PED2025

Pedestrian and Evacuation Dynamics 2025

Prague
9–12 September

Book of Abstracts

updated 8. 9. 2025

FACULTY OF INFORMATION TECHNOLOGY CTU IN PRAGUE

FACULTY OF CIVIL ENGINEERING CTU IN PRAGUE

Content

Version: 8. 9. 2025

Pedestrian and Evacuation Dynamics

Pedestrian and Evacuation Dynamics (PED) is a bi-annual international conference series established in 2001. This booklet contains the abstracts of the contributions to its 12th edition hosted by Faculty of Information Technology and Faculty of Civil Engineering of the Czech Technical University in Prague (FIT CTU in Prague and FCE CTU in Prague) between 9 and 12 September 2025.

The conference covers the whole PED research range, which is an inter- and multi-disciplinary area. The conference welcomes contributions from engineering, psychology, sociology, computer science, automated vision, applied physics, applied mathematics and other disciplines contributing to crowd dynamics research.

The PED 2025 edition especially highlights three topics covered by keynote talks:

- **Data acquisition from pedestrian experiments**, a topic focusing on obtaining the crowd and evacuation data for model calibration and comparison. The PhD workshop focuses primarily on this topic.
- **Artificial intelligence and pedestrian dynamics**, a new and rapidly developing topic deserving attention and discussion.
- **Coupling the fire and evacuation simulations**, a topic we believe should be reminded to the community as the origin of crowd motion research.

The scope of the conference includes, but is not strictly limited to, various topics related to pedestrian dynamics:

- **experiments and data acquisition,**
- **statistical evaluation and fundamental aspects of pedestrian flow,**
- **fire safety and safety aspects,**
- **psychological and behavioral aspects,**
- **model development, calibration and validation,**
- **simulation studies,**
- **applications and crowd management,**
- **machine learning, computer vision, and VR research in pedestrian dynamics.**

Organizing committee

Pavel Hrabák (Department of Applied Mathematics, FIT CTU in Prague)
Hana Najmanová (Department of Architectural Engineering, FCE CTU in Prague)
Daniel Vašata (Department of Applied Mathematics, FIT CTU in Prague)
Jana Vacková (Department of Applied Mathematics, FIT CTU in Prague)
Vladimír Mózer (Department of Architectural Engineering, FCE CTU in Prague)

Conference secretary

AMCA, spol. s r. o.
Academic and Medical Conference Agency
Vyšehradská 320/49 Prague 2, 128 00

Support and sponsors

Institutional support

Faculty of Information Technology CTU in Prague
Faculty of Civil Engineering CTU in Prague

FACULTY OF INFORMATION TECHNOLOGY CTU IN PRAGUE

FACULTY OF CIVIL ENGINEERING CTU IN PRAGUE

Silver level sponsor

Thunderhead Engineering

THUNDERHEAD ENGINEERING

Contacts and updated information

Web: https://www.ped25.cz

E-mail: ped25@cvut.cz (organizing commitee),
ped25@amca.cz (conference secretary)

Venue: **Czech Technical University in Prague**, Faculty of Civil Engineering,
Thákurova 7/2077, 166 29, Praha 6, Czech Republic
(campus of Czech Technical University in Prague in Dejvice)

Scientific Committee

Juliane Adrian	Forschungszentrum Jülich, Germany
Martyn Amos	Northumbria University, United Kingdom
Cecile Appert-Rolland	CNRS & University of Paris-Saclay, France
Nikolai Bode	University of Bristol, United Kingdom
Maik Boltes	Forschungszentrum Jülich, Germany
Mohcine Chraibi	Forschungszentrum Jülich, Germany
Alessandro Corbetta	Eindhoven University of Technology, Netherlands
Arturo Cuesta	University of Cantabria, Spain
Winnie Daamen	Delft University of Technology, Netherlands
Maria Davidich	Siemens, Germany
John Drury	University of Sussex, United Kingdom
Dorine Duives	Delft University of Technology, Netherlands
Iñaki Echeverria-Huarte	University of Navarra, Spain
Claudio Feliciani	The University of Tokyo, Japan
Yan Feng	Delft University of Technology, Netherlands
Paul Geoerg	Vereinigung zur Förderung des Deutschen Brandschutzes e.V., Germany
Simo Hostikka	Aalto University, Finland
Anders Johansson	University of Bristol, United Kingdom
Ramachandra Rao K	Indian Institute of Technology Delhi, India
Max Kinateder	National Research Council Canada, Canada
Bryan Klein	Thunderhead Engineering, United States
Angelika Kneidl	accu:rate GmbH, Germany
Gerta Koester	Munich University of Applied Sciences, Germany
Milan Krbalek	Czech Technical University in Prague, Czechia
Tobias Kretz	PTV Group, Germany
Petr Kučera	VŠB - Technical University of Ostrava, Czechia
Peter Lawrence	University of Greenwich, United Kingdom
Chung-Min Lee	California State University Long Beach, United States
Eric Wai Ming Lee	City University of Hong Kong, Hong Kong
Jian Ma	Southwest Jiaotong University, China
Alexandre Nicolas	CNRS & Université Claude Bernard Lyon 1, France
Katsuhiro Nishinari	The University of Tokyo, Japan
Daniel R. Parisi	Instituto Tecnológico de Buenos Aires, Argentina
Julien Pettre	INRIA, France
Enrico Ronchi	Lund University, Sweden
Meead Saberi	The University of New South Wales, Australia
Andreas Schadschneider	University of Cologne, Germany
Armin Seyfried	Forschungszentrum Jülich, Germany
Anna Sieben	Forschungszentrum Jülich, Germany
Weiguo Song	University of Science and Technology of China, China
Michael Spearpoint	OFR Consultants, United Kingdom
Anne Templeton	University of Edinburgh, United Kingdom
Antoine Tordeux	University of Wuppertal, Germany
Federico Toschi	Eindhoven University of Technology, Netherlands
Giuseppe Vizzari	University of Milano-Bicocca, Italy
He Wang	University College London, United Kingdom
Jarosław Wąs	AGH University of Science and Technology, Poland
Daichi Yanagisawa	The University of Tokyo, Japan
Francesco Zanlungo	ATR-IRC, Japan
Jun Zhang	University of Science and Technology of China, China
Iker Zuriguel	University of Navarra, Spain
Ezel Üsten	Forschungszentrum Jülich, Germany

Keynote Speakers

Maik Boltes

Forschungszentrum Jülich, Germany

Maik Boltes studied mathematics and computer science at the RWTH Aachen and Fern Universität Hagen, Germany focusing on computer graphics and scientific visualization. For his Ph.D. at the University of Cologne he developed computer vision methods for measuring pedestrian dynamics in crowds. Since 2018 he is heading the division "Pedestrian Dynamics – Empiricism" within the institute "Civil Safety Research" at Forschungszentrum Jülich, Germany. His research activities include the identification of parameters influencing crowd dynamics, the acquisition of these parameters, studying sensor techniques capturing corresponding data, and analyzing the collected and fused data. All his activities are guided by the principles of open science.

Data Acquisition from Pedestrian Experiments (Wed 9:15 — 10:15)

Empirical data is the basis for studying and thus understanding the dynamics inside crowds, which could increase safety and comfort for pedestrians as well as the performance of pedestrian facilities. The results enable the development of models reflecting the real dynamics. Controlled reproducible experiments allow the quantitative description of pedestrian dynamics by investigating influencing aspects and enable the analysis of selected parameters under well-defined constant conditions. Data of these experiments has to be collected by appropriately selected and utilized sensors.

In my presentation, I will address the implementation of laboratory experiments, with a particular focus on the collection of experimental data. I will discuss both the opportunities and limitations of various data collection techniques and methods, as well as their practical applications. The fusion of carefully calibrated and synchronized data enables the correlation of different influencing factors. Linking individual characteristics to specific subjects within a dataset makes it possible to analyze the impact of personal attributes on the specific dynamics. The use of standardized methods for data acquisition, measurement, and storing data significantly enhances the comparability of experimental results. Furthermore, the availability of open data and open-source software is essential for ensuring the reproducibility of findings and for facilitating the reuse of the often laboriously collected experimental datasets. These aspects will also be explored in my presentation.

He Wang

University College London, United Kingdom

He Wang is an Associate Professor in the Department of Computer Science at University College London, a core member of the UCL Centre for Artificial Intelligence, and a Visiting Professor at the University of Leeds. His research focuses on computer graphics, computer vision, scientific machine learning, and deep learning. Previously, he was an Associate Professor at the University of Leeds and a Senior Research Associate at Disney Research Los Angeles. He has led or co-led research projects of several million pounds funded by the EU and UKRI. He is a former Turing Fellow and also serves as an Associate Editor for Computer Graphics Forum, an Academic Advisor at the Commonwealth Scholarship Council, and has held key roles in major international conferences.

Bridging Physics and AI: Learning Pedestrian Dynamics from Video Data (Thu 9:15 — 10:15)

Understanding pedestrian and crowd movements is a crucial challenge spanning multiple disciplines, from mathematics, physics, and computer science to public safety, event planning, policymaking, and psychology. Decades of research have provided valuable insights and powerful analytical tools, and since 2016, deep learning has emerged as a transformative force in this field. In this talk, I will introduce our latest research on pedestrian dynamics within the deep learning landscape. Moving beyond traditional explicit models and black-box AI, a new trend has gained momentum since 2022—integrating physics-based models with deep neural networks. This hybrid approach enhances predictive accuracy, improves explainability, and strengthens generalization, paving the way for a deeper understanding of complex human movement patterns.

Simo Hostikka

Aalto University, Finland

Simo Hostikka received his DSc (Tech) in 2008 from the Helsinki University of Technology. The field was Theoretical and Applied Mechanics. He worked several years as a fire safety researcher at VTT Technical Research Centre of Finland, developing the numerical methods of fire and evacuation simulations. Since his guest researcher period at the National Institute of Standards and Technology, USA, in 2000-2001, he became one of the principal developers of the Fire Dynamics Simulator -code, FDS. A bit later, he initiated the development of agent-based evacuation module FDS+Evac. Currently, he works as a professor of Fire Safety Engineering Aalto University, Finland, leading a team of about 10 doctoral and post-doctoral researchers. Main research topics include thermal radiation modelling, material flammability and toxicity, and fire and evacuation risk analyses.

Coupling the Fire and Evacuation Simulations – Needs, Challenges and Possibilities (Fri 9:15 — 10:15)

Fire and evacuation simulations are often conducted as part of a building's design process to ensure that occupants can evacuate or be rescued in the event of a fire, or as part of a fire investigation to assess the conditions and timing of a past incident. Despite the clear interdependence between fire development and evacuation processes, these simulations are usually performed independently. This presentation will discuss the reasons for and extent to which these simulations should be coupled, the technical challenges involved, and development opportunities to support practitioners in analyzing scenarios that account for the interactions between fire and human behavior.

Key motivations for coupling fire and evacuation simulations include the need to evaluate potential toxic effects and reduced visibility due to smoke, which is often modeled through walking speed reduction. Wayfinding difficulties are typically addressed by applying scenario- and location-specific visibility thresholds. The adequacy of using visibility as a surrogate for irritation will be examined in light of literature data. Beyond wayfinding as a physical task, efforts have been made to predict evacuees' decision-making processes; however, these methods have not yet matured into practical applications. Recently, increasing interest in wildfire evacuation has reignited this topic. In building fires, two-way coupling may also be necessary, as evacuee decisions could influence fire development.

Recent advancements in fire toxicity modeling have revealed that limitations in transferring toxicity data can lead to underestimated risks and non-conservative designs. This presentation proposes an approach to improve both the accuracy and computational efficiency of toxicity coupling by using effective surrogate species and optimizing the selection of transferred quantities. The potential role of Building Information Modeling (BIM) standardization in supporting these improvements will also be briefly discussed.

Conference Timetable

Tuesday, 9 September

8:00-20:00	Registration
9:00-17:00	PhD Workshop
18:00-20:00	Welcome drink

Wednesday, 10 September

8:00-9:00	Registration	
9:00-9:15	Welcoming	
9:15-10:15	Keynote lecture (Hall 1) **Data Acquisition from Pedestrian Experiments** Maik Boltes	
10:15–10:45	Coffee break	
10:45–12:05 (Hall2) **Controlled Experiments – Interactions** **1, 2, 3, 4**		**10:45–12:05** (Hall 3) **Crowd Management** **5, 6, 7, 8**
12:05-13:05	Lunch	
13:05-14:25 (Hall 2) **Crowd and Real World Data** **9, 10, 11, 12**		**13:05-14:25** (Hall 3) **Model Development and Calibration** **13, 14, 15, 16**
14:25-14:30	Coffee break (continues during Poster session)	
14:30-15:30	**Poster session, Odd numbers**	
15:30-16:30 (Hall 2) **Controlled Experiments – Velocity** **17, 18, 19**		**15:30-16:30** (Hall 3) **Modeling of Navigation Aspects** **20, 21, 22**
19:00-21:00	Social Event	

Thursday, 11 September

9:05-9:15 Short info		
9:15-10:15 Keynote lecture (Hall 1) **Bridging Physics and AI: Learning Pedestrian Dynamics from Video Data** He Wang		
10:15–10:45 Coffee break		
10:45–12:05 (Hall 2) **Field Data Measurements** **23, 24, 25, 26**	**10:45–12:05** (Hall 3) **Machine Learning and Microscopic Modeling** **27, 28, 29, 30**	
12:05-13:05 Lunch		
13:05-14:25 (Hall 2) **Behavioral Aspects** **31, 32, 33, 34**	**13:05-14:25** (Hall 3) **Modeling of Avoidance Behaviors** **35, 36, 37, 38**	
14:25-14:30 Coffee break (continues during Poster session)		
14:30-15:30 **Poster session, Even numbers**		
15:30-16:30 (Hall 2) **Controlled Experiments - Obstacles and Slow Walkers** **39, 40, 41**	**15:30-16:30** (Hall-3) **Modeling of Pedestrian Formations** **42, 43, 44**	
16:30-17:30 Steering committee meeting		
19:00-22:00 Conference dinner		

Friday, 12 September

9:05-9:15 Short info		
9:15-10:15 Keynote lecture (Hall 1) **Coupling the Fire and Evacuation Simulations – Needs, Challenges and Possibilities** Simo Hostikka		
10:15–10:45 Coffee break		
10:45–12:05 (Hall 2) **Controlled Experiments – Design** **45, 46, 47, 48**	**10:45–12:05** (Hall 3) **Case Study Simulations** **49, 50, 51, 52**	
12:05-13:05 Lunch		
13:05-14:25 (Hall 2) **Crowd Management and VR** **53, 54, 55, 56**	**13:05-14:25** (Hall 3) **Machine Learning and Macroscopic Modeling** **57, 58, 59, 60**	
14:25-15:00 Closing		
15:00-16:00 Farewell drink		

Talk Index

Poster Index

Abstracts of Oral Lectures

Experimental study on safety distance for pedestrians under different interaction angles

Liangchang Shen[1,2,3], Jialin Wu[1,2,4], Yushan Song[1,2], Jiayue Wang[5], and Wenguo Weng*[1,2]

[1] School of Safety Science, Tsinghua University, Beijing, China
[2] Beijing Key Laboratory of City Integrated Emergency Response Science, Tsinghua University, Beijing, China
[3] Department of Architecture and Civil Engineering, City University of Hong Kong, Hong Kong, China
[4] College of Safety Science and Engineering, Nanjing Tech University, Nanjing, China
[5] School of Public Order, People's Public Security University of China, Beijing, China

Abstract Pedestrians must adjust their motion behaviors to avoid collisions with other moving objects in real-world scenarios. Here, a series of pedestrian interaction experiments were conducted to investigate the safety distance maintained during collision avoidance across various interaction angles. The results demonstrated that the safety distance between pedestrians decreased from 2.31 m to 0.95 m as the interaction angles decreased from 150° to 30° (increments of 30°). This finding provides a valuable empirical foundation for advancing research on collision avoidance algorithms.

Keywords collision avoidance, pedestrian interactions, safety distance

Instruction

In recent years, new devices such as self-driving cars and service robots have appeared in people's daily lives. They have embedded motion models to plan their routes and avoid collisions with other objects [1–3], which include social force models [4,5], cellular automata models [6], behavioral heuristics models [7], etc. These models have shown promising prospects and results in current device navigation [3] and crowd simulation [8]. However, shortcomings of the models also exist, such as lower validity and a lack of accuracy, which might result in misprediction and collision accidents. Therefore, studying the collision avoidance behavior of moving objects, especially pedestrians, is essential for more accurate modified motion models.

In this study, we conducted well-controlled experiments on interacting pedestrians. The optical motion capture system directly tracked the alternating movement of the two legs of each pedestrian, enabling a full investigation of the collision avoidance process of interacting pedestrians. The effects of step length and different interaction angles were examined. In the future, the decision-making process and basis of pedestrians in the collision avoidance process will be systematically analyzed.

We recruited 16 participants (10 males and 6 females) from Tsinghua University. The age range of all participants was 18-24. The height was 1.7 ± 0.1 m, and the BMI was within the normal range.

As shown in Figure 1a, the experimental measurement area was a circular area with a radius of 5 m with the intersection point of the two planned participants' routes as the center. Twelve equally spaced labels were placed on the boundary of the circular measuring area in the field so that the subjects knew their starting and ending positions. We took Figure 1b as the diagram and took black and green pedestrians as examples to further illustrate the experimental process. The green and black pedestrians were assumed to be participants A and B. The green and black lines were the motion routes of A and B. The red center of the circle was the intersection of green and black lines. The other blue lines were the planned walking routes assigned to the subjects according to the experimental needs of different interaction angles. The numbers on the periphery of the circular area are designed to help pedestrians understand their starting and target positions in the experiment. Different experimental routes represent different interaction angles.

Email of the corresponding author: wgweng@tsinghua.edu.cn

Timetable
Talk index

(a) (b)
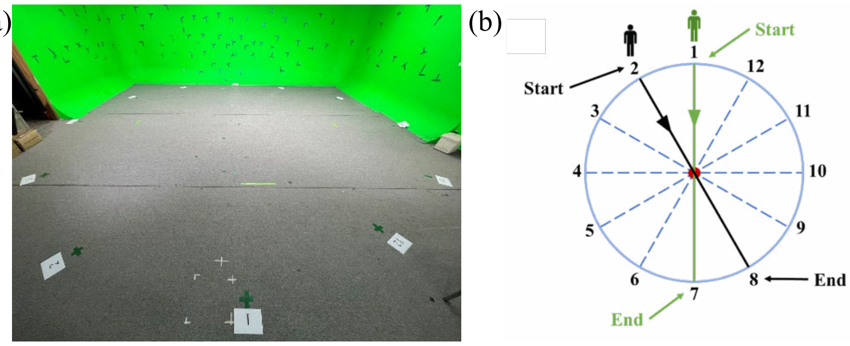

Figure 1: **(a)** The experimental measurement area, **(b)** A diagram of the experimental scene.

As shown in Figure 2, the safety distance seemed to be negatively correlated with the interacting angle. In five different interacting angles (150°, 120°, 90°, 60°, and 30°), the safety distances were 2.31 (±0.75) m, 1.44 (±0.545) m, 1.31 (±0.476) m, 1.14 (±0.361) m, and 0.95 (±0.345) m, respectively. A previous study showed that the safety distance increased with speed [9,10], so pedestrian speed might also be a factor affecting the safety distance. The correlation between the speed product of two pedestrians and their safety distance at five different interaction angles was analyzed, and the absolute value of the Pearson correlation coefficient at five interaction angles is less than 0.2 (Table 1). Within the range of pedestrian speed in this experiment, the safety distance of pedestrians seems to have little relationship with the walking speed of pedestrians.

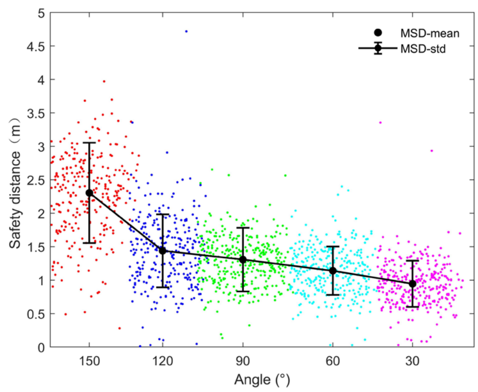

Figure 2: The relationship between the safety distance and the interaction angle.

Table 1: The Pearson correlation coefficient at different interaction angles

Angle	**150°**	**120°**	**90°**	**60°**	**30°**
PCC	0.006	0.115	0.0269	-0.0269	0.0203

Bibliography

[1] Itoh M, Horikome T and Inagaki T 2013 Effectiveness and driver acceptance of a semi-autonomous forward obstacle collision avoidance system Applied Ergonomics 44 756–63

[2] Richards D and Stedmon A 2016 To delegate or not to delegate: A review of control frameworks for autonomous cars Applied Ergonomics 53 383–8

[3] Rudenko A, Palmieri L, Herman M, Kitani K M, Gavrila D M and Arras K O 2020 Human Motion Trajectory Prediction: A Survey The International Journal of Robotics Research 39 895–935

[4] Helbing D, Farkas I and Vicsek T 2000 Simulating Dynamical Features of Escape Panic Nature 407 487–90

[5] Wang J, Sarvi M, Ma J, Haghani M, Alhawsawi A, Chen J and Lin P 2022 A modified universal pedestrian motion model: Revisiting pedestrian simulation with bottlenecks Build. Simul. 15 631–44

[6] Weng W G, Chen T, Yuan H Y and Fan W C 2006 Cellular automaton simulation of pedestrian counter flow with different walk velocities Phys. Rev. E 74 036102

[7] Moussaïd M, Helbing D and Theraulaz G 2011 How simple rules determine pedestrian behavior and crowd disasters Proc. Natl. Acad. Sci. U.S.A. 108 6884–8

[8] Wang C, Ni S and Weng W 2019 Modeling human domino process based on interactions among individuals for understanding crowd disasters Physica A: Statistical Mechanics and its Applications 531 121781

[9] Yuan Gao, Tao Chen, Luh P B, and Hui Zhang 2014 Experimental study on pedestrians' collision avoidance Proceeding of the 11th World Congress on Intelligent Control and Automation (Shenyang, China: IEEE) pp 2659–63

[10] Wang Q, Chen J and Ma J 2021 Experimental study on individual level interaction between bicycle and pedestrian J. Stat. Mech. 2021 093403

Quantifying Contact Pressure in High Competitive Pedestrian Evacuations

Iñaki Echeverría Huarte*[1], Ángel Garcimartín[1], Diego Maza[1], and Iker Zuriguel[1]

[1]Departamento de Física y Matemática Aplicada, Facultad de Ciencias, Universidad de Navarra, Pamplona, Spain

Abstract Understanding how crowds behave during evacuations is key to ensuring safety. Yet, while density and flow have been extensively studied, direct measurements of contact pressure remain scarce. Here, we employed a dynamic pressure mapping sensor to capture real-time pressure at the exit door during high-competitive evacuations. The results reveal that pressure at the doorjamb can be nearly an order of magnitude higher than on the wall, and that strategically placed obstacles help reduce these peaks and ease pressure surges caused by clogs.

Keywords Contact Pressure, Evacuation Safety, Pedestrian Dynamics.

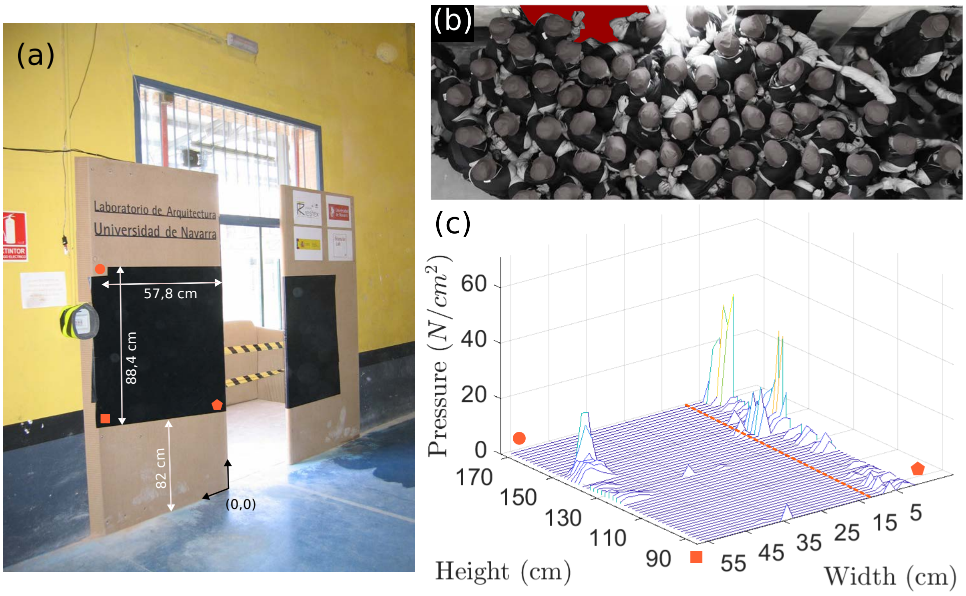

Figure 1: **(a)** Photograph of the door equipped with a dynamic pressure mapping sensor, with the sensor area featuring a black adhesive lining on the left. **(b)** Top view of a high-competitive evacuation experiment. The location of the pressure sensor is highlighted in red. **(c)** An instantaneous pressure field captured during a high-competitive evacuation. The dashed line divides the analyzed area into the doorjamb region (on the right) and the wall region (on the left), while the symbols mark three key spatial reference points.

Over the past two decades, research in pedestrian dynamics has primarily focused on metrics such as density and flow rates to gauge safety during evacuations. Seminal works by Helbing *et al.* [1] introduced phenomena like the "faster is slower" effect and the potential use of obstacles to modulate crowd movement. Despite these advances, the direct measurement of contact pressure (a critical parameter linked to life-threatening compressive asphyxia) has received limited quantitative attention. A recent literature review on contacting force measurement methods for pedestrian crowds [2] underscores that current techniques often lack sufficient spatial resolution, temporal accuracy, and integration with dynamic models. These shortcomings hinder our ability to capture the transient, localized force peaks that precipitate crowd disasters. Here, we addressed this gap by conducting controlled evacuation drills with 180 soldiers under high competitive conditions [3]. A dynamic pressure mapping sensor was installed along the exit door of

*Email of the corresponding author: `iecheverriah@unav.es`

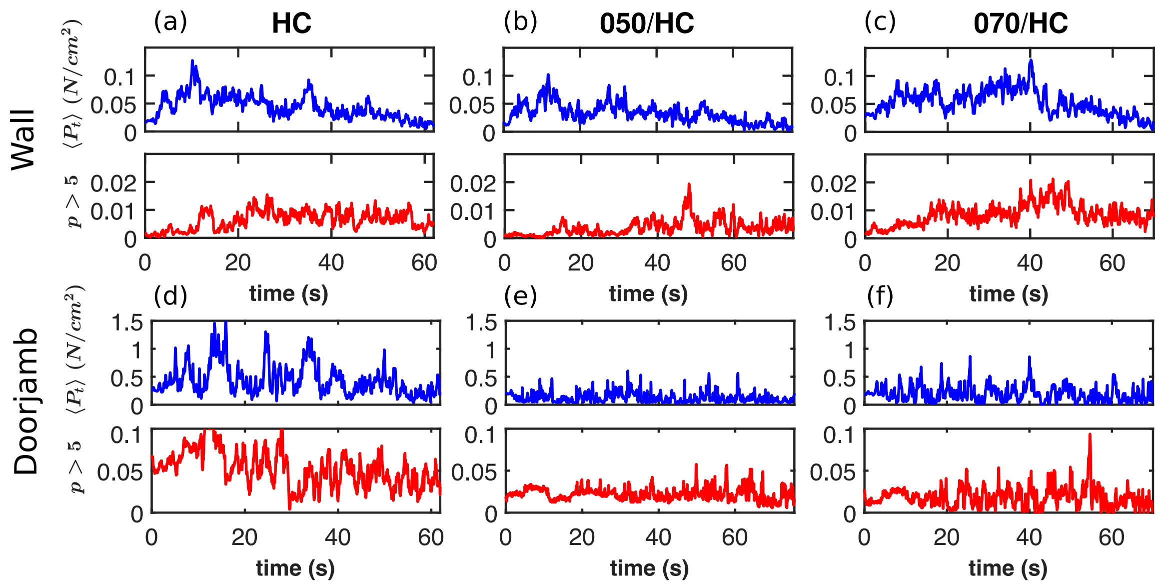

Figure 2: Temporal evolution of the mean pressure (blue) and the probability of detecting sensor pressure values above 5 N/cm² (red) under three diferent experimental conditions: High competitiveness without obstacle (HC), HC with an obstacle at 50 cm, and HC with an obstacle at 70 cm. The obstacle was centered in front of the door. At each time, the mean pressure $\langle P_t \rangle$ is computed as the average across all sensor units in the two distinct regions—the wall (a-c) and the doorjamb (d-f). The probability (p) of detecting high-pressure values is calculated as the fraction of sensor units registering pressures above 5 N/cm² divided by the total number of units in each region.

the room (Fig. 1a) to capture real-time contact pressures during the evacuation (Fig. 1b). Our experiments reveal that the pressure does not distribute uniformly across the sensor (as seen in Fig. 1c), where clear spatial heterogeneities are evident. This observation prompted us to define two distinct zones for the analysis: the wall zone and the door edge (doorjamb).

Detailed analysis shows that the pressure levels in these two zones differ markedly. In particular, the mean pressure $\langle P_t \rangle$ along the wall (panels a-c in Fig. 2, shown as blue lines) is nearly an order of magnitude lower than that at the doorjamb (panels d-f). This is clearly underscored by the change in the y-axis scale between the plots representing these two regions. Moreover, the probability (p) of recording high-pressure values (exceeding 5 N/cm², indicated in red) is considerably higher at the door edge than along the wall (notice again the change in the scale), suggesting that the doorjamb region is more susceptible to pressure surges that can lead to clogs and, ultimately, crowd disasters.

Furthermore, our study demonstrates the impact of strategically positioning an obstacle in front of the exit. When placed approximately 50 cm from the door (second column of Fig.2), the obstacle serves as an effective buffer, mitigating the pressure peaks. This intervention results in a substantial reduction in $\langle P_t \rangle$ and a decreased likelihood of high-pressure events compared to the no-obstacle scenario (first column of Fig.2). Notably, the effect is most pronounced in the doorjamb region, where the obstacle alleviates the pressure surges associated with clogs and congestion. In contrast, when the obstacle is positioned at 70 cm (third column of Fig. 2), its mitigating effect, although present, is less pronounced than at the optimal 50 cm placement.

These findings not only validate previous hypotheses regarding the benefits of obstacle placement in crowd management [1] but also underscore the importance of integrating high-resolution, dynamic pressure measurements into pedestrian dynamics models to better predict and prevent crowd disasters.

Bibliography

[1] Helbing, D., Farkas, I., Vicsek, T., *Simulating dynamical features of escape panic*, Nature **407**, 487-490 (2000).

[2] Zhao, R., Rahman, A., Wei, B., Li, C., Ma, Y., Cai, Y., Han, L. *A literature review of contacting force measurement methods for pedestrian crowds*, Heliyon **10**, e39755 (2024).

[3] Zuriguel, I., Echeverría, I., Maza, D., Hidalgo, R.C., Martín-Gómez, C., Garcimartín, A., *Contact forces and dynamics of pedestrians evacuating a room: The column effect*, Safety Science **121**, 394–402 (2020).

12th International Conference on Pedestrian and Evacuation Dynamics (PED 2025)
Prague, Czech Republic - September 9-12, 2025

Experimental Study on Pushing Propagation in Moving Pedestrian Queues

Yushan Song[1,2], Haiyang Huang[1,2], Liangchang Shen[1,2,3], and Wenguo Weng*[1,2]

[1]School of Safety Science, Tsinghua University, Beijing, China
[2]Beijing Key Laboratory of City Integrated Emergency Response Science, Tsinghua University, Beijing, China
[3]Department of Architecture and Civil Engineering, City University of Hong Kong, Hong Kong, China

Abstract A series of controlled experiments were conducted on moving 5-pedestrian queues to investigate pushing propagation characteristics under different motion conditions, such as step frequency and gait cycle. The study compared and analyzed the relationships between initial impulse and variables including the propagation distance, propagation speed, and impulse ratios. Results showed that propagation speed decreased in moving conditions compared to static ($p = 0.0258$), and asynchronous stepping reduced the effect of initial impulse on propagation velocity ($p = 0.0297$), highlighting how pedestrian motion influences crowd dynamics.

Keywords Pushing propagation, Impulse, Pressure, Gait characteristics

Instruction

In dense crowds, physical interactions among individuals propagate similarly to shockwaves or turbulence, which have been identified as potential factors contributing to crowd crushes and stampede incidents [1,2]. Recently, pedestrian pushing experiments utilizing flexible pressure-sensing equipment have gained increased attention, aiming to investigate human responses to external forces and elucidate the mechanisms of force propagation within crowds. Wang et al. (2018) examined impulse and pressure propagation patterns in static pedestrian queues [3]. Li et al. (2021) measured mechanical and kinematic parameters involving one or two pedestrians, and analyzed the influence on body posture and stride behavior [4]; Feldmann et al. (2023) introduced inertial motion capturing technology to quantify mechanical responses and three-dimensional kinematics in a static queue of five individuals, assessing pushing propagation velocities from a kinematic perspective [5,6], and subsequently extended their analysis to larger pedestrian groups [7].

However, current controlled pedestrian pushing experiments have predominantly focused on static crowds. To investigate the propagation characteristics of pushes in moving crowds, we conducted a series of pushing experiments in moving pedestrian queues at Tsinghua University. Five male participants aged 22–28 years wore flexible pressure-mapping clothing (Xsensor), enabling continuous measurement of pressure levels on the chest, back, and arms. Additionally, an optical motion-capture system (Qualisys) recorded the three-dimensional trajectories of each participant's head and shoulders. To analyze the influence of movement speed and pedestrian stepping synchronization or asynchronization on pushing propagation, experiments were performed under multiple conditions at an interpersonal distances of elbow length (approximately 20 cm). Stepping frequencies of 45 bpm and 90 bpm represented slow and normal walking speeds, respectively. Gait conditions included synchronous, asynchronous, and random stepping, with two types of movements: swaying and walking. Under each condition, we performed 30 push trials of varying impulse magnitudes. A representative snapshot of the experimental setup is illustrated in Figure 1.

We analyzed the relationships between initial impulse and variables such as the number of individuals involved in pushing propagation, the propagation distance, propagation speed, and impulse ratios between adjacent individuals under different conditions. The results indicated that the pushing propagation threshold was significantly higher in asynchronous conditions compared to synchronous and static conditions. Additionally, the push propagation threshold increased with higher step frequencies, suggesting that pushes encountered greater resistance to forward propagation at higher stepping frequencies. Additionally, our analysis revealed that lateral propagation was more prominent under asynchronous conditions. Propagation velocities were calculated by fitting linear models to trajectory inflection points identified according to the methodology described in [5].

*Email of the corresponding author: wgweng@tsinghua.edu.cn

Statistical analyses demonstrated that propagation velocities were significantly influenced by both stepping conditions and initial impulses. Notably, propagation velocities during motion were significantly lower compared to static conditions ($p = 0.0258$). Furthermore, the interaction term analysis indicated that synchronous stepping conditions had a significant moderating effect ($p = 0.0297$), suggesting a pronounced reduction in the relationship between initial impulse and propagation velocity under asynchronous stepping conditions. Representative results are illustrated in Figure 2.

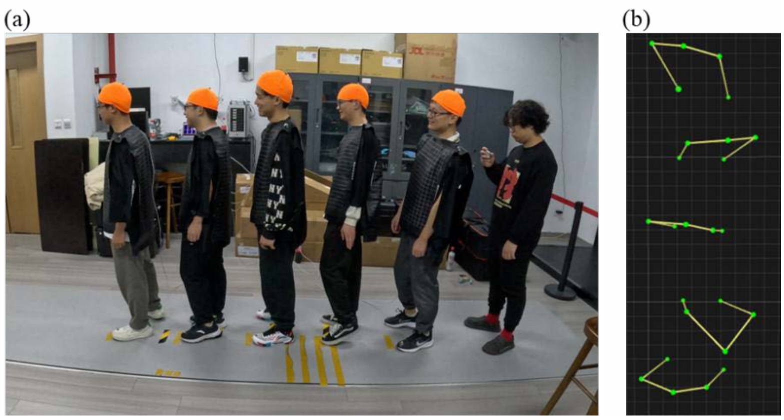

Figure 1: (a) side-view video recording and (b) Top-down view from Qualisys motion capture data, with trajectory points of the head, shoulders, and feet connected for clear differentiation, demonstrating the condition of asynchronous swaying at a step frequency of 45 bpm.

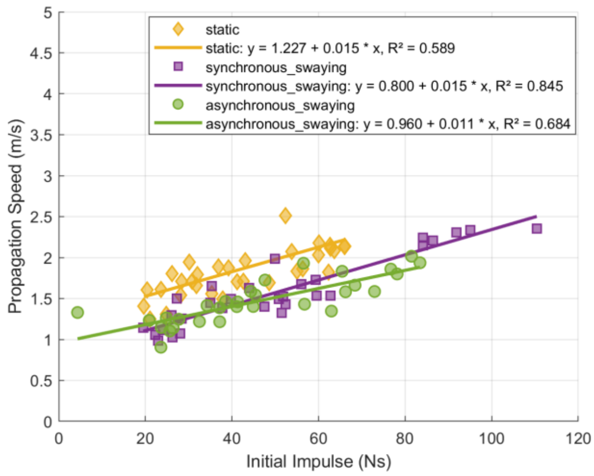

Figure 2: Pushing Propagation speed for different motion conditions and respective linear fitting equations.

Bibliography

[1] A. Bottinelli, D.T.J. Sumpter, J.L. Silverberg, Emergent Structural Mechanisms for High-Density Collective Motion Inspired by Human Crowds, Phys. Rev. Lett. 117 (2016) 228301. https://doi.org/10.1103/PhysRevLett.117.228301.

[2] J.J. Fruin, The causes and prevention of crowd disasters, Eng. Crowd Saf. 1 (1993) 99–108.

[3] C. Wang, W. Weng, Study on the collision dynamics and the transmission pattern between pedestrians along the queue, J. Stat. Mech. Theory Exp. 2018 (2018) 073406. https://doi.org/10.1088/1742-5468/aace27.

[4] X. Li, X. Xu, J. Zhang, K. Jiang, W. Liu, R. Yi, W. Song, Experimental study on the movement characteristics of pedestrians under sudden contact forces, J. Stat. Mech. Theory Exp. 2021 (2021) 063406. https://doi.org/10.1088/1742-5468/ac02c7.

[5] S. Feldmann, J. Adrian, Forward propagation of a push through a row of people, Saf. Sci. 164 (2023) 106173. https://doi.org/10.1016/j.ssci.2023.106173.

[6] S. Feldmann, T. Chatagnon, J. Adrian, J. Pettré, A. Seyfried, Temporal segmentation of motion propagation in response to an external impulse, (2024). https://doi.org/10.48550/arXiv.2402.19024.

[7] S. Feldmann, J. Adrian, M. Boltes, Propagation of Controlled Frontward Impulses Through Standing Crowds, Collect. Dyn. 9 (2024) 1–16. https://doi.org/10.17815/CD.2024.148.

Timetable
Talk index

Comparison of Different Methods to Determine Pedestrian Shoulder Orientation from Stereo Recordings

Deniz Kılıç*and Maik Boltes

Institute for Advanced Simulation 7: Civil Safety Research, Forschungszentrum Jülich, 52428 Jülich, Germany

Abstract This work compares imaging based methods for pedestrian orientation measurements. They are tested on overhead stereo recordings from corner-flow and bottleneck experiments with different densities. Classical computer vision based methods do not outperform using the movement direction and get worse with higher densities. A machine learning method outperforms the classical methods and does not degrade on higher densities.

Keywords Orientation, Shoulder, stereo computer vision, machine learning

Introduction

The orientation of the upper body of pedestrians can give insights into areas such as space requirements, collision avoidance and clogging or be used in further steps to e.g. determine social groups. To study the orientation of pedestrians, accurate measurements are needed. Different methods have been used in the literature such as IMUs [4], shoulder markers [1, 3], classical computer vision on depth data [2] or machine learning (ML) on depth data [5]. For large crowds, instrumentation of each individual is not feasible, so this contribution focuses on a comparison of the imaging based methods. Additionally, we compare to using the walking direction to determine the pedestrians orientation.

Method

All methods work with depth data from a stereo camera, except the movement direction based method. A stereo camera takes images from two cameras and computes the disparity between these images to determine the distance of objects from the camera. (1) The method from [2] is based on a PCA on points from the shoulder region. Said region is extracted from 3D imaging data using a segmentation algorithm based on growing clusters. Cluster growing starts with the highest points, making use of the fact that pedestrians are better separated at head height. It has been re-implemented with small changes to the segmentation method that have been observed to improve results on high density crowds by the authors. (2) Additionally, a self-developed method for the measurement of pedestrian orientation based on (1), working with constrained ellipsoid fitting instead of PCA was implemented. (3) To infer the orientation from the movement direction, the head trajectories were smoothed with a central moving average with a window size of 0.8 s. The orientation is then assumed to be orthogonal to the moving direction. (4) Finally, a neural network (NN) based approach was implemented by using the movement direction to automatically label data, albeit with large noise, similar to [5]. The NN uses patches of the depth image as input, centred around the point 32 cm below the head to counteract perspective distortion. These are generated from head trajectories. All of these methods were then applied on three runs of a corner flow experiment, with varying density ($0.54 \pm 0.14\,\mathrm{ped/m^2}$, $0.83 \pm 0.4\,\mathrm{ped/m^2}$, $1.84 \pm 0.66\,\mathrm{ped/m^2}$) and a bottleneck experiment ($1.82 \pm 1.31\,\mathrm{ped/m^2}$). Some data was manually annotated to estimate the error of the different methods.

Preliminary Results

Preliminary results for the corner flow can be seen in Figure 1. We see that method (3) using the movement direction is not outperformed by neither (1) nor (2). We also see that higher density leads

*d.kilic@fz-juelich.de

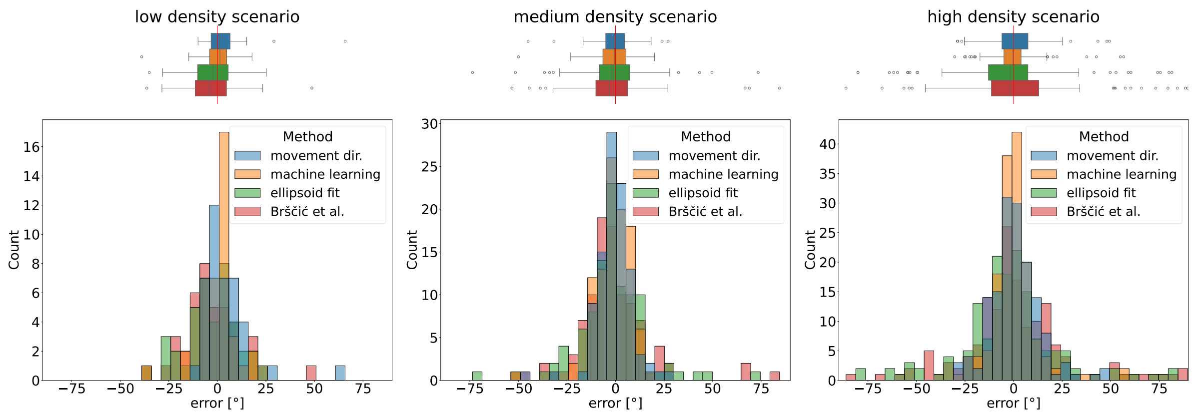

Figure 1: Error of different methods compared to manual annotation. Both the boxplot and the histogram use the same scale and colour scheme.

Figure 2: Frame from a RGB-D camera recording of bottleneck experiments from 10.34735/ped.2022.5 with shoulder markers.

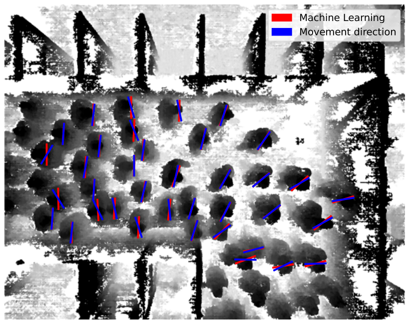

Figure 3: Comparison of ML method (4) and movement direction (3) on an example frame of the high density corner flow.

to worse results on the methods (1) and (2) and to lesser extent on method (3). The ML method (4) does not meaningfully degrade in performance with higher density and outperforms the methods (1) and (2) in all scenarios. However, the average error only gets lower than (3) in the high density scenario. It should be noted that the higher density scenario takes up a larger part of the training dataset, due to the higher number of pedestrians involved and the way of automatically creating the dataset. It should also be noted that we used laboratory experiments with an order of magnitude less training data than [5].

The bottleneck scenario a RGB-D recording (see Figure 2) including shoulder markers is available, which enables a comparison of all methods, including shoulder markers [1]. The high density is a challenge for the classical CV methods and the shoulder markers, while the low average speed mandates a different method for determining the walking direction from trajectory data.

References

[1] A. K. Boomers and M. Boltes. Shoulder Rotation Measurement in Camera and 3D Motion Capturing Data. In K. R. Rao, A. Seyfried, and A. Schadschneider, editors, *Traffic and Granular Flow '22*, pages 35–42, Singapore, 2024. Springer Nature.

[2] D. Brščić, T. Kanda, T. Ikeda, and T. Miyashita. Person Tracking in Large Public Spaces Using 3-D Range Sensors. *IEEE Transactions on Human-Machine Systems*, 43(6):522–534, Nov. 2013.

[3] L. Luo, G. Yang, C. Chen, Z. Yuan, and Z. Fu. Empirical study on pedestrian rotation mechanisms through bottlenecks. *Physical Review E*, 111(1):014103, Jan. 2025.

[4] J. Schumann. *Utilizing Inertial Sensors as an Extension of a Camera Tracking System for Gathering Movement Data in Dense Crowds*. PhD thesis, Forschungszentrum Jülich GmbH Zentralbibliothek, Verlag, 2022.

[5] J. Willems, A. Corbetta, V. Menkovski, and F. Toschi. Pedestrian orientation dynamics from high-fidelity measurements. *Scientific Reports*, 10(1):11653, July 2020.

Timetable
Talk index

12th International Conference on Pedestrian and Evacuation Dynamics (PED 2025)
Prague, Czech Republic – September 9-12, 2025

System Identification for Designing a Crowd Danger Controller in a Metro Station During Large Passenger Flow

Jun Zhang[1], Dongdong Shi[1], Lu Hu[1], Wei Yang[2], and Jian Ma*[1]

[1]School of Transportation and Logistics, Southwest Jiaotong University, Chengdu, 610031, China
[2]Anhui Provincial Key Laboratory of Urban Rail Transit Safety and Emergency Management, Hefei University, Hefei, 230601, China

Abstract Large passenger flows in metro stations may lead to potential safety issues. However, existing studies have primarily focused on service-oriented passenger flow control strategies [1]. To fill this gap, we investigate the potential for managing crowd risk by delaying the service time of the entrance ticket gates. We use crowd danger [2], the state-of-the-art definition of pedestrian dynamics, as an indicator for assessing crowd safety. Specifically, we develop a comprehensive microscopic pedestrian simulation model tailored to metro station scenarios, this model generates input-output data for the predictive model. The simulation scenario is shown in Figure 1, where the sensing area for crowd danger detection includes the paid area of the station hall, as well as the stairs and escalators. It is observed that high crowd danger values are primarily distributed near stairs and escalators, in reality, these areas experience the highest number of accidents [3]. Next, we develop a predictive model to capture the system dynamics, specifically the relationship between ticket gate delay time and crowd danger in the sensing area. This predictive model plays a crucial role in understanding the underlying mechanics of the system and enabling precise control. It serves as an accurate mathematical representation of the system, derived from input-output data generated by the simulation. The results indicate that entrance ticket gate delay time is highly sensitive to crowd danger in the sensing area. Moreover, the use of a linear state-space model effectively captures system dynamics and provides accurate multi-step predictions, demonstrating the potential of our proposed crowd management solution.

Keywords Metro station pedestrian regulation, Pedestrian microscopic simulation, Pedestrian dynamics, System identification, Crowd danger

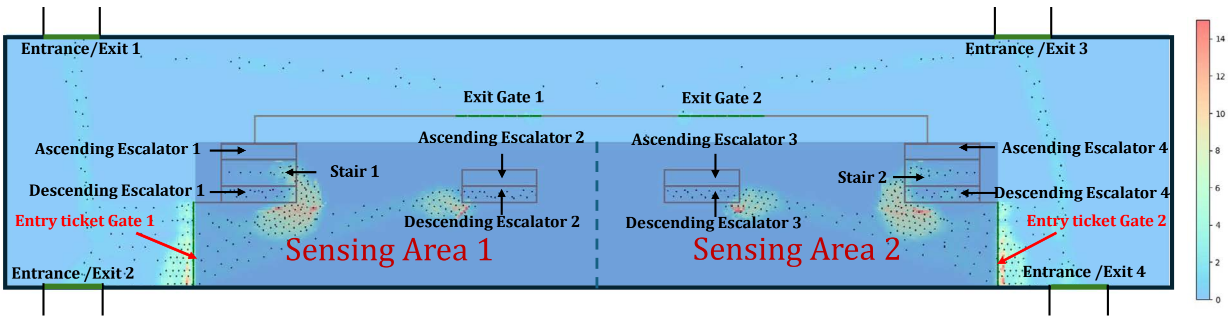

Figure 1: Metro station simulation scenario and pedestrian regulation solution.

Bibliography

[1] Zhu, G., Sun, R., Sun, X., Wei, Y., & Wu, B. (2023). Parallel and collaborative passenger flow control of urban rail transit under comprehensive emergency situation. *IEEE Transactions on Intelligent Vehicles*, 8(4), 2842-2856.

[2] Feliciani, C., Nishinari, K. (2018). Measurement of congestion and intrinsic risk in pedestrian crowds. *Transportation research part C: emerging technologies*, 91, 124-155.

[3] Xing, Y., Dissanayake, S., Lu, J., Long, S., Lou, Y. (2019). An analysis of escalator-related injuries in metro stations in China, 2013–2015. *Accident Analysis & Prevention*, 122, 332-341.

*Email of the corresponding author: `majian@mail.ustc.edu.cn`

12th International Conference on Pedestrian and Evacuation Dynamics (PED 2025)
Prague, Czech Republic – September 9-12, 2025

Crowd Simulations Beyond Evacuation Applications: A Use Case Study for Departure Scenarios at Major Events

Jette Schumann*[1] and Hauke Schmidt[2]

[1]Institute for Advanced Simulation (IAS-7), Forschungszentrum Jülich GmbH, Germany
[2]D.LIVE GmbH & Co. KG, Germany

Abstract We present an interdisciplinary work that brings together crowd simulations and safety planning. Crowd simulations were used to assist in planning of major events in Düsseldorf, Germany, with a particular focus on departure scenarios after the events have ended. This work describes the challenges of modeling these types of scenarios and how the results have been incorporated into safety planning.

Keywords Crowd simulations, Scenario modeling, Departure process, Major events, Crowd Management

Extended Abstract

Crowd simulations are an established method in fire safety engineering for investigating the effectiveness of escape routes and identifying congested areas for evacuation scenarios. The simulation scenarios are based on a variety of assumptions and model-specific parameters that are decisive for the simulation results and thus for the added value for practitioners. After defining a relevant scenario in terms of type of use and time of observation, several parameters must be determined for the input categories geometry, population (including the initial distribution of agents and individual characteristics such as free walking speed) and routes [2].

Scenario modeling becomes even more complex when it comes to modeling other types of processes, such as the departure of major events. Usually, the departure routes extend over a wide area to various transportation hubs (private and public transportation). The spatial start and end of the simulation area must be selected in such a way that the relevant dynamics of pedestrian streams can be represented and at the same time sufficient assumptions can be made for the parameters in this area. In addition to detailed modeling of the geometry, which can be particularly challenging in outdoor areas, assumptions must be made about the timing of the departure process. The spawned agents must be distributed to the destinations associated with the visitors' expected choice of transportation mode. In addition, there are often several available routes and crowd management measures on the way to a destination, which must be considered.

All assumptions made for modeling the scenario as well as model-related simplifications and restrictions (e.g. waiting behavior) must be taken into account when interpreting the simulation results to derive suitable measures for crowd management. The process of modeling such a simulation scenario and deriving findings for safety planning is a complex and iterative process, as illustrated in Figure 1, that requires close cooperation between simulation experts and safety planners at the respective event.

The authors have accompanied the planning of several major events in Düsseldorf, Germany. In the planning phase of the events, specific questions were identified that were to be answered with the help of crowd simulations. These questions were transformed into various scenarios and simulated using the research software JuPedSim [1]. The simulation results were interpreted in the context of crowd management. This was an iterative process, so that after the results were evaluated, changes were made to the scenario based on corrections and the updated planning status. An example of a simulation scenario examined is shown in Figure 2. The simulation results have helped to answer specific questions (e.g. what flow can be expected in that corridor after 30 minutes?) and to derive specific measures for crowd management, such as the routing to the various destinations. In addition, the visualization of the pedestrian streams helped to create a common planning basis that is also easier to understand for other stakeholders such as authorities.

*Email of the corresponding author: j.schumann@fz-juelich.de

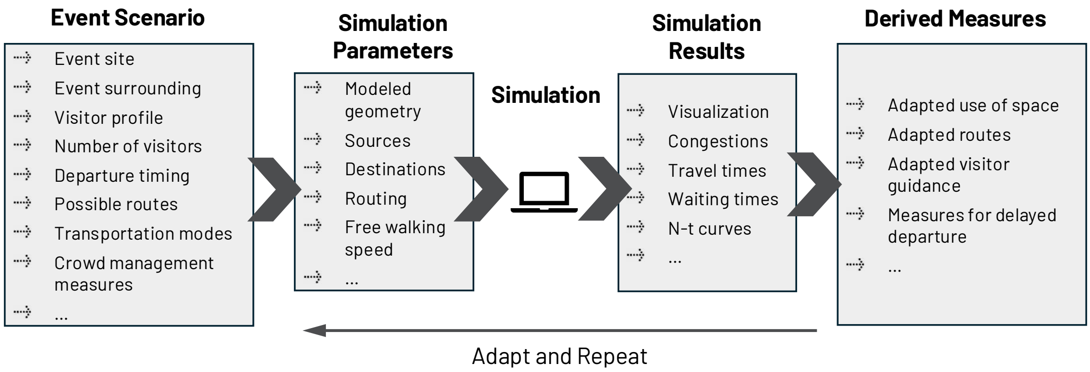

Figure 1: Schematic representation of simulation-aided planning starting from an event scenario to deriving measures.

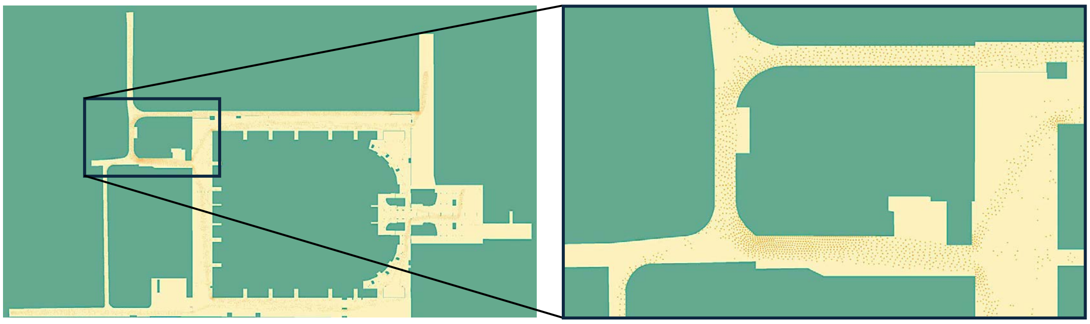

Figure 2: Snapshot of a simulation scenario that was created for the departure from the arena in Düsseldorf. For this scenario, for example, the choice and weighting of different routes in the surroundings of the arena were examined using simulations.

The proposed work provides an overview of the modeling process and the role of incorporation in the planning process of major events. It discusses the challenges and the use of the powerful tool of crowd simulations for scenarios beyond evacuation processes.

References

[1] Mohcine Chraibi et al. *JuPedSim*. Apr. 2024. DOI: `10.5281/zenodo.11093061`. URL: `https://doi.org/10.5281/zenodo.11093061`.

[2] RiMEA e.V. *Guideline for Microscopic Evacuation Analysis*. Jan. 2024. URL: `https://rimea.de/` (visited on 03/13/2025).

Timetable
Talk index

12th International Conference on Pedestrian and Evacuation Dynamics (PED 2025)
Prague, Czech Republic – September 9-12, 2025

The people at the gates : an analysis of the reasons of pedestrian flow management success in train stations at the Olympic Paris 2024 Games

Capucine-Marin Dubroca-Voisin,*[1,2]

[1]AREP Flux et Mobilités, Paris, France
[2]LVMT, École nationale des ponts et chaussées | Institut Polytechnique de Paris, Univ Gustave Eiffel, Marne-la-Vallée, France

Abstract Please, write here an abstract of 3 to 5 sentences summarizing the main essence of your extended abstract. During Paris 2024 Games, pedestrian flow management in train stations was a major challenge. It was yet successful thanks to a combination of actions and factors that this presentation will explore. Notably, massive use of trained staff, cooperation of passengers, exceptional maintenance and operational resources, and a lower ridership than expected were amongst these key factors.

Keywords pedestrian flow management, Olympic games, train stations, Paris

Introduction

One of the major challenges during the Paris 2024 Games was the management of pedestrian flows in train stations. The sheer number of visitors and athletes flocking to the city required an unprecedented level of coordination and infrastructure readiness. Train stations, being key nodes in the transportation network, were put to the test with the influx of people. Managing pedestrian flows small stations, such as Vaires Torcy which served the Nautical Stadium, presented its own unique set of challenges. These stations were designed for relatively modest commuter flows and not for major events.

Figure 1: Massive flows at Paris Est station

Solutions used

Careful flow management plans were built during the years preceding the Games, finding unidirectional solutions in these small stations, designing waiting areas to act as a buffer, and ensuring the connected

*Email of the corresponding author: `capucine-marin.dubroca-voisin@enpc.fr`

stations managed the connected flows to avoid overcrowding.

These plans, conceived by pedestrian flow experts, were adapted by local train operators' companies' staff in the months before the Games. Last minute adaptations were also made on the ground to correct the last details. While situation was expected to be potentially uncomfortable if not hazardous, smoothness of the operations was finally highlighted by the external observers. Observations made during the Games show that the massive presence of staff, who were adept at managing crowd situations, resolving issues swiftly, and providing clear guidance to passengers, was a key element to this success. The passengers themselves were highly cooperative and accepted waiting times for this event. Several other

Figure 2: Flow management layout at Vaires-Torcy station

key elements enabled this success. The transport network had been prepared with better maintenance capabilities than usual (for instance higher availability of replacement elements for elevators). There was an organized shortage of drivers before and after the Games to ensure there enough drivers during this period (which can be seen as a moderate sacrifice of the local population during the rest of the summer). A last key element of success was the fact that the number of passengers using public transport was overestimated. Patrons of the Games used public transport a bit less than expected, and travel demand management measures asking locals to avoid the city during the Games period.

Several elements were combined for this success: anticipation, cooperation between stakeholders, precise plans, travel demand management, efficient staff, enthusiastic patrons, quick adaptation, massive supervision, and a bit of luck. The experience from the Paris 2024 Games demonstrated the potential for shared governance and the necessity of treating pedestrian flow management as a common good.

Methodology

To determine the success factors in this presentation, we used a mix of participant observation (our team being in charge of the first version of the pedestrian flow management plan in train stations, and involved in the design of the solutions in the biggest stations), direct ground observation and data collection, plus interviews with selected stakeholders. We also relied on the numerous press reports reporting the organization of the Games as a success.

Timetable

Talk index

12th International Conference on Pedestrian and Evacuation Dynamics (PED 2025)
Prague, Czech Republic – September 9-12, 2025

A holistic guiding system for pedestrians: a proof of concept

Christina Maria Mayr[1] and Gerta Köster*[1]

[1]Hochschule München - University of Applied Sciences

Abstract Crowds could be made safer and flow more efficient by guiding pedestrians through an automatic system. Yet, no such system is being employed anywhere in the world. In former work we tackled obstacles to this goal: sensing and distribution of congestion information through a direct communication network, resolving congestion when facing limited compliance, and collecting data on compliance behavior. Here, we combine all into one socio-technical system and demonstrate through simulation how congestion at metro station Münchner Freiheit is resolved.

Keywords Socio-technical system, Guiding strategies, Compliance, Pedestrian modeling, Direct mobile communication, Survey

Building and investigating a system for crowd guidance

Whether at large events or in everyday traffic, crowds could be made safer and flow more efficient if one succeeded in guiding pedestrians towards better routes, as one does with cars. Ideally this would happen through an automatic system without involving human crowd managers. An app could make information available to anyone with a smartphone. Such a system is illustrated in Figure 1.

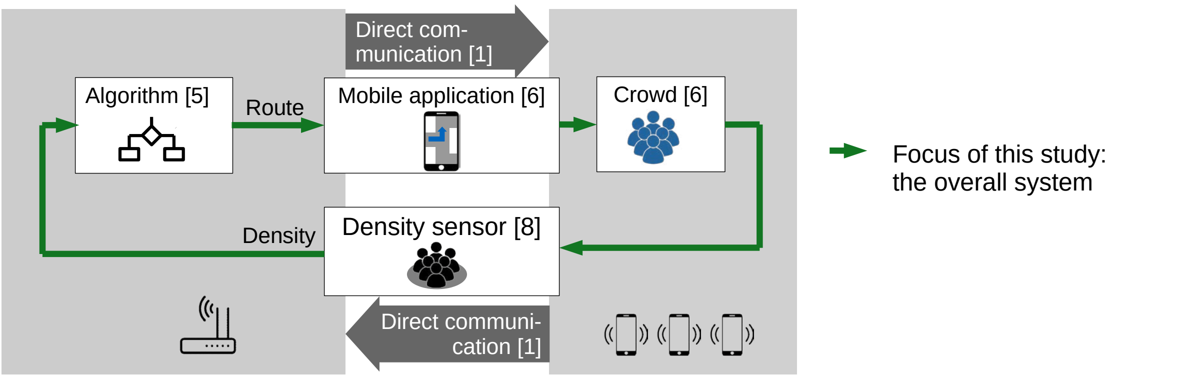

Figure 1: Components of a crowd guidance system that have been already analyzed in [1, 2, 3, 4]. The focus of this study is on the overall system. We integrate componontes into an overall concept and test it for a real life use case.

Yet, while the idea may seem obvious, as of today no such system is being employed anywhere in the world. A number of factors make the task more challenging than for car traffic. One is that we need a way to sense congestion in crowds that are often distributed over an area that may be hard to survey, even by cameras. Another issue is that instructions need to be distributed within the crowd. In preceding publications, e. g. Ref. [1], we suggested using direct mobile communication to do both, sense and transmit congestion information in a crowd, and showed that it is technically feasible.

However, most issues are non-technical. In particular, pedestrians need to perceive and understand instructions. Also information must be identical for all members of a group traveling together. Most importantly, unlike water molecules, people need to be convinced to comply. Even in the best of circumstances, compliance will be nowhere near 100% as often assumed in former concepts of control systems for pedestrian traffic, e.g. in Ref. [5, 6, 7]. The good news is that, compliance as low as 30 percent may suffice to resolve congestion as we demonstrated in an abstracted scenario with three routes in Ref. [2].

But will it work for real people in a real world scenario? In a survey with almost 1000 soccer fans we compiled realistic compliance distributions with respect to app designs that conveyed directional

*Email of the corresponding author: gerta.koester@hm.edu

suggestions. We saw that, when congestion information was added, compliance with route suggestions among soccer fans sufficed to significantly reduce jams [3].

All three aspects—information gathering and transmission, a robust guiding algorithm capable of handling low compliance, and mechanisms to foster compliance—are essential building blocks of a functional system. However, considering these elements in isolation is insufficient, as they interact. To assess whether the overall system is effective, it must be conceptualized and tested as an integrated whole. Therefore, in this contribution, we compose an overall concept—namely, a complex socio-technical system—and evaluate it through simulations.

We demonstrate, through a simulation study, how severe congestion on a preferred route at metro station Münchner Freiheit is relieved. Congestion is reduced on the preferred route to the trains during the rush before a Bayern München soccer match. A percentage of counterflow is estimated from a field study in 2020 Ref. [8]. In addition, we assume that only 40% of the people consult their smart phones for instructions. Compliance among these smart phone users is modeled after the survey data in Ref. [8]. See Figure 2.

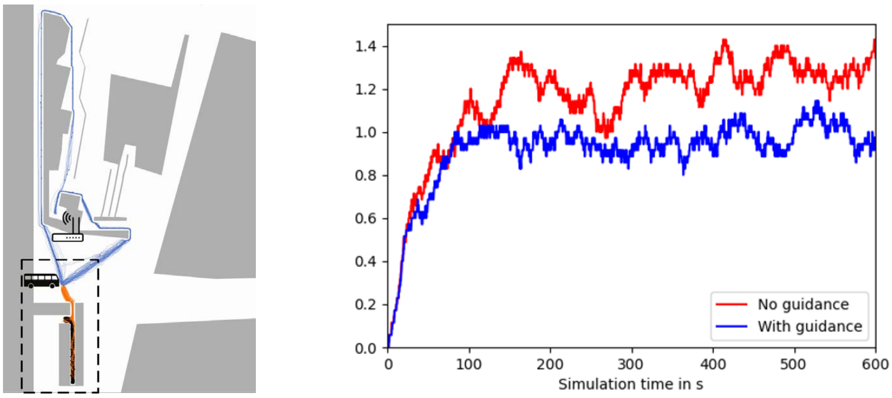

Figure 2: Left: Bird's eye schematic of three routes from the bus station to the train level. The shortest (orange) route is the preferred route for most. There is counterflow on that route. The guidance system points new arrivals to the least congested route. Right: Red: density without guidance system in persons/m^2 on the preferred route to trains. Blue: density with guidance, 40% app usage assumed, compliance among app users as in survey (about 40%), same counterflow as in unguided case.

References

[1] Christina Maria Mayr, Stefan Schuhbäck, Lars Wischhof, and Gerta Köster. Analysis of information dissemination through direct communication in a moving crowd. *Safety Science*, 142:105386, 2021.

[2] Christina Maria Mayr and Gerta Köster. Guiding crowds when facing limited compliance: Simulating strategies. *PLOS ONE*, 17(11):1–24, 11 2022.

[3] Christina Maria Mayr, Anne Templeton, and Gerta Köster. Designing mobile application messages to impact route choice: A survey and simulation study. *PLOS ONE*, 18(4):1–20, 04 2023.

[4] Stefan Schuhbäck, Lars Wischhof, and Jörg Ott. Cellular sidelink enabled decentralized pedestrian sensing. *IEEE Access*, 11:13349–13369, 2023.

[5] H. Ren, Y. Yan, and F. Gao. Variable guiding strategies in multi-exits evacuation: Pursuing balanced pedestrian densities. *Applied Mathematics and Computation*, 397, 2021.

[6] F. Gao, Y. Yan, Z. Chen, L. Zheng, and H. Ren. Effect of density control in partially observable asymmetric-exit evacuation under guidance: Strategic suggestion under time delay. *Applied Mathematics and Computation*, 418, 2022.

[7] Zhe Zhang, Limin Jia, and Yong Qin. Level-of-service based hierarchical feedback control method of network-wide pedestrian flow. *Mathematical Problems in Engineering*, 2016:1–14, 01 2016.

[8] Christina Maria Mayr and Gerta Köster. Estimating pedestrian flows using route distributions and sparse counting data. *Collective Dynamics*, pages 1–8, 2024.

12th International Conference on Pedestrian and Evacuation Dynamics (PED 2025)
Prague, Czech Republic – September 9-12, 2025

Modulation of pedestrian velocity along curves: a comparison between dyads and individuals

Adrien Gregorj[1], Zeynep Yücel*[1,2,3], Francesco Zanlungo[2,4,5], and Takayuki Kanda[2,6]

[1]Okayama University, Okayama, Japan
[2]ATR International, Kyoto, Japan
[3]Ca' Foscari University of Venice, Venice, Italy
[4]Osaka International Professional University, Osaka, Japan
[5]University of Palermo, Palermo, Italy
[6]Kyoto University, Kyoto, Japan

Abstract This study investigates how pedestrians adjust their velocity along curved trajectories, comparing individuals and dyads. By analysing ecological data from the DIAMOR underground pedestrian street network, we aim to determine whether dyads exhibit different velocity patterns compared to individuals along curved paths. Our findings indicate dyads begin to reduce their velocity when encountering higher curvature values as compared to individuals, and at very high curvature values, their velocity profile aligns increasingly closely with that of individuals.

Keywords Pedestrian dynamics, social groups, pedestrian behaviour, curvature

Groups, particularly groups of two (dyads), serve as a fundamental building block of pedestrian crowds and influence both local and large-scale movement patterns [1]. Studying dyads is essential for understanding pedestrian behaviour in various contexts, such as evacuation scenarios, urban planning, and crowd management.

Understanding how pedestrians adjust their velocity when navigating curves is crucial for modeling human movement and designing pedestrian-friendly environments. Unlike walking in straight paths, curved trajectories introduce additional biomechanical and perceptual challenges that influence trajectory planning. While previous research explored how individuals regulate speed based on curvature [2, 3] the effect of social factors such as walking in pairs remains less understood. Social interactions, spatial constraints, and coordination between partners may influence their walking speed, when adapting to curved paths.

This study investigates how pedestrians modulate their velocity along curved trajectories, comparing individuals and dyads. Analysing ecological trajectories, we aim to determine (i) whether dyads exhibit different velocity patterns compared to individuals and (ii) how curvature influences these adjustments.

Trajectories were collected from uninstructed pedestrian movement data recorded in the DIAMOR underground facility, in Japan. *Passage points* (i.e., the locations where pedestrians entered and exited the recording area) were identified in the environment and all dyad and individual trajectories traversing between two passage points were studied.

For each pair of passage points, we computed a *reference trajectory* for both dyads and individuals. The reference trajectory was defined as the average path taken by all individuals (resp. dyads) between the two passage points (see Figure 1).

Curvature and velocity were calculated along these reference trajectories (see Figure 2). Velocity-curvature relationship between dyads and individuals is contrasted to identify differences in speed regulation.

A log-log plot of velocity versus curvature revealed that at low curvature, pedestrians maintain a relatively stable velocity, while at higher curvature, velocity decreases (see Figure 3). This pattern suggests a threshold effect, where only sufficiently sharp turns require notable speed adjustments. Dyads consistently exhibited lower velocities than individuals, which may be attributed to social coordination, such as maintaining mutual awareness and synchronization. We can explain these findings by assuming a delicate balance between the attention that dyad members can allocate to social interaction and the demands of walking. Namely, they must divide their energy between engaging in social interactions and

*Email of the corresponding author: `zeynep@atr.jp`

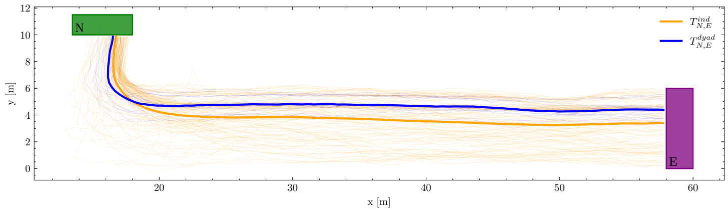

Figure 1: Reference trajectories for dyads and individuals between two passage points. Reference trajectories are showed with the thicker line, and the original trajectories are shown with the thinner lines.

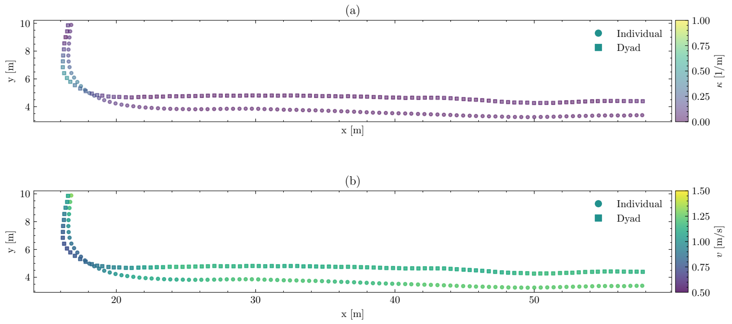

Figure 2: (a) Velocity and (b) curvature values along the reference trajectories of dyads and individuals.

navigating their surroundings, particularly when traversing curved paths. As the curvature of the path increases, walking becomes more challenging. This reflects on individuals as a decrease in velocity as soon as curvature starts increasing. In the case of dyads, they can maintain a steady pace even as the curvature increases by reallocating their energy from social interaction to walking, but only until their velocity matches that of individuals navigating similar curves. Once the dyads' speed aligns with that of the individuals, it indicates that they have reached their limit, necessitating a reduction in their velocity.

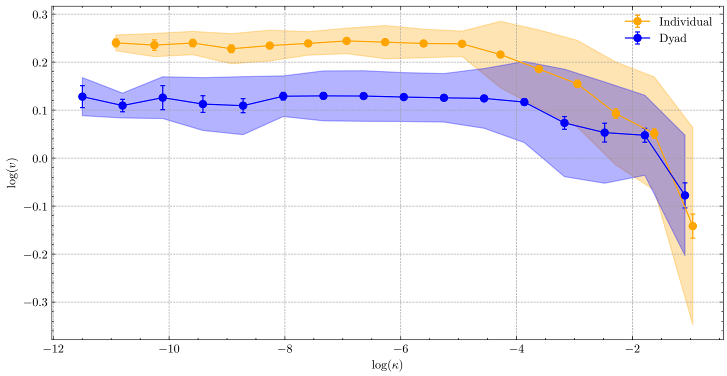

Figure 3: Log-log plot of velocity versus curvature for dyads and individuals.

These findings provide insight into how pedestrians regulate their speed in response to curvature, with implications for pedestrian dynamics modeling and urban planning. A next step is to examine how the inner and outer pedestrians within a dyad adjust their velocities differently, as their relative positions may influence movement coordination and speed regulation.

Bibliography

[1] Moussaïd, M., Perozo, N., Garnier, S., Helbing, D., and Theraulaz, G., *The Walking Behaviour of Pedestrian Social Groups and Its Impact on Crowd Dynamics*, PloS ONE **5**, e10047, 2010.

[2] van der Vleuten, G. G. M., Toschi, F., Schilders, W., and Corbetta, A., *Stochastic Fluctuations of Diluted Pedestrian Dynamics along Curved Paths*, Physical Review E **109**, 014605, 2024.

[3] Hicheur, H., Vieilledent, S., Richardson, M. J. E., Flash, T., and Berthoz, A., *Velocity and Curvature in Human Locomotion along Complex Curved Paths: A Comparison with Hand Movements*, Experimental Brain Research **162**, 145–154, 2005.

High Density Measurements from Ramadan at Makkah, 2025

Anders F. Johansson*[1], Rainald Löhner[2], Jürgen Bradatsch[3], Knut Haase[4], Salim Al Bosta[5], and Muttlaq Elfaleh[6]

[1]School of Engineering Mathematics and Technology, University of Bristol, UK
[2]Center for Computational Fluid Dynamics, George Mason University, Fairfax, VA, USA
[3]SLRasch GmbH, Stuttgart, Germany
[4]Desior GmbH, Hamburg, Germany
[5,6]Royal Commission for Makkah City and Holy Sites, Makkah, KSA

Abstract We provide an extensive set of measurement data from Ramadan 2025 at Makkah, KSA. A great number of cameras has been installed in critical locations in and around the Holy Mosque, so that not only the areas in the immediate vicinity of the Kaaba are evaluated, but also entrances, passages and other walkways. We regard this as a unique opportunity to compile data for crowd movement in the high density, multi-cultural, multi-age, multi-fitness regime, data that is needed to further understand the movement and behaviour of high density crowds in order to guarantee safety and comfort.

Keywords High Density Crowds, Fundamental Diagram, Maximum Capacity, Pedestrian Safety

Fundamental Diagrams

Two of the key criteria when designing places for safe pedestrian motion is the maximum throughput and the density at which this maximum occurs. The reason is obvious: a channel or passage can only handle a certain maximum throughput; if the incoming flux of pedestrians exceeds this capacity, people will accumulate, driving the density to dangerous levels (asphyxia, crowd crushes). As can be seen from the data compiled by Holl[1], Löhner et al.[2], and Helbing et al.[3] shown in Figures 1,2, there is a wide discrepancy of so-called fundamental diagrams.

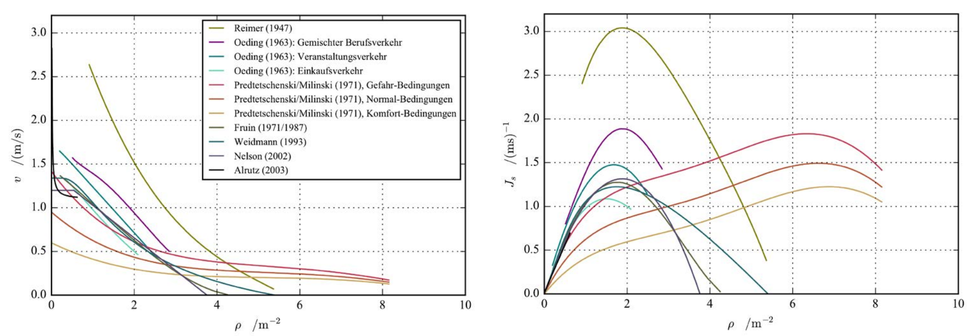

Figure 1: Compilation of Fundamental Diagrams: Velocity (left) and Flux (right) (from [1])

The most immediate differences one can discern are:
a) A series of measurements where the maximum flux peaks at 1.8-2.0 p/sqm, and others where the peak is at 6-7 p/sqm;
b) A series of measurements where the pedestrian motion stops completely at 3.8-5.4 p/sqm, and others where the motion never stops, even for densities greater than 8.0 p/sqm;
c) The large variation in maximum densities measured: which range from 2.0 p/sqm to greater than 8.0 p/sqm.
There are a number of possible reasons for this discrepancy; the two most obvious being:
a) Some of the authors were actually never able to measure situations with such high densities, and simply extrapolated curves;

*Email of the corresponding author: anders@johansson.ltd

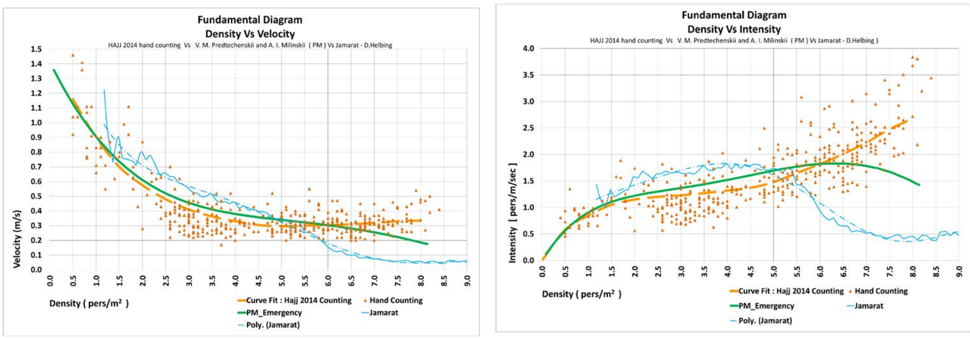

Figure 2: Fundamental Diagrams Sites in Makkah, KSA: Velocity (left) and Flux (right) (from [2])

b) Some of the authors report controlled experiments and not field data; this implies that the individuals being measured had no need to reach a certain place at a certain time and had the option of simply stopping if they so desired.

In order to increase our knowledge and understanding of high density flows, and the possible differences between them, an experimental campaign is being prepared for the upcoming Ramadan season. A great number of cameras has been installed in critical locations in and around the Holy Mosque, so that not only the areas in the immediate vicinity of the Kaaba are evaluated (as in [2]), but also entrances, passages and other walkways. We regard this as a unique opportunity to compile data for crowd movement in the high density, multi-cultural, multi-age, multi-fitness regime, data that is urgently needed not only for static analysis but also for network and micro/agent models.

The final paper will provide an extensive compilation of the measurements, elaborate on the observations, and thus expand on previous empirical studies in Makkah by the authors, such as [2] and [3].

Bibliography

[1] Holl, S., *Methoden für die Bemessung der Leistungsfähigkeit Multidirektional Genutzter Fußverkehrsanlagen*; Schriften des Forschungszentrums Jülich, IAS Series Band/ Volume **32**, ISBN 978-3-95806-191-0 (2016).

[2] Löhner, R., Muhamad, B., Dambalmath, P. and Haug, E., *Fundamental Diagrams for Specific Very High Density Crowds*; Collective Dynamics **2**, 2018. doi: http://dx.doi.org/10.17815/CD.2017.13

[3] Helbing, D., Johansson, A. and Al-Abideen, H.Z., *Dynamics of Crowd Disasters: An Empirical Study*; Physical Review E **75**, 046109 (2007).

Timetable
Talk index

Expected evacuation distance affects the evacuation efficiency of crowds in super high-rise buildings: an empirical analysis

Yayun You[1], Zhiming Fang[1*], Jun Zhang[2], Weiguo Song[2], Wei Lv[3]

[1]Business School, University of Shanghai for Science and Technology, Shanghai 200093

[2]State Key Laboratory of Fire Science, University of Science and Technology of China, Hefei, 230027

[3]School of Safety Science and Emergency Management, Wuhan University of Technology, Wuhan, 430070

Abstract This study focuses on the evacuation characteristics of pedestrians in super high-rise buildings. Three experiments are conducted, including evacuation drills in two iconic super high-rise buildings: Shanghai Tower and Jinmao Tower, as well as evacuation experiments with different expected evacuation distances on an evacuation test platform for simulating super high-rise buildings. The findings indicate that the expected evacuation distance exerts significant influence on the desired speed of pedestrians during long-distance stairwell evacuation. Pedestrians with longer expected evacuation distances who depart from higher floors prefer to evacuate with relatively lower speeds at the early stage of the evacuation to conserve physical strength for the whole procedure. Conversely, as they get closer to the safety area, the expected evacuation distance gradually decreases and speed-up behavior enabling rapid completion of final evacuation stages are observed.

Keywords Super high-rise buildings; Expected evacuation distance; Experiment; Evacuation speed

Experiments

Continuous downward movement through stairwells can easily lead to physical exhaustion or reduced speed among evacuees, while complex group behaviors further affect evacuation efficiency. The complexity of speed variations during ultra-long distance stairs evacuation inadequately explored. The acquisition of empirical data on super high-rise evacuation dynamics remains constrained by architectural complexities and pedestrian safety, making it challenging to conduct analysis of localized evacuation behavior. Hence, three sequential super high-rise building evacuation experiments were systematically conducted, focusing on the speeds variation of pedestrians facing long-distance stairs evacuation.

Experiment A was conducted in the Shanghai Center Tower, which is the tallest building in China with a height of 632m and 126 floors above ground. 69 participants whose ages ranged from 20 to 51 years old were divided into two groups: Group 1 (41 participants) initiated evacuation from the 126th floor, while Group 2 (28 participants) commenced evacuation from the 117th floor when the participants of Group 1 reach. The experiments ended when all the participants reach the ground floor. Localized evacuation characteristics were extracted and analyzed using surveillance video data of each floor from the stairwells of the Shanghai Tower, with the exception of a few floors without surveillance cameras.

Experiment B was conducted on an evacuation test platform for simulating super high-rise buildings based on a 12-story building. Panoramic camera equipment installed on all levels. Participants moved from the 12th floor to the 1st floor and then took the elevator back to the 12th floor, which was defined as one lap. They were asked to repeat multiple laps to simulate the evacuation distance of super high-rise buildings. Different expected evacuation distances were achieved by asking participants to run 9, 10, and 11 laps (11 laps is the 132nd floor, others are similar). A total of 24 participants were recruited for the experiment, with a male to female ratio of 1:1, and were evenly divided into 4 experimental groups. Each participant was tested individually in sequence.

Experiment C was conducted at the Shanghai Jinmao Tower, a 420m tall skyscraper with 88 stories. Surveillance cameras were deployed at 4-floor intervals within stairwells to capture evacuation dynamics. 60 participants were allocated into four groups (14-16-14-16 configuration) and dispatched to initiate evacuation from the 87th, 75th, 63rd, and 51st floors respectively. The evacuation sequence was as follows: Evacuee on the 87th floor first evacuate, then once any evacuee reached the platform on the 75th floor, evacuee on the

Timetable
Talk index

75th floor could commence, and so on.

Conclusions

The results of experiment A showed in Figure 1(a) demonstrated two stages of speed variation. In the first stage, the merge of pedestrians led to a high density within the space, causing a decline in crowd speed; in the second stage, as pedestrians gradually dispersed and spatial density decreased, the speed gradually increased and returned to the free speed. Meanwhile, under the influence of expected evacuation distances, Group 1 exhibited a significantly lower average evacuation speed of 0.730 ± 0.213 m/s compared to Group 2 (0.767 ± 0.217 m/s). The phenomenon revealed that pedestrians, influenced by spatial density and the longer evacuation distances, tend to choose lower evacuation speeds to cope with the increased physical exertion and psychological pressure. Based on experiment A, we argued that, during long-distance stairwell evacuations, the expected evacuation distance significantly affects the desired speed of evacuees due to body energy limitations.

The experiment B was conducted to validate this hypothesis. The experimental results (Figure 1(b)) showed that pedestrian speed exhibit a decreasing trend with increasing evacuation distance. The longer the expected evacuation distance, the smaller the average evacuation speed of pedestrians. Furthermore, a phenomenon on the speed fluctuation was also observed: once or twice speed boosts were prone to occur when the expected evacuation distance decreased, especially when pedestrians were close to the target node. This non-linear pattern of speed variation revealed that evacuees in long-distance stairwell evacuations adopt a speed reduction strategy to save on physical exertion based on the judgement of the expected evacuation distance, and will have a speed-up behavior when approaching the target node (with a shorter expected evacuation distance). The findings validate that evacuees' speed selection is significantly governed by expected evacuation distances during super high-rise building evacuations.

Finally, the experiment C results verified that the average evacuation speed for higher departure floors (those with longer expected evacuation distances) was smaller than those for lower departure floors, as shown in Figure 1 (c). Figure 1(d) gave the expected evacuation distance governs pedestrians speed selection in super high-rise evacuations. A significant convergence in crowd speed distribution was observed as evacuation distance increases. The experiments further confirmed the impact of expected evacuation distance on crowd evacuation speed.

Through a series of experiments, we have drawn the following conclusions: expected evacuation distance affects pedestrian evacuation speed, with longer expected distances prompting individuals to adopt speed reduction strategies to rationally allocate body energy. Simultaneously, pedestrians' speed increases after taking a rest. Additionally, the confluence phenomenon in stairwells significantly reduces overall evacuation efficiency. These findings emphasize the need to integrate distance-dependent speed modulation into evacuation strategies for improved emergency management. It is crucial to optimize existing norms and emergency management strategies based on more detailed crowd-movement data.

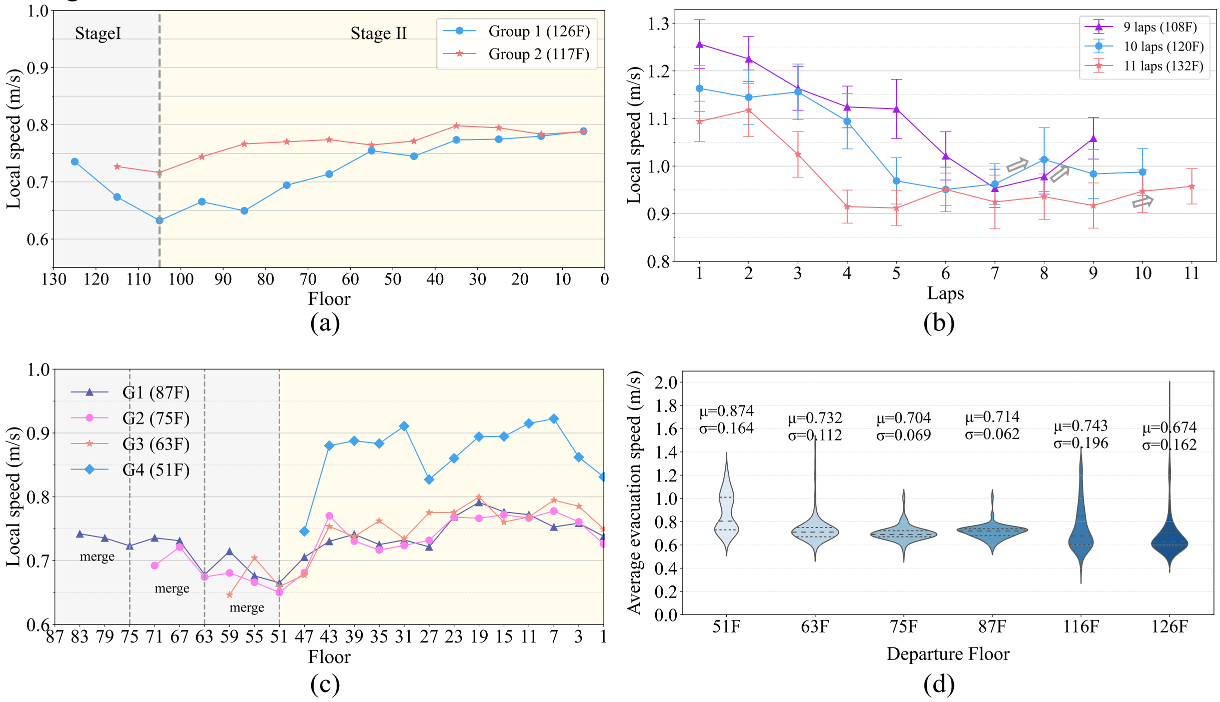

Figure1: Local speed results for different experiments. (a) Variation of local speed with floor for two experimental groups in experiment A. (b) Variation of local speed in different experimental groups in experiment B. (c) Variation of local speed with floor for different experimental groups in experiment C. (d) Evacuation speed data for the first 48 floors of each experimental group in experiments A and C.

*Email of the corresponding author: Zhmfang2015@163.com

Timetable
Talk index

12th International Conference on Pedestrian and Evacuation Dynamics (PED 2025)
Prague, Czech Republic – September 9-12, 2025

Understanding pedestrian-geometry interactions via real-world measurements in variable environments

Chiel van der Laan*[1,2], Fenn Zeelenberg[1], Anjo Korthout[1], and Alessandro Corbetta†[1,2]

[1]Applied Physics and Science Education, TU/Eindhoven, The Netherlands
[2]Eindhoven Artificial Intelligence Systems Institute, TU/Eindhoven, The Netherlands

Abstract We present a real-world experimental campaign to investigate the impact of spatial geometry on real-life pedestrian dynamics. It hinges on weekly changes of the location of obstacles in a trafficked venue. We show that the geometry effects on trajectories can be quantitatively captured by a continuous variational principle. Notably, our setup bridges the gap between controlled laboratory experiments and large-scale real-world data collection, offering both experimental control and high statistical resolution.

Keywords Pedestrian dynamics, geometry dependency, real-life experiment, variational modeling

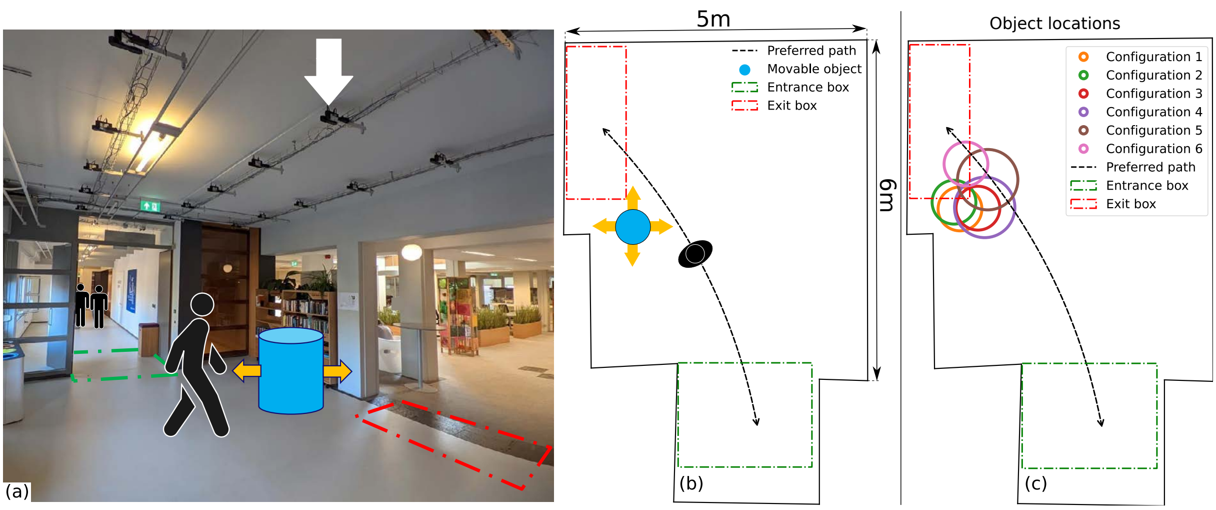

Figure 1: **(a)** Measurement venue at the entrance of the University of Twente library (**(b)**, overhead sketch). On a weekly basis, we perturb the geometry in the proximity of the preferred path (dashed black line) by changing the position of an obstacle (blue cylinder). We anonymously track each pedestrian crossing the area via a grid of overhead sensors (one highlighted by the white arrow), collecting up to 5.000 trajectories per day. **(c)** Obstacle size and position for six configurations between November 2024 and January 2025 (cf. Fig. 2a).

Navigating built environments is key to pedestrian dynamics. Understanding the impact of geometric changes on pedestrian behavior is an outstanding challenge. In fact, the effect of environmental geometry unavoidably couples with individual stochasticity and mutual interactions. Ideally, one could disentangle such an effect through systematic measurements of pedestrian trajectories across numerous geometrical variations. Laboratory measurements offer fine control over the geometry and thus have been used to investigate prototypical scenarios (e.g. bottlenecks [3, 5] and obstacle navigation at crossings [6]). However, the number of trajectories is constrained by participant availability, hindering the capability of quantifying stochastic effects beyond averages. In contrast recent advancements in automated vision have enabled accurate large-scale collection of pedestrian trajectories in real life [2]. While allowing highly-resolved statistics, these campaigns are limited by static or uncontrollable environments.

In this study we combine the strengths of laboratory-based and real-life measurements to understand how generic geometric configurations influence pedestrian movement We achieve this by introducing weekly geometric perturbations in a trafficked real-world environment while anonymously tracking the

*c.v.d.laan@tue.nl
†a.corbetta@tue.nl

crossing pedestrians (setup in Fig. 1); thousands of users per day, cf. Fig. 2(a)). We observe that each obstacle configuration produces a different position probability and velocity field, one of which is depicted in Fig 2(b).

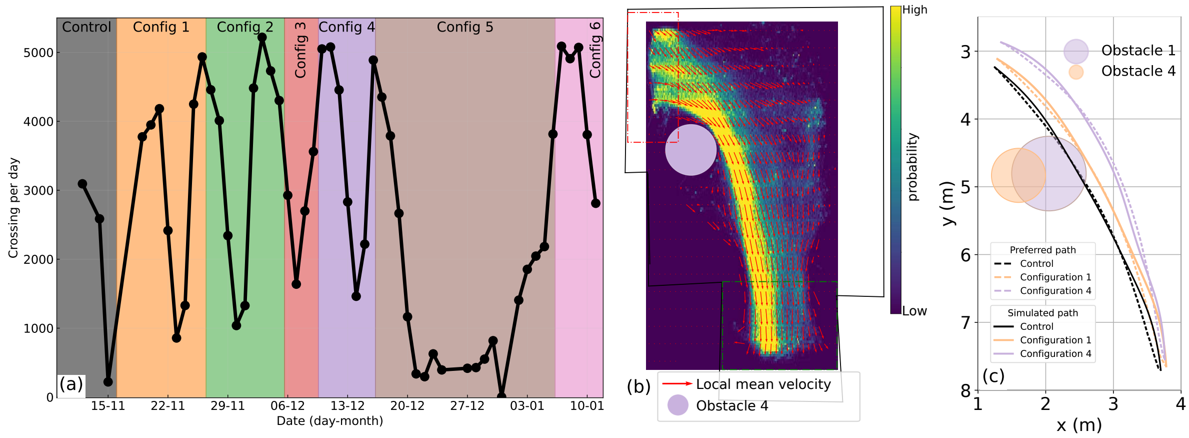

Figure 2: **(a)** Number of trajectories per day, background shades distinguish the configurations (same color coding of Fig. 1(c)). **(b)** Obstacles in different locations reflect in different position probability and velocity fields: case of configuration 4, restricted to trajectories moving from the red to the green area. **(c)** Average pedestrian trajectory in three configurations including control (i.e. no obstacle), comparison between empirical data and prediction by the variational model in Eq. 1.

To understand the mechanisms that regulate the pedestrian-geometry interaction, we assume a rational pedestrian model [4], according to which individual decision-making is driven by the minimization of a hidden cost function (e.g. an interplay between comfort and efficiency). To this end, we explore various continuous variational principles that generalize the proposal by Arechavaleta et al. [1] by including an obstacle penalty term. In Fig. 2c, we report predictions of the average trajectories according to the cost

$$C = \int_0^T \left(\lambda_1 ||\mathbf{v}(t)||^2 + \lambda_2 \kappa(t)^2 + \frac{\lambda_3}{d(t)^2} \right) dt, \qquad (1)$$

which models an interplay of three key terms: a velocity term ($||\mathbf{v}||^2$) that penalizes high unrealistic speeds; secondly, a curvature term (κ^2) that penalizes sharp uncomfortable turns; and lastly a distance-based term (d^{-2}) that penalizes close proximity to obstacles. We estimate the weights $\{\lambda_i\}$ and systematically validate our models by comparing temporal and spatial characteristics of the predicted trajectories with the empirical data.

Bibliography

[1] Gustavo Arechavaleta, Jean-Paul Laumond, Halim Hicheur, and Alain Berthoz. An optimality principle governing human walking. *IEEE Transactions on Robotics*, 24(1):5–14, 2008.

[2] Alessandro Corbetta, Jasper A. Meeusen, Chung-min Lee, Roberto Benzi, and Federico Toschi. Physics-based modeling and data representation of pairwise interactions among pedestrians. *Phys. Rev. E*, 98:062310, Dec 2018.

[3] A Garcimartín, D Maza, J M Pastor, D R Parisi, C Martín-Gómez, and I Zuriguel. Redefining the role of obstacles in pedestrian evacuation. *New Journal of Physics*, 20(12):123025, dec 2018.

[4] Serge Hoogendoorn and Piet H.L. Bovy. Simulation of pedestrian flows by optimal control and differential games. *Optimal Control Applications and Methods*, 24(3):153–172, 2003.

[5] Weichen Liao, Armin Seyfried, Jun Zhang, Maik Boltes, Xiaoping Zheng, and Ying Zhao. Experimental study on pedestrian flow through wide bottleneck. *Transportation Research Procedia*, 2:26–33, 2014. The Conference on Pedestrian and Evacuation Dynamics 2014 (PED 2014), 22-24 October 2014, Delft, The Netherlands.

[6] Oksana Severiukhina, Daniil Voloshin, M.H. Lees, and Vladislav Karbovskii. The study of the influence of obstacles on crowd dynamics. *Procedia Computer Science*, 108:215–224, 2017. International Conference on Computational Science, ICCS 2017, 12-14 June 2017, Zurich, Switzerland.

Timetable
Talk index

12th International Conference on Pedestrian and Evacuation Dynamics (PED 2025)
Prague, Czech Republic – September 9-12, 2025

Pedestrian behavior model considering gaze and head direction

Ryo Sasaki[1], Shohei Yasuda*[1], and Takashi Fuse[1]

[1]Department of Civil Engineering, Faculty of Engineering, The University of Tokyo

Abstract Evidence suggests that pedestrians' gaze direction influences their movement as they look at advertisements, shop windows, and other pedestrians in facilities. However, the existing Social Force Model, which is widely used for facility design, has not quantitatively addressed this relationship. This study introduces a simulation framework that integrates pedestrians' gaze fluctuations and the resulting movement changes. The model's performance is validated against real-world data, demonstrating that incorporating gaze and head direction into the Social Force Model has a measurable impact on pedestrian flow simulation.

Keywords Pedestrian dynamics, Head direction, Gaze direction, Social Force Model

Introduction

As the urban population continues to grow globally, ensuring that various facilities are safe and comfortable for pedestrians has become increasingly important. Microscopic pedestrian behavior models enable the distinction of individual pedestrians and the simulation of their movement, thereby facilitating the evaluation of multiple design proposals. Among microscopic pedestrian behavior models, the Social Force Model (SFM) [1] is particularly notable for its lack of spatial resolution constraints, ease of implementation, and high interpretability, making it widely used for facility design. The SFM conceptualizes pedestrian movement through the application of virtual forces and determines acceleration using equations of motion.

Despite suggestions that pedestrians' gaze direction influences their movement [2], existing SFM has not quantitatively addressed the relationship between gaze and locomotion, or only discrete visual attentional state (looking at a store or not) has been addressed [3]. Since pedestrians in facilities direct their gaze toward various objects, such as advertisements, shop windows, and other pedestrians, incorporating gaze into the SFM used for facility design holds significant potential.

Methodology

This study examines the relationship between pedestrian movement, head orientation, and gaze direction using data from a laboratory experiment [4]. Specifically, it analyzes angles between the head and gaze direction vectors, originating from the pedestrian's position, and the movement direction vector on a top-down 2D plane (θ for head and φ for gaze), speed over one second divided by 90 percentile (V), and directional change over the same period (ψ).

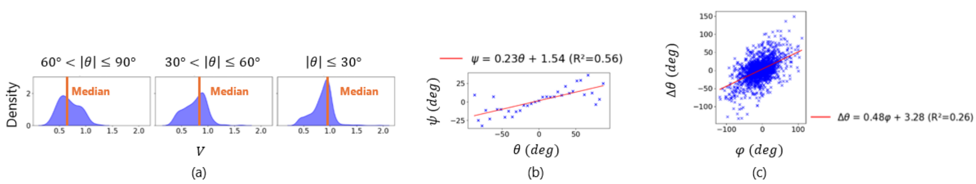

Figure 1: (a) Kernel density distribution of V across different θ, with orange lines indicating medians. The median values follow a ratio of 0.75:0.9:1.0. (b) Relationship between θ and ψ, where θ is binned in 5° intervals, and ψ represents the bin-wise average. (c) Relationship between φ and $\Delta\theta$ (change in θ).

The analysis in Figure 1 indicates that pedestrian speed and movement direction changes are influenced by θ, which in turn is affected by φ. Based on this, the simulation framework was designed to predict movement using a modified SFM, where φ is impacted by visual attractors in the environment (Figure 2).

*Email of the corresponding author: `s.yasuda@civil.t.u-tokyo.ac.jp`

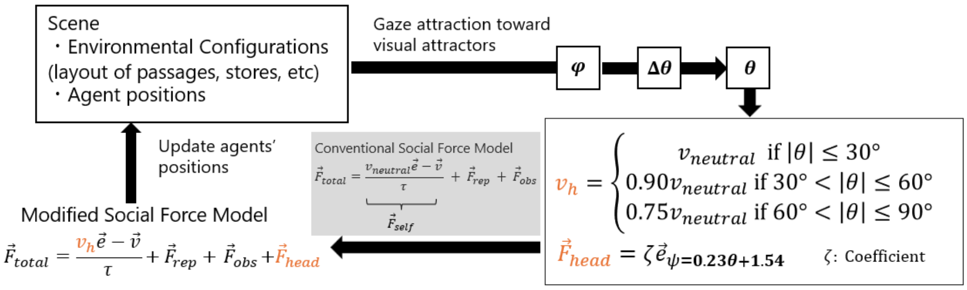

Figure 2: The simulation framework. The conventional SFM is from equations(7)-(10) in [5]. $\vec{F}_{total}$: The total force. $\vec{F}_{self}$: The driving force. $\vec{F}_{rep}$: The repulsive force of other pedestrians. $\vec{F}_{obs}$: The repulsive force of obstacles. τ : The relaxation time. $\vec{v}$: The current speed vector. $\vec{e}$: The unit vector toward a destination. $\vec{e}_{\psi=0.23\theta+1.54}$: The unit vector in the direction of $\psi = 0.23\theta + 1.54$.

At each time step, given agent positions and environmental configurations, φ is sampled based on gaze attraction toward visual attractors, while θ is updated via $\Delta\theta$ sampled from the normal distributions centered at the regression line in Figure 1(c). This θ induces a reduction in the desired speed $v_{neutral}$ following Figure 1(a) and a virtual force $\vec{F}_{head}$ in the direction of $\psi = 0.23\theta + 1.54$. These effects are incorporated into the conventional SFM to formulate the modified model, which then updates agent positions.

Result and Conclusion

A 45-minute bidirectional pedestrian flow dataset in an underground metro station corridor [3] was used for the model evaluation. A convenience store on one side of the corridor serves as a visual attractor, with the dataset providing binary labels indicating whether pedestrians look at the store at each time step. The corridor is divided into 12 parallel lanes, each approximately 45 cm wide. For each lane, the proportion of pedestrians looking at the store is calculated, and when simulating, φ is sampled accordingly from a distribution oriented either toward the store or along the current speed vector.

In the dataset, lane-wise average speed decreases as the lane gets closer to the store. To evaluate the model's ability to reproduce this spatial distribution, lane-wise Mean Absolute Errors (MAE) between the dataset's average speed and the simulated average speed over a 45-minute simulation were computed using both the modified and conventional SFM.

As shown in Table 1, the modified SFM achieves lower MAE in the majority of lanes, suggesting that quantitatively incorporating head and gaze direction enhances the model's ability to simulate pedestrian flows.

Table 1: MAE (cm/s) for each lane, averaged over 100 simulation runs with different random seeds for agent initial positions, φ, and $\Delta\theta$ samplings. Lane 1 is closest to the convenience store, with distance increasing as the lane number grows. The smallest MAE values for each lane are highlighted.

Lane	1	2	3	4	5	6	7	8	9	10	11	12
Modified	13	**4.6**	1.3	**1.3**	**1.6**	**2.8**	**3.8**	**4.4**	**1.5**	**1.5**	**2.0**	16
Conventional	13	6.3	**1.2**	8.9	13	17	14	9.3	12	2.2	3.0	**4.5**

Bibliography

[1] Helbing Dirk and Molnar Peter, *Social force model for pedestrian dynamics*, Physical review E **51**, 4282, 1995.

[2] Mark A Hollands and Aftab E Patla and Joan N Vickers, *"look where you're going!": gaze behaviour associated with maintaining and changing the direction of locomotion*, Experimental brain research **143**, 221-230, 2002.

[3] Li Danrui and Schwartz Mathew and Sohn Samuel S and Yoon Sejong and Pavlovic Vladimir and Kapadia Mubbasir, *Microscopic modeling of attention-based movement behaviors*, Transportation Research Part C: Emerging Technologies **162**, 104583, 2024.

[4] Schreiter T and Rodrigues de Almeida T and Zhu Y, *THÖR-MAGNI: A large-scale indoor motion capture recording of human movement and robot interaction*, The International Journal of Robotics Research **0**, 0, 2024.

[5] Xu Chen, Martin Treiber, Venkatesan Kanagaraj and Haiying Li, *Social force models for pedestrian traffic – state of the art*, Transport Reviews **38**, 625-653, 2018.

12th International Conference on Pedestrian and Evacuation Dynamics (PED 2025)
Prague, Czech Republic – September 9-12, 2025

Open Access Crowd Simulations Using a Humanoid Paradigm.

Thomas Chatagnon *[1] and Xiaoyun Shang[2]

[1]Institute for Advanced Simulation, Forschungszentrum Jülich, Germany
[2]School of Systems Science, Beijing Jiaotong University, Beijing 100044, PR China

Abstract Dense crowds can pose real safety risks, yet existing crowd simulation paradigms struggle to capture the complex physical interactions at stake. Recent studies have highlighted the role of whole-body motion in high-density conditions. To integrate these findings into simulation, we propose to implement a new simulation paradigm involving humanoid-shaped agents in the open-source crowd simulation software JuPedSim [3], enabling more realistic crowd simulations.

Keywords Crowd Simulation, Humanoid shape, Whole body motion, Representation Paradigm.

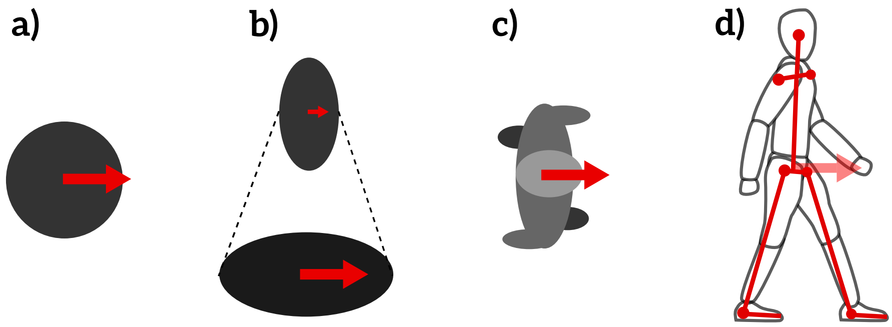

Figure 1: Overview of classical spacial representations of pedestrians for microscopic crowd simulations. a) Circular shape, used in first modelling approaches, up to modern simulations [11, 4]. b) Representation using shape-changing ellipsoids with variations as a function of pedestrian velocity [2]. c) Two-dimensional humanoid shape proposed in [10]. d) Simplified three-dimensional humanoid representation proposed in [8].

Introduction

Major events around the world have been shown to be prone to uncontrolled incidents, leading to discomfort, injury or even death [6]. One of the responses to such problems from the research community have been to create models and simulations in order to prevent such fate. So far, one of the most advocated purpose of crowd simulation is to be able to predict and prevent incidents in dense crowds [11]. However, crowd simulation seems to be mostly limited to the use of two main types of simulation paradigms.

The first type is a macroscopic simulation. In such simulations, the crowd is considered as a continuum medium, and only high-level quantities such as crowd density and flow volume are considered. These models are usually computationally efficient, but are based on continuum theory and struggle to capture complex mechanisms associated with physical interactions. Another classic paradigm for crowd simulation is microscopic simulation. In these, the simulated agents are independent entities driven by a set of rules. The overall crowd dynamics result from the interaction of the agents following the guidance of the rules to which they are bound. However, these models have been designed to handle light to medium densities where physical interactions do not occur. For dense crowds, this simulation paradigm is usually used with oversimplified, reciprocal and isotropic repulsion forces [4] or very limited balance recovery models [7].

In the meantime, recent experimental studies have attempted to provide a better picture of the mechanisms involved due to physical interaction in dense crowds [1, 9]. In particular, these mechanisms

*Email of the corresponding author: t.chatagnon@fz-juelich.de involve whole-body movement of pedestrians [5]. Even without physical interaction, high levels of density modify the gait cycle and involve advanced shoulder rotation [12].

In order to implement this new experimental knowledge, crowd simulations have to adapt to sub-microscopic representations of the human body that include different body parts. To this end, we decided to implement a novel representation paradigm for simulated agents in the open source software JuPedSim [3]. This new type of simulation is directly derived from the work of Shang et al. (2024) [8] who proposed a *Humanoid Model* for crowd simulation. The aim of this work is to provide the community with an accessible simulation framework that allows direct use of this new simulation paradigm through notebooks and direct comparison with experimental results.

References

[1] Thomas Chatagnon et al. "Standing balance recovery strategies of young adults in a densely populated environment following external perturbations". In: *Safety Science* 177 (2024), p. 106601. ISSN: 0925-7535. DOI: doi.org/10.1016/j.ssci.2024.106601.

[2] Mohcine Chraibi, Armin Seyfried, and Andreas Schadschneider. "Generalized centrifugal-force model for pedestrian dynamics". In: *Phys. Rev. E* 82 (4 Oct. 2010), p. 046111. DOI: 10.1103/PhysRevE.82.046111. URL: https://link.aps.org/doi/10.1103/PhysRevE.82.046111.

[3] Mohcine Chraibi et al. *JuPedSim*. Version v1.1.0. URL: https://github.com/PedestrianDynamics/jupedsim.

[4] E. Cristiani et al. "An all-densities pedestrian simulator based on a dynamic evaluation of the interpersonal distances". In: *Physica A: Statistical Mechanics and its Applications* 616 (2023), p. 128625. ISSN: 0378-4371. DOI: doi.org/10.1016/j.physa.2023.128625.

[5] Sina Feldmann et al. "Temporal segmentation of motion propagation in response to an external impulse". In: *Safety Science* 175 (2024), p. 106512. ISSN: 0925-7535. DOI: doi.org/10.1016/j.ssci.2024.106512.

[6] Claudio Feliciani et al. "Trends in crowd accidents based on an analysis of press reports". In: *Safety science* 164 (2023), p. 106174. DOI: 10.1016/j.ssci.2023.106174.

[7] Sujeong Kim et al. "Velocity-Based Modeling of Physical Interactions in Dense Crowds". In: *The Visual Computer* 31.5 (May 2015), pp. 541–555. ISSN: 1432-2315. DOI: 10/f696cv.

[8] Xiaoyun Shang et al. "Development and experimental validation of a humanoid pedestrian model that captures stepping behavior and body rotation". In: *Transportation Research Part C: Emerging Technologies* 158 (2024), p. 104446. ISSN: 0968-090X. DOI: doi.org/10.1016/j.trc.2023.104446.

[9] Liangchang Shen et al. "Experimental study on mechanical transfer regularity and step distance of individuals under different collision impulse". In: *Journal of Statistical Mechanics: Theory and Experiment* 2024.7 (July 2024), p. 073404. DOI: 10.1088/1742-5468/ad613c.

[10] Peter A. Thompson and Eric W. Marchant. "A computer model for the evacuation of large building populations". In: *Fire Safety Journal* 24.2 (1995), pp. 131–148. ISSN: 0379-7112. DOI: https://doi.org/10.1016/0379-7112(95)00019-P. URL: https://www.sciencedirect.com/science/article/pii/037971129500019P.

[11] Wouter van Toll et al. "SPH crowds: Agent-based crowd simulation up to extreme densities using fluid dynamics". In: *Computers & Graphics* 98 (2021), pp. 306–321. ISSN: 0097-8493. DOI: doi.org/10.1016/j.cag.2021.06.005.

[12] Jiayue Wang et al. "Step styles of pedestrians at different densities". In: *Journal of Statistical Mechanics: Theory and Experiment* 2018.2 (Feb. 2018), p. 023406. DOI: 10.1088/1742-5468/aaac57.

12th International Conference on Pedestrian and Evacuation Dynamics (PED 2025)
Prague, Czech Republic – September 9-12, 2025

A game-theoretic perspective on how pedestrian behaviour changes with crowd density

Tao Jin* [1], Ryan Palmer[1], and Nikolai W.F. Bode[1]

[1]School of Engineering Mathematics and Technology, University of Bristol, Bristol, UK

Abstract Social and physical interactions between pedestrians significantly influence their behaviour and in scenarios such as evacuation can affect the overall departure efficiency. This study aims to explore such interactions in bottlenecks from a game-theoretic perspective, using a public goods game framework. Simulation and experiments can be developed to validate our model, and the results will reveal different macroscopic patterns of pedestrian movement.

Keywords Bottleneck, Game theory, Public goods game, Nash equilibrium, Movement patterns

Introduction

Game theory is a useful tool to explore behavioural interactions among dynamic and finitely rational agents because this theory can produce self organising behaviours by defining a utility function that can easily be adapted. Some examples include the use of mean field [1, 2] and evolutionary games [3].

We consider the bottleneck evacuation a scenario in which crowds share limited public resources, including exit and available space. Each pedestrian can benefit from these resources that affect the efficiency of evacuation, which we refer to as public goods benefit. At the same time, they can also contribute to these resources because of an aggressive movement strategy (e.g., every move is giving up a certain amount of space for others to occupy). The limited nature of the resources could lead to selfish behaviour and competition, or such constraints could be resolved through cooperation. Here, we thus develop a multi-stage public goods game for pedestrians to explore this tension between individuals maximising their own benefits and regarding others' needs. We can adjust a pedestrian's consideration of their own interests and the overall evacuation efficiency through changing the model parameters and make suggestions based on the corresponding Nash equilibrium results. As the strategies pedestrians choose in our game model relate to movement directions and speeds, we can explore the change of congestion and other crowd behaviours.

Methods

The public goods game model for pedestrians supposes that pedestrian behaviours are multi-stage games consisting of a series of games, denoted by t interactions. Pedestrians are all successfully evacuated through T stages. Importantly, our model should not be interpreted as a physical model, as pedestrians can overlap. Rather, the model should be viewed as describing movement intentions of individuals depending on their surroundings. Our model is outlined in the following.

Agents: the agents of the game are each pedestrian denoted in a set $N = \{1,\ 2,\ 3,\ \cdots,\ n\}$.

Strategies: in interaction t, each pedestrian $i \in N$ decides a movement strategy $\boldsymbol{p}_{i,t}$ (i.e., the target position), which involves a footstep $v_{i,t}^{max}$ (step length) and a movement direction related to θ:

$$v_{i,t}^{max} = v_{max} \cdot \left(1 - \frac{\rho_{i,t}}{\rho_{max}}\right), \tag{1}$$

$$\boldsymbol{p}_{i,t} = (x_{i,t}, y_{i,t}),\ \forall\ i \in N,\ \ t \in T,\ \ \text{and} \parallel \boldsymbol{p}_{i,t} - \boldsymbol{p}_{i,t-1} \parallel \leq v_{i,t}^{max}, \tag{2}$$

where $x_{i,t}, y_{i,t}$ are the spatial position of pedestrians, $v_{i,t}^{max}$ is the maximum footstep of the pedestrian i in t according to the density, v_{max} is the maximum footstep for pedestrians, $\rho_{i,t}$ is the true number of people around the pedestrian i and ρ_{max} is the maximum number of people that can be around pedestrians (the value of this can be set based on physical or psychological considerations). The angle θ is defined as the angle between the direction of pedestrian movement and the direction facing the exit.

*Email of the corresponding author: taotao0612.jin@bristol.ac.uk

Utility: the possible strategies of pedestrians are associated with a public goods benefit $f(G_t)$, expressed by the following equations:

$$f(G_t) = r \cdot \frac{G_t}{n_t}, \quad G_t = \sum_{i=1}^{n_{t-1}} d^e_{i,t-1} = \sum_{i=1}^{n_{t-1}} \frac{\| \boldsymbol{p}_{i,t-1} - \boldsymbol{p}_{i,t-2} \| \cdot |\cos\theta|}{v_{max}}, \tag{3}$$

where r is a magnification factor (a free parameter), and G_t is the contribution obtained at t from the pedestrian strategy made at $t-1$, and it is related to the effective distance pedestrians have travelled on the shortest path to the exit $d^e_{i,t-1}$.

The utility of pedestrian i in stage t is:

$$u_{i,t}(\boldsymbol{p}_{i,t}, \boldsymbol{P}_{-i,t}) = W_{i,0} + f(G_t) - C_{i,t}(\boldsymbol{p}_{i,t}), \tag{4}$$

where $\boldsymbol{P}_{-i,t} = \{\boldsymbol{p}_{j,t} : \forall j \in N, \text{ and} j \neq i\}$, and $\boldsymbol{P}_{-i,t}$ refers to the strategy for all pedestrians except i. $W_{i,0}$ is the initial benefit value of pedestrians obtained from their initial position (pedestrians closer to the exit will have higher initial benefits). A cost function $C_{i,t}(\boldsymbol{p}_{i,t})$ for pedestrian movement is defined based on the position of pedestrians in space and the density of their surroundings. In general, it contains the cost associated with deviating from the shortest path to the exit and the cost of fatigue of moving to areas of high pedestrian density.

Objectives: each pedestrian i will adopt a Nash equilibrium strategy $\boldsymbol{p}^*_{i,t}$ which is obtained by maximising $u_{i,t}(\boldsymbol{p}^*_{i,t}, \boldsymbol{P}^*_{-i,t})$. At this point, the strategies of the rest pedestrians $\boldsymbol{P}^*_{-i,t}$ are all Nash equilibrium strategies as well.

Results

We now present some initial results. In general, as the acceptable crowd density increases one would expect that the evacuation may also become more efficient in terms of time step for all pedestrians to exit. However, in our model, the effect of the pedestrian willingness to accept the maximum number of people around them (ρ_{max}) is not always linear, as shown in Figure 1. A larger ρ_{max} leads to a higher slope evacuation efficiency, but can also result in a longer congested movement pattern, making evacuation times longer. This may be attributed to the expected increased acceptance of high density crowds by pedestrians, and the increased behaviour of following the flow of the crowd resulting in pedestrians not avoiding the congestion. It reveals the possibility that the evacuation efficiency of a high-density crowd is better than that of a low-density crowd, and it is necessary to explore the mechanisms involved further to understand why this may happen.

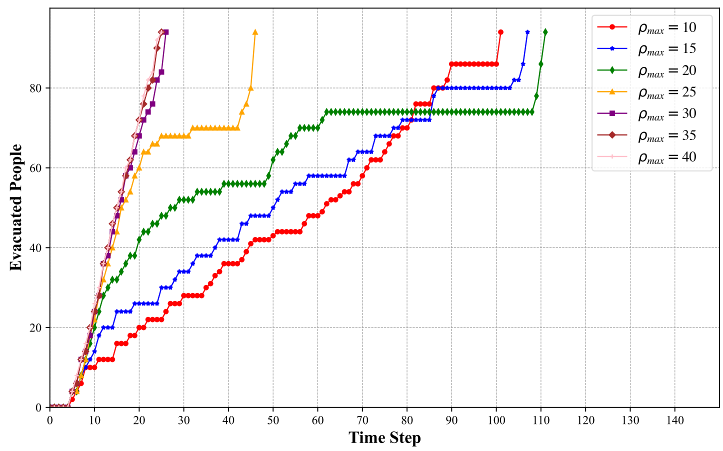

Figure 1: The impact of ρ_{max} on on the number of individuals evacuated in Nash equilibrium. The value of the maximum footstep for pedestrians v_{max}, magnification factor r, the weight κ, the weight α are 0.2, 2, 10, 1, respectively.

Bibliography

[1] Thibault B, Matteo B, Théophile B, Iñaki E.H, Antoine S, Alexandre N, Cécile A.A, Denis U, *Pedestrians in static crowds are not grains, but game players*, Physical Review E **107**, 024612, 2023.

[2] Lachapelle A, Wolfram M.T, *On a mean field game approach modelling congestion and aversion in pedestrian crowds*, Transportation Research Part B: Methodological **45**, 1572-1589, 2011.

[3] Hao Q.Y, Jiang R, Hu M.B, Jia B, Wu Q.S, *Pedestrian flow dynamics in a lattice gas model coupled with an evolutionary game*, Physical Review E **84**, 036107, 2011.

12th International Conference on Pedestrian and Evacuation Dynamics (PED 2025)
Prague, Czech Republic – September 9-12, 2025

Bridging Empirical Research and Standards in Pedestrian Dynamics: Towards Enhanced Verification and Validation

Mohcine Chraibi*[1], Alessandro Corbetta†[2], Claudio Feliciani[3], and Bryan Klein[4]

[1]Forschungszentrum Jülich, Germany
[2]Eindhoven University of Technology, Netherlands
[3]The University of Tokyo, Japan
[4]Thunderhead Engineering, USA

Abstract As our quantitative knowledge of pedestrian dynamics keeps growing thanks to more and more accurate measurements, so increase our capability of validating models. We introduce here a benchmarking framework. It hinges on one side on the latest experimental evidence, and on the other on a Continuous Integration (CI) pattern for automatic and independent simulation software testing during development and maintenance phases. Ultimately, the framework allows researchers, practitioners, and standardization organizations to work together to improve the reliability and applicability of pedestrian simulations in real-life scenarios.

Keywords Verification, Validation, Pedestrian dynamics, Evacuation Software, Standards

Introduction

Mathematical models, a cornerstone of the scientific method, are developed to investigate, explain, and possibly predict the properties of real-world systems. Pedestrian dynamics is no exception: models are developed to analyze crowd behavior at all scales. This ranges from microscopic-level individual locomotion and interactions to coarse-grained properties, e.g. the capacity of a train station to operate within safety limits. Reproducing with models emergent features measured in real world systems that have not been themselves explicitly included in the model underlies validation, and to probe for limitations. Ultimately, models are translated into software to provide crowd management managers with convenient tools to assess design scenarios and evaluate potential interventions.

Recent advances in empirical research on pedestrian and crowd dynamics unlock a wealth of new data that are describing the behavior of crowds with higher and higher levels of detail. These include characterization of stochastic behavior, universal features, dependency on type of crowd, surrounding geometry, and more [2, 5]. Naturally, these provide invaluable sources for significantly improving the way current models are designed and, more importantly, validated and verified. Existing standards, such as those described in [3, 1], continue to play an important role in providing foundational benchmarks (for example, ensuring that agents walking 10 meters at 1 m/s cover that distance in 10 seconds). However, they often predate recent experimental findings and may miss critical nuances of pedestrian flow. To address this gap, new test frameworks, supported by up-to-date empirical studies, are necessary to capture complex behaviors more faithfully.

This contribution critically discusses recent pedestrian dynamics experimental data and how these can be tailored into the next generation of references and benchmarks to validate the effectiveness of current and forthcoming crowd models. In particular, we will address the following:

- Model validation benchmarks; i.e. how well the model—and its software implementation—reflect (statistic-level) empirical observations of actual systems (cf. e.g., Fig. 1 (bcd)).
- Model verification tests; i.e., to what extent the implemented software correctly simulates the behaviors prescribed by the underlying mathematical model and whether those simulation outcomes reliably mirror the real-world system.

Although validation and verification are closely related, they have distinct goals. The former is about capturing physical behavior whereas the latter is about building trust around the consistency of the model

*Email of the corresponding author: m.chraibi@fz-juelich.de
†Email of the corresponding author: a.corbetta@tue.nl

implementation. In practical terms, this contribution will introduce an automated online testing suite, using the well-established Continuous Integration development paradigm to enable automated, online, and unbiased testing, standard for all.

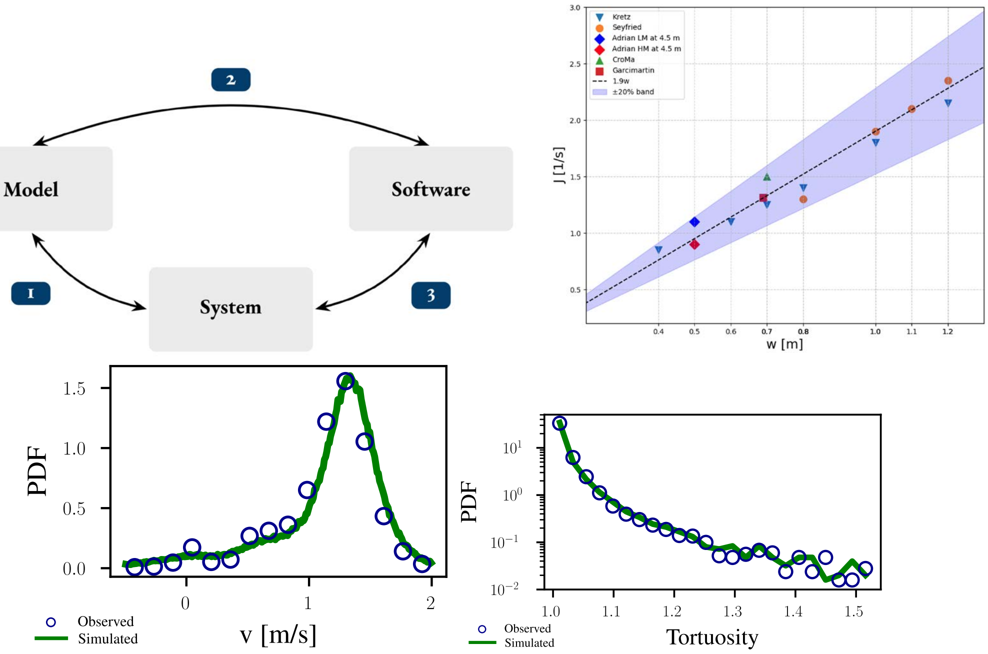

Figure 1: (a) Validation process involving a model, software, and real system. [1] and [3] validate the results of the model and its implementation against real-world observations, while [2] verifies that the model is implemented faithfully in the software. (b) Flow versus width of bottleneck for different experiments from the literature. (c,d) Examples of complex statistical features of pedestrian dynamics, here velocity and trajectory tortuosity. Figures reproduced from [4].

Figure 1(a) illustrates how verification and validation interact among the three main elements: the real-world system, the model, and the software. Steps [1] and [3] deal with validating outcomes against real-world data, whereas step [2] ensures that the software correctly implements the model's logic. Figure 1(b) illustrates an experiment that highlights the linear relationship between flow and the width of the bottleneck. Simulation results falling within the blue band are considered realistic. Figure 1(c,d) show complex statistics of pedestrians trajectories, such as velocity or tortuosity, that realistic simulations should be able to capture.

By backing each of these steps with state-of-the-art empirical insights and by carefully choosing which data to include, researchers, software developers, and standards bodies can collaboratively strengthen the reliability and realism of pedestrian models. Ultimately, this improves confidence in simulated outcomes, enabling better-informed decisions for crowd management and urban planning.

References

[1] ISO/TC 92/SC 4 20414:2020. *Fire Safety Engineering — Verification and Validation Protocol for Building Fire Evacuation Models*. Standard 20414. ISO, Nov. 2020, p. 69.

[2] A. Corbetta and F. Toschi. "Physics of human crowds". In: *Ann. Rev. Conden. Matter Phys.* 14.1 (2023), pp. 311–333.

[3] IMO. *Revised guidelines on evacuation analysis for new and existing passenger ships*. Tech. rep. 2016.

[4] Koen Minartz et al. "Discovering interaction mechanisms in crowds via deep generative surrogate experiments". In: *Scientific Reports, to appear. arXiv:2412.01491* (2025).

[5] A. Schadschneider et al. "Pedestrian Dynamics: From Empirical Results to Modeling". In: *Crowd Dynamics, Vol. 1*. Ed. by L. Gibelli. Modeling and Simulation in Science, Engineering and Technology. Springer, 2018, pp. 63–102.

Inhomogeneities in dense crowds: a case study on active and passive pedestrians

Mira Küpper*[1,2] and Juliane Adrian[1]

[1]Forschungszentrum Jülich, Germany
[2]University of Wuppertal, Germany

Abstract Until now in bottleneck experiments crowds with homogeneous instructions and therewith equal motivation levels were studied. In this study, we investigate how the presence of both active and passive participants influences the dynamics within the crowd and compare the results to those of a homogeneous crowd. We are interested in density profiles, changes in neighborhood, waiting time and fairness.

Keywords experiments, bottleneck, high density

Instruction

Generally, high density is one of the main causes for dangerous situations within pedestrian crowds. Therefore, it is important to understand potentially dangerous dynamics and investigate their origin to prevent accidents. However, currently the knowledge about how dangerous dynamics are triggered is limited as the factors which cause these dynamics are not yet fully understood.

Until now in bottleneck experiments crowds with homogeneous instructions and therewith equal motivation levels were studied. However, real crowds are heterogeneous, meaning that individuals have e.g. different levels of motivation. While some people actively move forward and are willing to get in contact with others, e.g. by pushing to reach their goal faster, others adopt a more passive waiting posture and like to avoid contacts.

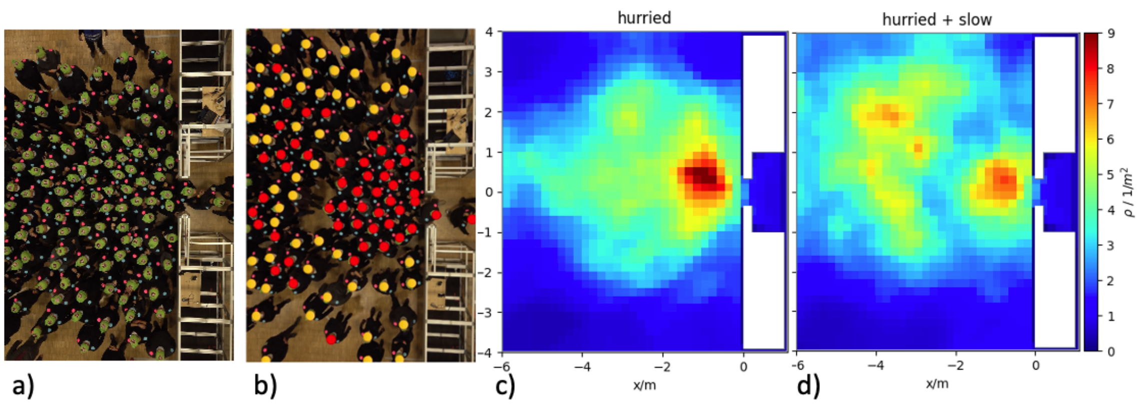

Figure 1: High motivation in bottleneck: a) homogeneous crowd b) inhomogeneous crowd: active participants (red) try to get closer to their goal, while passive participants (yellow) wait and create gaps. c) density profiles for homogeneous crowd (all hurried), d) density profiles for inhomogeneous crowd (20% (secretly) instructed to move slowly).

In this study, we investigate how the presence of both active and passive participants influences the dynamics within the crowd and compare the results to those of a homogeneous crowd. As case study we use laboratory bottleneck experiments [1] performed during the projects CrowdDNA (EU) and CroMa (BMBF). One of the experimental parameters, that was systematically varied to study its impact on the dynamics, was the level of motivation. There were three defined levels being either *normal*, *hurried* or *full commitment*. Generally, all participants were given the same instructions. Following the assumption

*Email of the corresponding author: mi.kuepper@fz-juelich.de

that most participants followed the instructions, we define these crowds as being more homogeneous. However, in one experimental run 20% of the participants were (secretly) given the instruction to move slowly (meaning that they should reduce their motivation), while all others were told to hurry. This run will be our case study of an inhomogeneous crowd which is being compared to the other experimental runs. The data set consists of individual head trajectories extracted with PeTrack [2] from over-head video recordings. For the data analysis we mainly use the software PedPy [3].

In the video recordings it is visible that in experiments with inhomogeneous instructions not all participants actively move forward (e.g. by closing gaps or pushing), but some adopt a more passive waiting posture (see Figure 1a-b). In the density profiles (Figure 1c-d), it can be seen how this affects the spatial structure of the crowd, as this behaviour leads to different space requirements. Additionally, we plan to investigate how this affects the dynamics within the crowd by e.g. studying the waiting-time to target-distance relations, fairness as well as changes in neighborhood.

Bibliography

[1] Boomers, A.K., Boltes, M., Adrian, J., Beermann, M., Chraibi, M., Feldmann, S., Fiedrich, F., Frings, N., Graf, A., Kandler, A., Kilic, D., Konya, K., Küpper, M., Lotter, A., Lügering, H., Müller, F., Paetzke, S., Raytarowski, A.K., Sablik, O., Schrödter, T., Seyfried, A., Sieben, A., Üsten, E., *Pedestrian Crowd Management Experiments: A Data Guidance Paper*, Collective Dynamics **8**, 1-57, 2023.

[2] Software *PeTrack*, 10.5281/zenodo.14056465, 2024.

[3] Software *PedPy*, 10.5281/zenodo.14906931, 2025.

Understanding Pedestrian Congestion in Merging Corridors: A Speed and Velocity Variance Approach

Jiawei Zhang*[1], Sakurako Tanida[1], Xiaolu Jia[2], Claudio Feliciani[1], Daichi Yanagisawa[1], and Katsuhiro Nishinari[1]

[1]School of Engineering, The University of Tokyo, Tokyo, Japan
[2]Beijing Key Laboratory of Traffic Engineering, Beijing University of Technology, China

Abstract Crowd dynamics in high-density scenarios challenge congestion analysis and risk mitigation. This study introduces speed and velocity variances as metrics to quantify movement irregularity and assess congestion. Experiments in a T-shaped corridor show that velocity variance detects directional disruptions at turning corners, while speed variance identifies congestion near merging points. Their distinct probability distributions provide deeper insights into localized movement instabilities, improving congestion assessment.

Keywords Pedestrian dynamics, Collective behaviors, Interactions, Voronoi diagram

Introduction

Collisions in crowded environments highlight the need to accurately assess congestion as a key characteristic of crowd dynamics. Although density, which measures the number of pedestrians per unit area, is the most common crowding indicator, it often overlooks critical factors such as individual behavior, localized interactions, and emergent turbulence in high-density conditions. Traditional models like Fruin's level-of-service [1] rely on density, flow, and speed thresholds but fail to capture multidirectional flows, self-organization, and turbulence in pedestrian movement.

T-shaped merging corridors, common in train stations, stadiums, and event venues, create natural "pinch points" where converging pedestrian streams lead to sudden congestion and disruptions. The interplay of turning angles and varying densities makes movement patterns highly complex, posing challenges for congestion assessment.

Existing metrics struggle to fully capture these dynamics. Congestion Number (CN) further quantifies flow disruptions and transitions to disorganized states [2], but do not account for directional conflicts in merging flows, and its data and computation demands limit real-time application. Entropy-based measures assess disorder [3] but may miss localized interactions crucial in confined merging spaces.

To address these limitations, we propose a new metric specifically designed for T-shaped corridors, offering a complementary perspective on pedestrian dynamics and contributing to more effective risk mitigation strategies.

Model and Methods

This study proposes two indicators: speed variance and velocity variance, which capture both magnitude and directional fluctuations in pedestrian movement. Speed variance (V_s) measures how an individual's

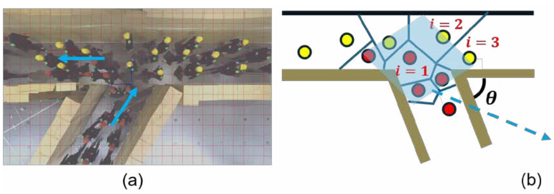

$V_s = \frac{1}{N}\sum_i^N (v_i - \bar{v})^2, \; V_v = \frac{1}{N}\sum_i^N \|\mathbf{v}_i - \bar{\mathbf{v}}\|^2$

i : Each point adjacent to the reference point

N : Total people of one area

Figure 1: (a) Real-experiment setup of merging corridor (b) Concept of calculation

*Email of the corresponding author: `zhang-jiawei@g.ecc.u-tokyo.ac.jp` scalar speed deviates from the local average, while velocity variance (V_v) incorporates direction by treating speed as a vector quantity. Voronoi diagrams facilitate detailed spatial assessments of local congestion by adaptively partitioning pedestrian space.

These indicators were tested in a T-shaped corridor experiment (Fig. 1), designed to simulate pedestrian merging flows under different turning angles and crowd sizes.

Result and discussion

Heatmap analysis of density and speed/velocity variance reveals congestion hotspots. Density increases after merging (Fig.2(a)). Figure 2(b) shows a 120° merging corridor where speed variance is concentrated after the turn, highlighting abrupt accelerations and decelerations due to interactions. In contrast, velocity variance peaks at the turning corner (Fig.2(c)), capturing directional disruptions at sharp turns. This distinction suggests that velocity variance detects pre-collision shifts, while speed variance marks collision-prone zones.

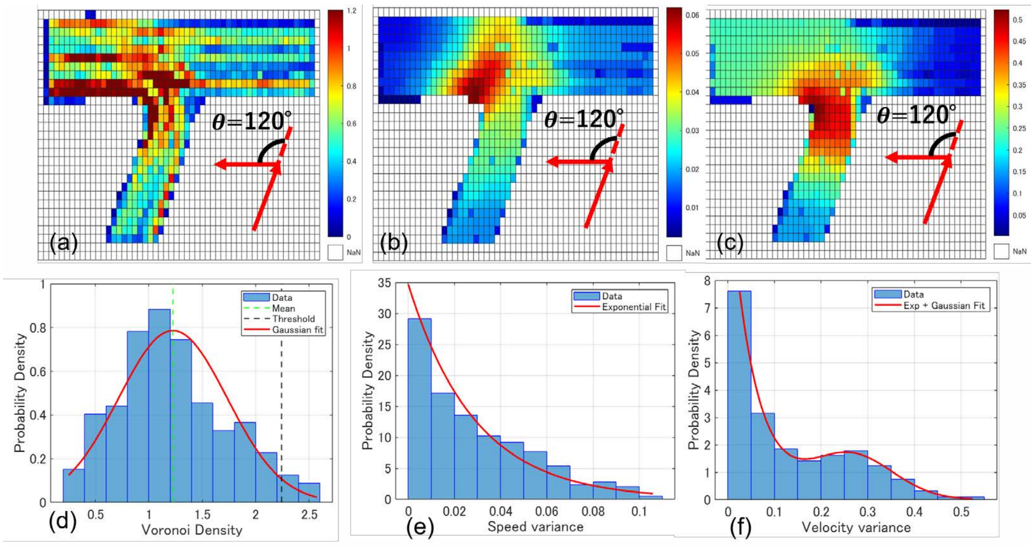

Figure 2: Heatmap of (a) Density, (b) Speed variance, (c) Velocity variance; Distribution of (d) Voronoi density, (e) Speed variance, (f) Velocity variance.

To further understand crowd behavior, we examine the probability distribution functions (PDFs) at the merging point. Voronoi density follows a Gaussian distribution (Fig.2(d)), indicating moderate crowding symmetry. Speed variance exhibits an exponential decay (Fig.2(e)), meaning small fluctuations dominate, but occasional large variations occur due to collision avoidance. Velocity variance (Fig. 2(f)) follows a mixed exponential-Gaussian pattern, suggesting that while minor directional changes are common, sharp turns cause significant disruptions. Thus, Voronoi density reflects overall crowding, while speed and velocity variance capture critical movement instabilities essential for collision risk assessment.

Summary

This study examines pedestrian congestion using speed variance and velocity variance as indicators of movement irregularity. Heatmap analysis in a T-shaped merging corridor demonstrates that velocity variance is highly sensitive to turning angles, effectively detecting directional shifts before collisions, while speed variance identifies congestion zones near merging points, where sudden speed fluctuations occur.

References

[1] Fruin.J., *Pedestrian Planning and Design*, Metropolitan Association of Urban Designers and Environmental Planners, 1971.

[2] Francesco.Z et al., *A pure number to assess "congestion" in pedestrian crowds*, Transp. Res. C, **148**, 104041, 2023.

[3] Yiping.Z et al., *Entropy analysis of the laminar movement in bidirectional pedestrian flow*, Physica A, **566**, 125655, 2021.

Impacts of Water Depth on Pedestrian Speed, Gait, and Stability: results from an experimental study

Xintong Li[1,2], Weiguo Song*[1], Jun Zhang[1], and Nikolai W.F. Bode[2]

[1]State Key Laboratory of Fire Science/University of Science and Technology of China
[2]School of Engineering Mathematics and Technology/University of Bristol

Abstract Evacuation and rescue operations during floods often necessitate walking in water. We conducted controlled experiments with 188 volunteers under four water depths (0 m, 0.35 m, 0.60 m, and 0.90 m) to analyze the effects of water depth on movement. These findings elucidate the impact of water depth on pedestrian dynamics, show gender-related correlations in this context, and provide critical insights into gait characteristics in varying water depths.

Keywords Flood evacuation, Evacuation experiment, Pedestrian dynamics, Walking speed, Gait characteristics

Introduction

In the context of emergency evacuations and rescue operations during flooding events, both affected individuals and rescuers frequently encounter the necessity of traversing through water. Consequently, a thorough understanding of pedestrian dynamics in flood environments is imperative for ensuring the safety of evacuees.

Researchers have undertaken individual pedestrian speed experiments in water tanks [1, 2] and swimming pools [3] featuring varying water depths. These experiments have demonstrated a substantial reduction in pedestrian movement speed in water compared to on land. Moreover, an exponential correlation between pedestrian speed and the specific flood force per unit width (derived from the combination of flood depth and speed) has been observed, indicating a decrease in pedestrian speed with increasing water depth. However, existing research has yet to reach consensus regarding the impact of gender on movement speed, and there remains a paucity of data on pedestrian gait characteristics.

To address this gap, we conducted experiments to examine pedestrian movement at four distinct water depths (0 m, 0.35 m, 0.60 m, and 0.90 m), representing no water, below-knee, above-knee, and waist-high water conditions. The objective was to elucidate the effects of gender and water depth on pedestrian speed, uncover gait characteristics at varying depths of water, and contribute richer data on the dynamics of pedestrian movement.

Experiments and Results

The experiments were carried out within a 1.8 m wide and 8 m long corridor built by guard poles. Figure 1 illustrates the experimental setup. We recruited 188 student volunteers (101 males and 87 females) to participate in our experiments. Before each trial, participants gathered on the left side of the *Start Line*. Upon the start signal, each volunteer began from the *Start Line*, simulating an emergency evacuation by proceeding quickly and safely through the *Measurement Area* to the *End Line*. To avoid interference, each volunteer was individually tested. After the current volunteer completed their traversal of the measurement area and left the corridor, the next volunteer would then begin their test.

A camera recorded the entire experiment. *PeTrack* software was used to calibrate the video, converting 2D pixel coordinates into real-world 3D coordinates. Pedestrian trajectories within the measurement area were extracted for data analysis.

We discussed the effects of water depth and gender on speed, quantified the pedestrian's lateral swaying amplitude, step frequency and step length by calculating the trajectory curvature, and introduced the coefficient of variation as a measure of the stability of step frequency and step length during walking. Our results indicate that water depth significantly affects pedestrian speed and gait characteristics: when

*Email of the corresponding author: wgsong@ustc.edu.cn

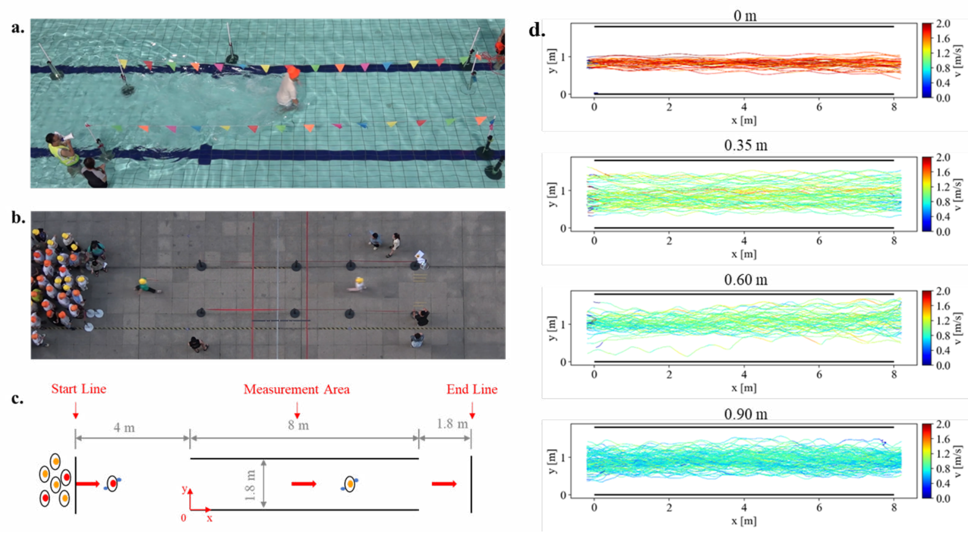

Figure 1: a). A video frame from the in-water experiment; b). A frame from the on-land (0 m depth) experiment; c). A schematic of the experimental layout. d). Pedestrian trajectories across different water depths, with the color bar indicating instantaneous speed. From top to bottom, the trajectories correspond to water depths of 0 m, 0.35 m, 0.60 m, and 0.90 m, respectively.

water depth increased from 0 m to 0.35 m, pedestrian speed declined significantly (by 38.6% for males and 44.8% for females), lateral swaying amplitude increased notably (69% in males and 133.3% in females), and step length shortened substantially (37.0% in males and 32% in females). Further increases in water depth, however, produced a diminishing effect on these measures. Furthermore, water presence accentuated gender differences in speed, while gender differences in step frequency, step length, and lateral swaying amplitude were primarily seen at 0 m depth. At water depths of up to 0.90 m, the Coefficients of Variation (CV) for step length and step frequency increased, suggesting reduced gait stability.

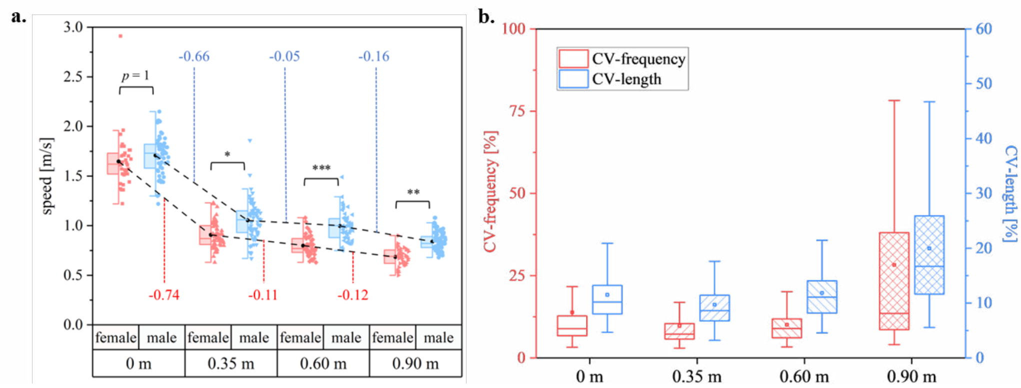

Figure 2: a). Boxplot of pedestrian movement speeds by gender across water depths,Dunn's post-hoc test significance markers are also included: *** for $p < 0.001$, ** for $p < 0.01$, and * for $p < 0.05$, denoting significant differences across water depths; b). Boxplots of coefficient of variation for step length and step frequency. The red box plot represents the coefficient of variation of step frequency, which corresponds to the left red axis, and the blue box plot represents the coefficient of variation of step length, which corresponds to the right blue axis.

Bibliography

[1] C. Dias, N.A. Rahman, A. Zaiter, *Evacuation under flooded conditions: Experimental investigation of the influence of water depth on walking behaviors*, International Journal of Disaster Risk Reduction **58**, 102192, 2021.

[2] G. Bernardini, E. Quagliarini, M. D'Orazio, M. Brocchini, *Towards the simulation of flood evacuation in urban scenarios: Experiments to estimate human motion speed in floodwaters*, Safety Science **123**, 104563, 2020.

[3] H. Lee, W. Hong, Y. Lee, *Experimental study on the influence of water depth on the evacuation speed of elderly people in flood conditions*, International Journal of Disaster Risk Reduction **39**, 101198, 2019.

12th International Conference on Pedestrian and Evacuation Dynamics (PED 2025)
Prague, Czech Republic – September 9-12, 2025

Interaction of 3D pedestrian flow in a congested railway station: Structural estimation based on Mean Field Game theory

Takahiro Matsunaga[1] and Eiji Hato*[1]

[1]Department of Civil Engineering, The University of Tokyo, Japan

Abstract This paper establishes a new approach for the description and estimation of pedestrian interaction by introducing mean field game (MFG) theory into the network-based route choice model. The mean field dynamics is endogenized in the model and parameters are estimated through repeated structural estimation. The proposed method presents better validation likelihood and shorter computation time than the conventional method.

Keywords pedestrian, 3D route choice model, interaction, mean field game, structural estimation

Introduction

Network-based discrete route choice models are coarser in resolution than simulation-based models in continuous space (Ref. [4]) but can be easily statistically estimated and interpreted with real data based on utility maximization theory. In modeling pedestrian behaviors, description of interaction is important, tackled by several approaches such as social force model (Ref. [3]), cellular automata (Ref. [2]), and discrete choice models (Ref. [1]). Under congested conditions where the number of agents is sufficiently large, considering interactions between each pedestrian is computationally expensive and not realistic. Mean field game (MFG) theory (Ref. [6]) is an effective approach to address this issue. MFG treats agents as a density distribution, reducing calculation costs and enabling simultaneous description of individual strategies and group dynamics (Figure 1). The description is achieved by solving the time evolution of agents' value function and the entire density distribution simultaneously. Ref. [5] introduced MFG into a pedestrian model by Ref. [4], for example, but existing works focus on simulation-based approach and calibrations with real data have not been conducted.

This paper integrates Bellman equation of dynamic route choice and expected pedestrian flow on a discrete network in a MFG framework and constructs structural estimation in which mean field is endogenized by model itself. The contribution of this study is to enable simultaneous estimation of route choice parameters and endogenized mean field using real data by maximum likelihood estimation.

Methodology

To model pedestrians' sequential route choice behaviors, we adopt the discount Recursice Logit (RL) model (Ref. [7]), where each agent is driven by Bellman equation with discount factor β, destination d. In our model, the utility function includes the mean field dynamics M:

$$V^d(k) = E\left[\max_{a \in A(k)} \left\{v(a|k) + \beta V^d(a) + \varepsilon(k)\right\}\right], \qquad v(a|k) = \sum_i \theta_i X_{i,a|k} + \gamma M_{a|k}. \tag{1}$$

The term $\gamma M_{a|k}$ corresponds to the impact of the mean filed on agents moving from node k to a. M is defined as a innor-product of a link vector $\vec{e}$ and average flow vector $\vec{f}$ weighted by an expected density ρ ($M^t_{a|k} = \vec{f}^t_k \cdot \vec{e}_{a|k}$). $\vec{f}$ and ρ are defined at each node and time:

$$\vec{f}^t_k = \sum_{a \in A(k)} \rho(k,t) P^t(a|k;\theta,\gamma,M)\vec{e}_{a|k}, \qquad \rho(k,t) = \sum_{a' \in K(a)} \rho(a',t-1)P^{t-1}(k|a';\theta,\gamma,M). \tag{2}$$

The point here is that M is structurally endogenized in the model instead of given exogenously. Also, according to the concept of MFG, we treat behaviors of other agents as probabilistic distribution P rather than actual choice results. As shown in Figure 1, we estimate parameters by minimizing the log-likelihood function repeatedly until convergence (*structural estimation*). The value function (model parameters) and the mean field are updated iteratively in the process.

*Email of the corresponding author: `hato@bin.t.u-tokyo.ac.jp`

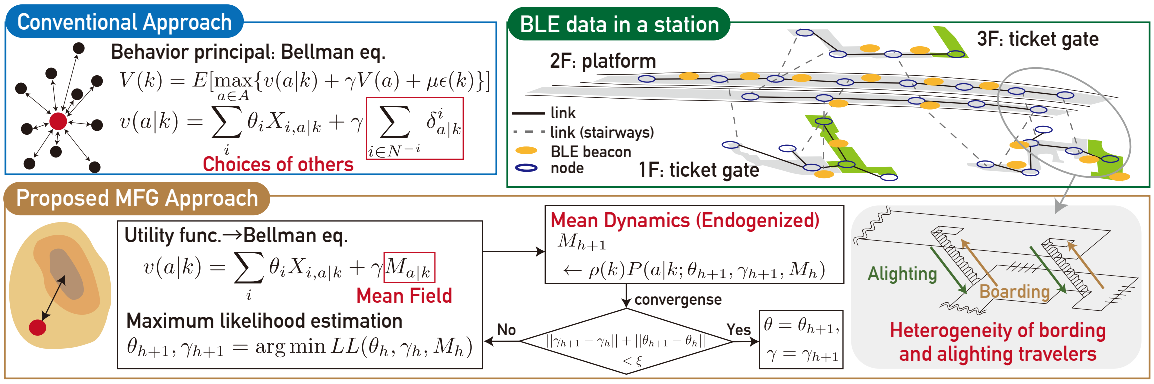

Figure 1: Framework

Table 1: Results

	Sunday morning	Sunday evening	Monday morning	Monday evening
validation LL (not-MFG)	-5.56	-7.69	-6.67	-8.29
validation LL (MFG)	-5.51	-7.75	-7.31	-8.29
time (not-MFG) [s]	7074	1438	1989	1693
time (MFG) [s]	6932	1906	2540	2220
γ_{off} (MFG) (t-val)	0.19 (2.37)	0.16 (2.03)	-0.13 (-0.61)	-0.25 (-1.43)
γ_{on} (MFG) (t-val)	0.16 (0.61)	-0.73 (-2.49)	-0.32 (-1.57)	-0.30 (-1.37)

Results and Discussion

As the case study, we installed BLE beacons to capture BLE signals from travelers' devices in JR Shibuya station, one of the busiest stations in Tokyo, Japan (Figure 1). The data was collected on Sunday and Monday morning (8:30-8:45) and evening (17:30-17:45) on January 29th and 30th, 2023. Agents' footprints are extracted by sorting boarding and alighting trajectories based on MAC addresses, enabling a comparison of interaction effects across groups. Each time slot includes approximately 1,000 agents.

Table 1 shows the comparison of the average validation likelihood (10-fold cross validation) and computation time of the proposed and conventional method as well as the parameter estimates of interaction terms with the MFG-based model. The upper part reveals the MFG-based approach achieves significantly lower calculation cost and equivalent or better validation likelihood (devided the number of path). The lower part presents γ_{off} (interaction parameter for alighting travelers) is significantly positive on Sunday, while that of boarding (γ_{on}) is generally negative or statistically insignificant. Since there are fewer commuters on Sundays, meaning that more passengers are unfamiliar with the station layout than on weekdays, alighting passengers may tend to be guided by others rather than avoiding congestion. It is suggested that the 3D pedestrian flow in a congested station exhibits different effects on boarding and alighting travelers, and these properties dynamically change depending on day and time.

Our result indicates that the MFG-based approach is effective in estimating the impacts of interaction in a space with many agents both in terms of estimation accuracy and computation time. The adaptation of MFG to pedestrian flow control problems is expected as a future work.

References

[1] Gianluca Antonini, Michel Bierlaire, and Mats Weber. Discrete choice models of pedestrian walking behavior. *Transportation Research Part B: Methodological*, 40(7):667–687, 2006.

[2] Victor J. Blue and Jeffrey L. Adler. Cellular automata microsimulation for modeling bi-directional pedestrian walkways. *Transportation Research Part B*, 35(3):293–312, 2001.

[3] Dirk Helbing and Peter Molnar. Social force model for pedestrian dynamics. *Physical Review E*, 51(5):4282–4286, 1995.

[4] Serge P. Hoogendoorn and Piet H.L. Bovy. Pedestrian route-choice and activity scheduling theory and models. *Transportation Research Part B: Methodological*, 38(2):169–190, 2004.

[5] Aimé Lachapelle and Marie-Therese Wolfram. On a mean field game approach modeling congestion and aversion in pedestrian crowds. *Transportation Research Part B: Methodological*, 45(10):1572–1589, 2011.

[6] Jean-Michel Lasry and Pierre-Louis Lions. Mean field games. *Japan Journal of Mathematics*, 2:229–260, March 2007. Based on the 1st Takagi Lectures, Kyoto University, 2006.

[7] Yuki Oyama and Eiji Hato. A discounted recursive logit model for dynamic gridlock network analysis. *Transportation Research Part C*, 85:509–527, 12 2017.

12th International Conference on Pedestrian and Evacuation Dynamics (PED 2025)
Prague, Czech Republic – September 9-12, 2025

Comparative Analysis of Evacuation Strategies: Awareness and Pathfinding *

Álvaro Serrano[1], Giuseppe Vizzari[2], and Marin Lujak[†1]

[1]CETINIA, University Rey Juan Carlos, Madrid, Spain
[2]Department of Informatics, Systems, Communication, University of Milano-Bicocca

Keywords Pedestrian evacuation, Pathfinding, Agent-Based Simulation, Dynamic Routing

Extended Abstract

Efficient evacuation planning is crucial during emergencies. Agent-based simulations offer a controlled environment to evaluate how different routing strategies and levels of situational awareness affect evacuation efficiency [1, 4, 5]. In our study, we model evacuees as agents grouped by their starting locations within a building layout, represented as a graph. The agents move toward exits using one of the following two strategies: the *Efficient Paths* approach, which allows agents to dynamically re-compute their routes on the fly in response to changing conditions, and the *Agile Evacuation Routes (AER)* approach. This method dynamically identifies Agile Evacuation Routes by assessing the number, safety, and evacuation time of the paths originating from their intermediate nodes. It evaluates each node's evacuation centrality, ensuring evacuation that is resilient to the fluctuating safety conditions posed by unpredictable hazard dynamics [2]. Additionally, agents are modeled with either *High Awareness* (i.e. they receive continuous updates on the presence of risks in the environment) or *Low Awareness* (gaining information by local perception as they progress in space) [3]. The high awareness approach is only possible in environments able to locate the pedestrians (e.g. smart buildings with indoor localization facilities) and when evacuees can actually receive awareness information about the best route to be followed (e.g. through smart wearable or portable devices, or variable message panels positioned in the environment). The low awareness approach has lower technology requirements and, essentially, a static evacuation plan positioned in strategic locations in the building. The high-awareness scenario is applicable to emergency response systems in environments with controlled access, including hospitals and airports. Here, dynamic routing or static signage is tailored to the available technological infrastructure. Our analysis offers valuable insights into how adaptive routing and the availability of information affect evacuation performance.

Methodology – The simulation employs a building layout (Fig. 1) featuring multiple exits, key waypoints, and designated starting positions. For pedestrian simulation, we employ JuPedSim with the Collision Free Speed Model[1], focusing on pedestrian routing choices. Each evacuee, initially randomly located in the building, selects between two strategies: *Efficient Routes*, which are dynamically computed shortest paths that adapt as hazards evolve, and *Agile Evacuation Routes*. Evacuees with high awareness receive continuous updates that allow them to re-plan their routes as conditions change [4], whereas Low Awareness evacuees rely on information gathered as they progress [3]. Figure 2 illustrates the trajectories of evacuees under different scenarios. In the Low Awareness Agile Evacuation Routes case, evacuees traverse the central corridor until they reach an intersection and initially head toward exit EA; however, upon reaching node 3G, they observe that node 3H is hazardous and thus reverse course to proceed toward exit EB. Conversely, in the High Awareness Agile Evacuation Routes scenario, evacuees use the same corridor but, being pre-informed of the hazard on the path to EA, they directly choose exit EB. Regarding the Efficient Paths strategy, in the Low Awareness scenario, evacuees from the red group follow the shortest route to exit EB without encountering hazards, while those in the blue group attempt to use the shortest path toward the nearest exit (EA); upon arriving at node N, they detect that node O is hazardous and consequently re-route to exit AB via the shortest path. In the High Awareness Efficient Paths scenario, both groups proceed directly to exit AB along the shortest route.

*This work was partially supported by the grant COSASS: PID2021-123673OB-C32 funded by MCIN/ AEI/ 10.13039/501100011033 and by "ERDF A way of making Europe."

†Email of the corresponding author: `marin.lujak@urjc.es`

[1]`https://www.jupedsim.org/stable/pedestrian_models/index.html`

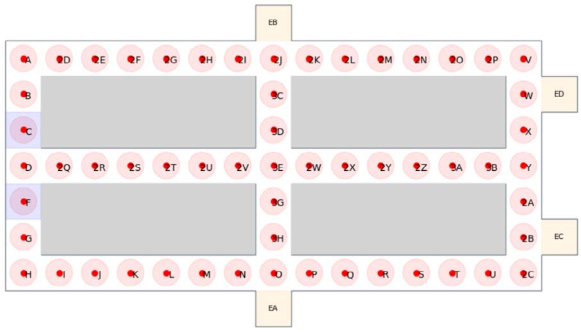

Figure 1: Layout of the simulation environment: zones C and F are starting positions; red markers are potential waypoints/hazards; EA, EB, ED, and EC are exits.

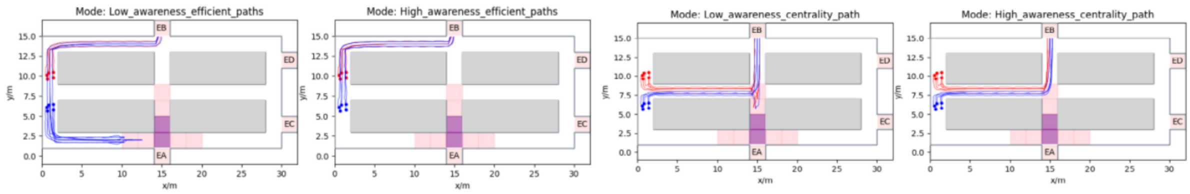

Figure 2: Colored dots are evacuees' initial positions, with colors associated to the two groups considered; lines show their trajectories. Purple areas are hazard zones, while pink areas may become risky over time.

Awareness Level	Pathfinding Algorithm	Time (s)
Low Awareness	Efficient Paths	66.52
High Awareness	Efficient Paths	30.56
Low Awareness	Agile Evacuation Routes	37.40
High Awareness	Agile Evacuation Routes	34.92

Table: Evacuation Times for Different Scenarios

Results – The evacuation times for each scenario are summarized in Table 2. Notably, the *High Awareness + Efficient Paths* combination yielded the fastest evacuation, while the *Low Awareness + Efficient Paths* scenario was the slowest. These findings confirm that dynamic route adjustment plays a critical role in reducing evacuation time [1]. High Awareness significantly reduced evacuation times, particularly when paired with the Efficient Paths algorithm [4]. Although the Agile Evacuation Routes method proved robust under limited information [2], the dynamic re-routing of Efficient Paths only showed its full potential in this simple environment when agents were well-informed [3].

Conclusion – Our simulation environment demonstrates that situational awareness is essential for rapid evacuations. Dynamic shortest-path algorithms provide the best performance when agents receive continuous, real-time information in this context [4], while Agile Evacuation Routes remain a reliable alternative when information is limited [2]. The layout of our simulation environment was relatively simple. In future work, we will perform experiments in more complex layouts with multiple egress possibilities and security conditions that change rapidly in time and space. We also intend to investigate more complex behavioral models and multi-level environments to further refine evacuation strategies.

Bibliography

[1] D. Helbing, I. Farkas, and T. Vicsek, "Simulating dynamical features of escape panic," *Nature*, vol. 407, no. 6803, pp. 487–490, 2000.

[2] M. Lujak and S. Giordani, "Centrality measures for evacuation: Finding agile evacuation routes," *Future Generation Computer Systems*, vol. 83, pp. 401–412, 2018.

[3] S. Ossowski and M. Lujak, "Evacuation Route Optimization Architecture Considering Human Factor," *AI Communications*, vol. 45, pp. 78–89, 2017.

[4] G. Vizzari, L. Crociani, and S. Bandini, "An Agent-Based Model for Plausible Wayfinding in Pedestrian Simulation", *Engineering Applications of AI*, vol. 87, 2020.

[5] K.A.U. Wagoum, A. Seyfried and S. Holl, "Modeling the dynamic route choice of pedestrians to assess the criticality of building evacuation", Advances in Complex Systems, 15(07), p.1250029, 2012.

Timetable
Talk index

12th International Conference on Pedestrian and Evacuation Dynamics (PED 2025)
Prague, Czech Republic – September 9-12, 2025

Learning mid-term human navigation through crowds

Céline Finet *[1], Jean-Bernard Hayet[2], Ioannis Karamouzas[3], and Julien Pettré[1]

[1]Inria Rennes
[2]CIMAT
[3]University of California, Riverside

Abstract This article presents a method for modeling and predicting sequences of human decisions during a crowd navigation task. We focus on the mid-term navigation, i.e., where navigation is modeled as a sequence of traversed gaps between people. By leveraging data from a virtual reality experiment, the method divides the space into triangles using Delaunay triangulation the vertices of which are humans forming the crowd. A binary classifier is used to predict a participant's sequence of traversed triangle edges. The goal is to find a minimal configuration that effectively models human trajectories, balancing prediction accuracy and model complexity.

Keywords Human navigation, Crowd Modeling, Prediction, Multi-scale algorithm, Decision sequences

1 Introduction

Crowd simulation consists of proposing algorithms to reproduce, imitate, understand or predict the behavior of (human) crowds in various situations. This work focuses on microscopic approaches whose simulation models detail individual movement, and are based on the principle that inter-individual interactions are able to account for phenomena emerging at the macroscopic scale of the crowd. By exploring recent surveys in the field [5], we find that the simulators most frequently focus on the case of pedestrian simulation. Individual trajectories are calculated by taking into account two main elements: the 'motivation', or desired destination of the agents, and local interactions, the main one being collision avoidance between agents. The desired destination generally results from a trajectory planning stage which allows, for example, the presence of obstacles in the environment to be taken into account. Collision avoidance results from the adaptation of this plan on a local scale, for which there are a very large number of solutions. It is worth noting that the mid-term scale is rarely taken into account in simulation models. Yet this would make it possible to establish dynamic strategies for adapting long-term navigation plans, beyond a single purely local vision. Some work does exist, however, such as that of Julien Bruneau, who shows that constructing a trajectory as a sequence of multiple interactions makes it possible to improve the realism of simulations [6]. Similarly, Andrew Best, with his DenseSense algorithm, models density-dependent behavior by simulating trajectories that respect speed/density relationships [2], while W. Van Toll proposes a topological approach to resolve conflicts between global planning and local collision avoidance [4]. The work presented here is in line with these ideas. We seek to propose a method that is capable of reproducing human medium-term navigation strategies. To do this, we introduce the idea that navigation within crowds can be modeled as a sequence of gap crossings. In this idea, a trajectory is a sequence of points of passage between 2 individuals. We are seeking to establish an approach that is capable of reproducing the strategy of human navigation, i.e. reproducing real human trajectories of movement in a crowd. To do this, we have a dataset that we present in the following section, as well as our method for learning the strategy from this data.

2 Data and methods

To address the problem of learning mid-term navigation strategies in crowds, we modeled computing a Delaunay triangulation of which vertices are humans in the crowds. This method optimally divides the space into triangles, maximizing angles and avoiding overly elongated triangles. Delaunay triangulation is particularly suited to our context as it effectively captures the spatial relationships between humans. Our method is tested on data were acquired during an experiment conducted by Martin and colleagues[3],

*Email of the corresponding author: `celine.finet@inira.fr`

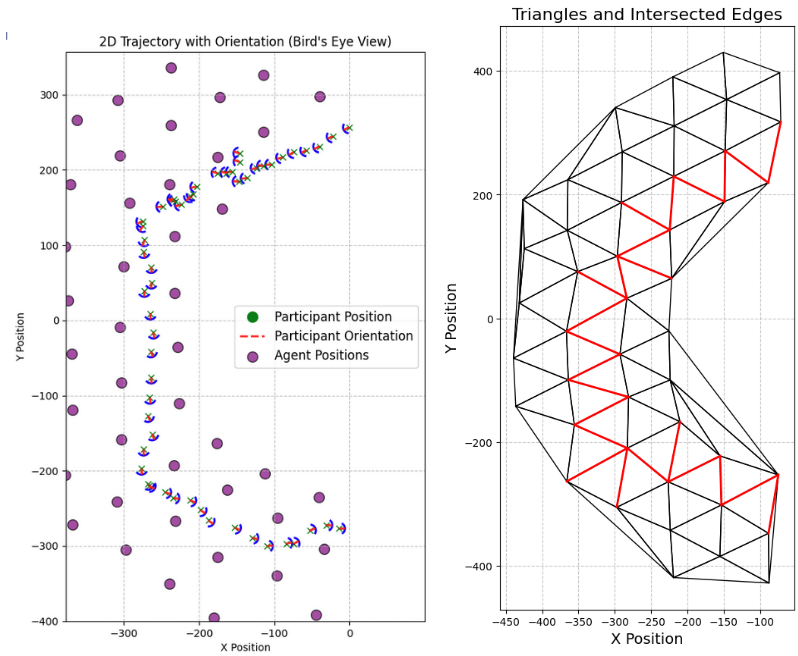

Figure 1: Left: example of a trajectory (green crosses) through a crowd of humans (purple disks) recorded in a Virtual Reality environment. Right: Crowd modeled as a Delaunay triangulation, and result of path prediction (traversed triangle in red)

in which participants had to walk through a circular corridor and navigate through stationary agents in virtual reality (VR). This experiment aimed to understand whether the appearance of the stationary agents influenced the participants' navigation. These data allow for the complete trajectories followed by the participants in the virtual environment to be recreated for each condition (varying density) and with the position of all stationary agents. The problem then reduces to solving the participant's navigation within an independent triangle to understand their local choice. Subsequently, we can recursively develop their navigation across all triangles to obtain their global trajectory, guided by the person's distant goal. In the case of semicircle data, the trajectory is guided by the tangent to the circle. The method used for learning is a binary classifier, which takes as input the edge through which the participant passes and predicts the edge through which they will exit (to their right or left). In the first implementation, the input data for the algorithm to learn the exit label (right or left) are the geometric features of the triangle. Each triangle is transformed into the same base to eliminate the orientation bias in the data. Thus, the model does not learn directly from the global coordinates of the problem but rather locally. This problem is egocentric as the trajectory prediction is relative to the participant's frame of reference. Using this approach, we aim to capture the participants' local decisions and chain them coherently to form a sequence of choices that achieve a global objective. The goal of this method is to find the optimal parameters, i.e., the fewest parameters possible, necessary for accurate modeling. By varying the depth at which we evaluate the succession of triangles, we seek to determine the minimal configuration that achieves a reliable prediction of the participant's navigation choices. This approach aims to balance the complexity of the model with the precision of the prediction, ensuring that the model remains lightweight and efficient.

Bibliography

[1] van den Berg J, Lin M and Manocha D *Reciprocal velocity obstacles for real-time multi-agent navigation.*, IEEE International Conference on Robotics and Automation 2008

[2] Best, A, Narang, S, Curtis, S, et al. *DenseSense: Interactive Crowd Simulation using Density-Dependent Filters.* Symposium on Computer Animation. 2014.

[3] Martin, J, Hoyet, L, Pinsard, E, et al. *Virtual Crowds Rheology: Evaluating the Effect of Character Representation on User Locomotion in Crowds.*, IEEE Transactions on Visualization and Computer Graphics, 2024.

[4] Van Toll, W, Pettré, J. *Connecting global and local agent navigation via topology.* In: Proc. of the 12th ACM SIGGRAPH Conference on Motion, Interaction and Games. 2019.

[5] Van Toll, W, Pettré, J. *Algorithms for microscopic crowd simulation* Computer Graphics Forum. 2021.

[6] Bruneau, J and Pettré, J. *Eacs: Effective avoidance combination strategy.* In : Computer Graphics Forum. 2017.

Timetable
Talk index

12th International Conference on Pedestrian and Evacuation Dynamics (PED 2025)
Prague, Czech Republic – September 9-12, 2025

Analysis of Staircase Emergency Evacuation of Pedestrian after Earthquake

Xuheng Chen[1], Weiguo Song*[1], and Jun Zhang[1]

[1]State Key Laboratory of Fire Science/University of Science and Technology of China

Abstract In this paper we try to use the surveillance footage to capture the characteristic of staircase evacuation after a real earthquake. We got the time marks when entering and exiting stairs of 143 pedestrians and, based on this data, calculated evacuation time, average travel speed, average regional speed etc.

Keywords Pedestrian Evacuation Dynamics, Staircase, Earthquake, Emergency

Introduction

Earthquakes, as sudden and devastating natural disasters, pose significant threats to urban safety. In densely populated cities where high-rise buildings are increasingly common, the safety of citizens during such events is paramount. According to Chinese fire regulations, elevators are prohibited for use during emergencies, necessitating the use of staircases for evacuation. This makes the study of high-rise building evacuations during earthquakes critically important.

For staircase evacuation, researchers organized various experiments aimed at quantitative analysis. Usually, volunteers were recruited to participate experiments in specific scenarios. Speeds of walking downstairs or upstairs, crowd density are direct parameters[1] as a result from videotape of experiments, helping quantifying evacuation characteristics. Hard to get around the fact that, differences of pedestrians' performance between control experiment, fire drill and true emergency are not clear. Thanks to permission from the relevant authorities, we obtained valuable raw footage of a building from which students and teachers evacuated following a distinctly perceptible 4.7-magnitude earthquake tremor. This real-world emergency scenario provided critical data for analyzing evacuation behaviors under genuine threat conditions.

Method and Analysis

The spontaneous emergency evacuation happened in a 9-story building at a university in Hefei[2]. The building contained 2 identical staircases with 26 steps per floor (except between 1st floor and 2nd floor, 2nd floor and 3rd floor, which had 32 steps), located at both ends of the corridor. After the sudden shock of the ground, totally 143 students and teachers evacuated quickly through the 2 series of stairs, specifically 71 through the East one and 72 through the West one. To discover the evacuation characteristics when emergency from videotape, we conducted several analyses as evacuation time, average travel speed, average regional speed, and regional density.

Evacuation time: By analyzing timestamps embedded in videos recorded at the stairwell entrances and exits, the evacuation time of each pedestrian can be determined, as shown in Tab. 1.

Average travel speed: With the estimation of the spacial travel distance on stair, average travel speed can be calculated for every pedestrian. Following Tab. 1 shows maximum, minimum, mean and medium value of average travel speed.

Average regional speed: With the help of frame-level analysis software as the open-source video player 'VLC' and trajectory tracking software 'PeTrack', velocity diagram for the pedestrian passing through 3.652m before the exit can be provided and the histogram is shown below as Fig. 1.

Spacial evacuation behavior: All pedestrians followed the regulation of not using elevators. Under the influence of social relationships, some pedestrians delayed their evacuation to accompany friends.

*Email of the corresponding author: wgsong@ustc.edu.cn

Result

Out of 143 pedestrians, 114(approximately 79.7%) evacuated at an average travel speed of less than 1.0 m/s. However, there were individuals who reached speeds up to 2.44 m/s, indicating that some pedestrian may accelerate under emergency conditions. Comparing the two figures in Fig. 1, the percentage of individuals with average regional speeds exceeding 1.0 m/s(56.3%) is significantly higher than those with average travel speeds(4.2%). As illustrated in Fig. 2, which compares the two types of pedestrian speeds, nearly all pedestrians exhibited a higher regional speed immediately before exiting compared to their average travel speed during the entire evacuation. This suggests that the merging of pedestrians from different floor occurred before reaching the exit, after which pedestrians accelerated, possibly due to a heightened sense of threat. There were up to 6 pedestrians in the 3.264 square meter stairwell because the people were walking side by side. Men were generally faster than women, but to less than 20%. In addition, the Voronoi diagram during evacuation is analyzed.

	Time use	Counts	Maximum v	Minimum v	Mean v	Medium v
West stair	144s	72 peds	2.44m/s	0.60m/s	1.09m/s	0.83m/s
East stair	187s	71 peds	1.13m/s	0.52m/s	0.66m/s	0.62m/s
Total	189s	143 peds	2.44m/s	0.52m/s	0.85m/s	0.91m/s

Table 1: Preview of Evacuation Time and Average Travel Speed

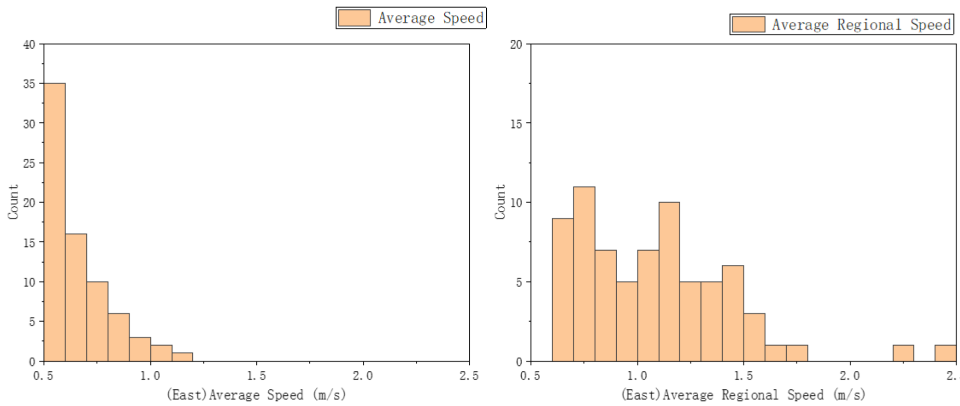

Figure 1: Average Travel Speed(left) and Average Regional Speed(right) on the East stair

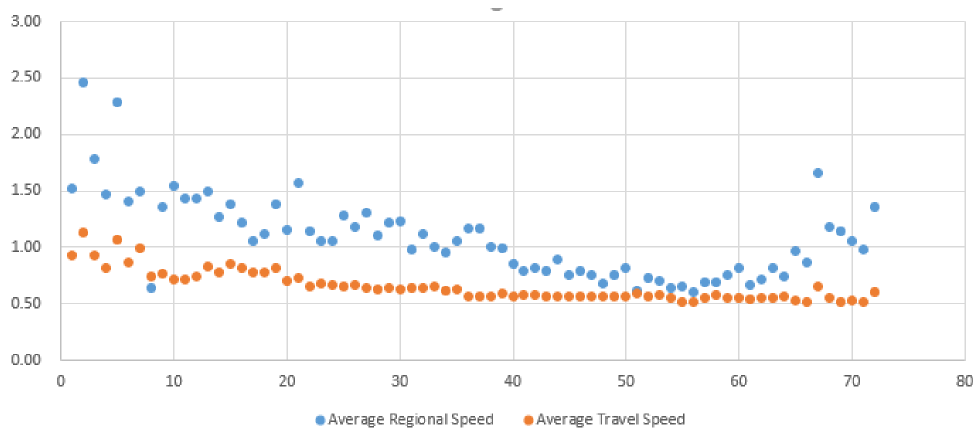

Figure 2: Comparison of Average Travel Speed and Average Regional Speed of Every Pedestrian

Bibliography

[1] Huang, Z., et al. *Performance of occupant evacuation in a super high-rise building up to 583 m.* Physica A: Statistical Mechanics and its Applications 589, 2022.

[2] Zeng, Y., et al. *Experimental study on walking preference during high-rise stair evacuation under different ground illuminations.* Physica A: Statistical Mechanics and its Applications 479: 26-37, 2017.

12th International Conference on Pedestrian and Evacuation Dynamics (PED 2025)
Prague, Czech Republic – September 9-12, 2025

Exploring pedestrian nudging: Current advancements and future challenges

Claudio Feliciani*[1] and Alessandro Corbetta[2]

[1]Graduate School of Engineering, The University of Tokyo, Tokyo, Japan
[2]Department of Applied Physics and Science Education, Eindhoven University of Technology, Eindhoven, The Netherlands

Abstract Pedestrian nudging represents a simple and yet valid solution to change people's behavior in walking environments. However, research by the authors reveal that effectiveness can vary depending on environment and experimental context, making it difficult to draw general conclusions and, eventually, automated protocols. To prove this, we present a summary from our experiments while extending the call to participants of the PED2025 conference to increase the overall sample size (of studies) and help to find patterns providing valid evidence to support future implementations of nudging solutions in pedestrian spaces.

Keywords Crowd control, Nudging, Environmental stimuli, Lighting, Crowd sensing

Introduction and background

Crowd control is a multi-layer process in which members of a crowd receive increasingly disrupting instructions to change their behavior [3]. When risk and urgency is low, crowd control is performed using simple and neutral information, usually through signage allowing people to find their way. On the other hand, when risk is judged high, and countermeasures need to be taken depending on the situation, barriers or deviations are prepared and physical layout is changed to steer people and reduce density in critical locations.

"Pedestrian nudging" also represents a layer of crowd control and follows the principles proposed under the nudge theory: a concept in behavioral economics that suggests that positive reinforcement and indirect suggestions can influence people's decisions and behavior without restricting their freedom of choice. From a practical perspective, pedestrian nudging can be performed by modifying the environment where people walk, for example changing lighting conditions, using music or sounds, or automatizing signage to prioritize underutilized routes. In the frame of crowd control, nudging takes a special role for several reasons: 1) It allows to change people's behavior without restricting their freedom of choice, 2) It has the potential of being automated measuring crowd conditions, and 3) It is relatively cheap to operate, thus minimizing or delaying the need of human intervention.

However, little research has been performed on pedestrian nudging and results are not always coherent and encouraging. One of the difficulties is that such research is not possible (or very difficult) in a laboratory setting and experiments are often performed in ecological scenarios where a number of (hidden) variable also influence crowd motion. For instance, the dynamics of people is different when there are social groups or people have a strong social identity (football supporters of the same team, for example). Such factors often go undetected when pedestrian data are collected to measure the efficacy of nudging solutions, therefore potentially contributing to information gap and, ultimately, conflicting results.

Representative results

To provide evidence in support of the arguments raised above, we will present several studies, some sharing very similar conditions, yet resulting in different outcomes.

Light was tested in four different experiments: at the Glow 2027 festival in Eindhoven (The Netherlands), in the jellyfish area of a large aquarium (Kaiyukan) in Osaka (Japan), at the 2024 Iwaki firework display (Japan), and through a long-term experiment in a university in Tokyo (Japan) [4]. Among the four

*Email of the corresponding author: feliciani@g.ecc.u-tokyo.ac.jp

experiments only the latter two managed to change people's behavior using light above a 10% threshold, possibly because of the relative importance played by lighting in those contexts.

Further, three experiments employing a visual indication (such as an arrow) are also considered: the already mentioned Glow 2027 festival [1] and long-term experiment in Tokyo, and, in addition, another experiment in the Kaiyukan aquarium. In this case, all three experiments managed to change people's motion to some extent, although the degree of "intrusion" can be considered somewhat large and, still, the efficacy in changing people's motion was in the order of 5-10% (20% at the most).

Finally, sound was also tested in the long-term experiment in Tokyo without satisfactory results in term of steering efficiency while worked oppositely respect to expectations in experiments performed in Eindhoven [2].

Results for the above experiments are summarized in Table 1. From a quick glance, it should be already clear that results are diverse depending on the setup, although some patterns start to emerge. For example, experiments using visual indications appears to be more effective compared to other solutions.

Table 1: Summary of the results from the experiments presented above. Efficacy is always evaluated in regard to the measured variable (speed, density, waiting time, etc.).

Name (location & year)	Stimulus used	Efficacy	Notes
Glow festival (Eindhoven, 2017)	Light	$\leq$ 5%	Density dependance
Kaiyukan jellyfish area (Osaka, 2024)	Light	None	Dark environment
Firework display (Iwaki, 2024)	Light	10-15%	Outdoor event
University entrance (Tokyo, 2023)	Light	$\approx$5%	Change over 2 months
Glow festival (Eindhoven, 2017)	Stimulus array	5%	Large bright arrow
University entrance (Tokyo, 2023)	LED display arrow	$\approx$5%	Change over 2 months
Kaiyukan Pacific Ocean tank (Osaka, 2024)	Wall projection	15-20%	Text and animation
University entrance (Tokyo, 2023)	Sound	None	Sound on transit
TU/Eindhoven (Eindhoven, 2022)	Sound	5%	16 loudspeakers used

Discussion

When people move in an ecological context a number of variables affect their behavior. This would require a large sample size to perform valid statistical tests and underline patterns in the data. However, sample size for nudging experiments is very limited, making such approach not possible, for the moment. A potential reason is that nudging studies often do not get published for several reasons, making a (meta) review difficult. In some cases the study was too simple to become a standalone publication, in others there were negative (yet valid) results, and/or, sometimes, study are simply hard to find in the literature.

The purpose of this work is to bring the problematic to the audience of PED2025 and potentially find a sufficient number of studies to expand the database presented in Table 1. The authors are aware of several unpublished studies which could help obtaining a better overall picture on nudging. However, there are likely more and PED2025 represents an ideal opportunity to spread the message and raise awareness that, in a proper context, a negative or non-conclusive study can still represent a significant piece of information for research in pedestrian nudging.

References

[1] Alessandro Corbetta et al. A large-scale real-life crowd steering experiment via arrow-like stimuli. *Collective Dynamics*, 5:61–68, 2020.

[2] Alessandro Corbetta, Toros Senan, Lex Wöstemeier, and Bart Hengeveld. Public-space sonification for pedestrian trajectory nudging. In *International Conference on Traffic and Granular Flow*, pages 207–214. Springer, 2022.

[3] Claudio Feliciani, Kenichiro Shimura, and Katsuhiro Nishinari. *Introduction to crowd management: Managing crowds in the digital era: Theory and Practice*. Springer Nature, 2022.

[4] Claudio Feliciani, Sakurako Tanida, Xiaolu Jia, and Katsuhiro Nishinari. Influencing pedestrian route choice through environmental stimuli: A long-term ecological experiment. *Journal of Disaster Research*, 19(2):325–335, 2024.

12th International Conference on Pedestrian and Evacuation Dynamics (PED 2025)
Prague, Czech Republic – September 9-12, 2025

Spontaneous synchronization of motion in a group of marathon runners

Hiroaki Furukawa*[1], Hisashi Murakami[2], and Kazutoshi Kudo[1]

[1]The University of Toyo, Tokyo, Japan
[2]Kyoto Institute of Technology, Kyoto, Japan

Keywords Synchronization, Step timing, Marathon runner, Relative phase

Various synchronization phenomena have been reported in nature. Synchronization phenomena have also been reported to occur between people, such as the stride patterns of two people walking side by side [1], and are referred to as interpersonal synchronization. Interpersonal synchronization has been suggested to occur not only in daily activities such as walking [1] and simple limb movements [2]., but also in athletic situations such as sprinting [3]. Here we show a case of synchronization occurring among marathon runners. We analyzed the step timing of five runners who formed the leading group in the Osaka International Women's Marathon 2021. This marathon had a limited lead group of five or fewer runners and was held on a flat 2.8 km loop course, which controlled for the influences of group size and terrain. Based on each runner's step timing, the relative phase of each pair was calculated, and synchronization was evaluated by the localization of the relative phase occurrence distribution. As a result, pairs with significant localization at relative phases of 0° or 180° were observed (Figure 1). These results indicate that interpersonal synchronization can occur even during marathon competitions and influence step timing. We expect that our findings will provide new insights into understanding how and why human groups synchronize their motion.

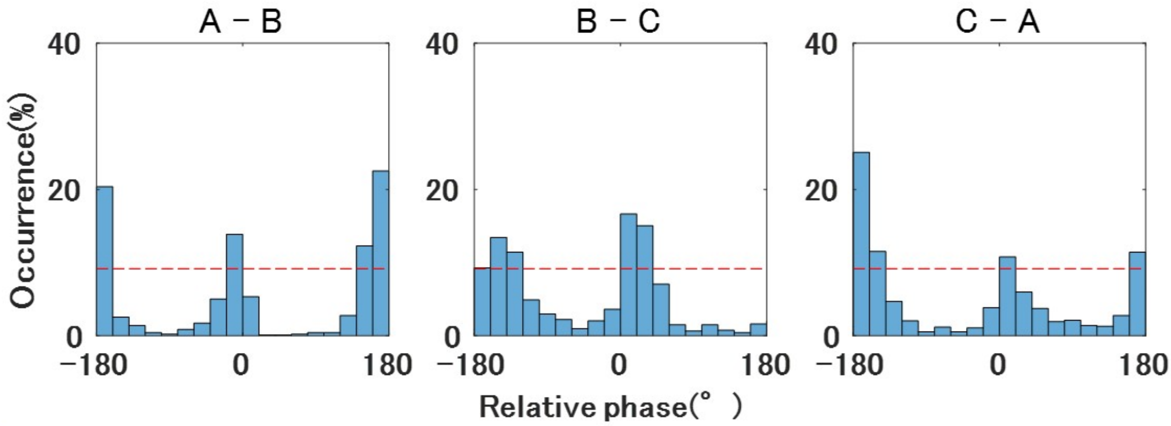

Figure 1: Typical examples of the relative phase distribution of each pair. A, B, and C represent the runner's ID. The red horizontal dotted lines were the significance threshold.

Bibliography

[1] Ma et al., *Spontaneous synchronization of motion in pedestrian crowds of different densities*, Nat. Hum. Behav. **5**(4), 447-457, 2021.

[2] Schmidt et al., *Phase transitions in visual coordination Phase transitions and critical fluctuations in the visual coordination of rhythmic movements between people*, J. Exp. Psychol.: Hum. Percept. Perform. **16**(2), 227, 1990.

[3] Varlet and Richardson, *What would be Usain Bolt's 100-meter sprint world record without Tyson Gay? Unintentional interpersonal synchronization between the two sprinters*, J. Exp. Psychol.: Hum. Percept. Perform. **41**(1), 36, 2015.

*Email of the corresponding author: `furukawa.hiroaki95@gmail.com`

12th International Conference on Pedestrian and Evacuation Dynamics (PED 2025)
Prague, Czech Republic – September 9-12, 2025

Nudging pedestrian choice behavior with light color in a station

Arco van Beek*[1], Yan Feng[1], Serge P. Hoogendoorn[1], and Dorine C. Duives[1]

[1]Department of Transport & Planning, Delft University of Technology, Delft, the Netherlands

Abstract This study focuses on the effect of light color on pedestrian choice behavior in a station hall. Lights are added into the existing environment and dynamically switched between different light conditions, consisting of white, green and red lights. Preliminary findings show promising results with respect to use of lights to nudge pedestrians.

Keywords Pedestrian choice behavior, lights, crowd management, field study,nudging

Background

Crowd management becomes more important over time in order to manage larger crowds in their pedestrian infrastructures. Light is one of the potential crowd management measures and an ideal solution for many crowd operators. Since light is already present in most environments, it offers a cost-effective and easily adoptable solution compared to other measures. Additionally, it can be dynamically changed, highlighting an advantage for real-time crowd management. Previous works indicate that light affects pedestrian choice behavior [1, 2, 3]. Their findings show that pedestrians prefer pathways with brighter lights, and [1] also highlights the potential of using light color to nudge pedestrians to a particular path.

This study aims to build on these insights by conducting a large-scale field study at a train station. Because of regulations at the station, this study is limited to the effects of light color on pedestrian choice behavior. Within the train station, two different experimental designs were used to study whether the effects of the lights are universal in context.

Methodology: Description of the field study

This field study takes place at train station Amsterdam Bijlmer-Arena in the Netherlands. The station is well-known for its proximity to three large event venues, but it also serves thousands of daily commuters for work purposes. This makes the station an ideal environment to study crowd management, given its diversity in crowd population and variety in density.

This field study uses two experimental designs within the station. Firstly, an experimental set-up with two lights is used to investigate whether pedestrians can be nudged with light color when they only need to make a slight deviation from their path. Figure 1a shows that both doors are less than one meter apart. Thereafter, a second experimental set-up is used to study whether the effect observed in the first set-up remains when the deviation from their path becomes larger. This design employs lights above four adjacent doors with 2-5 meters between each, as shown in Figure 1b. The first set-up was used from 5 November 2024 to 5 February 2025, whereas the second set-up started on 5 February 2025 and is still ongoing.

In both experimental designs, we installed Philips Hue LED strips above the exit doors of the station hall. These lights were added to the existing environment and did not serve as ambient lighting. The first set-up employed three different light conditions - white (W), green (G), and red (R) - resulting in seven different conditions. These conditions included WW, WG, WR, GW, GR, RW, and RG, where the letters represent the light color enforced above door 1 and door 2, respectively. See Figure 1a for light condition GR. These conditions are dynamically changed, ensuring that each light condition is systematically shown at different moments of the day and week. Additionally, the second experimental set-up includes seven different conditions as well, which were determined based on the preliminary findings of the first set-up.

The data is collected by the crowd operator, NS, the Dutch railway operator. An overlapping system of stereo-vision and depth-sensors is used to derive anonymous trajectory data of pedestrians within the field of view of the sensor network. The dataset regarding the first set-up consists of approximately

*Email of the corresponding author: a.h.n.vanbeek@tudelft.nl

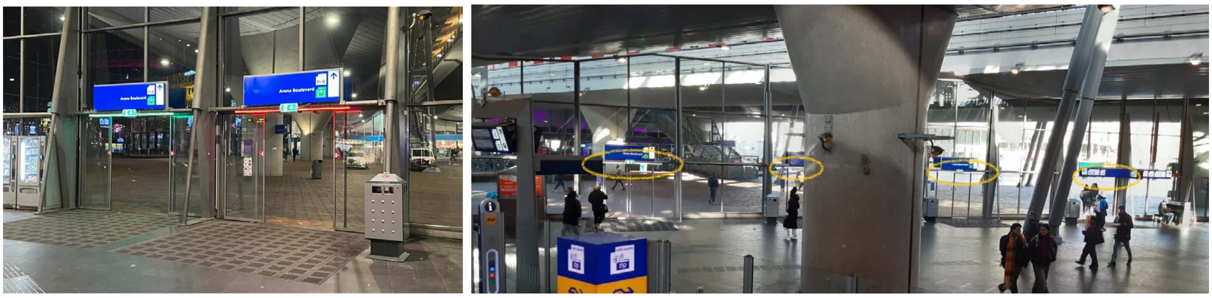

(a) Set-up 1, condition: Green - Red.
(b) Set-up 2, condition: White - White - White - White.

Figure 1: The experiment uses two different set-ups: (a) lights installed above two exit doors, and (b) lights installed above four adjacent exit doors, highlighted with yellow contours.

1,125,000 pedestrian trajectories, excluding pedestrians only transferring between platforms. Since the lights are installed inside the station hall, the authors argue that nudging is more likely for pedestrians leaving the hall. Therefore, the preliminary findings focus solely on the leaving pedestrians, consisting of almost 500,000 trajectories.

Preliminary findings and conclusion

Figure 2a indicates the percentage of pedestrians that left the station hall through door 1 - which is the left door in Figure 1a - for each light condition individually. Here, light condition WW is used as the baseline scenario, consisting only of standard colored lights. Figure 2b shows the variation in door usage for every condition compared to the baseline condition WW.

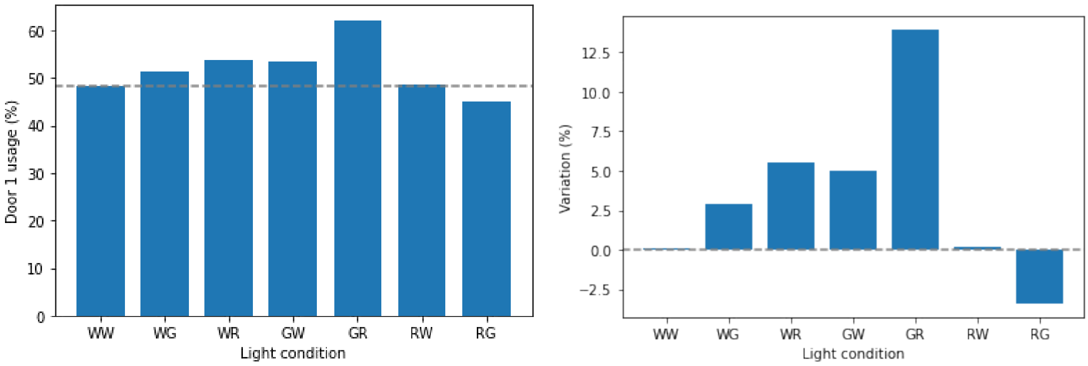

(a) Door 1 usage.
(b) Variation.

Figure 2: (a) Door 1 usage for every light condition, (b) the variation to the baseline condition WW.

The figures highlight an apparent effect of light color on the pedestrian exit choice. Specifically, when the light condition GR is used, there is a variation of more than 10% compared to the baseline condition. This highlights the potential of light color to nudge crowds; however, further data analysis is needed before drawing definitive conclusions.

In the upcoming period, we will analyze the gathered experimental data more in-depth, for instance, studying the impact of crowd density, time of day, type of crowd, and origin location. Thus, does the efficiency of light color intervention change due to external parameters? At the conference, we will present the findings of both set-ups at the train station.

Bibliography

[1] van Beek, A., Feng, Y., Duives, D.C., Hoogendoorn, S.P. *Studying the impact of lighting on the pedestrian route choice using Virtual Reality*, Safety Science **174**, 106467, 2024.

[2] Vilar, E., Rebelo, F., Noriega, P., Duarte, E., Mayhorn, C.B. *Effects of competing environmental variables and signage on route-choices in simulated everyday and emergency wayfinding situations*, Ergonomics **57(4)**, 511-524, 2014.

[3] Feliciani, C., Tanida, S., Jia, X., Nishinari, K. *Influencing pedestrian route choice through environmental stimuli: A long-term ecological experiment*, Journal of Disaster Research **19(2)**, 325-335, 2024.

12th International Conference on Pedestrian and Evacuation Dynamics (PED 2025)
Prague, Czech Republic – September 9-12, 2025

Deep Learning Approach to Force-Based Modeling of Pedestrian Flow in Bottleneck Scenarios

František Koutenský*[1,2], Daniel Vašata[1], and Pavel Hrabák[1]

[1]Faculty of Information Technology, Czech Technical University in Prague, Czechia
[2]Czech Institute of Informatics, Robotics and Cybernetics, Czech Technical University in Prague, Czechia

Abstract This work introduces a hybrid force-based concept for modeling pedestrian flow through bottlenecks, integrating Graph Neural Networks with the Social Force Model. While the model dynamics is driven by the social-force based equation of motion, the goal-directed, interaction, and environmental forces are learned from trajectory data in the Bottleneck Caserne dataset [3] using a neural network. Through data-driven simulations, this approach has been shown to be applicable to bottleneck flow modeling, accurately predicting pedestrian dynamics even in unseen scenarios.

Keywords pedestrian modeling, neural networks, bottleneck flow, crowd dynamics, force prediction.

Introduction and Model Architecture

Due to the increasing popularity of artificial intelligence, machine learning (ML) methods find applications in various scientific fields, including pedestrian flow modeling. Recent studies focus on the possibility of using ML methods as an alternative or supplement to classical knowledge-based (KB) models such as the Social Force Model (SFM) [2]. While deep learning models excel at capturing complex patterns, knowledge-based models offer interpretability and physical realism. Hybrid models aim to combine these strengths by embedding neural networks within KB frameworks [1].

This work proposes a novel hybrid approach, integrating a graph neural network based deep learning model into the SFM. The idea is to drive the dynamics by the social-force equation of motion

$$\ddot{\boldsymbol{x}}_t = \boldsymbol{F}_{\text{total}}\left(\boldsymbol{x}_t, \dot{\boldsymbol{x}}_t\right) = \boldsymbol{F}_{\text{goal}}\left(\boldsymbol{x}_t, \dot{\boldsymbol{x}}_t\right) + \boldsymbol{F}_{\text{int}}\left(\boldsymbol{x}_t, \dot{\boldsymbol{x}}_t\right) + \boldsymbol{F}_{\text{obs}}\left(\boldsymbol{x}_t, \dot{\boldsymbol{x}}_t\right), \tag{1}$$

letting the neural network learn the goal-directed, interaction, and environmental forces from trajectory data. The model is designed as Markovian, i.e., only current pedestrian positions, velocities, obstacles, and goals are used to predict the acting force. The model consists of three force modules, as shown in Figure 1.

Force Modules The goal-directed module uses *individual features* ($\mathbf{X}_{\text{ind}} \in \mathbb{R}^6$): current velocity (v_x, v_y), distance to goal (d_{goal}), direction vector to goal (d_x, d_y), and velocity toward goal (v_{goal}). Interaction module processes *interaction features* ($\mathbf{X}_{\text{int}} \in \mathbb{R}^{k\times 5}$) for k pedestrians including distance to pedestrian, direction vector, relative velocity, and alignment. Obstacle module processes *obstacle features* ($\mathbf{X}_{\text{obs}} \in \mathbb{R}^{m\times 9}$) for m obstacles including distances and direction vectors to obstacle endpoints and the closest point.

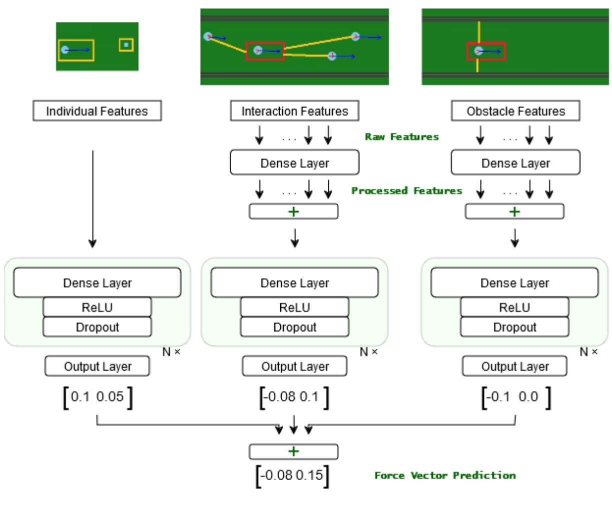

Figure 1: Model architecture.

Feature Transformation and Core Network Interaction and obstacle features are projected to a higher-dimensional space to enhance their representation before being aggregated via summation in a graph neural network way. The core network processes individual and aggregated interaction/obstacle features through feedforward blocks. The final force is the sum of the outputs from each force module analogous to (1).

*Email of the corresponding author: `koutefra@gmail.com`

Results and Conclusion

The network has hidden layer dimensions of 512, 1024, 512, 256, and 128. The first of these layers, with 512 dimensions, handles the pre-aggregation projection. Velocities are approximated using backward finite differences. The model is trained by minimizing the L_2 loss between predicted and true positions over 32 frames, using the ADAM optimizer (learning rate 0.001, dropout 0.5, batch size 64). We evaluate our model on the Bottleneck Caserne dataset [3], which provides diverse scenarios of pedestrian flow through bottlenecks. Scene `b160` was excluded from training for generalization testing. The training lasted 5 epochs.

Figure 2 shows predicted and true trajectories across scenes, including the unseen `B160` scene, demonstrating strong generalization. A video showcasing our model's performance, including the unseen `B160` scene, is available on YouTube: `https://youtu.be/E4YjcGl7qtw?si=zmSZiT57Dxf2-aix`. The model-generated trajectories qualitatively align with the true trajectories, validating our approach. However, the predicted trajectories exhibit higher speeds in the corridor after the bottleneck.

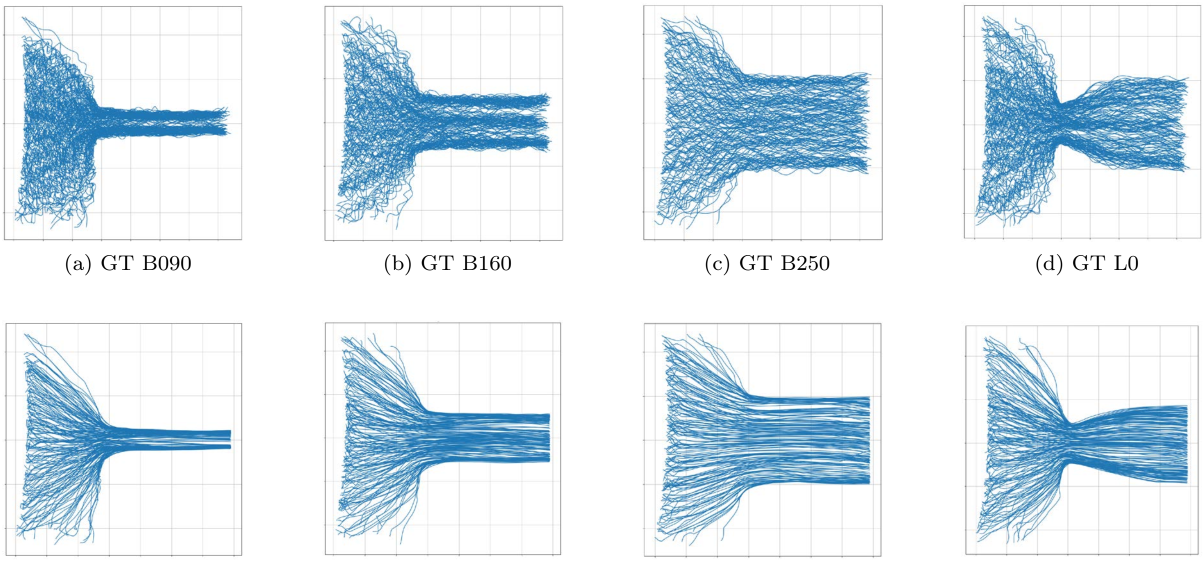

(a) GT B090 (b) GT B160 (c) GT B250 (d) GT L0

(e) Model B090 (f) Model B160 (g) Model B250 (h) Model L0

Figure 2: Comparison of ground truth (GT) and model-predicted trajectories across different scenes.

To summarize, the introduced data-driven neural network approach is capable to effectively capture pedestrian dynamics in bottleneck scenarios and even generalizes well to unseen scenes. However, this conclusion is limited only to the Caserne dataset [3], yet, the presented results promise that the concept can be applicable in more general layouts as well, which is the aim of our future work.

The source code will be released upon acceptance.

Acknowledgments: The work was supported by the CTU internal grant SGS23/210/OHK3/3T/18 and by the Ministry of Education, Youth and Sports within the dedicated program ERC CZ under the project ARTEMIS no. LL2405.

References

[1] Alessandro Antonucci, Gastone Pietro Rosati Papini, Paolo Bevilacqua, Luigi Palopoli, and Daniele Fontanelli. Efficient prediction of human motion for real-time robotics applications with physics-inspired neural networks. *IEEE Access*, 10:144–157, 2022.

[2] Raphael Korbmacher and Antoine Tordeux. Review of pedestrian trajectory prediction methods: Comparing deep learning and knowledge-based approaches. *IEEE Transactions on Intelligent Transportation Systems*, 23(12):24126–24144, 2022.

[3] Armin Seyfried, Maik Boltes, Bernhard Steffen, Tobias Rupprecht, Andreas Schadschneier, and Andreas Winkens. Bottleneck Caserne dataset, 2006. Data available at `http://ped.fz-juelich.de/da/2006bottleneck`.

Timetable

Talk index

12th International Conference on Pedestrian and Evacuation Dynamics (PED 2025)
Prague, Czech Republic – September 9-12, 2025

RL-Godot Pedestrian Simulation: Curriculum–Based Reinforcement Learning for Pedestrian Simulation

Giuseppe Vizzari*[1], Andrea Falbo[1], Ruben Tenderini[1], and Daniela Briola[1]

[1]University of Milano-Bicocca, Italy

Abstract The abstract describes a research effort aimed at developing a Reinforcement Learning based open source software system supporting the study of pedestrian and crowd dynamics. We briefly discuss the system and a first experimental application aimed at evaluating its adequacy to simulate medium to high local density situations.

Keywords Reinforcement Learning, Curriculum Learning, Pedestrian simulation

Extended abstract

Reinforcement Learning (RL) [1] is a machine learning approach in which an agent learns how to behave in a given environment in which it is situated, thanks to a feedback signal provided by the environment itself as a consequence of an action carried out by the agent. This feedback, a scalar reward signal, is much less informative than the loss function value typical of neural network training. Nonetheless, it is applicable in cases where there are difficulties in achieving sufficiently large and varied data sets for supervised training, but an evaluation of the quality of an action can be computed.

Pedestrian simulation, despite being a very active field of research, has provided empirical evidence allowing for such an evaluation. Recent works have shown that Deep Reinforcement Learning (DRL) (i.e. RL techniques employing deep neural networks in their functioning) can produce policies producing plausible pedestrian behaviors. In particular, [2] employed a system based on Unity and the associated ML-Agents toolkit[1], as technical enabling technologies, coupled with a curriculum learning approach, to achieve a general model that produces plausible pedestrian behaviors in environments not approached during training. Employing a game engine allows both performing simulations and exporting data for external analyses, but it also allows employing the achieved models within games, interactive applications, even in Vitual Reality experiments for acquiring empirical data about pedestrian behavior.

Unity, however, is not an open source platform, and ML-Agents does not represent a generalized library providing a wide range of DRL algorithms, but rather an ancillary complement to Unity. We decided therefore to develop an analogous platform only employing open source technologies and in particular: (i) the **Godot** [2] game engine, (ii) the **Godot RL Agents** library [3] that grants the possibility to connect Godot to external RL and DRL libraries such as **Stable Baselines** [4], an open source library providing a set of reliable implementations of a large number of DRL in PyTorch; data about the simulated scenarios can then be plotted employing **PedPy**[5], an open source e library for pedestrian movement analysis. The result is RL-Godot Pedestrian Simulation [6], a system granting the possibility to perform simulations in an environment created respecting specific requirements employing some already available agent behavioral models, or even customize the training process to generate new behavioral models.

First of all, we reproduced the results of the above-mentioned work [2], then we considered situations characterized by a higher level of pedestrian density, such as the scenarios described in [3] and [4]: in this kind of situation, the model achieved through the previous work, and the enclosed training process, did not lead to plausible results. Our conjecture was that the reward function was excessively penalizing agents for getting close to other ones. We performed a new training process, reducing the penalization for the invasion of proxemic space, as well as including in the training curriculum additional scenarios in which learning agents encountered higher density situations.

*Email of the corresponding author: `giuseppe.vizzari@unimib.it`
[1]`https://github.com/Unity-Technologies/ml-agents`
[2]`https://godotengine.org/`
[3]`https://github.com/edbeeching/godot_rl_agents`
[4]`https://github.com/DLR-RM/stable-baselines3`
[5]`https://pedpy.readthedocs.io/`
[6]`https://github.com/Ruben-2828/RL-Godot-Pedestrian-Simulation`

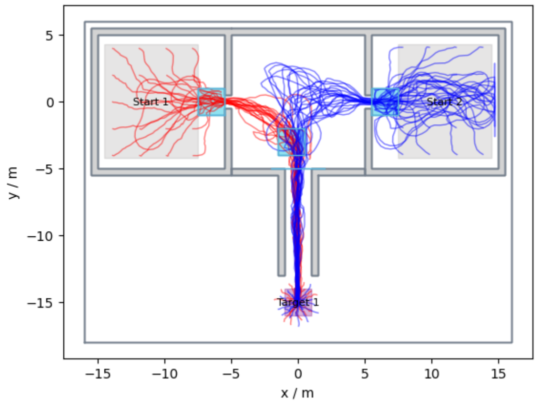

(a) Trajectories generated by agents in the center door connection

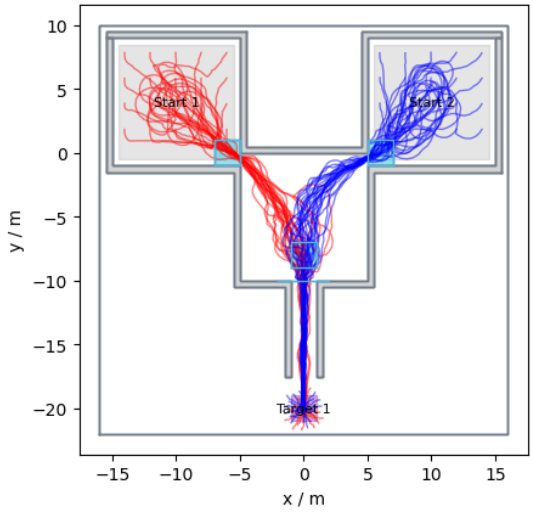

(b) Trajectories generated by agents in the corner door connection

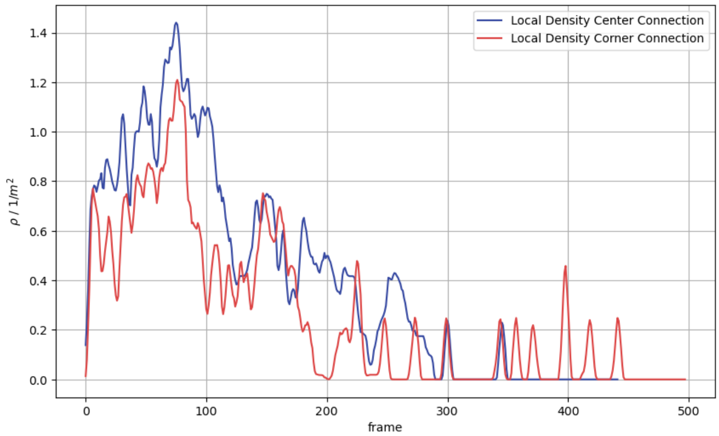

(c) Overall measured density in the central room

Figure 1: Results achieved in the scenario discussed in [3].

The achieved pedestrian behavioral model performed significantly better than the previous one: Fig. 1(a) and Fig. 1(b) respectively show trajectories in the two considered spatial configurations of the environment, and Fig. 1(c) show the level of density in the monitored area (highlighted as a cyan square in the previous figures) throughout the simulation. Results are encouraging and comparable to those reported in the cited papers.

Bibliography

[1] Sutton, R.S. and Barto, A.G., 1998. Reinforcement learning: An introduction (Vol. 1, No. 1, pp. 9-11). Cambridge: MIT press.

[2] Vizzari, G. and Cecconello, T., 2022. Pedestrian simulation with reinforcement learning: A curriculum-based approach. Future Internet, 15(1), p.12.

[3] Ezaki, T., Yanagisawa, D. and Nishinari, K., 2012. Pedestrian flow through multiple bottlenecks. Physical Review E—Statistical, Nonlinear, and Soft Matter Physics, 86(2), p.026118.

[4] Adrian, J., Seyfried, A. and Sieben, A., 2020. Crowds in front of bottlenecks at entrances from the perspective of physics and social psychology. Journal of the Royal Society Interface, 17(165), p.20190871.

12th International Conference on Pedestrian and Evacuation Dynamics (PED 2025)
Prague, Czech Republic – September 9-12, 2025

Generative Agents in Crowd Simulation: A Cognitive Approach with Large Language Models

Nizar Ntarouis*[1] and Roland Geraerts[2]

[1]Independent Researcher
[2]Utrecht University

Abstract Crowd simulation is a powerful tool used in fields such as urban planning, emergency response, and entertainment to model and predict human movement and behavior in various scenarios. As society becomes increasingly complex and interconnected, the need for simulations that accurately capture human behavior at both the individual and group level grows. Understanding these interactions can help institutions and experts develop more effective mitigation strategies in dynamic social environments. This research explores the potential of the power of Large Language Models (LLMs) in crowd simulations, leveraging their capabilities to model individual behavior and enable the emergence of realistic crowd dynamics through agent-level interactions. We propose a novel architecture that integrates key cognitive components—such as perception, planning, memory, reflection, and action—on an algorithmic level. This approach allows generative agents to process environmental and social contexts in a human-like manner. Our findings show that these agents exhibit diverse and contextually appropriate behaviors, closely resembling human decision-making, particularly in crisis situations.

Keywords Crowd Behavior, Large Language Models, Cognitive Models, Crisis Scenarios

Introduction

In the rapidly advancing field of crowd simulation, emulating the complexity of human interaction is essential, as its fidelity has profound implications for crisis management, urban planning and public safety. Central to this quest is the process of pattern extraction through the concept of Patterns of Life (PoL) [1], which refers to the repetitive and structured aspects of existence, whether societal, individual, or organizational level. These patterns may involve cycles, rhythms, or structures that are recurrent and contribute to the overall order and functioning of a particular system.

Large Language Models (LLMs) offer a transformative capability in this regard, enabling the nuanced simulation of individual behaviors and interactions [2] [3]. Our goal is to study patterns related to observation and analysis of behaviors in crisis and evacuation scenarios. This includes examining the thought processes of individual actors, as well as the interactions and collisions that occur both internally (within the actors' minds and their mental models of the world) and externally with nearby actors.

Figure 1: Festival in Full Swing: Generative agents mingle, form clusters, and navigate through a vibrant festival, showcasing the emergent complexity of crowd dynamics.

Traditional Methodologies and PoL research often fall short, oversimplifying human cognition and complexities by generalizing and focusing on clusters of group movement and navigation [4]. These

*Email of the corresponding author: `nizardarwish001@gmail.com`

methods typically overlook subtleties of individual cognition -the thoughts, decisions, and interactions that result in the passive formation of crowds. Addressing this gap necessitates a shift from group-centric modeling to ones centered on individual cognition. Furthermore, understanding crowd dynamics involves recognizing emergent properties that arise from individual interactions but are not inherent in isolated individuals.

In our exploration of the vast network of human behavior, we pose the question: Can Large Language Models be used to simulate realistic crisis scenarios? This inquiry unfolds into two avenues of exploration, which underpin aspects and challenges of the complex network of interplay that defines crowd behavior:

- Can LLM-based agents exhibit human-like reasoning and communication, leading to emergent behavioral patterns that closely resemble those observed in real-world human interactions?
- What are the performance and scalability limitations of LLM-based simulations, particularly in complex scenarios involving large populations?

Methodology

Achieving the creation of artificial agents capable of natural language interactions and emergent social behaviors [5] [6] represents a significant challenge in artificial intelligence, particularly at the micro level of human behavior. This study leverages recent advancements in generative AI and cognitive models, centering around a Large Language Model (LLM) as the primary architecture controller [7]. The architecture integrates cognitive modules that enable agents to navigate environments and facilitate communication between the LLM and geometric simulations. We aim to determine whether generative agents within this setup could effectively coordinate, form relationships, carry out activities, and respond dynamically in a virtual context.

We propose a novel architecture for crowd simulation that integrates cognitive components—such as perception, planning, memory, reflection, and action—on an algorithmic level to enable generative agents to process environmental and social contexts in a human-like manner [8]. Inspired by dual-process theories of cognition [9], we deploy two systems embedded inside the agentic framework: the Intuitive and Deliberative systems.

Two Thinking Systems

System 1 operate automatically, driven by heuristics from previous experiences and emotions. In the context of generative agents, it is activated for events requiring immediate responses, using predefined symbolic decisions to each agent's personality.

System 2 involves deliberate and logical processing, requiring more cognitive resources. Representing the LLM architecture, System 2 is responsible for analyzing significant events and constructing rational responses. This system enables agents to process information, consult memories, and develop plans effectively.

Generative agents operate within dynamic environments, influenced by current settings and past experiences. This study proposes an innovative agent architecture that integrates a large language model with mechanisms for gathering, processing, and utilizing information.

Architecture Design

The architecture comprises a profiling module, memory module, reflection module, planning module, and action module, all working in harmony to enable for real-time dynamic simulations, critical for multi-agent environments.

This comprehensive framework allows generative agents to exhibit sophisticated behaviors that closely resemble human cognition, enhancing the realism and applicability of simulations. As a result, agents naturally form group patterns that reflect real-world human behavior.

Results

Evaluating the realism and effectiveness of generative agents is inherently complex, requiring a nuanced approach that examines behavior across multiple crisis scenarios. We conducted experiments in various simulated evacuation scenarios, comparing the emergent behaviors of LLM-based agents to those observed in human studies. Furthermore, a subjective evaluation was conducted to assess the agents' realism, emotional intelligence, behavioral diversity, and resemblance to human traits. Our evaluation framework concentrates on four critical indicators:

- **Pattern Comparison:** Agents' behaviors were aligned with documented real-world patterns, evaluated on both micro and macro scales. Participants confirmed the realism of the simulated behaviors, although some robotic and uncanny actions were noted.
- **Crowd Scalability:** The architecture's scalability was tested by examining the relationship between scalability and real-time responsiveness. Our trials demonstrated that the system maintained performance with up to 150-200 agents before encountering computational bottlenecks, primarily due to the processing constraints of the LLM models used.
- **Agent Interviews:** We leveraged the generative agents' ability to engage in natural language by conducting interviews. Through these interactions, we analyzed their capacity to recall, reflect, plan and reason about past experiences and memories. Results indicated that agents could plan future actions, understand concepts of time and place, perceive their surroundings, and respond appropriately to events within their simulated lifetime.
- **Patterns of Life Scoring:** Utilizing Silverman's scoring matrix for Patterns of Life (PoL) simulations [10], our model achieved a score of 8/9, indicating a high level of behavioral fidelity.

Our findings demonstrate that the agents exhibit diverse and contextually appropriate behaviors, closely resembling human decision-making in crisis situations. Future research could explore the use of fine-tuned LLMs to capture a broader spectrum of human emotions and decision-making nuances. Further enhancing agents' emotional intelligence and their ability to respond to complex social cues.

Bibliography

[1] R. Hubal and E. A. C. Hubal, "Simulating patterns of life: More representative time-activity patterns that account for context," *Environment International*, p. 107753, 2023.

[2] L. Wang, C. Ma, X. Feng, Z. Zhang, H. Yang, J. Zhang, Z. Chen, J. Tang, X. Chen, Y. Lin *et al.*, "A survey on large language model based autonomous agents," *Frontiers of Computer Science*, vol. 18, no. 6, p. 186345, 2024.

[3] S. Yao, J. Zhao, D. Yu, N. Du, I. Shafran, K. Narasimhan, and Y. Cao, "React: Synergizing reasoning and acting in language models," 2023. [Online]. Available: https://arxiv.org/abs/2210.03629

[4] P. Charalambous, J. Pettre, V. Vassiliades, Y. Chrysanthou, and N. Pelechano, "Greil-crowds: Crowd simulation with deep reinforcement learning and examples," *ACM Transactions on Graphics (TOG)*, vol. 42, no. 4, pp. 1–15, 2023.

[5] J. S. Park, L. Popowski, C. Cai, M. R. Morris, P. Liang, and M. S. Bernstein, "Social simulacra: Creating populated prototypes for social computing systems," in *Proceedings of the 35th Annual ACM Symposium on User Interface Software and Technology*, ser. UIST '22. New York, NY, USA: Association for Computing Machinery, 2022. [Online]. Available: https://doi.org/10.1145/3526113.3545616

[6] L. Wang, J. Zhang, X. Chen, Y. Lin, R. Song, W. Zhao, and J.-R. Wen, "Recagent: A novel simulation paradigm for recommender systems," 06 2023.

[7] S. S. Kannan, V. L. N. Venkatesh, and B.-C. Min, "Smart-llm: Smart multi-agent robot task planning using large language models," 2024. [Online]. Available: https://arxiv.org/abs/2309.10062

[8] J. S. Park, J. O'Brien, C. J. Cai, M. R. Morris, P. Liang, and M. S. Bernstein, "Generative agents: Interactive simulacra of human behavior," in *Proceedings of the 36th Annual ACM Symposium on User Interface Software and Technology*, 2023, pp. 1–22.

[9] D. Kahneman, *Thinking, Fast and Slow.* New York: Farrar, Straus and Giroux, 2011.

[10] B. G. Silverman, G. Bharathy, and N. Weyer, "What is a good pattern of life model? guidance for simulations," *Simulation*, vol. 95, no. 8, pp. 693–706, 2019.

12th International Conference on Pedestrian and Evacuation Dynamics (PED 2025)
Prague, Czech Republic – September 9-12, 2025

Variational Modeling for paths through static crowds

Apoorva Singh*[1], Rui M. Castro[2], Maarten Schoukens[3], and Alessandro Corbetta[1]

[1]Department of Applied Physics and Science Education, TU Eindhoven, The Netherlands
[2]Department of Mathematics and Computer Science, TU Eindhoven, The Netherlands
[3]Department of Electrical Engineering, TU Eindhoven, The Netherlands

Abstract We use variational modeling to quantitatively predict the path of an intruder undergoing the N-to-1 interaction while crossing a static crowd. Leveraging large-scale real-life data from Eindhoven Centraal Station, NL, we learn a cost model that stochastically generates trajectories over a discretized domain.

Keywords Pedestrian dynamics, Real-life Data, Variational modeling, Pedestrian paths

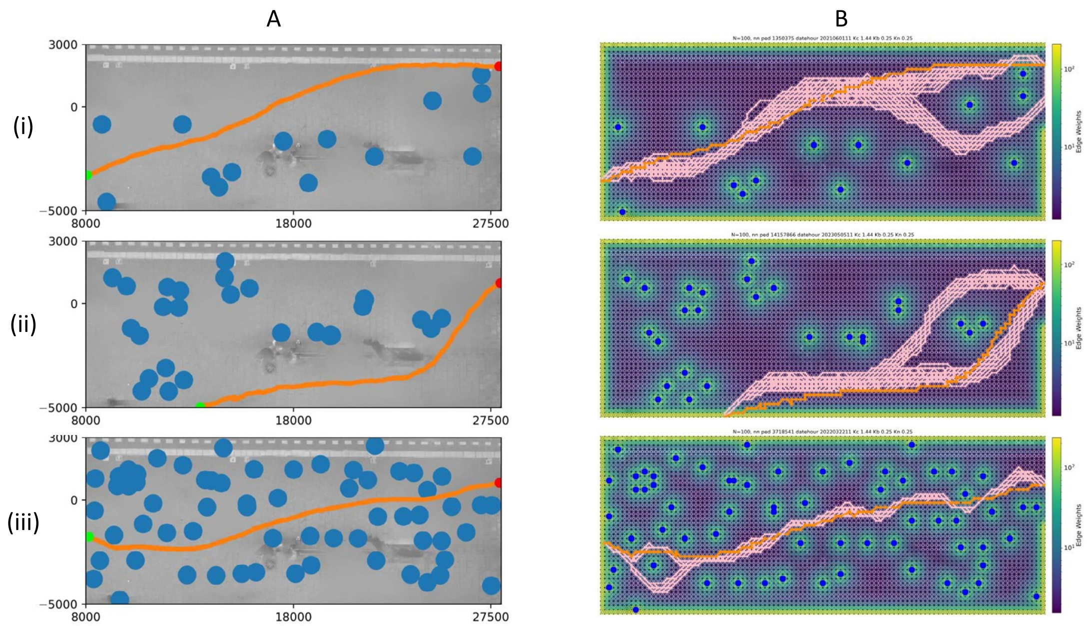

Figure 1: A: Examples of instances of N-to-1 interaction for different sizes of static crowd. Blue dots represent static pedestrians and orange curves represent intruder trajectories. B: Corresponding discrete cost landscapes with original trajectories in orange and stochastically generated trajectories in pink.

The interactions between individuals in a crowd are a major driver of crowd dynamics. In this work, our aim is to develop quantitative, stochastic models for a key type of interaction, which we call the N-to-1 interaction, where an intruder moves through a crowd of stationary pedestrians. Most prior efforts have focused on analyzing laboratory data [1, 2], which is constrained by limited sample size and may not accurately reflect real-world conditions. In contrast, we leverage large-scale, real-life data, which enables us to better understand and quantify the inherent stochasticity in path choice. Empirical evidence suggests that most pedestrians seek to minimize discomfort by avoiding excessive proximity to others while simultaneously reducing effort by choosing shorter, straighter paths [3]. To capture this trade-off, various models for 'rational pedestrians' have been proposed, where pedestrians optimize utility [4]. In these models the pedestrians walk by minimizing a cost function that accounts for factors such as proximity to others, total path length, anticipation of others' movements, etc. [5]. However, without real-life data for validation, such models remain largely qualitative. By utilizing real-world data, we can develop quantitative models that more accurately describe pedestrian behavior.

*Email of the corresponding author: a.singh2@tue.nl

The purpose of this study is to understand the factors that inform an intruder's choice of path while crossing, and build a stochastic model that predicts the path. We establish a cost function C that penalizes the following along the intruder's path: total distance walked, interaction with crowd members $I_C(l)$ $(= K_C\, r_{crowd}^{-2}(l))$, and interaction with boundary/obstacles $I_B(l)$ $(= K_B\, r_{obs}^{-3}(l))$. We add a noise $\xi(l) = K_n \mathcal{N}^l(0,1)$, to account for the stochasticity in choice. $\theta \equiv \{K_C, K_B, K_n\}$ are the model parameters. The intruder chooses a path Υ that minimizes the cost $C(\Upsilon)$ over it:

$$C(\Upsilon) = \int_{\Upsilon} (1 + I_C(l) + I_B(l) + \xi(l))dl \qquad (1)$$

One of our research questions is the choice of model for I_C (and I_B), with candidates such as linear superposition (similar to the 'social force' model), nearest-neighbor interaction, and K nearest-neighbor interaction. We start with a crowd interaction term that goes as $1/r^2$ to mimic a repulsion force.

We use pedestrian trajectory data over a region $(20m \times 8m)$ of the platform of the Eindhoven Central train station, The Netherlands (tracking accuracy about 1cm at 10Hz, $\sim$ 3 years of data). From this data we extract instances of N-to-1 interaction at varying densities (Fig.1 A): we build a dataset of 1864 distinct instances. To numerically approximate the path that minimizes the cost in equation (1), we discretize the region of consideration by overlaying a gridded spatial network on it (Fig.2(a)). The weight at any edge is according to the interaction terms in eq. 1, and the cost of a path on the graph is the sum of weights of all the edges it passes through. Using Dijkstra's algorithm we can determine the path with the least cost. Different realizations (with different random noise) generate different paths. Figure 1 shows some instances from the dataset in column A, and the corresponding discrete cost landscapes, created using the nearest-neighbour interaction model with manually chosen parameters, and predicted paths in column B. The predicted paths (in pink) typically diverge into two or more distinct groups of paths, showcasing a meta-stable phenomena, successfully capturing the real-life stochasticity. Fig. 2(b) shows the distribution of costs of the real life trajectories, using manually selected parameters θ, according to different crowd interaction models. It suggests that the nearest-neighbours model (for the chosen parameters) is closest to reality as the cost distribution is minimum. The results highlight the strong quantitative potential of the modeling approach. To get a better fit, the model parameters can be learned from the dataset. The weights and thus cost function can be parameterized in terms of the parameters θ. In this contribution, we will provide a formal model estimation of a parameterized cost function using data driven techniques like system identification and machine learning.

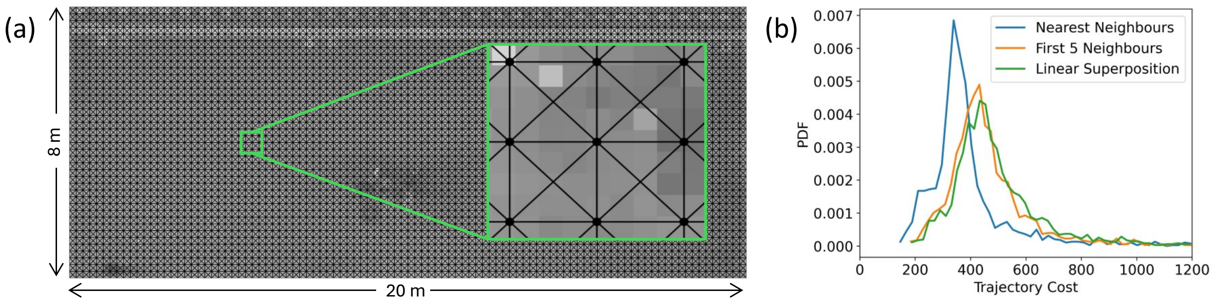

Figure 2: (a) Gridded spatial network overlaid on the region of consideration. (b) Distribution of costs for the real life trajectories from the dataset according to different crowd interaction models.

References

[1] Wang, J., Lv, W., Jiang, H., Fang, Z., & Ma, J. (2023). *Exploring crowd persistent dynamism from pedestrian crossing perspective: An empirical study.* Transportation research part C: emerging technologies, 157, 104400

[2] Nicolas, A., Kuperman, M., Ibañez, S., Bouzat, S., & Appert-Rolland, C. (2019). *Mechanical response of dense pedestrian crowds to the crossing of intruders.* Scientific reports, 9(1), 105.

[3] Arechavaleta, G., Laumond, J. P., Hicheur, H., & Berthoz, A. (2008). *An optimality principle governing human walking.* IEEE Transactions on Robotics, 24(1), 5-14.

[4] Cristiani, E., Piccoli, B., & Tosin, A. (2014). *Multiscale modeling of pedestrian dynamics* (Vol. 12). Springer.

[5] Hoogendoorn, S., & HL Bovy, P. (2003). *Simulation of pedestrian flows by optimal control and differential games.* Optimal control applications and methods, 24(3), 153-172.

[6] Pouw, C. A. S., van der Vleuten, G. G. M., Corbetta, A., & Toschi, F. (2024). Data-driven physics-based modeling of pedestrian dynamics - dataset: Pedestrian trajectories at Eindhoven train station [Data set]. Zenodo. https://doi.org/10.5281/zenodo.13784588

12th International Conference on Pedestrian and Evacuation Dynamics (PED 2025)
Prague, Czech Republic – September 9-12, 2025

Different ways of coordinating behavioral repertoires in crowds

Anna Sieben*[1,2], Mira Küpper[1,2], Tom Postmes[3], and Armin Seyfried[1,2]

[1]Forschungszentrum Jülich, Institute for Advanced Simulation (IAS-7), Germany
[2]Bergische Universität Wuppertal
[3]University of Groningen, Faculty of Behavioural and Social Sciences, Netherlands

Abstract This study explores four modes of crowd coordination: mechanical (uniform movement with a leader or predefined choreography), physical (movement dictated by environmental constraints), organic (dynamic leadership in small interactive groups), and individual (independent movement requiring coordination to avoid collisions). Experiments manipulating physical and social factors confirmed that these modes influence crowd organization, movement patterns, and leadership dynamics. The findings highlight how different coordination modes shape crowd behavior, contributing to varying levels of homogeneity and heterogeneity in movement.

Keywords Behavioral repertoires, Crowd movement, Coordination, Crowd experiments

Movement repertoires in pedestrian behavior

Questions about the supposed homogeneity and heterogeneity of crowd behavior may be more than a century old, but they remain a central puzzle for our field. In prior research we have developed an analytical framework to describe and understand the different movement behaviours seen in crowds [1]. Based on past behavioral observation work [2, 3] we developed a method which focuses on forms of behavior seen in crowds that observers and participants are likely to see as socially meaningful. We call these behavioral repertoires. Some repertoires are specific for individuals (standing aside), some for small interactive subgroups (chatting) and some for larger subgroups (queueing). The fact that these behaviours are socially meaningful to participants and onlookers is consequential: it means that all involved have cultural and embodied understandings not just of how to move in relation to other actors, but also what norms apply, what atmosphere and emotions are fitting, etc.

Current research: Coordination in crowds

The transitions between these ways of behaving can occur fluently, typically without overt gesturing, and sometimes rapidly [1]. This raises the question: how do these patterns emerge and propagate? To study this, we conducted a set of small experiments (20-30 participants). We directly manipulated the physical, collective and inter-personal factors by which we hypothesize crowds coordinate their movement. We hypothesise that there is not one way to coordinate in crowds but several, and that each mode of coordination has its own characteristic pathways for social organisation. First, members of a crowd can feel as one and intend to move in uniform (collective/mechanical). In this case, the movement could be choreographed from the beginning (a dance performance in which everyone knows the steps, marching soldiers who know the drill) or there could be an initiator or 'leader'. Second, members can move uniformly for non-social reasons, for example when the physics of the situation forces them to form lanes or keep a certain formation, speed or distance (physical). They may orient themselves to relevant physical cues, or coordinate with other people's bodies and movement. Third, crowd coordination can start from interactive dyads or small groups who communicate, often non-verbally, how they are going to move together (organic). In this configuration, leadership is dynamic and there are potentially several leaders of small groups in the crowd. Finally, people can move within a crowd on their own, following their own rhythm but still, they need to coordinate to avoid collisions or blockages (individual).

In our analysis of the experiment we have tried to include and where possible integrate the physical and social psychological characteristics of the movement in each of these four conditions. Thus, we have developed a set of quantitative movement parameters to describe the different forms of coordination, unity and 'leadership'. These results are complemented by post-experimental questionnaires which shed light

*Email of the corresponding author: an.sieben@fz-juelich.de

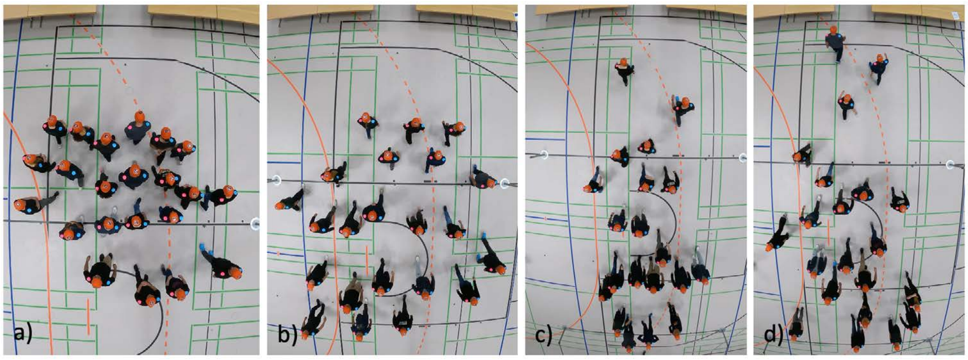

Figure 1: Coordination of movement: a) collective/mechanical, b) physical, c) organic/small groups, d) individual.

on the subjective experience of these variables. Finally, with qualitative analysis of observational data, we dig deeper into the behavioral dynamics of coordination and leadership across the four conditions.

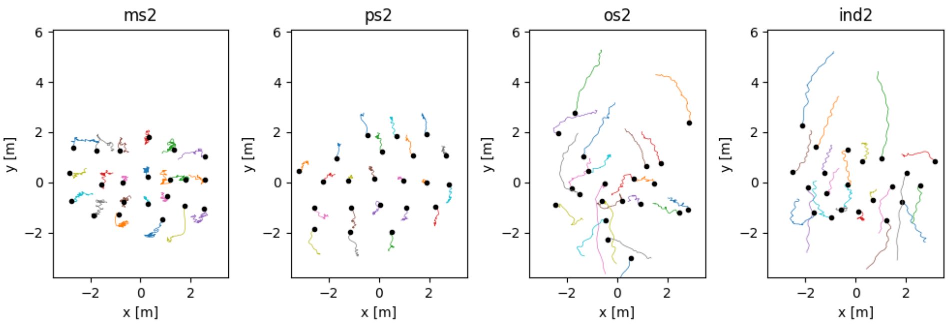

Figure 2: Crowd synchrony plots. In order to visualise the relative changes in position of the participants in relation to one another, the graph shows the 'trajectories' of the centre of mass system (center of mass at (x,y) = (0,0)). Conditions from left to right: 'mechanical', 'physical', 'organic' and 'individual'. While the relative positions change only slightly for the condition 'mechanical' and 'physical', the variation is significant for the individual and organic conditions. In the organic condition, parallel trajectories indicate the movement of small groups or couples.

Together, the results suggest that it is useful to distinguish between these four modes of coordination in crowds, that these coordination modes are consequential for the kinds of actions displayed and hence also for the degree of homogeneity and heterogeneity found in crowds, and that these coordination modes are associated with fundamentally different ways of attending and responding to others, their movements and gestures.

Bibliography

[1] Sieben, A., Postmes, T.*Behavioural repertoires in moving crowds: an observational approach*, Royal Society Open Science **12(2)**, 241561, 2025.

[2] Philpot, R., Levine, M. *Evacuation Behavior in a Subway Train Emergency: A Video-based Analysis*, Environ Behav. **54(2)**, 383–411, 2022.

[3] Schweingruber, D., McPhail, C., *A Method for Systematically Observing and Recording Collective Action*, Sociol Methods Res. **27(4)**, 451–98, 1999.

12th International Conference on Pedestrian and Evacuation Dynamics (PED 2025)
Prague, Czech Republic – September 9-12, 2025

Improving Railway Platform Safety via Awareness Campaign

Stephanie Baumann*[1] and Ernst Bosina[1]

[1]SBB AG

Abstract To address the challenges of managing crowded platforms during peak hours at Swiss railway stations, we implemented a sensitization campaign to enhance passenger safety, using Sursee Station as a case study. The campaign employed auditory announcements and visual posters to raise awareness about train passage risks. Results showed that auditory announcements were more effective, with 40% of passengers reporting increased awareness and behavioural adjustments. Future research will focus on the long-term impact and the potential for periodic reinforcement to sustain safety improvements.

Keywords railway station, platform safety, pedestrian tracking, real-life observation

Introduction and Background

At Swiss railway stations, no physical barrier exists between the danger zone at the platform edge and the safety zone in the middle of the platform. Therefore, the platform design and the behaviour of the users must ensure the passenger safety, also during peak hours and while considering the expected increase in passenger demand. One common approach to accommodate more passengers involves platform expansions. However, such expansions are costly, spatially constrained, and can take several years to implement. Consequently, there is an need for alternative solutions that can be deployed swiftly while still providing significant benefits to passengers. One crucial aspect of these alternatives is the ability to influence passenger behaviour to enhance safety and efficiency on the platforms [1].

Sursee Station, located in Central Switzerland, is a medium-sized station featuring an island platform and a side platform. The island platform (2/3) is relatively narrow and is already highly utilized during peak hours. Additionally, two trains frequently stop on the same track (track 2) simultaneously. Specifically, the S-Bahn from Lucerne stops at the far end of the platform, necessitating that all disembarking passengers walk at least 100 meters to the nearest exit (see Figure 1). During this circulation period, an intercity train passes through on track 3. The direction of travel obscures the approaching train from the passengers' view, leading to recurrent hazardous situations. Passengers tend to walk close to the platform edge and are often startled by the approaching train. Although no accidents have occurred to date, this scenario poses a significant risk that needs to be addressed.

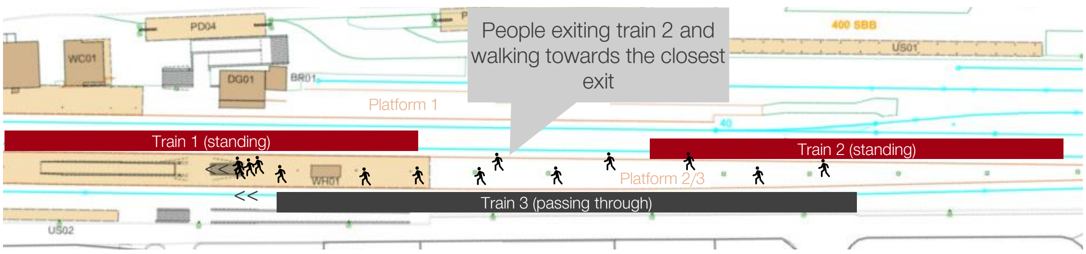

Figure 1: Station layout and the train positions during the alighting process from train 2

Method

Given that a platform expansion is not feasible in the near term for Sursee Station, alternative approaches were explored. We implemented a sensitization campaign, aimed at increasing passengers' awareness of the risks associated with train passages and encouraging them to remain within the designated safety lines, thereby avoiding the danger zone. The campaign disseminated this information through both auditory

*Email of the corresponding author: stephanie.baumann@sbb.ch announcements in the incoming train and visual posters displayed at the station. Both messages were kept short so that they can be quickly grasped.

Conducted over a two-week period in the spring of 2024, the campaign's efficacy was evaluated using a multi-method approach. Surveys were distributed at the station before, during, and after the campaign. The survey was done by distributing leaflets with a QR-code and a small chocolate as an incentive. Passenger movements on the platform were recorded and analysed using a sensor, which records anonymous tracking data as well as the nearby train movement.

Results and Discussion

For the survey, 3000 leaflets were distributed which resulted in an overall return rate of 22%. The participants showed a good distribution concerning age, gender and frequency of the station usage. The results revealed that visual posters were largely ineffective; only approximately 25% of passengers noticed and read the posters, and a mere 8% reported that the posters influenced their behavior (see Figure 2). Conversely, auditory announcements proved more effective: nearly 40% of passengers indicated that the announcements heightened their awareness of train passages and prompted them to adjust their behaviour accordingly. Analyses to determine whether age and/or gender had an impact on the results were also conducted. The older the passengers were, the more they listened to the announcements (under 18 years: 31%, over 60 years: 68%). Gender did not show a significant difference in response to the announcements, but men noticed the posters significantly more often than women (29% compared to 12%). The survey conducted after the campaign showed a slight reduction in the percentage of people who reported a change in behaviour. Therefore, the long-term effectiveness is not necessarily guaranteed and requires further consideration.

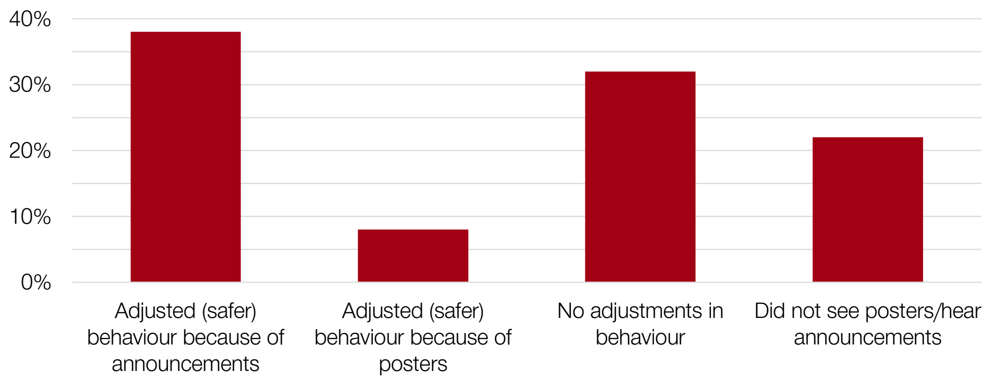

Figure 2: Self declared impact of the campaign on the customers

Sensor data corroborated these findings, showing a consistent decline in the number of individuals in the danger zone during the campaign and in comparison to the initial measurements before. Initially, an average of 5% of passengers were outside the white safety lines during the described situation in the morning. After the campaign, this number decreased to 3.1%. In the evening, a reduction was also measurable, although slightly less pronounced than in the morning. Future research will focus on assessing the long-term impact of the campaign by distributing follow-up surveys at the station. It is hypothesized that the campaign's effect may diminish over time. Therefore, periodic reinforcement of the campaign and announcements throughout the year is being considered. A permanent implementation is avoided due to the anticipated habituation effect.

The findings highlight the potential of auditory announcements as a cost-effective and immediate measure to enhance passenger safety on overcrowded platforms. Further studies are warranted to explore additional behavioral interventions and their long-term efficacy in various station environments.

Bibliography

[1] Schneider, A., Krueger, E., Vollenwyder, B., Thurau, J., Elfering, A., *Understanding the relations between crowd density, safety perception and risk-taking behavior on train station platforms: A case study from Switzerland*, Transportation Research Interdisciplinary Perspectives **10**, 100390, 2021.

12th International Conference on Pedestrian and Evacuation Dynamics (PED 2025)
Prague, Czech Republic – September 9-12, 2025

Crowding Perceptions at Large Business Events: Insights from Beacons and Surveys

Sakurako Tanida[1,2], Hyerin Kim[3], Claudio Feliciani[1,2], Xiaolu Jia[4,1,2], Akira Takahashi[5], Tetsuya Aikoh[3], and Katsuhiro Nishinari[1,2]

[1]Department of Aeronautics and Astronautics, School of Engineering, The University of Tokyo
[2]Research Center for Advanced Science and Technology, The University of Tokyo
[3]Research Faculty of Agriculture, Hokkaido University
[4]Beijing Key Laboratory of Traffic Engineering, Beijing University of Technology
[5]D3 Center, Osaka University

Abstract We quantitatively assess how attendees perceive congestion based on survey responses compared to crowd levels measured by beacon data. Our findings show that attendees demonstrated better perception accuracy than random guessing for time and location, whereas density recognition from images was less effective. Additionally, we identified a temporal bias, with attendees tending to report congestion at times closer to when they filled out the survey. These insights contribute to enhancing crowd management strategies and the overall experience at large-scale events.

Keywords Crowd management, Beacon data, Survey analysis, Congestion perception, Crowd dynamics

Introduction

Managing the flow and density of people at large-scale events, such as international conferences and business exhibitions, is critical for maintaining a lively atmosphere while minimizing the negative effects of excessive congestion. To achieve this, it is essential to understand how attendees perceive congestion at these events. However, quantitative evaluations of congestion perception remain unclear, especially for large-scale gatherings.

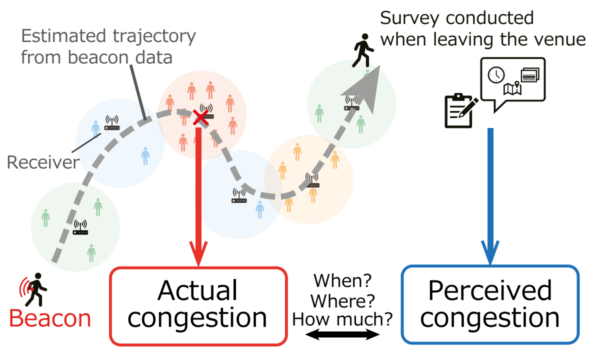

Figure 1: Schematic representation of the combined beacon and survey methodology used in this study.

Recent technological advances offer promising solutions: various sensors now enable real-time counting and tracking of people's movements [1, 2], while large-scale analyses of crowd dynamics, such as controlled laboratory experiments involving hundreds of participants [3] have revealed the complex phenomena involved. Despite these advancements, establishing a clear correlation between perceived and actual crowding at large-scale events has been challenging, particularly when drawing on extensive survey data collected in real facilities.

In this presentation, we introduce our recent study on the quantitative comparison of perceived congestion and measured crowd levels at events exceeding 10,000 participants [4]. Specifically, we investigated the relationship between measured and perceived crowding by analyzing how location, time, and crowd density affect individual attendees at large-scale events.

Methodology

To investigate discrepancies between how attendees perceive crowding and how it is actually measured, we combined questionnaire-based data collection with sensor measurements using beacon tags (Fig. 1).

Timetable
Talk index

Over two consecutive editions, we conducted surveys and Bluetooth-based mobility analyses at Tokyo Big Sight, one of Japan ’ s largest exhibition and conference venues.

Survey respondents provided information about congestion in three ways: (1) They reported specific times they felt crowded through open-ended questions. (2) They marked perceived congestion locations on venue maps that were subdivided into smaller sections. (3) They selected photographs that most closely matched their personal sense of crowd density.

Simultaneously, beacon-based trajectory analyses tracked participant movement to capture the timing, location, and extent of crowding they encountered (Fig. 1). The beacon tags continuously recorded timestamps and estimated each participant ’s position within the venue. We assumed that the number of beacons detected by each receiver within specified time intervals would correlate with local crowd density. By cross-referencing each participant ’ s trajectory with crowd data across various locations and times, we identified peaks in measured crowding in terms of time, location, and density.

Results

In 2022 and 2023, the number of visitors to the targeted events was 10,607 and 31,137, respectively. The higher attendance in 2023, roughly three times that of 2022, primarily reflected shifting attitudes toward COVID-19 [5].

To explore how participants qualitatively perceived congestion, we examined the ratio of responses to the crowding-time questions among those who provided answers. The data indicate that as the maximum crowd size increased, the proportion of participants who reported experiencing congestion also increased.

Next, we compared quantitative perceptions of crowding with measured crowd levels. Our findings indicate that while participants accurately identified the most heavily congested times overall, their reported congestion times tended to align more closely with their departure times than with actual peak crowding. This pattern suggests a recency bias in how participants recall congestion.

With regard to location, most participants displayed a fairly accurate understanding of which larger zones (approximately 100 m $\times$ 100 m) were crowded, although many mistakenly identified adjacent smaller zones (around 20 m in distance) as crowded. Moreover, participants ’ selections of crowd-density photographs showed only a weak correlation with the measured congestion levels, implying that factors beyond spatial density (e.g., personal comfort thresholds or expectations) play a significant role in shaping perceived crowd intensity.

Discussion and Conclusion

By combining questionnaire data and beacon-derived crowd measurements, this study offers, to the best of our knowledge, the first attempt to compare perceived and actual crowding at an event attracting over 10,000 attendees. Our results reveal how and when attendees tend to notice or recall congestion and underscore the importance of psychological factors, such as recency bias, that can affect perceptions of crowd density.

These insights broaden our understanding of crowd perception and carry direct implications for event management and planning. For instance, by addressing congestion closer to expected departure times, organizers may be able to enhance overall attendee experiences without compromising safety or operational efficiency. Taken together, our findings provide a foundation for strategies aimed at optimizing crowd flow while preserving the many benefits of large-scale gatherings.

Bibliography

[1] Teixeira, T. *et al.*, *A survey of human-sensing: Methods for detecting presence, count, location, track, and identity*, ACM Computing Surveys **5**(1), 59–69, 2010.

[2] Feliciani, C. *et al.*, *Introduction to Crowd Management: Managing Crowds in the Digital Era: Theory and Practice*, Springer, 2022.

[3] Boomers, A.K. *et al.*, *Pedestrian crowd management experiments: A data guidance paper*, Collective Dynamics **8**, 1–57, 2023.

[4] Tanida, S. *et al.*, *Quantifying crowding perception at large events using beacons and surveys*, Scientific Reports **15**, 991, 2025.

[5] Kim, H. *et al.*, *Investigating visitors ’ perceptions and behaviors in a crowded situation at a large-scale exhibition*, Journal of Disaster Research **19**(2), 370–378, 2024.

12th International Conference on Pedestrian and Evacuation Dynamics (PED 2025)
Prague, Czech Republic – September 9-12, 2025

Simulating and quantifying the influence of covert and explicit leaders on human crowd motion

Kei Yoshida*[1], Sina Feldmann[1], and William H. Warren[1]

[1]Department of Cognitive and Psychological Sciences, Brown University, Providence, USA

Abstract We previously reported an experiment in which covert or explicit leaders (confederates) were placed in a group of walking pedestrians in order to test leader influence on human crowd motion [1]. Here we simulate the participant trajectories with variants of an empirical pedestrian model, treating the covert leaders' motion as input, and test model agreement with the experimental data. We are currently using reconstructed influence networks [2] to modify the model weights in order to simulate the influence of explicit leaders. The results help us to understand how leader influence propagates via local interactions in real human crowds.

Keywords Pedestrian dynamics, Leadership, Modelling, Experiment, Influence networks

Motivation

Collective motion of human crowds is thought to be a self-organizing phenomenon that emerges from local interactions between neighboring individuals. Some positions in a crowd are more influential than others, resulting in the emergence of strong leaders [2]. We recently conducted an experiment in which confederates were strategically placed in these positions to test their influence on crowd motion [1]. The results showed that both covert and explicit leaders can steer a crowd, but explicit leaders are significantly more influential and can also split a crowd. Reconstruction of the influence networks revealed that explicit leaders change the network topology.

In the present study, we simulate the data with an empirical model of human locomotion, the SCruM (Self-organized Collective Motion) model. First, using the motions of covert confederates as input, we simulate the participant trajectories with visual and 'omniscient' versions of the model, to investigate the local coupling between neighbors that accounts for the experimental data. Second, we use the reconstructed network topology [2] to modify the local weights in the model, to estimate the influence of explicit leaders. The results help us to understand how leader influence propagates through a crowd based on local interactions.

Methods

Experiment

In each session, a group of pedestrians (N=16 to 22) was instructed to walk across a field together. Four confederates, whose presence was either unknown ("covert") or visually specified by pennants ("explicit"), simultaneously turned about 25°mid-way through the trial. We varied the turn direction of each confederate, creating three trial conditions: "control" (no turns), "steer" (all confederates turn left or right), or "split" (2 confederates turn left and 2 turn right). Data were recorded by a camera drone (50 Hz). Head positions were extracted by a data processing pipeline using multiple-object tracking frameworks.

Pedestrian Models

The SCruM model controls the heading direction and speed of an agent based on input from its environment. We evaluate two variants of the model: (i) Omnisicient SCruM, based on neighbor velocities without occlusion [3] and (ii) Visual SCruM, based on visual variables (optical expansion, angular velocity, and eccentricity of neighbors) with visual occlusion [4].

*Email of the corresponding author: kei_yoshida@brown.edu

Two model components are used here: the goal component orients the agent's heading toward a distant goal, while the alignment component attracts the agent toward the mean heading and speed of its neighbors. In the simulations, the trajectories of the confederates are taken from the human data, while the movements of participants are simulated, with initial conditions taken from their data.

Analyses

Figure 1 presents the probability density distributions of the change in heading direction for participants on each trial, with covert confederates. We statistically compared the distributions for the simulated data (B and C) with the human data (A).

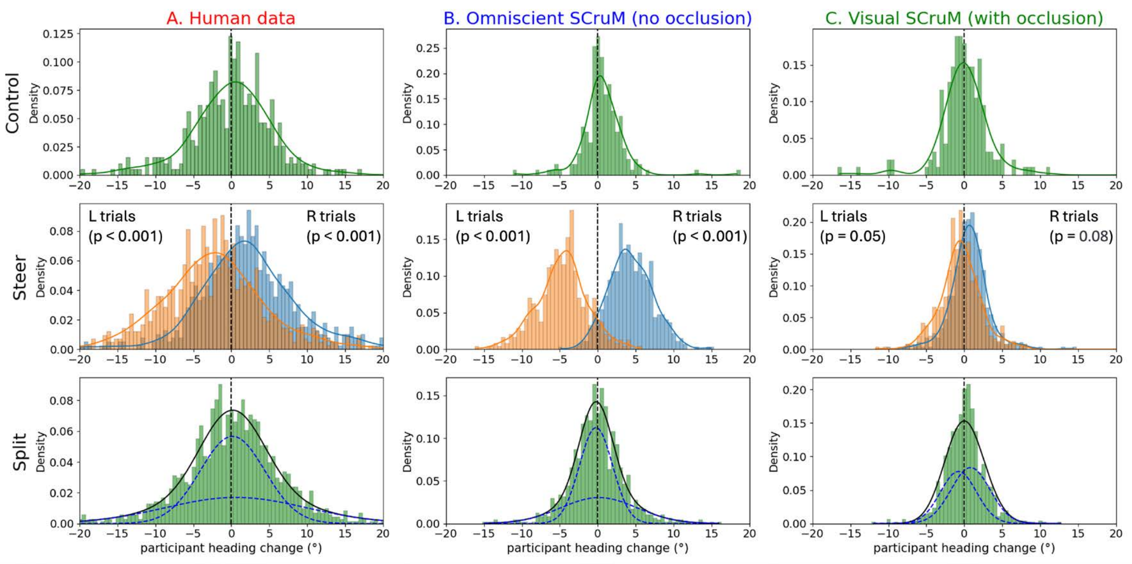

Figure 1: Probability density distributions of heading change by participants on each trial when covert confederates are present. From the top, rows represent control, steer (left-turning in orange, right-turning in blue), and split trials. **A.** Experimental data of participants. **B,C.** Simulated data of non-confederate agents using the SCruM model, without (B) or with (C) occlusion.

In the Control condition, neither omniscient SCruM ($p = 0.16$) or visual SCruM ($p = 0.94$) was significantly different from the human data, although Kolmogorov-Smirnov (KS) tests indicated significant distributional differences (both $p < 0.001$). In the Steer condition, for both left and right turns, omniscient SCruM turned significantly more than humans ($p < 0.001$), whereas visual SCruM turned significantly less than humans ($p < 0.001$), although the left/right difference was still significant; both models exhibited distributional differences from the human data (KS, $p < 0.001$). In the Split condition, omniscient SCruM was marginally different from the human mean ($p = 0.05$), whereas visual SCruM was not significantly different ($p = 0.23$), although both exhibited distributional differences (KS, $p < 0.001$).

In sum, human crowds are surprisingly resistant to Splitting, consistent with both models, due to averaging the influence of neighbors. In the Steer condition, the omniscient model over-steered whereas the visual model was somewhat closer to human behavior. To model the influence of explicit leaders, we are currently modifying the local weights in the alignment component based on the topology of the reconstructed networks [2]. The results will help us to understand how leader influence propagates via local interactions in real human crowds.

Bibliography

[1] Yoshida, K., Taylor, H., Warren, W.H., *The Influence of Explicit and Covert Leaders on Human Crowd Motion*, Traffic and Granular Flow (TGF) Proceedings, 2025.

[2] Yoshida, K., di Bernardo, M., Warren, W.H., *Visual Influence Networks in Walking Crowds*, biorxiv (`https://doi.org/10.1101/2025.01.29.635594`).

[3] Dachner, G.C., Wirth, T.D., Richmond, E., Warren, W.H., *The visual coupling between neighbours explains local interactions underlying human 'flocking'*, Proceedings of the Royal Society B: Biological Sciences **289**, 20212089, 2022.

[4] Wirth, T.D., Dachner, G.C., Rio, K.W., Warren, W.H., *Is the neighborhood of interaction in human crowds metric, topological, or visual?*, PNAS Nexus **2**, pgad118, 2023.

Modelling the effect of adherence behaviour on infection spread in crowds

Sophia Johanna Wagner*[1] and Gerta Köster[1]

[1]Hochschule München - University of Applied Sciences

Abstract People's adherence to health measures significantly impacts the spread of infectious diseases. Using a crowd dynamics model for simulating infection spread, we model varying adherence levels for mask-wearing and physical distancing, looking at adherence of infectious and susceptible agents separately. We find that mask-wearing is highly effective in a direct manner, while adherence to physical distancing can indirectly change the infectious agent's behavior which then has surprising effects on infections spread.

Keywords Infection modeling, Adherence behaviour, Infection prevention measures, Crowd modeling

Simulating how people's adherence influences infection spread

In this work, we want to connect infection modelling with people's behaviour, since the effectiveness of measures strongly depends on people's compliance. To our knowledge, this has not been explored in small-scale contexts. We argue, that combining these fields can improve our understanding of how to manage and predict the spread of infectious diseases based on human behavior.

Our model builds on the transmission framework by Rahn et al. [1, 2], incorporating agents — either infectious or susceptible — navigating from an ingress to a destination. Infectious agents exhale aerosol clouds that impact susceptible agents who may inhale these aerosols. One can then measure the exposure of susceptible agents for different conditions.

In this work, we simulate a scenario to examine the impact of varying adherence levels for two measures: physical distancing and mask-wearing. We aim to determine which adherence levels are needed to effectively control disease spread. Additionally, we explore the impact of an infectious agent's adherence compared to other agents and whether proper mask-wearing can replace the need for physical distancing.

We simulate a bottleneck scenario, shown in Figure 1, representing an entrance, exit, or food court at a sports event, with 100 susceptible agents and one infectious agent. Each agent spends 15 seconds at the target, simulating ticket control, bag checks, or food ordering. Physical distancing is set to 1.5m, and mask filtration efficiency to 90%.

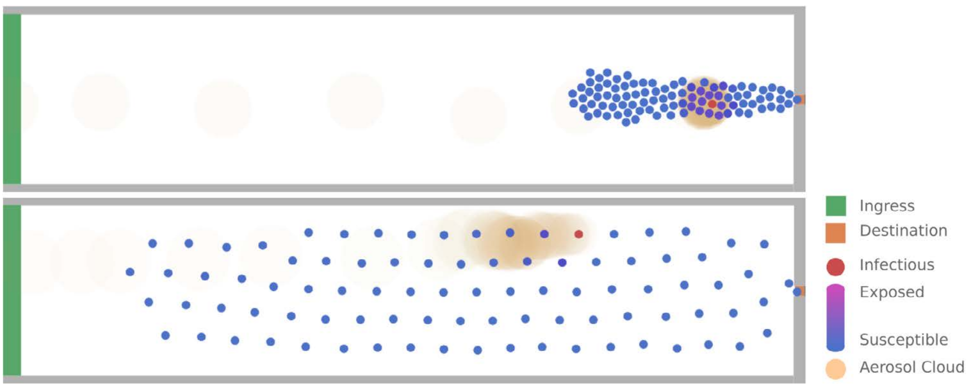

Figure 1: Bottleneck scenario with and without physical distancing.

Figure 2 depicts the average pathogen exposure of all agents in the bottleneck scenario, considering adherence probabilities of 0%, 50%, and 100% for susceptible agents, each condition with and without

*Email of the corresponding author: `sophia.wagner@hm.edu`

Timetable
Talk index

adherence by the infectious agent. For mask-wearing, exposure levels appear to decrease linearly as the adherence probability of susceptible agents increases. When all susceptible agents wear masks, exposure is reduced by a factor of 10 compared to scenarios with no mask use. The effect is even more substantial if the infectious agent wears a mask, decreasing exposure by a factor of 10 with only their adherence. Overall, when both susceptible and infectious agents wear masks, exposure can be reduced by a factor of 100.

For physical distancing, when the infectious agent does not adhere, exposure levels decrease as adherence probability increases. Interestingly, when the infectious agent adheres, the opposite occurs. This counterintuitive observation occurs because the adhering infectious agent changes its behavior by moving away from non-adhering susceptible agents to avoid close contact, thus preventing others from walking into its aerosol clouds. Conversely, if other agents also adhere, the infectious agent remains within the group, allowing others to pass through their aerosol trace. Therefore, the greatest effect is observed when the infectious agent behaves differently than the group, either fully adhering while the group does not or vice versa.

In conclusion, the most significant impact occurs when both the infectious agent and all susceptible agents wear masks. On the other hand, adherence to physical distancing can alter behavior based on awareness of infectiousness, and it is 20 times less effective than mask-wearing when everyone complies.

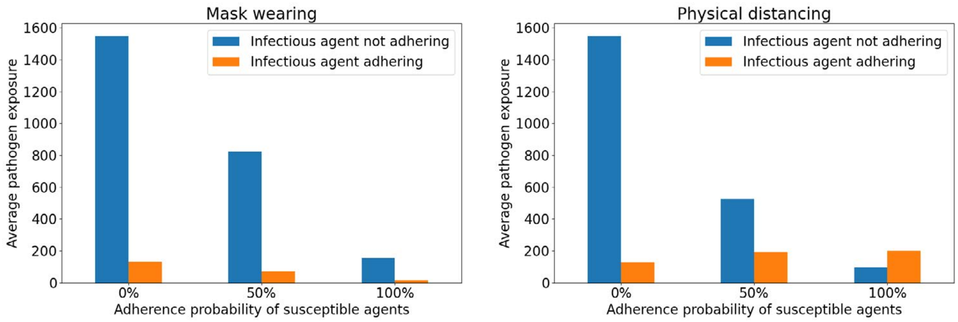

Figure 2: Average pathogen exposure for susceptible agents in the bottleneck for mask wearing (left) and physical distancing (right) for different adherence levels.

In the future, we plan to incorporate survey data on adherence at sports events, influenced by clarity of instructions, personal risk perception, shared social identity, and compliance of other people around. By combining infection modeling with crowd psychology, we aim to understand how these psychological elements influence adherence to Covid-19 guidelines and, consequently, disease spread. These insights are essential for developing effective public health strategies that reflect real-world behaviors.

References

[1] Simon Rahn, Marion Gödel, Gerta Köster, and Gesine Hofinger. Modelling airborne transmission of SARS-CoV-2 at a local scale. *PLOS ONE*, 17(8):1–24, 08 2022.

[2] Simon Rahn, Gerta Köster, and Hans-Joachim Bungartz. Toward unraveling airborne pathogen transmission in crowds: Parameter study for an agent-based exposure model. *Safety Science*, 175:106524, 2024.

12th International Conference on Pedestrian and Evacuation Dynamics (PED 2025)
Prague, Czech Republic – September 9-12, 2025

Emergent Phenomena Induced by Avoidance Behavior in Multi-Directional Pedestrian Flows

Andreas Schadschneider*[1], Priyanka Iyer[2], Rajendra Singh Negi[2], and Gerhard Gompper[1,2]

[1]Institute for Theoretical Physics, Universität zu Köln, 50937 Köln, Germany
[2]Theoretical Physics of Living Matter, Institute of Biological Information Processing and Institute for Advanced Simulation, Forschungszentrum Jülich, 52425 Jülich, Germany

March 7, 2025

Abstract Collision avoidance in multi-directional pedestrian streams can lead to self-organisation phenomena. A prominent example is lane formation in counterflow. We study a 3-way intersection using methods from active particle systems theory. A rich phase diagram with four different phases is found as function of the maneuverability and vision angle of the agents.

Keywords multi-directional flows, active particles, intersection, emergence, lane formation

Introduction

The collision avoidance behavior in multi-directional pedestrian streams is complex and not fully understood yet. In these scenarios it often competes with personal goals of the individuals which can lead to various macroscopic effects, especially the emergence of self-organisation phenomena. This is already known from bi-directional streams where lane formation is observed at intermediate densities. In this contribution we study theoretically the next simplest case of a 3-way intersection. A thorough understanding of crossing flows might help to improve safety and comfort in large crowds through appropriate crowd management methods.

Model

For modeling we adapt ideas from the theory of active particles, especially the concept of cognitive agents and intelligent active Brownian particles (iABPs) [1]. The simulation setup, shown in Fig. 1, is similar to circular antipode experiments as described e.g. in [2, 3]. To simplify matters and reduce the number of parameters we focus on a symmetric layout where all three streams have basically identical properties.

Motion of the agents is described by the overdamped limit of a Langevin equation to mitigate artefacts arising from inertia effects seen in force-based models. The focus is on effects of steering, not velocity adjustment. The interactions between the agents are based on local vision-based self-steering through torques that alter the direction of motion [4]. Since inertia effects are usually not overly important in pedestrian dynamics, assuming a constant speed of all agents is a reasonable approximation in modelling which helps to reduce the number of relevant parameters. For more details of the model definition we refer to [4].

Important parameters of the model are the strengths of goal fixation K, which controls the steering torque towards the goal, and the influence of visual perception Ω. With these two quantities we define the relative maneuverability $\Delta = \Omega/K$. Furthermore the influence of the vision angle ψ is taken into account.

Results

When varying the relative maneuverability Δ and the vision angle ψ, the agents show different dynamical states as shown in Fig. 1(b). For small Δ, goal alignment dominates over collision avoidance and agents

*Email of the corresponding author: as@thp.uni-koeln.de

Timetable
Talk index

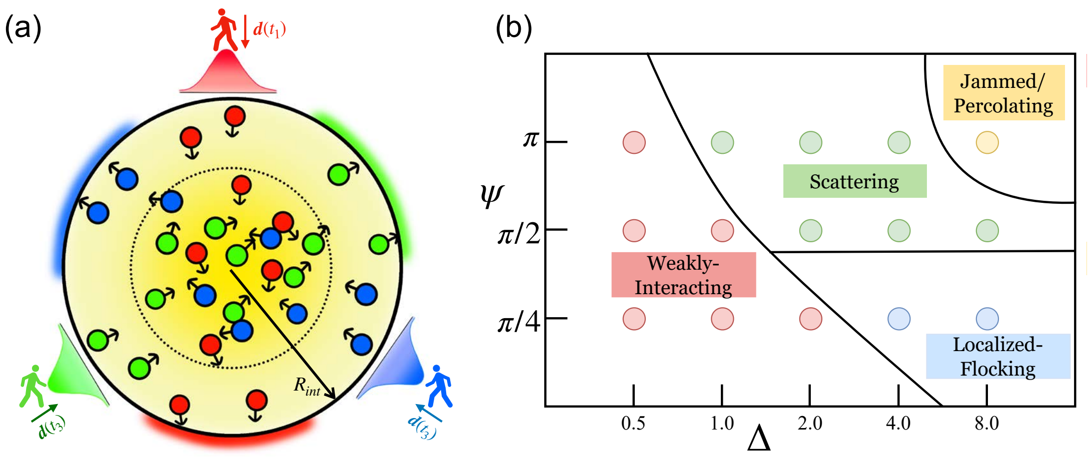

Figure 1: Model setup (left) and phase diagram (right).

head directly toward the goal. When Δ is increased, the agents in the stream interact more strongly with each other and more complex motion patterns evolve.

For large local avoidance Δ and narrow vision angles ψ, the agents in the interaction regime show avoidance-induced flocking. Neighboring agents with aligned motion can be arbitrarily close without noticing the presence of the other. If the vision angle is increased, agents start experience significant scattering and trajectories become convoluted. No stable order exists in this regime. If the vision angle is increased further, the systems enters a jammed state with percolated clusters where jamming is not caused by excluded volume effects but rather by strong steering avoidance.

Bibliography

[1] G. Gompper, H.A. Stone, C. Kurzthaler, D. Saintillan, F. Peruani, D.A. Fedosov, T. Auth, C. Cottin-Bizonne, C. Ybert, E. Clément et al., *The 2025 Motile Active Matter Roadmap*, J. Phys. Condens. Matter **37**, 143501 (2025) .

[2] Y. Xiao, Z. Gao, R. Jiang, X. Li, Y. Qu, Q. Huang, *Investigation of pedestrian dynamics in circle antipode experiments: Analysis and model evaluation with macroscopic indexes*, Transp. Res. Part C Emerg. **103**, 174 (2019).

[3] Y. Hu, J. Zhang, W. Song, *Experimental study on the movement strategies of individuals in multidirectional flows*, Physica A **534**, 122046 (2019).

[4] P. Iyer, R.S. Negi, A. Schadschneider, G. Gompper, *Directed motion of cognitive active agents in a crowded three-way intersection*, Commun. Phys. **7**, 379 (2024).

12th International Conference on Pedestrian and Evacuation Dynamics (PED 2025)
Prague, Czech Republic – September 9-12, 2025

Glimpsing into the Fluid Mechanics of Crowds Featuring Route Choice and Collision Anticipation

Maël LE GARFF[1,2], Jakob CORDES[3], and Alexandre NICOLAS*[1]

[1]Universite Claude Bernard Lyon 1, CNRS, Institut Lumière Matière, 69100 Villeurbanne, France.
[2]École polytechnique, 91128 Palaiseau, France.
[3]Forschungszentrum Jülich, Jülich, Germany.

Abstract Collision anticipation plays a key role in crowd dynamics, but was so far absent from the hydrodynamic equations typically used in crowd dynamics. We study how simple microscopic collision avoidance processes translate into the macroscale and unveil new hydrodynamic terms that bear the signature of collision anticipation. The results are validated by comparison to the corresponding agent-based simulations.

Keywords crowd hydrodynamics, collision anticipation, crowd theory, decision-making

Over the past few years, captivating crowd phenomena such as the backward propagation of soliton-like density waves through marathon corrals [1] or the oscillating motion of crowd 'patches' in very dense settings at festivals [2] have been successfully reproduced using hydrodynamic equations, in the wake of Toner and Tu's symmetry-based approach for active matter [3]. However, Toner and Tu explicitly stated that their approach holds for particles without 'compass', i.e., with no intrinsic directional preferences. Clearly, this assumption should not be taken for granted for pedestrians in general and we suspect that new relevant terms will arise in the fluid dynamical equations of agents with 'compasses'. Having in mind the goal to probe parts of the foundations of the fluid mechanics of pedestrian crowds, in the wake of [4], we study how *simple* microscopic descriptions accounting for collision anticipation translate into the macroscopic scale and we unveil the new contributing terms, with specific directions in space, that ensue in the hydrodynamic equations and reflect the process of collision anticipation.

Dimensionless numbers to classify crowd scenarios

First, in the spirit of Fluid Mechanics, we recently introduced two dimensionless numbers [5] that quantify (i) the strength of intrusions into personal spaces and (ii) the avoidance of imminent collisions in any given scenario; the latter is associated with collision anticipation. (Note that the aforementioned hydrodynamic studies took place in settings where settings where distance-based contributions, rendered by the first dimensionless number, are expected to dominate). These two dimensionless number are at the basis of a classification of a vast array of empirical crowd scenarios [6], represented in the left panel of the figure.

Collision anticipation at the microscopic scale

Then, we showed how the two dimensionless variables can help infer fairly generic *microscopic* equations of motion for pedestrians. In short, the velocity $\boldsymbol{v}_j(t)$ of a pedestrian j can always be expressed as the minimum of a suitably defined, ad-hoc function $\mathcal{C}_j^{(t)}(\boldsymbol{v})$, viz.,

$$\boldsymbol{v}_j(t) = \mathrm{argmin}_{\boldsymbol{v}}\, \mathcal{C}_j^{(t)}(\boldsymbol{v}). \tag{1}$$

Trading accuracy for simplicity, the foregoing reasoning based on dimensionless numbers helps propound a generic form for $\mathcal{C}_j^{(t)}(\boldsymbol{v})$. Following a perturbative approach *à la* Landau, fairly generic equations of motion are then obtained for the individual pedestrian [5]. In these equations, a variant of the anticipated time-to-collision accounts for collision anticipation.

*Email of the corresponding author: alexandre.nicolas@cnrs.fr

Bridging the gap with the macroscopic scale

Finally, we upscale these microscopic agents using Boltzmann's equation of motion, with a derivation that is not rigorous mathematically speaking, but does bridge the gap between the microscopic equation and the macroscopic one without having to posit artificial symmetries. This is achieved, notably, by coarse-graining the different terms into mesoscopic forces, by averaging over the distribution of spacings and velocities of interacting agents, and then into an effective macroscopic force. While the continuity equation (describing the conservation of particle number) does not change, we find that the modified equation describing the mean local velocity $\boldsymbol{v}_\alpha$ of agent type α takes the following schematic form,

$$\frac{\partial \boldsymbol{v}_\alpha}{\partial t} + (\boldsymbol{v}_\alpha \cdot \nabla)\boldsymbol{v}_\alpha = (\dots) + \sum_{\beta \neq \alpha} \rho_\beta \boldsymbol{D}^{(TTC)}_{\alpha,\beta} - \underline{\underline{T^{(TTC)}_{\alpha,\beta}}} \cdot \boldsymbol{\nabla} \rho_\beta, \tag{2}$$

where only the new terms signalling TTC-based collision anticipation are detailed on the right-hand side.

The resulting macroscopic description is tested and validated by comparing its predictions to the output of microscopic agent-based models featuring the same 'ingredients', in the case of intersecting perpendicular flows. This is illustrated in panel B of the figure, where we show the density field of the horizontal pedestrian stream (walking to the right) in the resolution of the hydrodynamic equations and in the agent-based simulations: we notice the same marked deviation of the stream towards the bottom, at the intersection with the perpendicular stream; this marked deviation vanishes if the new hydrodynamic terms exposed above are removed. Accordingly, at least qualitatively, the hydrodynamic contributions that were so far overlooked succeed in capturing the effect of collision anticipation.

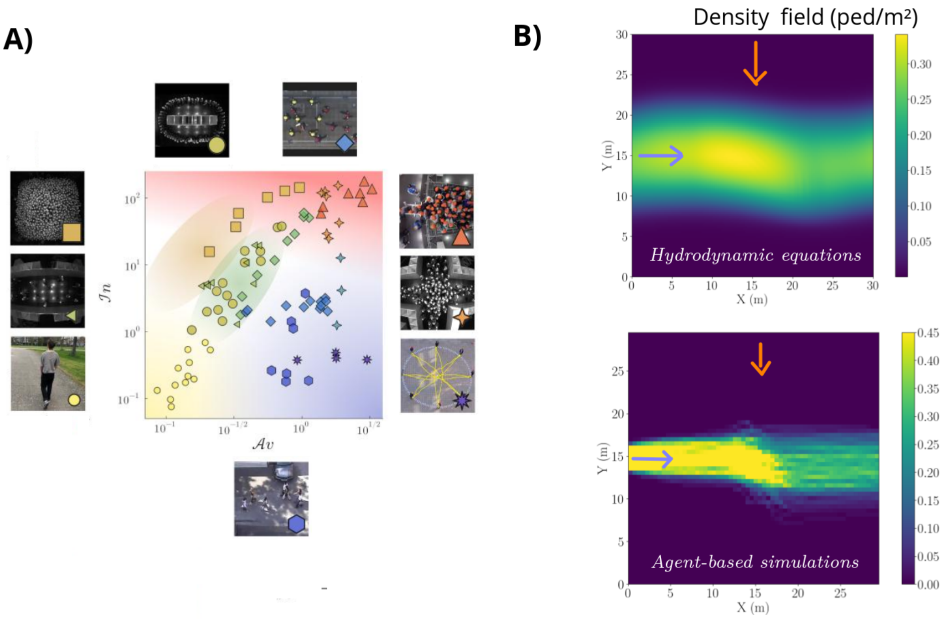

Figure 1: A) Classification of a wide range of empirical crowd scenarios (illustrated by the snapshots on the side) using our two dimensionless numbers, *In* and *Av*. Adapted from [5]. B) Simulated density field of the horizontal pedestrian stream in a perpendicular intersection scenario, by solving hydrodynamic equations (top) or microscopic agent-based simulations (bottom).

References

[1] N. Bain and D. Bartolo, "Dynamic response and hydrodynamics of polarized crowds," *Science*, vol. 363, no. 6422, pp. 46–49, 2019.

[2] F. Gu, B. Guiselin, N. Bain, I. Zuriguel, and D. Bartolo, "Emergence of collective oscillations in massive human crowds," *Nature*, vol. 638, no. 8049, pp. 112–119, 2025.

[3] J. Toner and Y. Tu, "Long-range order in a two-dimensional dynamical xy model: how birds fly together," *Physical Review Letters*, vol. 75, no. 23, p. 4326, 1995.

[4] P. Degond, C. Appert-Rolland, J. Pettré, and G. Theraulaz, "Vision-based macroscopic pedestrian models," *arXiv preprint arXiv:1307.1953*, 2013.

[5] J. Cordes, A. Schadschneider, and A. Nicolas, "Dimensionless numbers reveal distinct regimes in the structure and dynamics of pedestrian crowds," *PNAS nexus*, vol. 3, no. 4, p. pgae120, 2024.

[6] J. Cordes, A. Nicolas, and A. Schadschneider, "Classification of pedestrian crowds by dimensionless numbers," *Collective Dynamics*, vol. 9, pp. 1–10, 2024.

Timetable
Talk index

12th International Conference on Pedestrian and Evacuation Dynamics (PED 2025)
Prague, Czech Republic – September 9-12, 2025

Simulating crossing pedestrian flows with a vision-based model of collision avoidance

Sina Feldmann*[1], Kyra Veprek[1], and William H. Warren[1]

[1]Department of Cognitive and Psychological Sciences, Brown University, Providence, USA

Abstract Previous simulations of crossing flows using a vision-based collision-avoidance model reproduced lanes and stripes but showed larger heading adjustments during crossing than the human data. Here we investigate two possible explanations. First, we tested participants walking through a virtual crowd under two density conditions, refit the collision avoidance model, and resimulated the crossing flows data. Our findings reveal little influence of moderate densities on human collision avoidance behavior. Second, we are testing mutual collision avoidance between two participants to determine whether a revised model better approximates the crossing flows data.

Keywords Pedestrian, Collision Avoidance, Modeling, Experiment, Heading Control

Motivation

Individual interactions between pedestrians in a crowd can lead to emergent patterns of collective motion, such as the formation of stripes in crossing flows [1]. In previous research, we found that an empirical, vision-based pedestrian model (Visual SCruM) including only two components, local collision avoidance and a common goal, could reproduce the perpendicular stripes observed in human crossing flows data [2].

However, the simulations consistently overestimated human heading adjustments during the crossing period to avoid collisions. Two hypotheses might explain that result. First, because model parameters were fit to data from participants avoiding a single obstacle moving on a fixed path, it might not scale up to crowds with higher densities. We refer to this as the density hypothesis. Second, the mutual avoidance hypothesis holds that heading adjustments might be smaller in a mutual avoidance scenario when both individuals avoid each other. Here, we present new data in which a participant walked through a crowd of avatars at two densities. Fitting the model parameters to this new scenario only slightly reduced the heading adjustments, inconsistent with the density hypothesis. We are also collecting data on collision avoidance between two participants to test the mutual avoidance hypothesis.

Methods

Crowd Experiment

We designed an experiment to test whether collision avoidance depends on crowd density, for moderate densities that allow for continuous walking. A human participant (N=12) walked in a $12\,\mathrm{m} \times 14\,\mathrm{m}$ area (the VENLab) while wearing a head-mounted VR display. The task was to walk through a virtual crowd (10 avatars) toward a goal while avoiding collisions with the avatars. The crowd had two initial densities (0.42 persons/m^2 and 0.36 persons/m^2) and the avatars walked at different speeds (all 1.0 m/s, all 1.2 m/s, or mixed). Head position was recorded at 90 Hz, and time series of heading and speed were computed.

Fitting Procedure

We fit the parameters of the visual SCruM model to the human trajectory data using an iterative search. For each trial, we initialized the model agent with the initial position, heading, and speed of the participant, and minimized the Root Mean Square Error (RMSE) between the positions of the model agent and the participant.

*Email of the corresponding author: sina_feldmann@brown.edu

Model Validation

We then used the new model parameters from the density experiment to predict the human crossing flows data [3]. In this dataset, a set of participants (N=36 or 38) was divided into two equal groups, which walked through each other at six different crossing angles ($30 - 180\,°$, increments of $30\,°$), with about 17 trials per angle. Simulations were carried out with model components for a goal, collision avoidance, and alignment. We report the within-subject standard deviation (SD) of heading for the human data and the model, with and without the new fit parameters.

Preliminary Results

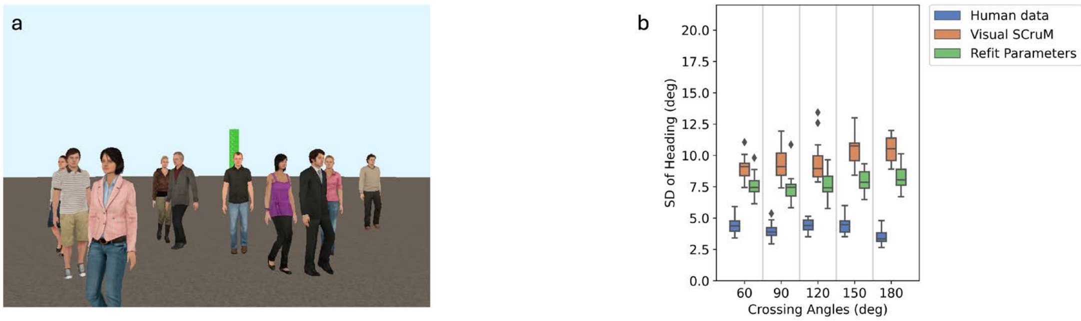

Figure 1: (a) Crowd experiment: A still from the virtual crowd stimuli. The initial positions of 10 avatars were randomly selected from within a bounded area. (b) Crossing flows: Boxplots of heading variation (mean within-subject SD) during the crossing period for human data (blue) and model simulations (previous parameters in yellow, parameters fit to the density experiment in green). Refit model parameters reduce the heading adjustments, but they are still significantly higher than the data.

To test the effect of crowd density, we fit the model parameters to the experiment data in each density condition separately. We then simulated the data in the other density condition and compared the performance between conditions. For the parameters fit to the higher density condition, a t-test found no statistical difference in model performance between the two conditions ($t = 0.34363$, $p = 0.7312$). Similarly, there was no statistical difference for the parameters fit for the lower density condition ($t = -0.85283, p = 0.3939$).

We then fit the model parameters to all the experimental data, and simulated the crossing flows data. The simulated heading adjustments are slightly improved with the re-fit parameters, but are still significantly larger ($p < 0.001$) than the human data (Fig.1). Based on this result, we conclude that the exaggerated heading adjustments in our crossing flows simulations cannot be attributed to the density hypothesis.

We are currently testing the mutual avoidance hypothesis by conducting an experiment in which pairs of participants walk at various crossing angles and avoid colliding with one another. The collision-avoidance model will be refit to this experimental data, and then used to simulate the crossing flow data. The mutual avoidance hypothesis predicts that heading adjustments will be reduced to levels similar to the human data.

Bibliography

[1] Naka, Y., *Mechanism of cross passenger flow—Study on Complicated Passenger Flow in Railway Station (Part I) (in Japanese)*, Trans Arch Inst Jpn, 258: 93–102, 1977.

[2] Feldmann, S., Veprek, K., Warren, W.H., *Formation of lanes and stripes in crossing pedestrian flows using an empirical human model.*, Poster presented at *Traffic and Granular Flow*, Lyon, France., 2024.

[3] Mullick, Pratik, Sylvain Fontaine, Cécile Appert-Rolland, Anne-Hélène Olivier, William H. Warren, and Julien Pettré., *Analysis of emergent patterns in crossing flows of pedestrians reveals an invariant of 'stripe' formation in human data.*, PLoS computational biology 18, 6, 2022.

12th International Conference on Pedestrian and Evacuation Dynamics (PED 2025)
Prague, Czech Republic - September 9-12, 2025

Specific flow rate at openings for pedestrians including slow walkers

Kenichi Takayama[1], Tomoaki Nishino[2]

[1] Takenaka Corporation, Japan
[2] Disaster Prevention Research Institute, Kyoto University, Japan

Using laboratory walking experiments, this paper investigates the effect of the ratio of slow walkers, such as elderly people, on pedestrian flow behavior. Specifically, we quantify the specific flow rates at a bottleneck opening by parametrically varying both the ratio of slow walkers to normal walkers and the width of the opening. The results show that the measured specific flow rates at the opening exceeded the rate of 1.5 persons/m/s, which is commonly used in building fire safety design in Japan, even with high percentages of slow walkers. This finding, given the opening width and the ratio of slow walkers, enables more accurate assessments of the fire evacuation time.

Keywords Elderly person, Evacuation experiment, Specific flow rate

1. Introduction

Currently, the global aging population is approximately 10%; this percentage is expected to exceed 16% by 2050. In particular, Japan exhibits the highest aging rate in the world, with elderly individuals comprising approximately 29% of its total population. This increasing aging population presents new challenges for building fire safety design. Evacuation time assessments typically assume uniform walking capabilities and neglect mobility-impaired evacuees. To deal with the demographic shifts in aging societies, improving evacuation time assessments is essential. A critical parameter in evacuation time assessments is the specific flow rate through bottlenecks, which is defined as the number of people passing through an opening with a unit width per unit time. In Japan, a value of 1.5 persons/m/s, derived from station platform observations by Togawa [1], is commonly used; however, experimental studies [e.g., 2, 3, 4] have demonstrated specific flow rates higher than 1.5 persons/m/s [1].

Kretz et al. [2] conducted full-scale experiments to investigate the flow capacity through a 40-cm-thick wall opening under normal conditions, with opening widths ranging from 40 cm to 160 cm. The flow capacity showed a linear decrease from 2.2 persons/m/s to 1.8 persons/m/s as the bottleneck width increased from 40 cm to 70 cm, while maintaining a constant capacity of approximately 1.8 persons/m/s for wider openings between 70 cm and 120 cm. In large-scale evacuation experiments, Daamen and Hoogendoorn [3] studied emergency door capacity while examining diverse population compositions and various opening widths. Their results demonstrated specific flow rates greater than 2.25 persons/m/s in most cases. Jo et al. [4] examined the relationship between the spatial conditions and the pedestrian flow behavior via walking experiments and demonstrated that both the pedestrian trajectories and the specific flow rates were significantly influenced by the spatial configuration of the passageways and openings. However, the influence of higher proportions of slow walkers on pedestrian flow characteristics has not been sufficiently investigated in the context of aging populations. Accordingly, this study investigates the flow behavior at openings with a special focus on pedestrians including unassisted slow walkers as a preliminary investigation into aging population effects. Experiments with participants were performed to quantify the specific flow rates under controlled laboratory conditions.

2. Experimental setup

The experiments were conducted on December 15, 2019, using an opening with a variable width installed in a room with a size of 14 m × 7 m, where 24 participants started walking simultaneously from designated starting positions through the opening to a specified destination area (Figs. 1 and 2). The flow behavior of the participants was recorded using three video cameras to count the number of participants passing through the opening as a function of time and to evaluate the specific flow rates.

*Email of the corresponding author 1: takayama.kenichi@takenaka.co.jp
*Email of the corresponding author 2: nishino.tomoaki.3c@kyoto-u.ac.jp

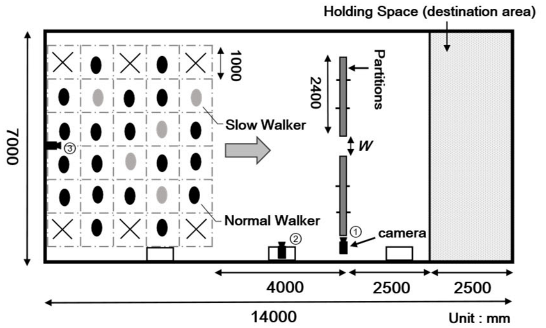

Figure 1. Plan of the experimental setup.

Figure 2. Images taken during the experiment (blue caps for typical walkers and red for slow walkers).

The 24 able-bodied participants comprised 21 males and 3 females (22 in their 20s, 1 in their 30s, and 1 in their 40s) initially positioned at 1-m intervals as shown in Fig. 1. The participants were assigned two types of roles: typical walkers and slow walkers. The walking speed of each role was controlled using metronomes with different beats per min (BPM); participants were instructed to synchronize their steps with the metronome beats via portable audio players. The metronomes were set at 102 BPM for typical walkers and 63 BPM for slow walkers. These BPMs were calibrated via preliminary trials such that the free walking speeds of each role were on average close to 1.0 m/s (standard deviation = 0.09 m/s) and 0.6 m/s (standard deviation = 0.06 m/s), respectively. That is, possible variabilities in walking capability were simplified into two categories focusing on the free walking speed from a practical viewpoint. The participants were visually distinguished by colored caps corresponding to their assigned roles (blue for normal walkers and red for slow walkers).

The experimental conditions comprised 18 cases with two varying parameters: the opening width W (0.9 m, 1.2 m, and 1.5 m) and the slow walker percentage Φ (0%, 10%, 20%, 30%, 40%, and 100%), with slow walkers distributed uniformly except in the last row in the direction of movement. Each trial was initiated by a simulated fire evacuation announcement and ended when all participants reached the designated destination area, with participants instructed to keep walking to the destination area without stopping even after passing through the opening.

3. Results and discussion

Figure 3 shows the relationships between the specific flow rate at the opening, calculated by dividing the total participant count by the product of the opening width and total passage duration, and the slow walker percentage. The results show that the specific flow rate at the opening decreases with increasing slow walker percentage. Approximately all of the measured specific flow rates exceeded Togawa's value of 1.5 persons/m/s [1], while those for $\Phi = 0\%$ were consistent with previous experimental observations [2, 3, 4]. For $W = 0.9$ m, an increase in the slow walker percentage had a relatively small effect on the specific flow rate at the opening compared with the other opening-width conditions. An opening width of 0.9 m is not sufficient for persons to pass through in two rows; therefore, many participants leaned their bodies when passing through the opening; this efficient behavior resulted in higher specific flow rates relative to the other opening-width conditions.

4. Conclusions

The specific flow rates through openings were quantified depending on two parameters: the slow walker ratio and the opening width. Although further investigation is necessary, the results enable more accurate assessments of the fire evacuation time, given the opening width and the slow walker ratio.

Figure 3. Relationships between the specific flow rate N and the slow walker ratio Φ.

References

[1] Kikuji Togawa, Report No.14, Building Research Institute, 1955

[2] Tobias Kretz, Anna Gr¨unebohm, Michael Schreckenberg, Experimental study of pedestrian flow through a bottleneck, Journal of Statistical Mechanics Theory and Experiment, 2006

[3] Winnie Daamen, Serge Hoogendoorn, Capacity of Doors during Evacuation Conditions, Procedia Engineering, 2010

[4] Akihide Jo, Tomonori Sano, Yuka Ikehata, Yoshifumi Ohmiya, Analysis of Crowd Flow Capacity through a Door Connected to a Crowded Corridor., Transportation Research Procedia, 2014

12th International Conference on Pedestrian and Evacuation Dynamics (PED 2025)
Prague, Czech Republic - September 9-12, 2025

Mixed-Age Pedestrian Dynamics and Obstacle Avoidance Behaviors: An Experimental Analysis

Jiaming Liu[1], Hui Zhang*[1], and Majid Sarvi[2]

[1] Institute of Public Safety Research, Tsinghua University, Beijing, China
[2] Department of infrastructure Engineering, University of Melbourne, Melbourne, Australia

A mixed-age walking experiment was conducted to investigate the pedestrian dynamics of elderly and young participants under a notified evacuation without a visible disaster. The study analyzed walking speeds and fundamental diagrams and proposed a quantitative method for assessing pedestrian urgency. Furthermore, obstacle avoidance behaviors were examined and compared across different obstacle conditions, highlighting age-related differences in pedestrian movement.

Keywords: Elderly, Emergency, Urgency, Obstacles

Instruction

The global population is undergoing a significant demographic transition toward aging, with China being one of the most affected countries. Existing research on evacuation dynamics has predominantly relied on data from younger individuals. However, the presence of elderly individuals can significantly influence crowd movement patterns, potentially altering evacuation efficiency. Therefore, understanding of the impact of elderly individuals on group evacuation under emergency conditions is essential for improving evacuation strategies and ensuring the safety of aging populations.

A walking experiment was conducted on a university campus in China to examine pedestrian dynamics involving elderly individuals. It included 12 elderly participants (⩾60 years old) and 36 young adults (20–30 years old). Participants walked under a hypothetical emergency scenario, instructed to move as quickly as possible without running or pushing, simulating a notified evacuation without a visible disaster. The experiment varied corridor widths, elderly-to-young participant ratios, and obstacle placements. The scenarios included a straight corridor, a circular corridor, and intersecting straight corridors. All experiments were conducted under controlled conditions. Figure 1 presents the experimental setup and some of the results.

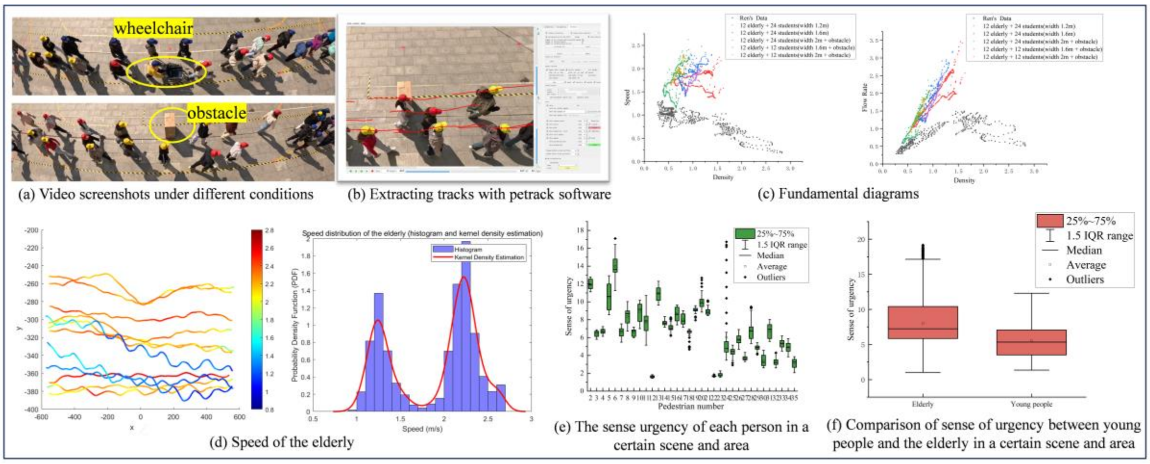

Figure 1: Experimental setup and some of the results.

*Email of the corresponding author: zhhui@tsinghua.edu.cn

Timetable
Talk index

After importing the top-view camera footage into the Petrack software [1], external and internal calibrations were performed to obtain each participant's position coordinates over time. The instantaneous velocities of elderly and young groups were calculated. The t-test results for velocity differences between elderly and young participants indicate a significant difference. A bimodal distribution of walking speeds was observed within both age groups. Video analysis revealed that female participants exhibited greater enthusiasm for walking at higher speeds, suggesting that gender contributed to the bimodal distribution. Notably, female participants, particularly elderly women, demonstrated the highest level of motivation in reaching the goal.

The Voronoi-based Thiessen polygon method [2] was used to calculate the average velocity, density, and flow rate in different regions (front, middle, and rear) of the straight corridor. The results indicate a gradual decrease in average velocity within the designated regions as the queue progresses. Additionally, we examined the fundamental diagram of the middle region, where pedestrian flow remains stable. Due to the limited number of participants, data points could not be obtained for the entire density range. Compared to previous studies [3], our data consistently exhibited higher values. This can be attributed to the predominantly low-density conditions in our experiment, where participants exhibited a conscious tendency to accelerate, as confirmed by our post-experiment questionnaire. Further comparisons across different conditions revealed that increasing corridor width led to lower density and a broader speed range. Additionally, increasing the proportion of elderly participants (reducing the number of students) resulted in a more continuous walking flow, eliminating the sudden drops in density caused by individual pedestrian slowing down.

During emergency evacuations, pedestrians tend to reduce their interpersonal distance and increase their walking speed [4] to reach a safe area more quickly. However, their perceived urgency varies. Asja's study suggests that at low densities, pedestrians walk at their preferred velocity with minimal interaction with others, a state referred to as the free regime [5]. In our experiment, pedestrian densities remained within this free state range. Therefore, in emergency scenarios, the relationship between a pedestrian's preferred velocity and the space maintained with others within their visible range can reflect their perceived urgency. To quantify this, we calculated the visible area using the K-nearest neighbors (KNN) method and measured psychological urgency using the dynamic pressure concept from fluid mechanics.

$$p = \rho_i v_i^2 \tag{1}$$

$$\rho_i = \frac{1}{S_i} \tag{2}$$

v_i represents the instantaneous velocity of a pedestrian i and S_i denotes the visible nearest-neighbor area. Under low-density conditions, the space maintained by pedestrians is largely subjective. The calculated dynamic pressure can serve as an indicator of perceived urgency. A pedestrian moving at a higher speed while maintaining a smaller interpersonal distance is likely experiencing a greater sense of urgency. The results indicate that in a notified evacuation without a visible disaster, elderly individuals exhibit a stronger sense of urgency than younger ones. Additionally, women of all ages demonstrate a higher urgency level than men. Furthermore, the front of the crowd experience significantly higher urgency than those at the back. Therefore, in a notified evacuation without a visible disaster, guiding personnel should prioritize raising evacuation awareness among pedestrians in the latter half of the crowd.

The experiment included various types of obstacles in different states. By extracting pedestrian trajectories and computing trajectory slope curves, we applied Fast Fourier Transform (FFT) to perform discrete Fourier analysis. By combining low and high frequency components, we corrected trajectory deviations caused by lateral body sway. Additionally, through segmented fitting of high-frequency components, we extracted key gait parameters. We analyzed and compared pedestrian avoidance behaviors for dynamic, static, same-direction, and opposite-direction obstacles, summarizing the differences between elderly and young participants. This study can provide fundamental parameters for pedestrian modeling in notified evacuations without visible disasters and have important implications for the design of elderly-friendly buildings.

Bibliography

[1] Boltes, M., & Seyfried, A. . (2013). Collecting pedestrian trajectories. Neurocomputing, 100(JAN.16), 127-133.

[2] Steffen, B., & Seyfried, A. . (2010). Methods for measuring pedestrian density, flow, speed and direction with minimal scatter. Physica A: Statistical Mechanics and its Applications, 389(9), 1902-1910.

[3] Ren, X., Zhang, J., Song, W., & Cao, S. . (2019). The fundamental diagrams of elderly pedestrian flow in straight corridors under different densities. Journal of Statistical Mechanics Theory and Experiment, 2019(2).

[4] Helbing, D., Farkas, I., & Vicsek, T. . (2000). Simulating dynamical features of escape panic. Nature, 407(6803), 487-90.

[5] Jelić, A., Appert-Rolland, C., Lemercier, S., & Pettré, J. (2012). Properties of pedestrians walking in line: Fundamental diagrams. Physical Review E—Statistical, Nonlinear, and Soft Matter Physics, 85(3), 036111.

Experimental analysis of firefighters crossing multiple obstacles under smoke and heat environment

Yixi Tao[1,2], Xuehua Song[1], Hang Yu[1], Weiguo Song*[1], and Jun Zhang[1]

[1]State Key Laboratory of Fire Science, University of Science and Technology of China
[2]Bishan Fire and Rescue Division, Chongqing Fire and Rescue Brigade

Abstract Firefighter movement experiments were conducted in a multi-factor coupled environment (dense smoke and high temperatures) to examine movement characteristics and influencing factors when crossing various obstacles. The study analyzed the effects of obstacle types and crossing postures on movement speed and explored the relationship between movement time and ten individual characteristics, categorized into three groups: basic information, firefighting experience, and psychological factors. The findings provide valuable insights for optimizing firefighting operations and improving firefighter safety training.

Keywords Smoke and heat environment, Multi-obstacle, Firefighter, Movement characteristics

Introduction

The firefighting and rescue environment is characterized by dense smoke, high temperatures, and complex obstacles, posing significant risks to firefighter safety. Existing research on firefighter movement primarily focuses on three aspects: (1) the effects of equipment load and carrying methods on mobility [1], (2) the relationship between air consumption and task intensity when using self-contained breathing apparatus (SCBA) [2], (3) the influence of search formations, spatial cognition, and information demands on wayfinding behavior [3]. However, existing experimental studies are conducted in simplified environments that differ significantly from actual firefighting and rescue scenarios. The combined effects of dense smoke, high temperatures, and multiple obstacles have not been adequately considered, leading to data and conclusions that may not effectively support firefighting operations.

Experimental setup

Based on these considerations, an experiment was conducted at the Bishan Fire and Rescue Division training facility in Chongqing, China (Fig.1(a)). This facility simulates complex firefighting environments, incorporating dense smoke, high temperatures, and multiple obstacles. Artificial smoke was released to reduce visibility to 0.5 meters, while high-power heating devices elevated the ambient temperature to 40 centigrade. The experimental route featured 13 obstacles, none of the participating firefighters had prior training on this route (Fig.1(d)). A total of 50 firefighters participated, all wearing full firefighting protective gear, including fire-resistant clothing, helmets, and self-contained breathing apparatus (SCBA), in accordance with operational requirements (Fig.1(b)). Each firefighter completed the experiment individually, with the process monitored and recorded using thermal imaging (Fig.1(c)). Data collection included movement time and SCBA air consumption. Additionally, a questionnaire was conducted to obtain individual characteristic data across three categories: basic information(years, BMI, physical fitness), firefighting experience(years of firefighting service, number of firefighting incidents, smoke and heat training, firefighter skill), and psychological factors(fear of darkness, fear of dense smoke, fear of unfamiliar and unknown)—encompassing ten variables.

Experimental analysis

In this study, five typical obstacles were selected to analyze movement speed under varying conditions, including differences across obstacle types and the impact of crossing postures on the same obstacle, as

*Email of the corresponding author: wgsong@ustc.edu.cn

shown in Fig.2. It was observed that obstacles requiring crawling or squeezing through, such as transverse barriers, significantly reduced movement speed. Similarly, obstacles that necessitated bending or crawling, such as height-restricted barriers, also imposed notable movement constraints. Additionally, for the same obstacle, the choice of crossing posture had a significant effect on movement speed. Building upon these findings, the relationship between individual characteristics and movement time was further examined. A correlation analysis was conducted on ten individual characteristics to assess their impact on movement time.

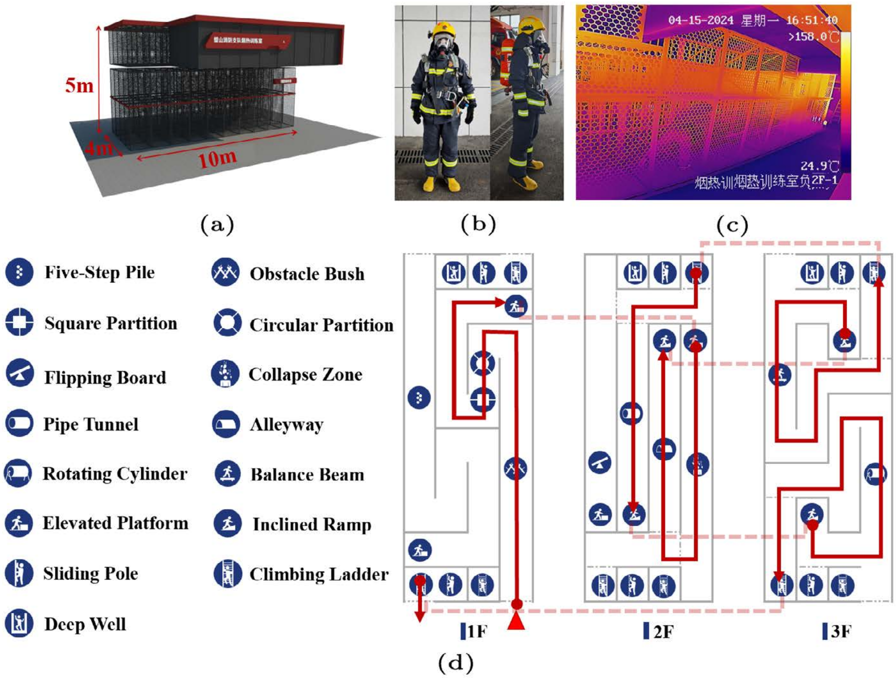

Figure 1: Experimental Overview.(a) Facility.(b) Firefighter gear.(c) Movement process.(d) Experimental route.

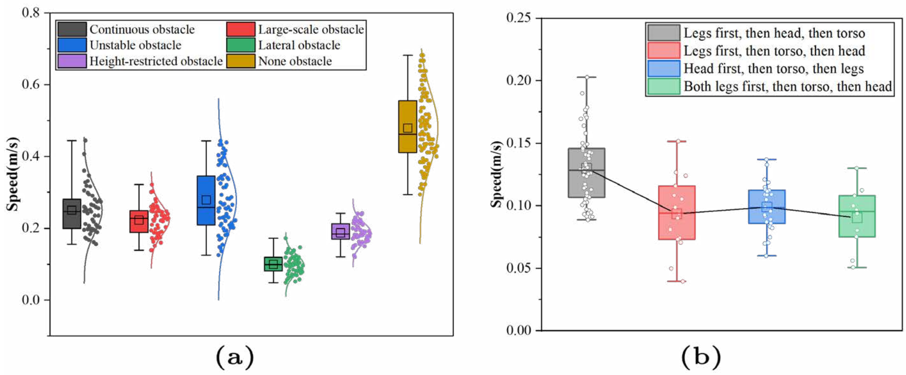

Figure 2: Experimental Analysis. (a) Movement speed across different obstacles. (b) Movement speed under different crossing postures for partitions.

Bibliography

[1] Latosinski, F., Cuesta, A., Alvear, D., Ferna´ndez, D., *Determinants of stair climbing speeds in volunteer firefighters*, Safety Science **171**, 106398, 2023.

[2] Wohlgemuth, K. J., Jesko, A., Frost, V., Conner, M. J., Mota, J. A., *Characteristics of slow and fast performers on a firefighter air consumption test*, Applied Ergonomics **118**, 104262, 2024.

[3] Chen, J. Y., Li, N., Shi, Y. M., Du, J.,*Cross-cultural assessment of the effect of spatial information on firefighters' wayfinding performance: A virtual reality-based study*, International Journal of Disaster Risk Reduction **84**, 103486, 2023.

12th International Conference on Pedestrian and Evacuation Dynamics (PED 2025)
Prague, Czech Republic – September 9-12, 2025

Self-organisation in pedestrian dynamics simulation: a stochastic port-Hamiltonian approach

Rafay Nawaid Alvi*[1,2,3], Barbara Rüdiger[1,3], and Antoine Tordeux[2,3]

[1]Chair for Stochastics, University of Wuppertal, Germany
[2]Chair for Traffic Safety and Reliability, University of Wuppertal, Germany
[3]Institute for Mathematical Modelling, Analysis and Computational Mathematics (IMACM), University of Wuppertal, Germany

Abstract In this contribution, we use simulations to explore lane and stripe formation in pedestrian dynamics using a stochastic port-Hamiltonian system. Our approach is minimalist, enabling identification of fundamental modelling components and paving the way for further theoretical investigations.

Keywords Pedestrian dynamics, lane formation, stripe formation, stochastic port-Hamiltonian system

Extended abstract

The modelling of pedestrian dynamics is of great interest in safety, traffic, and civil engineering. Typical applications include simulation-based design and evacuation planning of complex infrastructures (such as train stations or stadiums) or the organisation of large public events (such as festivals or demonstrations). Pedestrian dynamics are mainly governed by local and nonlinear interaction mechanisms. Besides, pedestrian crowds are complex systems that describe self-organising phenomena [7]. For instance, when pedestrians move in opposite directions, they naturally form lanes to accommodate counter flows; while for cross flows, where they move in directions perpendicular to each other, they form stripes. Modelling and analysing the collective behaviour based on pedestrian interaction is not straightforward.

Port-Hamiltonian systems are well established modelling approaches of nonlinear physical systems [9]. The port-Hamiltonian modelling approach, which decomposes the dynamics into skew-symmetric terms, dissipation, input, and output is a meaningful representation of many systems. Interacting particle systems and pedestrian dynamics have also been modelled using port-Hamiltonian frameworks [5, 8].

In this contribution, we explore the dynamics of lane and stripe formation by simulation using stochastic port-Hamiltonian systems. The modelling approach is minimalistic and paves the way for further theoretical investigations. The pedestrian model is a stochastic formulation of a simplified (isotropic) *social force* model [2] given by

$$\begin{cases} \mathrm{d}q_n(t) &= p_n(t)\,\mathrm{d}t, \\ \mathrm{d}p_n(t) &= \gamma\big(u_n - p_n\big)\,\mathrm{d}t + \sum_{m=1}^{N} \nabla\mathcal{U}\big(q_m - q_n\big)\,\mathrm{d}t + \sigma\,\mathrm{d}W_n(t), \end{cases} \tag{1}$$

where $q = (q_n)_{n=1}^N \in \mathbb{R}^{2N}$ and $p = (p_n)_{n=1}^N \in \mathbb{R}^{2N}$ are the positions and velocities of the pedestrians, $\gamma \geq 0$ is the relaxation (dissipation) rate, $u_n \in \mathbb{R}^2$ is the desired velocity, $\mathcal{U}(x) = ab\exp\big(-|x|/b\big)$, $a \geq 0$, $b > 0$, is a short-range repulsive potential on the distance, W_n are standard Wiener process and σ is the noise volatility. The Hamiltonian of the system is

$$\mathcal{H}(z) = \frac{1}{2}\sum_{n=1}^{N} p_n^\top p_n + \frac{1}{2}\sum_{n=1}^{N}\sum_{m=1}^{N} \mathcal{U}(q_m - q_n), \tag{2}$$

where $z = [q, p]^\top$ describes the system state. The port-Hamiltonian formulation of the system is given by [8, 3]

$$\mathrm{d}z(t) = \begin{bmatrix} 0 & I_N \\ -I_N & -\gamma I_N \end{bmatrix} \nabla\mathcal{H}\big(z(t)\big)\,\mathrm{d}t + \begin{bmatrix} 0 \\ \gamma I_N \end{bmatrix} u\,\mathrm{d}t + \begin{bmatrix} 0 \\ \sigma I_N \end{bmatrix} \mathrm{d}W(t), \tag{3}$$

where $u = (u_1, \dots, u_N)^\top \in \mathbb{R}^{2N}$. Different parameter settings lead to the formation of various patterns. If $\gamma = 0$, the deterministic system with $\sigma = 0$ is a strictly Hamiltonian colloid where the energy is conserved

*Email of the corresponding author: alvi@uni-wuppertal.de

(i.e. the Hamiltonian is constant), while the stochastic system accumulates the energy provided by the noise and diverges. Assume $\gamma > 0$ while $a = 0$, then the pedestrians no longer interact and the system is dissipative. Assume $\gamma, a > 0$ and $u_n = 0$ for all $n \in \{1, \ldots, N\}$, then the system is Hamiltonian-dissipative with stable deterministic crystallisation dynamics. In fact, the self-organization of lanes and stripes observed in pedestrian dynamics requires all port-Hamiltonian components and additionally a high relaxation rate γ and a low noise volatility σ.

In [8], a phase transition from disorder to collective phenomenon occurs in a deterministic framework as the input control parameter γ increases. In preliminary simulation results, we recover a comparable phase transition in the stochastic framework by increasing the noise volatility (see Fig. 1). This phenomenon is known in the literature as the *freezing by heating* effect [1]. Similar behaviour is observed for random initial conditions and for systems initially organised in lanes. This suggests that the system has a unique stationary distribution for a wide range of initial conditions. In contrast, further simulation results show that a *noise-induced ordering* effect [4] arises for stripe formation in 90 degree cross flow for low noise volatility.

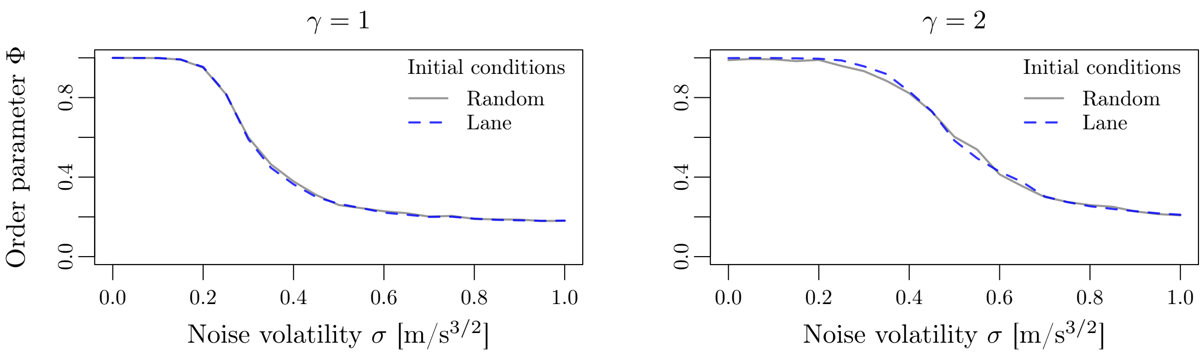

Figure 1: Mean lane formation order parameter Φ for noise volatilities ranging from 0 to 1 in 0.05 steps in a counterflow experiment where $u_n = (-1, 0)$ for half of the pedestrians while $u_m = (1, 0)$ for the remaining pedestrians with $\gamma = 1$ (left panel) and $\gamma = 2$ (right panel). A phase transition occurs as the noise volatility increases. The lower the dissipation rate, the earlier the transition. Simulation results obtained using a leapfrog Maruyama scheme with time step $\delta t = 0.01$. The order parameter is averaged over 20 time units after a simulation time of 200 with an 11×5 periodic system with 32 pedestrians and where $a = 5$ and $b = 0.3$. The results are averaged over 100 simulations for each value of σ. The order parameter for lane formation is given by $\Phi = \frac{1}{N} \sum_{n=1}^{N} \phi_n$ with $\phi_n = \big[(L_n - \underline{L}_n)/(L_n + \underline{L}_n)\big]^2$ where $L_n = \operatorname{card}\big(m,\ |y_n - y_m| < 1/2,\ u_n = u_m\big)$ while $\underline{L}_n = \operatorname{card}\big(m,\ |y_n - y_m| < 1/2,\ u_n \neq u_m\big)$ [6].

References

[1] D. Helbing, I. J. Farkas, and T. Vicsek. Freezing by heating in a driven mesoscopic system. *Physical Review Letters*, 84(6):1240, 2000.

[2] D. Helbing and P. Molnàr. Social force model for pedestrian dynamics. *Physical Review E*, 51(5):4282, 1995.

[3] B. Jacob and C. Totzeck. Port-Hamiltonian structure of interacting particle systems and its mean-field limit. *Multiscale Modeling & Simulation*, 22(4):1247–1266, 2024.

[4] B. Khelfa, R. Korbmacher, A. Schadschneider, and A. Tordeux. Heterogeneity-induced lane and band formation in self-driven particle systems. *Scientific Reports*, 12(1):4768, 2022.

[5] I. Matei, C. Mavridis, J. S. Baras, and M. Zhenirovskyy. Inferring particle interaction physical models and their dynamical properties. In *2019 IEEE 58th Conference on Decision and Control (CDC)*, pages 4615–4621. IEEE, 2019.

[6] M. Rex and H. Löwen. Lane formation in oppositely charged colloids driven by an electric field: Chaining and two-dimensional crystallization. *Physical Review E*, 75(5):051402, 2007.

[7] A. Schadschneider, M. Chraibi, A. Seyfried, A. Tordeux, and J. Zhang. Pedestrian dynamics: From empirical results to modeling. *Crowd Dynamics, Volume 1: Theory, Models, and Safety Problems*, pages 63–102, 2018.

[8] A. Tordeux and C. Totzeck. Multi-scale description of pedestrian collective dynamics with port-Hamiltonian systems. *Networks and Heterogeneous Media*, 18(2):906–929, 2023.

[9] A. J. van der Schaft and D. Jeltsema. Port-Hamiltonian systems theory: An introductory overview. *Foundations and Trends in Systems and Control*, 1(2-3):173–378, 2014.

12th International Conference on Pedestrian and Evacuation Dynamics (PED 2025)
Prague, Czech Republic – September 9-12, 2025

“Valency” model of pedestrian group behaviour

Francesco Zanlungo*[1] and Zeynep Yücel[2]

[1]University of Palermo, Palermo, Italy
[2]Ca' Foscari University of Venice, Venice, Italy

Abstract We propose a model for social groups of any size in pedestrian crowds. This model allows groups with four of more members to walk in large U formations, while splitting in more stable subgroups (dyads and triads) when needed. The model is not based on a set of rules, but on a single cost function.

Keywords Social groups, mathematical model

Social groups are an important component of pedestrian crowds, and are well known to present characteristic behaviours, such as lower velocities and specific walking formations. For these reasons, they have been the subject of many research works, and are becoming an important component of crowd models and simulators. Most of the research on walking social groups has focused on groups of two (dyads) and three (triads) pedestrians, since these are the most commonly occurring ones, are obviously simpler than larger groups, and they represent the fundamental and dynamically stable components of larger groups [1], which arguably makes them also easier to observe.

A mathematical model of group behaviour, applicable in principle to groups of arbitrary size, is introduced by [2]. The fundamental idea is that pedestrians walking and socially interacting need to keep both their local goal (walking direction) and group partners in their field of view. This necessity may be modelled by introducing a function $U(\vec{\mathbf{r}}) = U(r, \theta)$ that each pedestrian tries to optimise, r being the distance to the partner and θ the angle formed between the relative position of the partner $\vec{\mathbf{r}}$ and the local goal direction (preferred velocity). Although in [2] quantitative computations are performed for a specific form of U and in the framework of a second order differential model, this approach can be used in any model in which pedestrians move to minimise a cost function. Furthermore, any function assuming two minima in $r = r_0, \theta = \pm\theta_0 \approx \pm\pi/2$, r_0 being the distance at which pedestrians prefer to walk, will reproduce the abreast walking of dyads, whose dynamics will be basically determined by the ratio of $\partial_r^2 U$ and $\partial_\theta^2 U$ in the minima. It is also shown that using $\theta_0 > \pi/2$ causes dyads to walk slower than individuals, while preserving abreast walking.

To apply the model to larger groups while preserving realistic behaviour, [2] assumes that pedestrians interact only with their first neighbours. In the case of triads, using the original proposed form leads to reproducing their behaviour (specifically the V formation and velocity) in a quantitative way without the need of a further calibration. When this approach is applied to groups with four or more members, it produces a U formation in agreement with the findings of [3]. Nevertheless, such U formations were not observed in the data set of [1, 2], which on the other hand presented four people groups splitting in two dyads, each of them presenting its typical abreast formation. The discrepancy with the results of [3] may be due to the different environments and crowd compositions of these ecological data sets, but also to the fact that in [1, 2] pedestrians were observed for a longer time, and thus had a higher probability to re-arrange in subgroups. This also suggests that larger groups may be also difficult to observe as that, since they may appear to be multiple dyads and triads.

On the other hand, dyads and triads cannot split as long as the members intend to continue interacting, since if they split, at least one of them would be alone. Basically, each pedestrian in a large group needs to have at least a partner, and must be able to accept another partner. We call this a “valency” model of large groups, since each pedestrian has the possibility to strongly interact with two other people from the large group, which will be positioned in their two U minima. Nevertheless, as soon as one minimum is filled, the pedestrian becomes “neutral”, and does not seek further interaction.

Mathematically, the valence model can be defined by modifying the function U (regardless of its specific definition) in the following way. First of all, we define, for each pedestrian i in the group the minimum value

$$U_0^i = \min_j U(\vec{\mathbf{r}}_{ij})$$

*Email of the corresponding author: francesco.zanlungo@unipa.it

Timetable

Talk index

where $\vec{\mathbf{r}}_{ij}$ is the relative position with respect to group partner j. We then define $\vec{\mathbf{r}}'$ as any vector satisfying the equipotential condition

$$U(\vec{\mathbf{r}}') = U_0^i, \; ||\vec{\mathbf{r}}'|| > r_0,$$

and define the new cost function using a new model parameter Δ_U as

$$U'(\vec{\mathbf{r}}) = \begin{cases} U(\vec{\mathbf{r}}), & \text{if } ||\vec{\mathbf{r}}|| \le r_0 \text{ or } U(\vec{\mathbf{r}}) < U_0^i, \\ U_0^i + \int_{\vec{\mathbf{r}}'}^{\vec{\mathbf{r}}} e^{-\frac{(U(\vec{\mathbf{s}})-U_0^i)^2}{\Delta_U^2}} \vec{\nabla} U(\vec{\mathbf{s}}) \cdot \mathrm{d}\vec{\mathbf{s}}, & \text{otherwise.} \end{cases} \tag{1}$$

Basically this assures that repulsive interactions with partners at a distance closer than r_0, and the interaction with the partner at the minimum value of the cost function will be unchanged, while the interaction (cost function gradient) with the others will be reduced as $\vec{\nabla} U'(\vec{\mathbf{r}}) = e^{-\frac{(U(\vec{\mathbf{r}})-U_0^i)^2}{\Delta_U^2}} \vec{\nabla} U(\vec{\mathbf{r}})$.

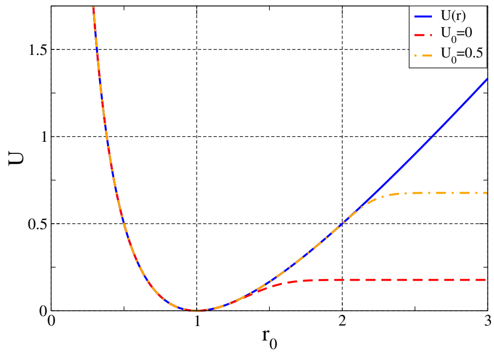

Figure 1: Radial dependence of cost function for first neighbours (blue), and for other partners when the first neighbour is in r_0 (red) or $2r_0$ (orange). Distance measured in multiples of r_0.

This modified cost function, shown in Figure 1 for the only radial dependence of the specific function proposed in [2], assures that while pedestrians will interact strongly with their closest (cost function wise) neighbour, they will be fundamentally neutral with respect to other partners. Nevertheless, partners walking alone will still be strongly seeking for interaction, trying to locate themselves in a free "minimum cost function" position. Once pedestrians have two partners occupying both minima they will strongly interact with both partners, but they will be ready to break one (but not both) link. As a result, large group U formations are possible, but based on initial conditions and/or collision avoidance will in general divide the large group into stable dyads and triads (Figure 2).

Figure 2: Left, blue: pedestrians walking (from left to right) in a large U formation. Right, red: pedestrians in the same group and using the same model, split in subgroups.

We stress that this is not done by introducing a set of rules, but just a single cost function. Furthermore, although to obtain figures the potential of [2] and a second order model have been used, the proposed approach can be used for any cost function based approach, and for any cost function reproducing the basic behaviour of dyads.

Bibliography

[1] Zanlungo, F., Kanda, T., *Do walking pedestrians stabily interact inside a large group? Analysis of group and sub-group spatial structure*, Proceedings of the Annual Meeting of the Cognitive Science Society, **35**, 35, 2013.

[2] Zanlungo, F., Ikeda, T., Kanda, T., *Potential for the dynamics of pedestrians in a socially interacting group*, Physical Review E **89.1** 012811, 2014.

[3] Schultz, M., Rößger, L., Fricke, H., Schlag, B., *Group dynamic behavior and psychometric profiles as substantial driver for pedestrian dynamics*, in *Pedestrian and evacuation dynamics 2012*, pp.1097-1111, Springer, 2014.

12th International Conference on Pedestrian and Evacuation Dynamics (PED 2025)
Prague, Czech Republic – September 9-12, 2025

Modeling metastable dynamics of dyads from large-scale data

Chiel van der Laan*[1,2], Tom Harmsen[1], and Alessandro Corbetta†[1,2]

[1]Applied Physics and Science Education, TU/Eindhoven, The Netherlands
[2]Eindhoven Artificial Intelligence Systems Institute, TU/Eindhoven, The Netherlands

Abstract Understanding of social groups behavior is crucial in pedestrian dynamics. In this study, we analyze and model the movement of dyads using millions of real-world trajectory at a train platform in Eindhoven The Netherlands. We identify key external parameters influencing dyad configurations and develop a data-driven differential modeling approach based on these parameters. The proposed model is validated by comparing simulated and empirical data on key statistical properties.

Keywords Pedestrian dynamics, groups, metastable dyads, real-life data, stochastic modeling

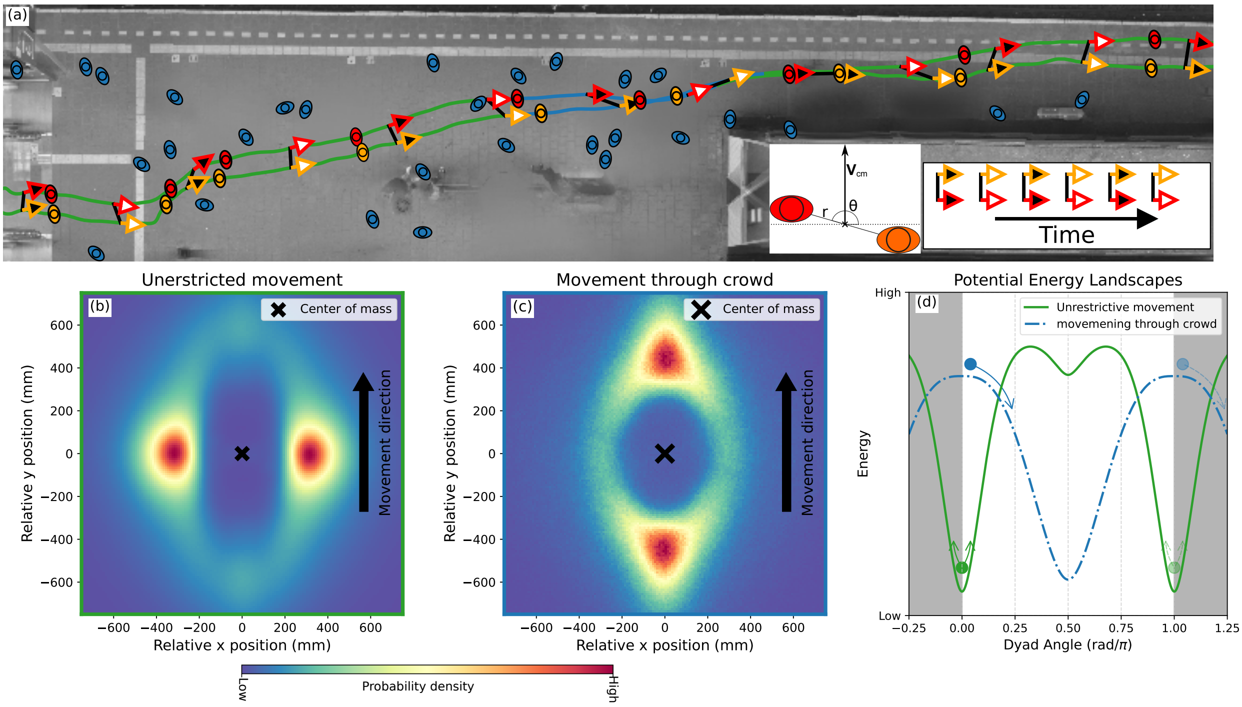

Figure 1: **(a)** Example of a dyad trajectory walking on the platform of Eindhoven Central Station. Arrows identify points in the trajectory happening simultaneously. In the initial and final part of the trajectories (green segments) the dyad traverses relatively empty areas, while in the middle part (blue segment) the dyad navigates through a denser crowd. The dyad formation along these segments conforms with the probability density functions respectively depicted in heatmaps **(b)** and **(c)**. In which the preferred walking direction is perpendicular and parallel to the walking direction respectively. **(d)** illustrates changes in the energy landscape as the dyad traverses the platform, driving a transition from a perpendicular to a parallel configuration.

In built environments, pedestrians often navigate as part of social groups. Understanding their behavior is essential for developing accurate predictive crowd simulations and represents a fundamental challenge in this field. Social group dynamics have been extensively studied in controlled laboratory settings or with small-scale annotated real-world data [1, 2, 5]. While dyads (social groups of two) prefer to walk side by side (perpendicular to the walking direction) [2], this behavior is mostly observed in low-density conditions, often relying on hand annotated data. A model incorporating basic assumptions about dyad social dynamics can effectively predict this configuration [4]. Recent advances in automated

*c.v.d.laan@tue.nl
†a.corbetta@tue.nl

vision allow for large-scale collection of pedestrian trajectories in real-world settings. This enables high resolution statistical analysis into the preferred configuration of dyads, outside of low-density conditions.

In this study, we identify and parameterize how external parameters influence preferred dyad configuration as they navigate through a wide variety of crowds scenarios in a real-world setting (a train platform at Eindhoven Central Station) An example trajectory is shown in Fig. 1a. We automatically identify more than three million dyads dyads by building on top of the graph-based method by Pouw at al. [3] in a wide variety of crowd scenarios.

We show that the preferred dyad configuration is driven by two key external parameters: the density of the surouding crowd (ρ) and the relative velocity ($\mathbf{v_r}$) between the dyad and this crowd. As reported in Fig. 1b, in low-density situations, the preferred configuration is perpendicular to the movement direction, while when navigating through stationary dense crowds (Fig. 1c), the preferred configuration is parallel, indicating that the system exhibits meta-stable behavior.

In the reference frame of the dyad center (parallel to the dyad velocity), any dyad configuration can be described by an angle, θ, and a distance, r, between the dyad pair (cf. Fig. 1a). We model the switching behavior between these two preferred configuration and the parallel configuration with a Langevin-like equation,

$$\ddot{\theta} = -\frac{\partial U\left(\theta, r, \rho, \mathbf{v_r}\right)}{\partial \theta} - \gamma\dot{\theta} + \eta(t), \tag{1}$$

where $U\left(\theta, \rho, \mathbf{v_r}\right)$ is a potential function, γ is a damping coefficient and $\eta(t)$ represents stochastic noise. To utilize this model we make the key assumptions that there is a Gibbs-like relation between probability $P(\theta, \rho, \mathbf{v_r})$ of the dyad being in configuration (θ, r) and the potential, which results in

$$U\left(\theta, \rho, \mathbf{v_r}\right) \propto -\log\left(P(\theta, \rho, \mathbf{v_r})\right). \tag{2}$$

We validate our modeling approach by comparing empirical observations of dyad pairs with simulated trajectories considering a wide range of observables including conditioned probability distributions on θ as function of time and autocorrelation functions (cf. Fig. 2).

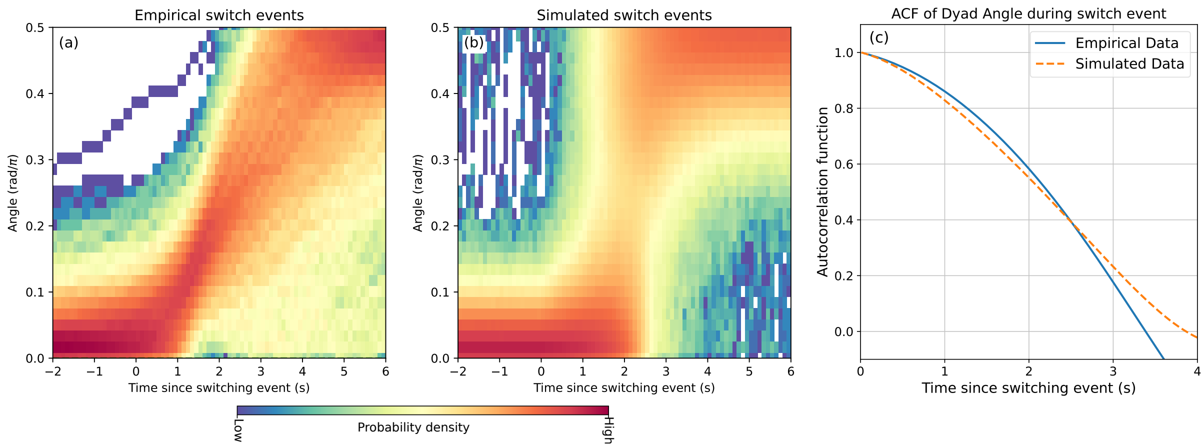

Figure 2: Transition dynamics of dyad pairs from a horizontal to a vertical configuration. **(a)** Probability distribution of switch events derived from empirical data. **(b)** Corresponding probability distribution obtained from simulated trajectories. **(c)** Autocorrelation function (ACF) for both the empirical and simulated trajectories for $\theta(t)$.

Bibliography

[1] Luca Crociani, Andrea Gorrini, Claudio Feliciani, Giuseppe Vizzari, Katsuhiro Nishinari, and Stefania Bandini. Micro and macro pedestrian dynamics in counterflow: the impact of social groups. 11 2017.

[2] Mehdi Moussaïd, Niriaska Perozo, Simon Garnier, Dirk Helbing, and Guy Theraulaz. The walking behaviour of pedestrian social groups and its impact on crowd dynamics. *PLOS ONE*, 5(4):1–7, 04 2010.

[3] Caspar A. S. Pouw, Federico Toschi, Frank van Schadewijk, and Alessandro Corbetta. Monitoring physical distancing for crowd management: Real-time trajectory and group analysis. *PLOS ONE*, 15(10):1–18, 10 2020.

[4] Francesco Zanlungo, Tetsushi Ikeda, and Takayuki Kanda. Potential for the dynamics of pedestrians in a socially interacting group. *Phys. Rev. E*, 89:012811, Jan 2014.

[5] Francesco Zanlungo, Zeynep Yücel, Dražen Brščić, Takayuki Kanda, and Norihiro Hagita. Intrinsic group behaviour: Dependence of pedestrian dyad dynamics on principal social and personal features. *PLOS ONE*, 12(11):1–26, 11 2017.

12th International Conference on Pedestrian and Evacuation Dynamics (PED 2025)
Prague, Czech Republic – September 9-12, 2025

Emergence of motion synchronization in pedestrian crowds

Yi Ma*[1], Meng Shi[2], Eric Wai Ming Lee[3], and Richard Kwok Kit Yuen[3]

[1]Institute for Disaster Management and Reconstruction, Sichuan University, Chengdu 610065, China
[2]School of Computer Science, South-central Minzu University, Wuhan 430074, China
[3]Department of Architecture and Civil Engineering, City University of Hong Kong

Abstract This study investigates when, how and why motion synchronization spontaneously emerges in pedestrian crowds through a pedestrian flow experiment that directly track the foot motion of pedestrians. We show that synchronization is most likely to emerge at the onset of jamming. We demonstrate that synchronization is essentially caused by insufficient interpersonal safety distance; it actually serves as a motion strategy that helps pedestrians avoid interpersonal collisions and maintain maximal collective movement efficiency under insufficient safety distance.

Keywords Pedestrian flow, synchronization, self-organized phenomenon

In pedestrian crowds, it is often observed that pedestrian individuals spontaneously synchronize their movements in the absence of external stimuli. However, it is unclear why this synchronization phenomenon spontaneously emerges in pedestrian crowds.

To address this question, we conducted a quasi-one-dimensional pedestrian flow experiment in a corridor with a length of 25.2 m and a width of 2.40 m. We performed 40 runs of experiments using different crowd sizes in the corridor, including using 20, 30, 40, 50, 60, 70, 80, 90, 100, 110, and 120 participants. In the experiment, we tracked and recorded the pedestrians' foot motion, then extracted the pedestrians' foot motion trajectories and footsteps from the recorded video clips.

Based on the experiment, we first investigated the probability of the synchronization at different pedestrian densities. Specifically, we calculated the proportion of synchronized steps for each pedestrian and linked it with pedestrian density (see Fig. 1(a)). The results show that when the density is approximately 1.80 persons/m^2, the proportion of pedestrian synchronized steps is the highest, suggesting that synchronization is most likely to spontaneously emerge at 1.80 persons/m^2. We found from the fundamental diagram obtained from the experiment that this critical density is exactly the jamming density (see Fig. 1(b)). This also means that the movement synchronization of pedestrians is most likely to emerge at the onset of jamming, similar to the occurrence of the synchronization of pedestrians in a one-dimensional single-file crowd environment [1].

For the detected synchronized pedestrian steps in the experiments, we also recorded the relative position of synchronized pedestrian and neighbor, and the directional angle of synchronized neighbor (i.e., the angle between the direction of the synchronized neighbor and the desired moving direction of the pedestrian) at the starting frame of each of these synchronized step samples. Figs. 1(c) and (d) show the relative positions and the distribution of the directional angles of synchronized neighbors over the collected synchronized step samples, respectively. From Fig. 1(d), we can see that the number of occurrences of a 0° directional angle is obviously larger than that of 90° and 270° directional angles. This result indicates that synchronization with neighbors in front is more likely to spontaneously occur than synchronization with neighbors on the left or right.

Why are pedestrians most likely to spontaneously synchronize their movements at the jamming density? To answer this question, we calculated the difference between the step length in each natural step and the interpersonal distance at the starting moment of pedestrian step, then linked this difference with the density at the starting moment of the step. The resulting relation diagram is shown in Fig. 1(e). The result shows that the difference is the minimal (only 0.22 m) at 1.80 persons/m^2 (i.e., at the jamming density). That is, if a pedestrian makes a step, the buffer distance between the adjacent neighbors and the body center of the pedestrian will only be 0.22 m. This means that if the neighbors stop suddenly, the

*Email of the corresponding author: yima23-c@my.cityu.edu.hk

body of the pedestrian will likely collide with the body of a neighbor, given that humans have a certain body thickness. However, if the pedestrian chooses to synchronize his or her stepping motion with the adjacent neighbors, the pedestrian will not only avoid potential collisions with the adjacent neighbors but also realize a stepping motion. This twofold benefit induces the pedestrian to synchronize with the adjacent neighbors. This is the reason why pedestrians are most likely to spontaneously synchronize their movements at the jamming density.

Our findings provide new insights into pedestrian flow dynamics.

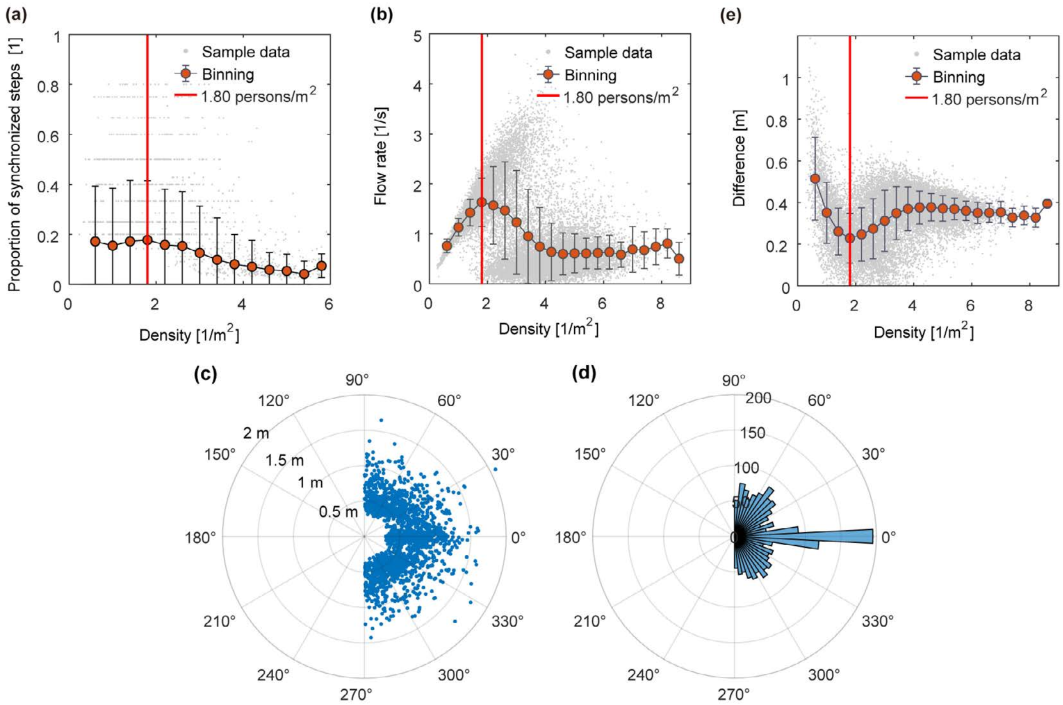

Figure 1: The experimental results. (a) Relation between the proportion of synchronized steps and pedestrian density. (b) Fundamental diagram. (c) and (d) are the relative positions and the distribution of the directional angles of synchronized neighbors over the collected synchronized step samples. (e) Relation between the distance difference and pedestrian density.

Reference

[1] Ma, Y., Lee, E. W. M., Shi M., Yuen R. K. K., *Emergence of motion synchronization in pedestrian crowds*, Nat. Hum. Behaviour **5**, 447-457, 2021.

12th International Conference on Pedestrian and Evacuation Dynamics (PED 2025)
Prague, Czech Republic – September 9-12, 2025

Density Dependent Gait Patterns in Crowds

Carina Wings*[1], Maik Boltes[1], and Uwe G. Kersting[2]

[1]Forschungszentrum Jülich, Germany
[2]German Sports University Cologne, Germany

Abstract Ensuring safety in dense crowds remains a critical challenge, partly due to a lack of detailed understanding of 3D motion dynamics such as foot positioning and base of support, which are critical for gait stability and fall prevention. This study aims to address this gap by examining gait patterns in dense crowds using a 3D motion capture system. The research focuses on how individual characteristics influence gait patterns changing as crowd density increases, e.g. to be able to identify indicators of potential falls or injuries.

Keywords Gait pattern, 3D motion capturing, Bottleneck experiment, Crowd safety

Introduction

Crowd safety is important issue and limited understanding of crowd behavior and individual movement can lead to serious incidents, including falls [6]. The relationship between crowd density and falls, along with the mechanisms causing them, requires further investigation.

Previous studies have identified factors such as step length and speed as influential in determining the likelihood of falls. Studies such as those by Boomers et al. [1] on walking speeds near bottlenecks, Chatagnon et al. [3] on recovery strategies following external pushes have all contributed valuable insights. Furthermore, one-dimensional pedestrian flow experiments by researchers like Jelic et al. [4], Wang et al. [5], and Cao et al. [2] have provided information about the gait patterns during density changes. These studies have already considered some aspects, but none of them have examined subjects within a crowd. However, a more detailed and nuanced understanding of how individuals behave within dense crowds is essential. This study aims to address this need by examining the gait patterns of individuals in a crowd, employing a 3D motion capture system to precisely record and analyze their movements. Specifically, the study will focus on two key objectives: First, to identify patterns or trends in gait behavior in general and especially these that may serve as indicators of potential crowd-related falls or injuries. Second, to explore how individual characteristics like height, gender, and age influence changes in gait patterns as crowd density increases.

Figure 1: Experimental setup and motion capture data. (Left) Top camera view from bottleneck experiment, and (Right) corresponding motion capture data from one participant, illustrating the detailed movement patterns recorded.

*Email of the corresponding author: `c.wings@fz-juelich.de`

Timetable
Talk index

Method

A mixed-methods approach will be used to achieve the study objectives. The 3D motion capture system will be used to record gait patterns, while trajectory analysis will provide data on crowd density. The experimental setup involves a crowd passing a bottleneck, as shown on the left of Figure 1, with some participants wearing XSens MVN Link suits to capture their 3D movements in detail. The recorded data for one person 3.5m in front of the bottleneck is shown on the right of Figure 1. A range of conditions are created to simulate real-world scenarios by varying the size of the crowd and the motivation of individuals to pass through the bottleneck over several experimental runs. An initial representation of the data for one person is shown in Figure 2, where the left and right heel strikes of a subject are given in the movement space of the experimental setup. The steps of the right foot are always red, and those of the left foot are always blue. The black line connecting consecutive steps helps to visualise the timing. The step lengths were determined based on these steps. Where the distance between heel strikes is Euclidean. This step length was then plotted against the Voronoi density of the subject at the moment of the heel strike, which is the start of the step. In the following, further subject data will be evaluated in order to conduct a statistical evaluation. On the basis of this statistical evaluation, correlations between density and step length in movement direction, as well as other gait characteristics like the step width, will be determined. In addition, step types will be examined in relation to walking speed and density.

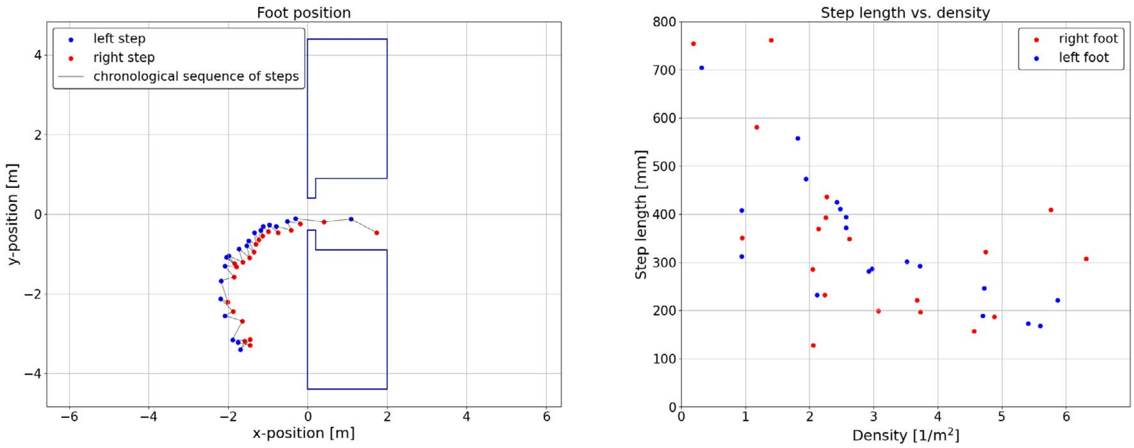

Figure 2: Data of one subject. (Left) Left and right steps of the subject in walking area of the test set-up, and (Right) the subject's step length in relation to the corresponding Voronoi density.

Bibliography

[1] Boomers, A.K., Boltes, M., Kersting, U. G., *How Approaching Angle, Bottleneck Width and Walking Speed Affect the Use of a Bottleneck by Individuals*, Sensors **24**, 2024.

[2] Cao, S., Zhang, J., Song, W., Shi, C., Zhang, R, *The stepping behavior analysis of pedestrians from different age groups via a single-file experiment*, J. Stat. Mech., 2018.

[3] Chatagnon, T., Feldmann, S., Adrian, J., Olivier, A.-H., Pontonnier, C., Hoyet, L., Pettré, J., *Standing balance recovery strategies of young adults in a densely populated environment following external perturbations*, Safety Science **177**, 2024.

[4] Jelic, A., Appert-Rolland, C., Lemercier, S., Pettré, J., *Properties of pedestrians walking in line. II. Stepping behavior*, Physical Review E, 2012.

[5] Wang, J., Weng, W., Boltes, M., Zhang, J., Tordeux, A., Ziemer, V., *Step styles of pedestrians at different densities*, J. Stat. Mech., 2018.

[6] Zeitz, K. M., Kadow-Griffin, C., *Injury Occurrences at a Mass Gathering Event*, Australasian Journal of Paramedicine, 2005.

12th International Conference on Pedestrian and Evacuation Dynamics (PED 2025)
Prague, Czech Republic – September 9-12, 2025

Single-file pedestrian flows with free density

Cécile Appert-Rolland*[1] and Julien Pettré[2]

[1]IJCLab, Univ. Paris-Saclay, CNRS, F-91405 Orsay, France
[2]Inria, Univ. Rennes, CNRS, IRISA, M2S, Rennes, France

Abstract We present single-file experiments in which the global density is not prescribed. It turns out that pedestrians choose their interdistances so as to be close to the jamming transition. Pedestrians seem quite efficient at forming a circle with unprescribed characteristics, though it implies collective decision.

Keywords Following behavior, fundamental diagram, decision making, single-file flow, headway

Pedestrian dynamics are quite complex as humans have little inertia and have a double control on their walking direction and speed. One-dimensional flows allow to restrict the dynamics to its longitudinal component, focusing on the following behavior between two successive pedestrians. Experiments investigating single-file (or one-dimensional = 1D) flows in controlled conditions [1, 2, 3] serve as a benchmark. They have allowed for example to compare the effect of cultural differences [4] or of age [5], or the influence of staircases [6] on 1D fundamental diagrams. They are intimately related to locomotion characteristics (step length, frequency) [7, 8, 9]. They can give rise to macroscopic phenomena such as stop-and-go waves [3, 10, 5]. Beyond 1D, following behavior can be involved in more complex flows as in large corridors [10]. Progress in pedestrian tracking allows now to compare controlled experiments with field data collected at real events [11].

While the first single file experiments were considering closed and prescribed trajectories, for which the total density is fixed, more recent ones have allowed to consider cases where pedestrians are free to choose their interdistance with the predecessor without global density constraint. We performed for example experiments in which pedestrians had to form a circle of unprescribed radius, or others in which pedestrians had to follow a straight line with freedom to choose the distance to the predecessor [12, 13].

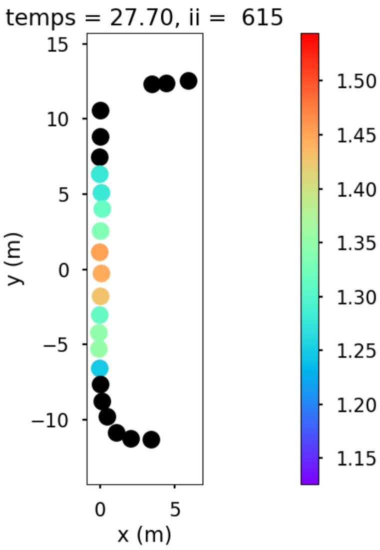

Figure 1: Top view of the line experiment at a given time. Each pedestrian is represented by a disk. Inside the measurement area, disks are colored according to the pedestrian's velocity.

We could have though that in the latter case, pedestrians would have chosen comfortable large interdistances. Actually it turns out not to be the case. Pedestrians rather seem to choose headways close to the jamming transition, possibly because of the social pressure coming from behind.

*Email of the corresponding author: `Cecile.Appert-Rolland@ijclab.in2p3.fr`

By giving instructions to the leader of the line, we could slow down the whole flow. We observe how the direction of propagation of density fluctuations switches from downstream at free speed to upstream at low speed.

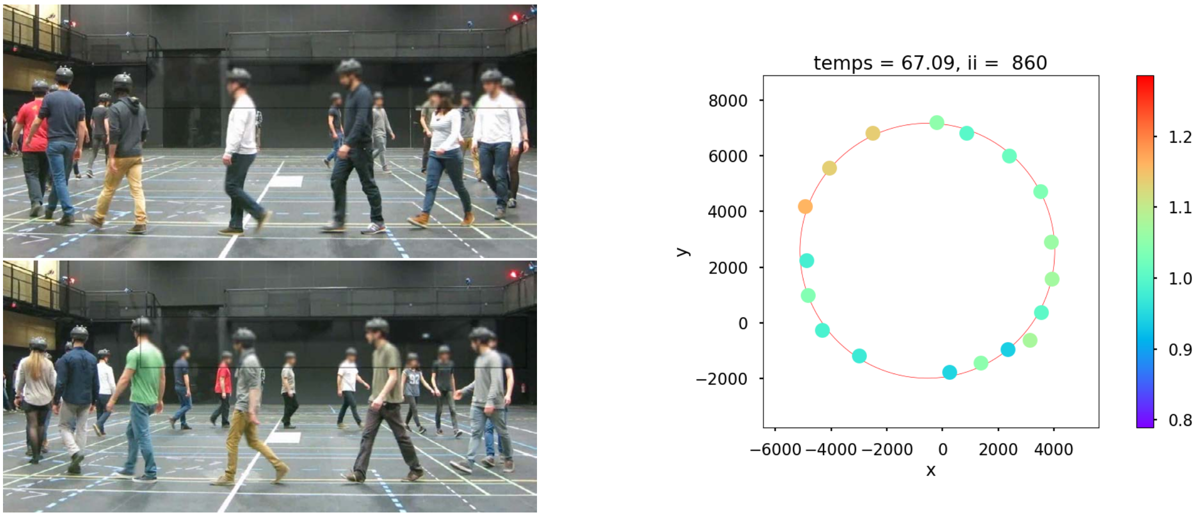

Figure 2: The circle experiment. (Left) Snapshots of the experiment, during the transient corresponding to the formation of the circle (Top) and once a permanent regime is established (Bottom). (Right) Top view of the circle experiment at a given time. Each pedestrian is represented by a disk colored according to the pedestrian's velocity. The line indicates the fitting circle.

While in the line experiment the decision about how much space to leave in front is individual, it is collective when the task is to form collectively a circle. Pedestrians seem quite efficient at this task, and for example the position of the circle center is quite steady. We present various observables allowing to characterize the circle formation process.

Bibliography

[1] A. Seyfried, B. Steffen, W. Klingsch, M. Boltes, *J. Stat. Mech.* , P10002 (2005).

[2] A. Seyfried *et al.*, In W. Klingsch, A. Schadschneider, M. Schreckenberg, editors, *Pedestrian and evacuation dynamics 2008* pages 145–156. Springer-Verlag Berlin (2010).

[3] A. Jelić, C. Appert-Rolland, S. Lemercier, J. Pettré, *Phys. Rev. E* **85**, 036111 (2012).

[4] U. Chattaraj, A. Seyfried, P. Chakroborty, *Advances in Complex Systems* **12**, 393 (2009).

[5] S. Cao *et al.*, *Phys. Rev. E* **94**, 012312 (2016).

[6] J. Chen, S. Lo, J. Ma, *J. Stat. Mech.* , 083403 (2017).

[7] A. Jelić, C. Appert-Rolland, S. Lemercier, J. Pettré, *Phys. Rev. E* **86**, 046111 (2012).

[8] Z. Fang *et al.*, *Physica A-Statistical Mechanics and its Applications* **391**, 307 (2012).

[9] S. Cao, J. Zhang, W. Song, C. Shi, R. Zhang, *J. Stat. Mech.* , 033402 (2018).

[10] S. Lemercier *et al.*, *Computer Graphics Forum* **31**, 489 (2012).

[11] S. Gulhare, A. Verma, P. Chakroborty, *Collective Dynamics* **3**, 1 (2018).

[12] C. Appert-Rolland *et al.*, *Collective Dynamics* **5**, 1 (2020).

[13] C. Appert-Rolland, A.-H. Olivier, J. Pettré, *Submitted, under revision, arXiv:2307.11548, hal-04237618* (2023).

Timetable
Talk index

Balancing Data Needs in Pedestrian Dynamics Experiments: Crowd Size, Number of Trials, and Trial Duration

Max Kinateder*[1], Paul Geoerg[2], and Nikolai Bode[3]

[1]National Research Council Canada
[2]Akkon University of Applied Sciences
[3]School of Engineering Mathematics and Technology, University of Bristol

Abstract Determining the required data for Pedestrian Evacuation Dynamics studies is essential but complex. Using an illustrative example from a study of pedestrians moving through a bottleneck, we discuss estimating crowd size, number of trials, trial duration, and how to report results. Critically, these considerations depend on the level of measurement, with different approaches needed for microscopic versus macroscopic measurements.

Keywords Sample size, Reproducibility, Pedestrian crowds, Power analysis

1 Introduction

Planning how many data points are needed to answer a research question reliably is critical to any empirical study. Many fields have established methods to estimate sample sizes, typically rooted in statistical procedures as well as theoretical and practical considerations. However, in Pedestrian Evacuation Dynamics, this answer is not necessarily straightforward, as sample size requirements can apply to the number of people needed in a single trial[1] (i.e., the crowd size) as well as the number and duration of trial repetitions for a single condition (either with the same participants or with a new crowd). Further, microscopic and macroscopic levels of measurement need to be considered. Here, we discuss three topics with relevance to *macroscopic* experimental studies of pedestrian dynamics: (1) crowd size, (2) sample size, i.e., the number of data points from the same conditions needed, and (3) duration of trials as avenues for increasing sample size. We begin with an illustrative example, demonstrate challenges, and provide recommendations for planning and reporting on each of the three topics.

2 Case study: effect of wheelchair users on egress times

The example uses a previously published study on a common experimental paradigm, in which crowds moved repeatedly through a bottleneck (crowd sizes ranged from 21 to 28). In the wheelchair condition, two participants used wheelchairs; in the control condition, all participants moved without any assistive devices [2]. Each condition was repeated more than 30 times. See [2] for details.

We sampled 30 trials per condition from the data and calculated egress times - defined as the last participant clearing the bottleneck in a given trial - from the trajectory data. Figure 1 shows the descriptive statistics of the conditions compared. The egress times were on average 4.3 s longer in the wheelchair condition compared to the control condition (t-test, $t(49.00) = 7.59$, $p < .001$), implying an effect size of $d = 2.04$ (Cohen's d - relates the mean difference to the variability).

Crowd size: Crowd size requirements fundamentally depend on the geometry of the study layout and desired microscopic or macroscopic measurements. In the example above, space was needed for the crowd to achieve a steady state of free flow before reaching the bottleneck and enough participants to generate sufficient densities at the bottleneck to impact free movement speeds. Data from pilot empirical or simulation studies can help to inform this decision.

*Email of the corresponding author: Max.Kinateder@nrc-cnrc.gc.ca

[1]A trial refers to an instance of data collection in an experiment; sometimes the term 'run' is used synonymously. For more information on terminology in pedestrian dynamics, see [1]

[2]There were other manipulations in the original study that are omitted from this analysis

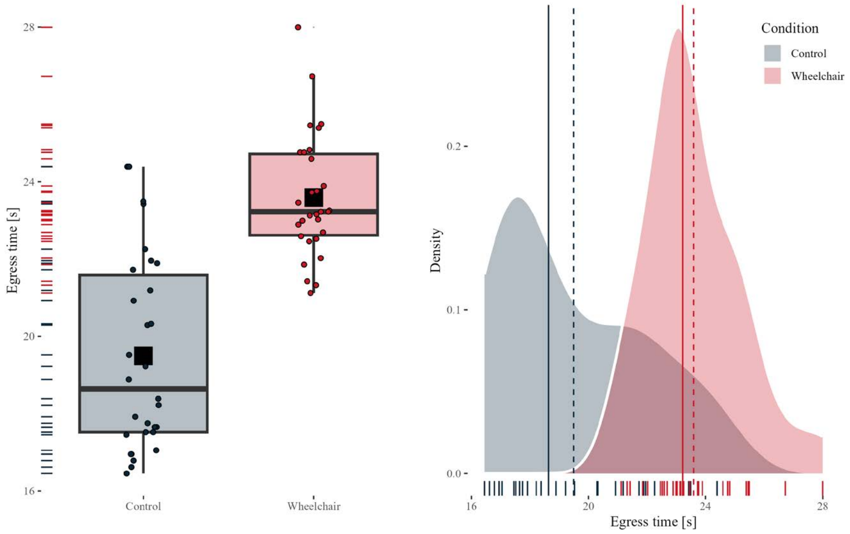

Figure 1: Egress times from multiple trials. Left: box-plot with overlaid scatter plots and marginal rug plot; squares indicate means. Right: density plot; solid lines indicate medians; dashed lines indicate means.

Sample size - number of replicate trials: The range of egress times varied considerably in the example: in 10 % of the trials in the control condition, egress times were longer than the median egress time in the wheelchair condition (Figure 1). That is, had the study only comprised a single trial per condition, it is entirely possible that the inverse results could have been observed.

Cohen introduced the concept of power analysis to estimate sample sizes [3]. Statistical power describes the likelihood of a significance test (e.g., t-test) detecting an effect when there actually is one. Power is sensitive to effect (e.g., Cohen's d) and sample size - the weaker the effect, the more data are needed to detect it reliably. For example, eight independent trials would be needed to detect an effect of $d = 2.04$ (the observed effect size in the example) with a power of 0.9. While effect sizes are often not known *a priori*, estimates can be derived from the literature or pilot studies (e.g., using simulations).

Duration of trials: Another relevant question is the duration of trials. Longer trial durations are a way to increase sample sizes by taking multiple measurements at different time points from one experimental trial. This approach is particularly useful to increase the sample size in macroscopic observations (e.g., flow). However, it assumes the time gaps between consecutive measurements are large enough to ensure independence of data, thus requiring typically relatively large crowd sizes.

3 Conclusion

Crucial in the consideration of sample size is the level of measurement. Statistically robust macroscopic findings require many replicate trials, or long time series for repeated independent measurements. Statistically robust microscopic measurements within crowds require careful accounting for interactions between individuals and the resulting correlations in their behaviour. Careful planning and transparent reporting practices allow researchers in pedestrian dynamics to generate reproducible insights.

References

[1] Juliane Adrian et al. "A Glossary for Research on Human Crowd Dynamics". en. In: *Collective Dynamics* 4 (Mar. 2019), pp. 1–13. ISSN: 2366-8539. DOI: 10.17815/CD.2019.19. URL: https://collective-dynamics.eu/index.php/cod/article/view/A19 (visited on 02/13/2025).

[2] Paul Geoerg et al. "Together Apart: the Influence of Increased Crowd Heterogeneity on Crowd Dynamics at Bottlenecks". en. In: *Collective Dynamics* 9 (June 2024), pp. 1–10. ISSN: 2366-8539. DOI: 10.17815/CD.2024.156. URL: https://collective-dynamics.eu/index.php/cod/article/view/A156 (visited on 02/13/2025).

[3] Jacob Cohen. *Statistical Power Analysis for the Behavioral Sciences*. en. Google-Books-ID: 2v9zDAsLvA0C. Routledge, 1988. ISBN: 978-1-134-74270-7. URL: https://doi.org/10.4324/9780203771587.

Timetable
Talk index

Evacuation simulations accounting for properties of the blended wing body aircraft

Yuming Dong*[1], Xiaolu Jia[2], Daichi Yanagisawa[1], and Katsuhiro Ninshinari[1]

[1]Department of Aeronautics and Astronautics, The University of Tokyo, Tokyo, Japan
[2]Beijing Key Laboratory of Traffic Engineering, Beijing University of Technology, Beijing, China

Abstract In this study, a blended wing body aircraft evacuation simulation model was developed to evaluate how the cabin layout can improve the evacuation efficiency of a blended wing body aircraft. Results demonstrate that an expanded aisle could be a simple method to evacuate a blended wing body aircraft in 90 seconds, while exit positions have limited influence.

Keywords Evacuation, Blended wing body, Cellular automaton, Stochastic processes, Simulation

Introduction

In an emergency landing, a fast and safe evacuation is the key to minimizing casualties. Currently, a full evacuation within 90 s is required by countries around the world for most passenger aircraft [1]. As a popular option for the next-generation passenger aircraft, the blended wing body (BWB) aircraft are anticipated to fulfill the ever-increasing requirements of good fuel economy and low emissions [2]. Previous studies on BWB aircraft evacuation often assume aisle widths and exit positions are similar to those of conventional aircraft. [3]. However, the BWB's large cabin is likely to provide more space for aisles, thus providing a viable option for improving evacuation efficiency and satisfy the 90-second rule.

Evacuation model

Live aircraft evacuation demonstrations are highly expensive and pose a significant risk to all participants. Consequently, computer-based evacuation simulations are indispensable for studying aircraft evacuations, especially for novel designs like the BWB aircraft. As shown in Figure 1, the evacuation model is based on the well-tested cellular automaton (CA) model. A 3D model of a BWB aircraft and the presumed cabin shape are also provided. This cabin poses a number of unique challenges for the emergency evacuation: larger cabin space, longer distance to exits, internal walls and supporting structures within the cabin, difficulty of placing emergency exits on the two sides, the higher likelihood of rear exit failures, etc.

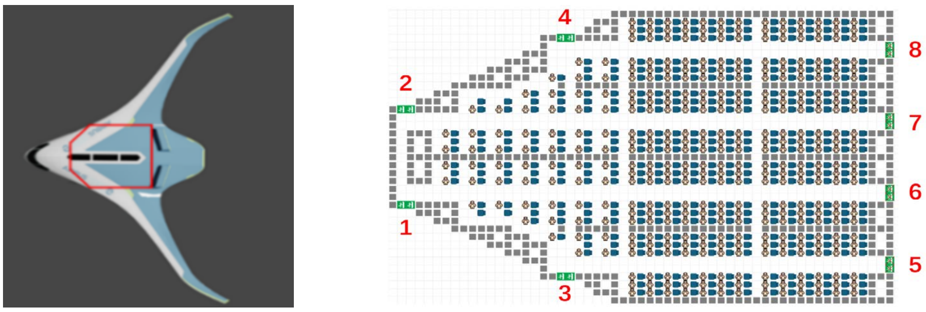

Figure 1: Left: 3D model of Airbus Maverick. The presumed cabin area is marked by a box.
Right: Overview of the evacuation model. It was designed to simulate a BWB cabin divided into four bays (mainly based on NASA's N2A-HWB), each with its own aisle. Exit 5, 6, 7, 8 are assumed to be unavailable to examine the worst-case scenario (longest distance to exits compared to other possibilities) for satisfying the 90-second rule.

*Email of the corresponding author: dong-yuming@g.ecc.u-tokyo.ac.jp

Once the simulation starts, 370 agents will mark the closest exit as their target and begin moving. If an agent cannot move forward because of congestion, it will attempt to randomly change target if possible. The total time required for all agents to leave the aircraft is recorded as the evacuation time. Considering the uncertainty in the cabin design of BWB, a number of cabin layouts were tested to find out how the following four factors can influence the evacuation efficiency: 1. The widths of four aisles: the BWB cabin may allow aisles wide enough for two agents; 2. The locations of exits: moving exit 3 and 4 further towards the tail; 3. The widths of exits: increasing the width of exit 3 and 4; 4. Areas near exits: how much space do exit 3 and 4 have, and the number of obstacles near exit 3 and 4.

Results and discussion

As shown in Figure 2, only aisle widths have a significant impact on the evacuation. All four aisles must be at least two cells wide to bring evacuation time below 90 seconds. The cabin should also allow small open areas near exit 3 and 4 to ensure a fast evacuation. Locations and widths of exit 3 and 4 have limited influence on the evacuation time. Considering that adding extra side doors could be a significant challenge for the BWB aircraft designer and manufacturer, increasing the aisle widths could be relatively straightforward and effective method to comply with the 90-second rule. Adjustments in supporting structures may also be necessary to create open areas near the exits. This indicates that no significant alteration is required for many existing BWB conceptual designs. For example, placing the cabin below the wing in order to create more side doors may not be necessary. Further study may include additional factors such as stress responses and passengers with disabilities.

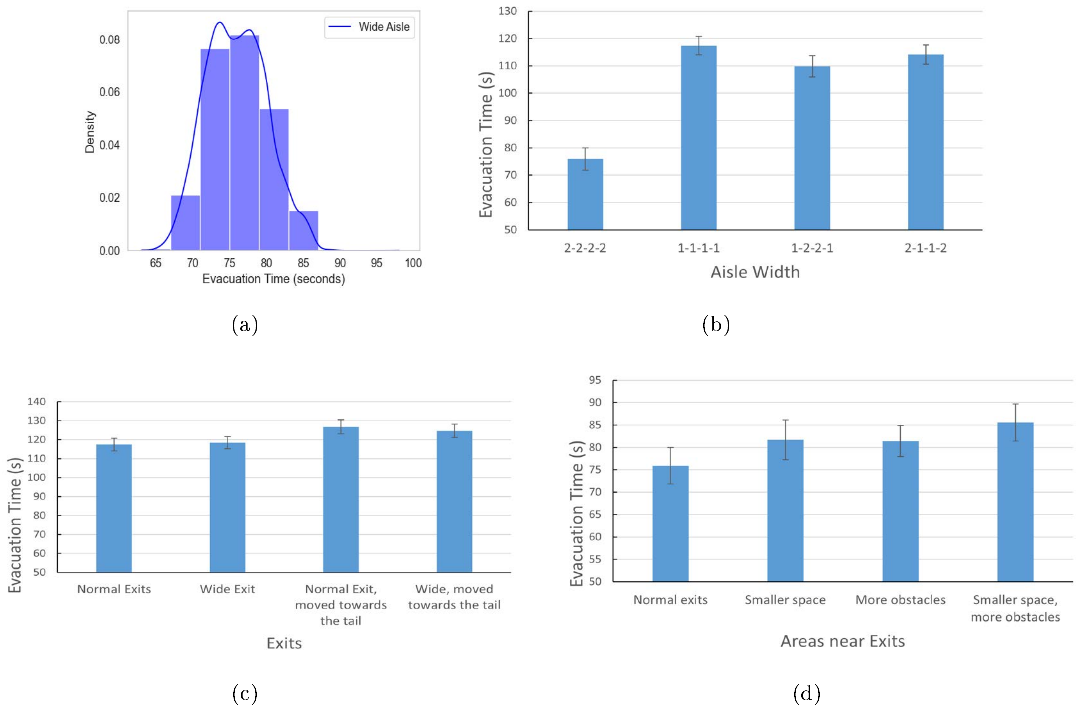

Figure 2: (a): Kernel density distributions of the evacuation time when all aisles are two cells wide.
(b): Evacuation time when widths of four aisles are different. The four numbers refer to aisle widths from left to right. For example, "1-2-2-1" means the two inner aisles are two cells wide, and the outer two aisles are one cell wide.
(c): Evacuation time when locations and exit 3 and 4 are different. All aisles are one cell wide.
(d): Evacuation time when areas near exit 3 and 4 are adjusted. All aisles are two cells wide.

Bibliography

[1] Galea ER, Wang Z, Jia F., *Numerical investigation of the fatal 1985 Manchester Airport B737 fire*, Journal Name **The Aeronautical Journal**, 287-319, 2017.

[2] Liebeck RH., *Design of the blended wing body subsonic transport*, Journal Name **Journal of aircraft**, 10-25, 2015.

[3] Chen K, Wang X, Li P, et al., *Modeling and evaluating passenger evacuation and risk in blended wing body aircraft using continuous displacement agents*, Journal Name **Discover Applied Sciences**, 1-17, 2025.

12th International Conference on Pedestrian and Evacuation Dynamics (PED 2025)
Prague, Czech Republic – September 9-12, 2025

Wildfire Evacuation Modelling of Tourist Campsites

Borja Rengel*[1], Enrico Ronchi[2], Amina Labhiri[2], Virginie Dréan[1], Bruno Guillaume[1] and Eric Guillaume[1]

[1]Efectis France, Research and Development Department, Saint Aubin, France
[2]Lund University, Division of Fire Safety Engineering, Sweden

Abstract Wildfires pose a serious risk to tourist campsites in the wildland-urban interface, where evacuation can be challenging due to limited access and transient populations. This study evaluates evacuation strategies at campsites through two French case studies, using crowd- and traffic-modelling simulations. Key findings highlight the impact of pre-movement delays, evacuation modes, and travel distances on overall evacuation efficiency. Recommendations include optimizing assembly points, improving communication, and establishing nearby safety zones.

Keywords Wildfire evacuation, tourist campsites, crowd and traffic modelling

Extended Abstract

Wildfires pose a serious threat to populations in the wildland-urban interface (WUI), where vegetation and urbanized populated areas intersect [1]. This risk is of special importance to tourist areas characterized by a mix of people with different cultures and languages, as well as a variety of infrastructures and emergency strategies. Tourists are transient populations who may come from non-wildfire-prone areas and be unfamiliar with their temporarily residential environment, thus meaning that they are potentially exposed to a risk they are not familiar with. Serious wildfires have occurred in tourist destinations worldwide, highlighting the numerous difficulties tourists may encounter during such events and potentially rendering them a vulnerable population. Notable examples include the 2016 Madeira fire in Portugal [2], the 2023 Maui Fire in the USA [3], and the 2023 Rhodes Fire in Greece [4].

Campsites, often located in remote, wooded areas, represent some of the most wildfire-hazardous vacation spots, particularly due to possibly rapid spread of fire. The number of tourists at campsites is typically higher during the summer season, coinciding with the peak risk of wildfires. These locations often have limited access roads and narrow pathways, which can significantly impede the evacuation process. The primary challenge lies in ensuring the safety of tourists and staff, especially when faced with the urgent need to evacuate most of the accommodations without fire protection measures due to a wildfire. Effective evacuation strategies are essential for mitigating risks in wildfire-prone camping areas; however, many campsites adopt their own strategies based on available resources and specific needs, which may not always be the most effective.

Crowd movement simulation models are highly valuable for evaluating evacuation strategies by identifying the safest routes, ensuring optimal resource allocation, and facilitating scenario analysis to uncover potential bottlenecks. They also implicitly consider the impact of variables such as weather and terrain on evacuation times, informing policy and decision-making for more effective evacuation strategies.

This paper aims to assess the evacuation strategies in campsites through two case studies in southeastern France, namely Le Bois de Pins and Le Bois Fleuri (see Figure 1), which differ significantly in terms of surface area, number of occupants, evacuation mode (by private vehicle or on foot), and types of accommodation. To achieve this, crowd-modelling simulations have been performed using Pathfinder [5], which can simulate the movement of tourists within the campsite. These simulations account for a set of behavioural itineraries, including tourists grouping by family members, reaching assembly points, returning to their accommodations to pick up belongings, and then either leaving the campsite or taking their vehicles. Additionally, traffic simulations with SUMO [6] have been conducted to estimate the travel time from the campsite to a site of relative safety.

For each campsite, different evacuation scenarios have been proposed, taking into account the occupant's state - whether they are awake or sleeping - as well as the possibility of blocked emergency exits. Tourists were distributed according to the accommodation capacity, with a significant number of children included, given that (i)

* Email of the corresponding author: borja.rengel@efectis.com

campgrounds are often family-oriented tourist destinations and (ii) children typically have reduced travel speed (a conservative assumption). Tourist profiles have been defined based on existing data [7-9], with adjustments for reduced movement speed due to terrain irregularities and possible obstacles along the main evacuation routes.

The results reveal that, as expected, pre-movement and waiting times at various locations significantly influence the overall evacuation time. Additionally, the distance between assembly points/exits and individual plots greatly affects the total evacuation time, particularly in larger campsites. The mode of evacuation (on foot or by car) also has a substantial impact on the time required for tourists to reach a safety point. Recommendations include (i) implementing multiple assembly points well-distributed throughout the campsite or bypassing them altogether by providing key evacuation information via sirens and other means (e.g. speakers and apps), and (ii) establishing a vegetation-free safety zone near the campsite (reachable on foot) to accommodate occupants.

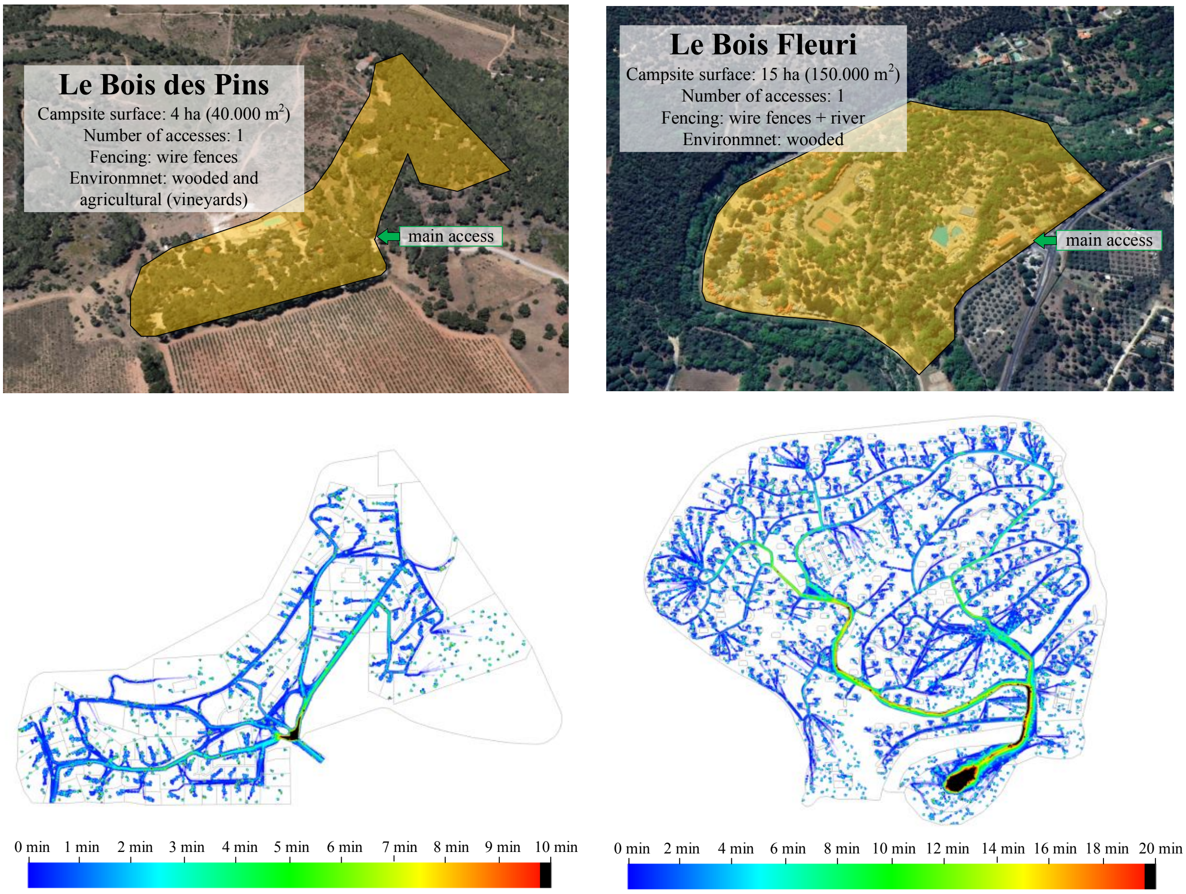

Figure 1: French campsites selected (up) and example of some Pathfinder results (down).

The information presented comes from the European-funded project called Wildland-Urban-Interface Fire Touristic Infrastructures Protection Solutions (Grant Agreement number 101101169, on call UCP-2021-PP in program UCPM2027). The project's main goal is to foster a harmonized understanding of wildfire risks in tourist areas, focusing on their impact on buildings, installations, cultural heritage, and infrastructure.

Bibliography

[1] Benichou, N., Adelzadeh, M., Singh, J., Gomaa, I., Elsagan, N., Kinateder, M., Ma, C., Gaur, A., Bwala, A., Sultan, M., National Guide for Wildland-urban interface fires: Guidance on hazard and exposure assessment, property protection, community resilience and emergency planning to minimize the impact of wildland-urban interface fires, National Research Council of Canada, 2021.

[2] Ronchi, E., Rein, G., Gwynne, S., Wadhwani, R., Intini, P., Bergstedt, A., e-Sanctuary: Open Multi-Physics Framework for Modelling Wildfire Urban Evacuation, Fire Protection Research Foundation, 2017.

[3] Gupta, G., The Maui fires are more deadly than Hawaii's 1960 tsunami, The New York Times (Digital Edition), 2023.

[4] Bubola, E., Kitsantonis, N., Greek Hotels Fear a Burning Future: 'Even the Animals Are Moving Away', International New York Times, 2023.

[5] Patfhinder Technical Reference Manual version 2023-2, Thunderhead Engineering, 2023.

[6] Alvarez Lopez, P., Behrisch, M., Bieker-Walz, L., Erdmann, J., Flötteröd, Y., Hilbrich R., Lücken, L., Rummel, J., Wagner, P., Wießner, E., Microscopic Traffic Simulation using SUMO, IEEE Intelligent Transportation Systems Conference (ITSC), 2018.

[7] Boyce, K., Shields, T., Silcock, G., Toward the characterization of building occupancies for fire safety engineering: capabilities of disabled people moving horizontally and on an incline, Fire Technology 35 (1), 51-67, 1999.

[8] Korhonen, T., Hostikka, S., Fire Dynamics Simulator with Evacuation: FDS + Evac Technical Reference and User's Guide, VTT Technical Research Center of Finland, 2009.

[9] Shields, T.J., Fire and disabled people in buildings, Building Research Establishment, Report BR231, 1993.

Timetable
Talk index

12th International Conference on Pedestrian and Evacuation Dynamics (PED 2025)
Prague, Czech Republic – September 9-12, 2025

The Lecture Hall Example as a Reference for Evacuation Simulations – An Updated Study

Angelika Kneidl*[1], Burkhard Forell[2], Gerald Grewolls[3], Rainer Könnecke[4], Tim Meyer-König[5], and Andreas Winkens[6]

[1]accu:rate GmbH, Munich, Germany
[2]Fire Safety Engineer, Cologne, Germany
[3]SIMTEGO GmbH, Ulm, Germany
[4]IST GmbH, Frankfurt am Main, Germany
[5]TraffGo HT GmbH, Flensburg, Germany
[6]BPK Ingenieure und Sachverständige für Brandschutz GmbH & Co. KG, Germany

Abstract A comparative study for the evacuation of a lecture hall, using six different microscopic software tools and two macroscopic approaches is presented. Reasons for differences in results, in particular for evacuation times and flow rates are discussed. The purpose of this study is to provide a basis for the definition of benchmarks for evaluating pedestrian dynamics to improve the prediciton quality of simulations.

Keywords Standardisation, crowd simulation, evacuation, fire safety, regulation

1 Introduction

Evacuation simulations play a vital role in ensuring safety during emergencies in complex environments. This study revisits the "Lecture Hall Example," Ref. [1], which was published in 2021 in German. The original study, which compared macroscopic and microscopic evacuation models, revealed deviations of up to 30% in evacuation times between models. These significant discrepancies led the RiMEA association Ref. [2] to form a working group to analyse the causes and propose solutions to improve the consistency of the modeling.

The study examines two evacuation scenarios for a lecture hall with 640 seats and 360 standing places, see Figure 1. Scenario 1 involves a single rear exit, while Scenario 2 includes two front exits. Key findings of the initial analysis revealed differences in geometric interpretations, inconsistencies in input data, and different route allocation among the simulation tools. For example, discrepancies in the modeling of stairs and seating arrangements contributed to varying congestion points and evacuation times. There was no clear pattern that models which predicted longer evacuation times in Scenario 1 do so in Scenario 2. These variations underline the importance of standardizing geometric and population parameters to ensure reliable results.

2 Results

To address these issues, the updated study implemented harmonized input data and repeated simulations with six microscopic tools (Aseri, buildingExodus, crowd:it, FDS+Evac, Pathfinder, PedGo) as well as two macroscopic calculation approaches (Capacity Analysis and Predtetschenski & Milinski). Adjustments included using uniform geometric dimensions based on the CAD file, equal distribution of 640 agents across seating areas, and consistent evacuation routes for outer seating rows. Despite these efforts, evacuation times still exhibited model-specific variations of 27% (Scenario 1) and 26% (Scenario 2) relative to the mean. This highlights the influence of internal algorithms, such as navigation and congestion handling, on the simulation output.

The study also analysed flow rates and their correlation with evacuation times. Sensitivity studies revealed that the assignment of agents to specific routes and the interpretation of geometries, such as stairs and exits, significantly impact evacuation outcomes.

*Email of the corresponding author: ak@accu-rate.de

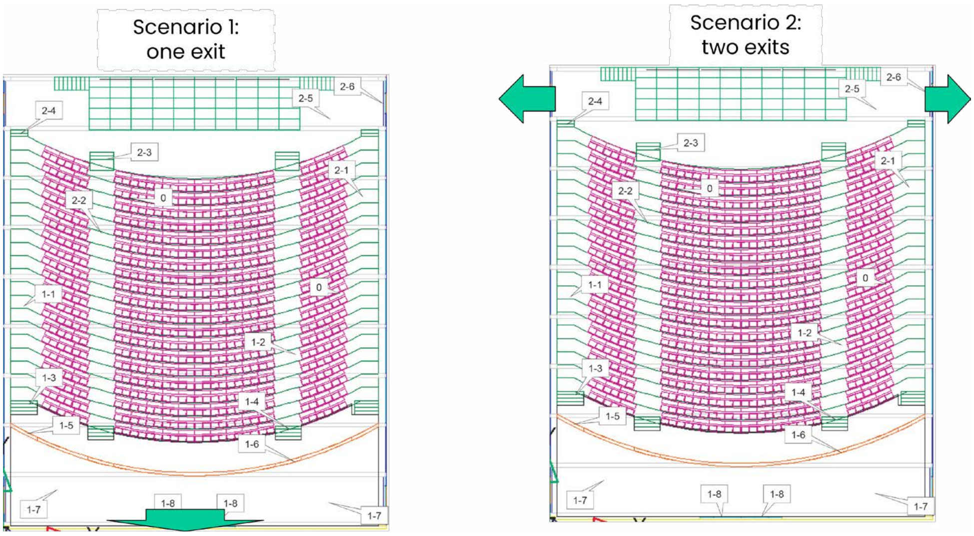

Figure 1: Floor plan of the two scenarios

The findings emphasize the need for robust validation frameworks, such as the RiMEA test cases Ref. [2] or the ISO 20414 Ref. [3], to evaluate model performance under standardized conditions. Sensitivity analyses of parameters such as population size, route allocation, and pre-movement times are recommended to address uncertainties. Furthermore, the study advocates for greater transparency and documentation in modeling decisions to enhance reproducibility and reliability.

3 Conclusion

In conclusion, the updated analysis demonstrates the complexity of evacuation simulations and the importance of harmonizing the input data and the methodologies. By standardizing test cases and conducting comprehensive sensitivity analyses, simulation tools can provide more accurate and actionable insights for safety engineering. This study serves as a critical step toward establishing benchmarks for evaluating pedestrian dynamics and ensuring safe evacuations in diverse environments.

Bibliography

[1] Schneider, V., Forell, B., *Personenstromsimulationen und Evakuierungsberechnungen*, Handbuch Brandschutz 2021.

[2] RiMEA e.V., *Guideline for microscopic evacuation analysis*, v4.0.1, 2024

[3] ISO 20414, *Fire safety engineering - verification and validation protocol for building fire evacuation models*, 2020

12th International Conference on Pedestrian and Evacuation Dynamics (PED 2025)
Prague, Czech Republic – September 9-12, 2025

How does the computational speed of pedestrian models depend on the characteristics of the simulated scenario?

Martijn Sparnaaij*[1], Dorine C. Duives[1], and Serge P. Hoogendoorn[1]

[1]Department of Transport and Planning, Delft University of Technology

Abstract Pedestrian models have many applications and there are also many different pedestrian models. But which model is best suited for which application? In addition to validity, the computational speed of a pedestrian is a key factor determining a model's applicability. This contribution presents how the computational speed of commonly used pedestrian models depends on the characteristics of the simulated scenario and what this means for which model is suitable for what application.

Keywords Model speed, Pedestrian models, Computational complexity, Model speed versus simulation scenario characteristics

Introduction

The computational speed of a pedestrian model is a key characteristic that determines the applications for which it is suitable. Can a model, for example, be used for real-time applications, where it needs to run faster-than-real-time? Or, can the model be used in simulation studies that need to deal with a lot of uncertainty in the input, which requires many simulations to be run? Many types of pedestrian movement dynamics simulation models have been developed in the last decades, and multiple studies (e.g., [1]) have reviewed the validity of these models. Hence, for this key characteristic, we have much insight into which types of models are well suited for which types of applications and why. For computational speed, this is unfortunately not yet the case.

To reduce this gap, we analysed how the computational speed of many different pedestrian model types depends on the simulated scenario. This analysis provides insight into how different characteristics of a simulation scenario, such as the size of the walkable space or the distribution of pedestrians over the space, affect a model's computational speed. This provides a first indication of what types of pedestrian simulation models are likely to be more suitable than others for certain types of simulation scenarios and why this is the case. Furthermore, this analysis provides important insights into what scenario characteristics should be included and tested when testing the computational speed of a particular model.

Our analysis consists of two steps. First, we identify the so-called pedestrian model archetypes. These capture the fundamental characteristics and features of a type of pedestrian model from a computational speed point of view. Accordingly, we use our recently developed APS (Assess Pedestrian model Speed) framework [2], in particular the test case creation procedure, to analyse how what scenario characteristics impact the speed of the pedestrian model archetypes and how it impacts their speed.

Pedestrian model archetypes

A pedestrian model archetype captures how the algorithm (the loops, data structure operation etc.) of a type of pedestrian model computes a simulation step. We identified a wide variety of commonly used pedestrian models and analysed how their basic algorithms differ from a computational point of view. From this analysis, we distilled six different pedestrian model archetypes that we present in Table 1.

We also identify variations of each basic archetype. For example, microscopic models that use discrete space, cover a wide range of models that share some basic characteristics, such as being a microscopic model using discrete space. But they also vary with regard to other characteristics, for example, in the update scheme they use. We capture these minor variations, from a computational perspective, in the identied variations. For each basic archetype and variation thereof, we describe their algorithm by pseudocode. This pseudocode forms the basis of the analysis.

*Email of the corresponding author: m.sparnaaij@tudelft.nl

Table 1: An overview of the six basic pedestrian model archetypes covering all three major pedestrian model classes

Microscopic models	1. Continuous space
	2. Discrete space
Mesoscopic models	3. Both continuous and discrete space and discrete time
	4. Discrete space in the form of cells and continuous time
	5. Discrete space in the form of a network and continuous time
Macroscopic models	6. Cell-based

Results

We apply the test case creation procedure (from the APS framework) to the pseudocode of each archetype and variation to obtain the scenario characteristics that impact each of them. We identified a total of 11 characteristics that impact the speed of one or more model archetypes. These are the following:

1. Walkable space size
2. Global density
3. # obstacles
4. Population heterogeneity
5. Spatial distribution pedestrians
6. Network complexity
7. Spatial distribution pedestrian classes
8. Spatial distribution obstacles
9. # Destinations
10. Movement base case
11. Scenario layout

Our analysis also reveals what the relationship is between these 11 characteristics and the model archetypes and variations. Table 2 presents an example of these detailed results. We observe that it depends strongly on the type of model what scenario characteristics impact its speed and how. Some scenario characteristics, like the walkable space size, impact all models in a similar way. Namely, as the space increases (whilst the density remains constant) the models become slower. Others, such as the global density, affect most models but not in the same way. The density affects the cell- and network-based models differently than, for example, the microscopic models. And then there are characteristics, like the number of obstacles of the population heterogeneity, that only impact the speed of a few models.

Table 2: The impact of four scenario characteristics whereby − indicates a negative relationship, 0 the model is not affected by this characteristic and +− the effect can be positive or negative depending on the value of the characteristic. The archetypes are identified by their number presented in Table 1.

Variable	1.	2.	3.	4.	5.	6.
Size walkable space	−	−	−			−
Global density	−	−	−	+−	+−	0
# Obstacles	−	0	0	0	0	0
Population heterogeneity	0	0	0	−	0	−

The results highlight the importance of using scenarios with different characteristics to test the speed of pedestrian models. That is, testing the speed of models whilst varying only one characteristic provides limited insights into their speed. Also, it can produce biased results when comparing models using a limited set of scenarios because not all characteristics impact each model or impact each model in the same way.

Furthermore, the results provide an indication regarding which type of model is particularly suitable for what sort of scenario from a computational speed perspective. For example, the results indicate that a microscopic model using continuous space (no. 1) is not particularly well suited for scenarios with lots of obstacles compared to all other models because it is the only model negatively affected by this scenario characteristic.

Lastly, we note that we study only one factor that determines the speed of a pedestrian model, the scenario characteristics. The model itself and the specific implementation of the model are both major determinants of the speed of the model. Therefore, the results only provide an indication regarding the suitability of a model type for a certain scenario. By applying the APS framework to particular implementations of models more detailed insights can be obtained.

Bibliography

[1] Duives, D. C., Daamen, W., & Hoogendoorn, S. P., *State-of-the-art crowd motion simulation models*, Transportation Research Part C: Emerging Technologies, **37**, 193–209, 2013.

[2] Sparnaaij, M., Duives, D. C., & Hoogendoorn, S. P., *How fast is my model? Part 1: A framework to systematically assess the computational complexity of pedestrian models*, Preprint Arxiv, 2025

12th International Conference on Pedestrian and Evacuation Dynamics (PED 2025)
Prague, Czech Republic – September 9-12, 2025

Toward Automatic Variations of Evacuation Simulations to Enhance Event Safety

Angelika Kneidl*[1], Felix Märtin[2], and Renate Häuslschmid[2]

[1]accu:rate GmbH, Munich, Germany
[2]Municipality of Freiburg i.Br., Freiburg im Breisgau, Germany

Abstract Mass gatherings pose significant challenges for organizers and safety authorities, as seen in past crowd disasters. Effective planning and rapid adaptation in case of danger are crucial to ensuring public safety. Our *Resilience & Event Management System (REMSY)* aims to solve a multitude of challenges surrounding event management but particularly addresses evacuation by enabling stakeholders to simulate and explore various "what-if" scenarios. Through an intuitive interface, planners can easily create and run multiple varied simulations to understand how crowd dynamics may evolve in diverging conditions. To enable data-driven decisions and optimize event planning, they are provided with various key safety indicators. A case study from Freiburg, Germany, will demonstrate the system's real-world applicability and value to stakeholders.

Keywords Event Safety, Crowd Simulation, Evacuation Planning, Emergency Preparedness, Mass Gatherings, Simulation-Based Decision Making, Crowd Management

Introduction & Motivation

Ensuring safety at open air large-scale events and mass gatherings is a complex challenge requiring a sophisticated, adaptive approach that integrates both preventive and responsive measures, such as evacuation planning. While evacuations are typically preplanned, they must be dynamically adapted to real-time conditions. Traditional static planning methods, i.e., the manual determination of evacuation routes and exits for a single event layout, often fail to account for the unpredictability of crowd dynamics and emerging hazards [6]. Unexpected factors—such as an unanticipated surge in visitors or an obstructed emergency exit—can significantly disrupt evacuation processes. Current approaches, being largely manual and scenario-specific, lack the flexibility to accommodate deviations from predefined conditions, forcing emergency responders to make rapid, high-pressure adjustments without a comprehensive situational overview. These ad hoc modifications are necessary but also come with a risk of suboptimal decisions. Therefore, an effective safety framework must encompass a broad range of potential scenarios to enhance the adaptability of evacuation plans, improve stakeholders' understanding of crowd dynamics and the impact of layout decisions during the planning phase.

The FreiburgRESIST[1] project embraces this necessity by developing a comprehensive system that supports the planning, execution, and evaluation of mass gatherings, called *REMSY* (Resilience & Event Management System). At the heart of the project is an event planning tool that allows for the simulation of multiple scenarios in relation to different event layouts. Instead of requiring the user to identify all relevant variations and run simulations individually, the tool automatically varies parameters and simulates all relevant combinations—providing a holistic overview to stakeholders and informing their decisions during event planning and execution.

From Manual to Simulation-based Event Planning

To identify the necessary key variations and decision factors, we conducted workshops and interviews with prospective system users, including Freiburg's police, fire department, department of public order, event organizers, and security services. These discussions revealed the need for an adaptive approach that allows for the evaluation of different scenarios and event layouts. Through these investigations, the following questions emerged as critical for informed decision-making:

- What happens if specific entry points or exit routes are blocked and cannot be used?

*Email of the corresponding author: ak@accu-rate.de

[1]The project *FreiburgRESIST* is funded through the *SIFOLife* program by the Federal Ministry of Education and Research of Germany (funding no. 13N15608, 13N15609 and 13N16812 to 13N16820).

- What if a danger emerges at location A and people start running away from it? What if it emerges at location B instead?
- How many people could be evacuated in both scenarios in a reasonable time?
- How would further or wider exit routes change the capacity?

To address these needs, *REMSY* will enable the execution of various evacuation simulations ('what-if' scenarios), providing users with in-depth insights into different situations.

Automatic Variation of Simulations

Evacuation simulations are a well-established tool for planning and assessing mass gatherings. Several models are available, each based on distinct methodologies, such as the Social Force Model ([2]) or the Optimal Steps Model [1].

For *REMSY*, we use crowd:it [3], an established tool on the market and well-validated by the tests of RiMEA [4] as well as the validation and verification tests of ISO 20414 [5]. The objective of this work is to extend the tool such that planners can easily test "what-if"-scenarios through an intuitive, user-friendly interface (see Figure 1) and receive feedback on the safety of their event layout.

A range of parameters can be adjusted to meet user requirements identified during the workshops, including visitor numbers, escape route widths, and exit availability. Users define parameter ranges (e.g., 10,000–20,000 visitors) that will be tested in multiple simulations. To exclude non-viable configurations, predefined criteria–such as a maximum evacuation time–can be applied. To maintain an overview of all variants, results are presented in a compact format, enabling users to quickly assess the validity of their layout. Figure 1 presents an exemplary simulation setup: visitor numbers and available exits are varied, discarding configurations where evacuation exceeds 15 minutes or congestion delays exceed 2 minutes. Results are displayed in a concise chart, showing that for 30,000 visitors, all exits must remain open, whereas with 20,000 visitors, the West Exit can be closed without compromising safety.

Since the multiplication and simulation of all combinations is very time-consuming, possible optimization approaches will be integrated in a next step to recognize and simulate only significant variants.

By enabling multiple simulations with varying parameters, *REMSY* users can develop a deeper understanding of the potential risks and vulnerabilities in their event planning. This allows them to make well-informed decisions and adjust their plans accordingly to ensure the safety of event visitors. The simulations can thus fundamentally alter the way events are planned and conducted.

If accepted, we will demonstrate this novel simulation approach using a real event in Freiburg, Germany, highlighting how varied simulations can enhance both safety and event planning.

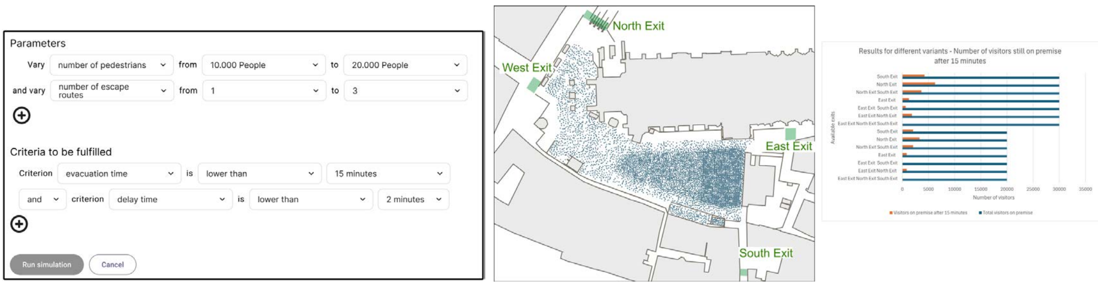

Figure 1: Left: Example mock-up of the future user interface for event planners. Right: Screenshot of one simulation run including a chart that displays the results of all parameter variation.

Bibliography

[1] M. J. Seitz and G. Köster *Natural discretization of pedestrian movement in continuous space, American Physical Society*, PHYSICAL REVIEW E **1**, 86, 046108, 2012.

[2] Helbing, D. *A fluid-dynamic model for the movement of pedestrians.* Complex Systems 6, p. 391–415, 1992.

[3] *crowd:it – Technical Description.* https://www.accu-rate.de/en/the-optimal-steps-model/

[4] RiMEA e.V., *Guideline for microscopic evacuation analysis*, v4.0.1, 2024

[5] ISO 20414, *Fire safety engineering - verification and validation protocol for building fire evacuation models*, 2020

[6] Sharma, A. et al. *Global mass gathering events and deaths due to crowd surge, stampedes, crush and physical injuries—lessons from the Seoul Halloween and other disasters*, Travel Medicine and Infectious Disease, **52**, 2023, Elsevier BV.

An Implementation of a Macroscopic Network-Based Simulation for Large-Scale Crowd Management

Weiming Mai*[1], Dorine Duives[1], and Serge Hoogendoorn[1]

[1]Department of Transport and Planning, Delft University of Technology

Abstract Current state-of-the-art macroscopic pedestrian models effectively simulate large-scale traffic, yet they focus primarily on descriptive analyses of pedestrian interactions rather than on implementing real-time control algorithms. Consequently, there is a need for a large-scale pedestrian simulation platform with integrated crowd intervention capabilities to support the development of network-wide control strategies.

Keywords Macroscopic pedestrian modeling, network model, crowd management

Introduction

Effective crowd flow management at large events to ensure pedestrian safety and preventing congestion. Existing research has focused mainly on managing crowds in localized areas such as corridors, intersections, or individual venues (e.g. [4, 5]). These studies primarily offer insights into micro-level pedestrian behavior. They often overlook the need for a comprehensive approach to coordinate the crowd in multiple interconnected locations, such as urban footpath networks and stadium complexes. This may limit the efficiency of the coordinating algorithm in a broader pedestrian network. Two key challenges currently hinder progress in network-wide controllers for crowd management. First, agent-based microscopic simulation models though rich in behavioral detail, are computationally prohibitive for simulating large crowds in large public areas. Second, macroscopic network-based models for pedestrian dynamics are underdeveloped. Existing frameworks such as the Link Transmission Model (LTM) [6] and other network-based pedestrian models (e.g. [1, 3]) are either adapted from vehicular traffic (ignoring pedestrian-specific behaviors) or not efficient enough for real-time control algorithms such as serving as the environment for reinforcement learning. This disconnect between simulation and control hinders the development of adaptive, network-wide crowd management.

To bridge this gap, we implemented a Python-based macroscopic pedestrian simulation model that is readily applicable to large-scale pedestrian simulation and can be integrated with real-time crowd management strategies (e.g. crowd redirect, capacity adjustment and flow separator). Compare to the continuum-based models, which are less suited for scenarios with complex route choices, our model can offer a more granular representation of pedestrian movement within a network. The model comprises two main modules: network loading, which simulates the propagation of pedestrian flows, and route split, which simulates the direction of the movement of the crowd. The subsequent sections will provide a detailed explanation of these modules.

Network Loading

Following Lilasathapornkit et al. [3], we implemented network loading using the LTM model. The pedestrian traffic propagation on links is assumed to follow kinematic wave theory and the conservation law, the link model in LTM defines the constraints of sending flow (upstream demand) and receiving flow (downstream supply) and the flow from upstream to downstream is constrained by the supply and demand. Detailed mathematical formulas for calculating the sending and receiving flow can be found in the original paper [6]. Note that the travel time on the link changes dynamically based on the link speed, which is influenced by the bidirectional pedestrian density and also the density-speed fundamental diagram on each link.

Turning Fractions

To simulate the route choice behavior of the pedestrians, we apply the route choice model described in [2] to calculate the turning fraction of the intersections (the nodes). First, k-shortest paths would be generated for each OD pairs. Then, the path condition such as the distance from the current node to the destination, the travel time, the comfort level of the path would be used to determine the utility of choosing a downstream link from a given upstream link, it is calculated using $U_i = \theta_i^T x_i + \epsilon$. In the equation, U_i represents the utility of choosing path i, and ϵ denotes the random error term, which follows a Gumbel distribution. The terms θ_i and x_i correspond to the calibrated coefficient and route condition factors, respectively. The conditional probability $P(\text{down} \mid \text{up}, \text{od})$ is computed using the softmax function: $P(\text{down} \mid \text{up}, \text{od}) = \frac{e^{U_i}}{\sum_j e^{U_j}}$.

*Email of the corresponding author: w.m.mai@tudelft.nl

The turning fraction $P(\text{down} \mid \text{up})$ is then obtained by applying the law of total probability:

$$P(down \mid up) = \sum_{od \in S} P(down \mid od, up) P(od \mid up). \tag{1}$$

Here, $P(od \mid up)$ depends on the real-time OD demands. The set S represents all ODs that can be reached by passing through the upstream node.

Preliminary Results

Figure 1 simulates the spill-back effect in the network caused by a bottleneck. To replicate this scenario, we intentionally set the capacity of the downstream link to a very low value to create the bottleneck condition. Figure 2 shows the simulation in a large sidewalk network in the center of Delft. There are two origins in the network and we can see the pedestrian propagate slowly from the origins (red nodes).

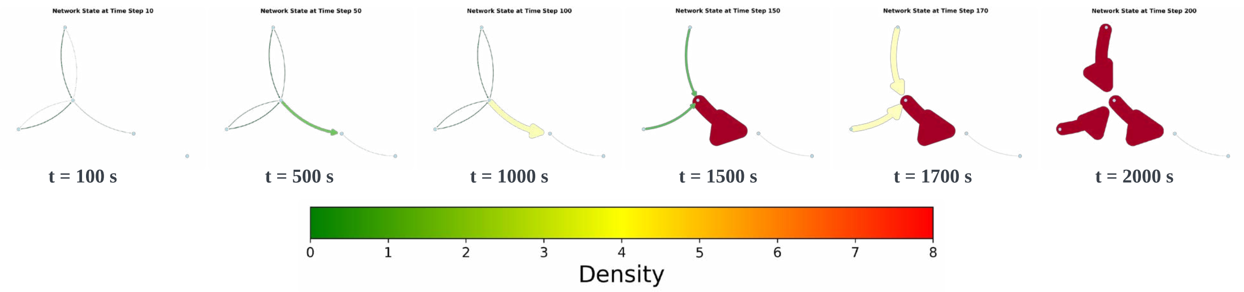

Figure 1: Simulating the spill-back of the flow in the forky intersection due to the bottleneck.

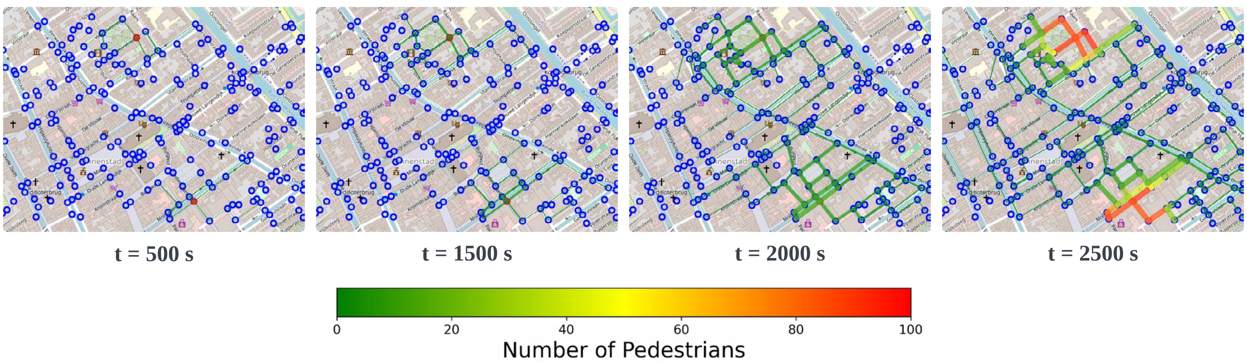

Figure 2: The evolution of the traffic state of the sidewalk network in Delft city center.

Bibliography

[1] Luc G Chalmet, Richard L Francis, and Patsy B Saunders. Network models for building evacuation. *Management science*, 28(1):86–105, 1982.

[2] Winnie Daamen. Modelling passenger flows in public transport facilities. 2004.

[3] Tanapon Lilasathapornkit and Meead Saberi. Dynamic pedestrian traffic assignment with link transmission model for bidirectional sidewalk networks. *Transportation research part C: emerging technologies*, 145:103930, 2022.

[4] Nicholas Molyneaux and Michel Bierlaire. Controlling pedestrian flows with moving walkways. *Transportation research part C: emerging technologies*, 141:103672, 2022.

[5] Nicholas Molyneaux, Riccardo Scarinci, and Michel Bierlaire. Design and analysis of control strategies for pedestrian flows. *Transportation*, 48(4):1767–1807, 2021.

[6] Isaak Yperman, Steven Logghe, and Ben Immers. The link transmission model: An efficient implementation of the kinematic wave theory in traffic networks. In *Proceedings of the 10th EWGT Meeting*, volume 24, pages 122–127. Citeseer, 2005.

Timetable
Talk index

12th International Conference on Pedestrian and Evacuation Dynamics (PED 2025)
Prague, Czech Republic – September 9-12, 2025

Validating applicability of VR technology to predict guidance effectiveness of crowd-control measures: A VR experiment to reproduce an empirical experiment

Shuhei Miyano*[1]

[1]Intelligent Systems Laboratory, SECOM Co., Ltd.

Abstract Various factors, such as congestion and environmental conditions, need to be considered in predicting the guidance effectiveness of crowd-control measures. Although it is expected that virtual reality (VR) can be used to simulate these complex contexts, further research is required to validate the applicability of the technology. In this study, an online nonimmersive VR experiment that reproduced an empirical experiment near a stadium was conducted. The route selection preferences between both experiments are compared. Compared to the empirical data, the VR data show a similar trend in guidance effectiveness but overestimated compliance rate, necessitating further analysis to fill the gap.

Keywords Crowd-Control Measures, Route Selection Preferences, Compliance Rate, Online Non-immersive virtual reality (VR) Experiment, Empirical Experiment

Introduction

Crowd control needs to be properly designed to ensure the safety and comfort of visitors at event venues. Several factors that can influence the route selection preferences of visitors, such as congestion and environmental conditions, need to be considered to effectively predict the guidance effectiveness of crowd-control measures. Although it is expected that virtual reality (VR) can help designers simulate such complex contexts, further research is required to validate the applicability of VR technology [1].

In this study, we conducted an online nonimmersive VR experiment that reproduced an empirical experiment in the vicinity of a stadium after baseball games. In the VR experiment, we replicated crowd-control measures, pedestrian flow, and spatial layout. We compared the route selection preferences between the VR and empirical experiments, and validated whether VR technology can be used to predict the guidance effectiveness of crowd-control measures under the complex contexts.

Experiments

Empirical experiment near a stadium after baseball games

We conducted an empirical experiment near a stadium after baseball games. Figure 1 (left) shows a snapshot of the experiment. Two routes can be adopted to make it to the train station, left and right. The right route is faster but tends to get congested; therefore, we guided stadium visitors to the left route. We investigated four crowd-control measures: 1) *no control*, 2) guidance using *handheld signs*, 3) guidance via *announcements*, and 4) guidance via a *combination* of handheld signs and announcements. We used each pattern on a different day and counted visitors passing each route.

VR experiment to reproduce the empirical experiment

We conducted an online nonimmersive VR experiment that replicated the crowd-control measures, pedestrian flow, and spatial layout of the empirical experiment. Figure 1 (right) shows an example of a VR scene. We gathered 1,026 participants that had visited the stadium within the past three years.

The VR experiment reproduced the same four patterns of crowd-control measures as in the empirical experiment. Accordingly, 165 VR scenes were generated for each pattern; therefore, we had 660 scenes in total. We presented 10 randomly selected scenes to each participant, and the participants answered with their preferred route—left or right—for each scene. We collected a total of 10,260 samples, but owing to differences in the number of samples for each scene, we randomly extracted eight samples for each scene.

*Email of the corresponding author: shu-miyano@secom.co.jp

Figure 1: Snapshot in the empirical experiment (left). Example of a reproductive VR scene (right).

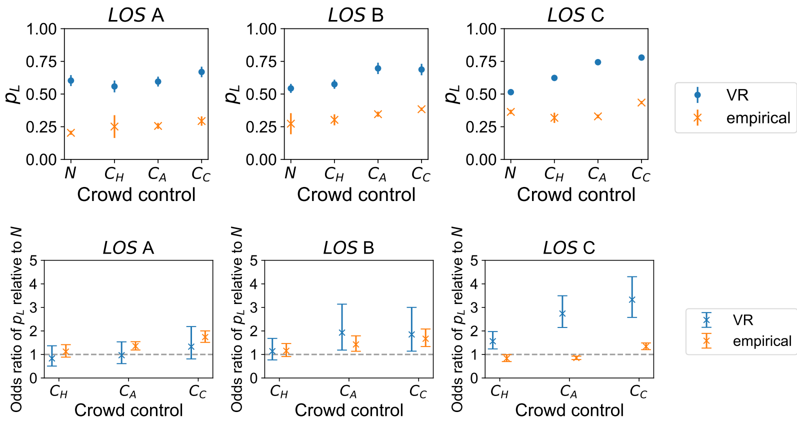

Figure 2: Left-route selection rate p_L (upper row) and odds ratio of p_L relative to *no control* cases (lower row) with congestion levels, represented as *levels of service* (*LOS*) [2]. N, C_H, C_A, and C_C denote *no control*, guidance using *handheld signs*, guidance via *announcements*, and guidance via a *combination* of handheld signs and announcements, respectively.

Owing to the lack of empirical data on pedestrian walking positions, we randomly assigned the walking position of the participant avatar. The avatar was set on a random point, 20 m from the junction, and it was moved along the path to a point 5 m from the junction. Pedestrian agents were walking around the avatar. Flow of pedestrian agents were set to have a range similar to that measured empirically. We randomly determined the number and route selections of agents in the flow range for each scene.

Results and discussion

Figure 2 shows the left-route selection rate p_L and odds ratios of p_L relative to *no control* cases for each crowd-control measure and congestion level. We consistently guided pedestrians to the left route, thus, p_L also denotes compliance rate, and the odds ratios reflect the guidance effectiveness. We calculated *LOS* [2] as congestion levels; *LOS* C was observed in the most congested conditions.

Figure 2 shows that p_L was overestimated in the VR experiment compared to that of the empirical experiment. The odds ratios of p_L diverged significantly in *LOS* C. However, the order of the odds ratios among crowd-control measures exhibited a similar trend for both experiments.

The similar trend of odds ratios suggest that the guidance effectiveness can be predicted using the VR data with some correction for the overestimation. The significant divergence in *LOS* C suggests that some factors associated with congestion caused the gap in the route selection preferences; for instance, real pedestrians in crowded conditions may have faced difficulty in changing their routes owing to interference from other pedestrians around them. Additionally, the walking position is another factor that may have caused the overestimation. We are currently conducting an analysis that considers these factors.

Conclusion

In this study, we conducted a VR experiment that reproduced an empirical experiment and compared the route selection preferences between both experiments. We found a similar trend of the guidance effectiveness for both experiments. However, the VR data overestimated the compliance rate compared to that of the empirical experiment, necessitating further analysis to fill the gap.

Bibliography

[1] Feng, Y., Duives, D., Daamen, W., Hoogendoorn, S., *Data collection methods for studying pedestrian behaviour: A systematic review*, Building and Environment **187**, 107329, 2021.

[2] Fruin, J.J., *PEDESTRIAN PLANNING AND DESIGN*, Metropolitan Association of Urban Designers and Environment, 1971.

12th International Conference on Pedestrian and Evacuation Dynamics (PED 2025)
Prague, Czech Republic September 9-12, 2025

Modeling the temporal dependency between factors affecting dynamic wayfinding behavior of heterogeneous pedestrians in VR

Zhicheng Dai[1,2] and Dewei Li*[1]

[1]Department of Traffic and Transportation/Beijing Jiaotong University, Beijing, China
[2]Department of Built Environment/Eindhoven University of Technology, The Netherlands

Abstract This study develops a virtual reality-based comprehensive transportation hub scenario to investigate the dynamic decision-making mechanisms underlying pedestrian route choices across various travel purposes, considering traveler heterogeneity. By integrating visual information and spatial knowledge, a dynamic Logit model incorporating spatial embedding autoregressive terms is proposed to quantify how these influencing factors evolve over temporal dimension.

Keywords Virtual reality, route choice, visual infomation, dynamic decision, discrete choice model

Instruction

Understanding the dynamic decision-making mechanisms underlying pedestrian route choices in public spaces is crucial for ensure pedestrian safety [1] and accurately forecasting crowd dynamics. Existing research on pedestrian wayfinding primarily relies on static decision-making models [2], rarely examining the temporal evolution of various influencing factors through virtual reality (VR) environments. Additionally, previous models generally neglect traveler heterogeneity, failing to effectively capture pedestrians' real-time, stepwise decision-making processes under varying conditions.

To address these limitations, this study develops a VR environment of a comprehensive transportation hub, as shown in Figure 1. By conducting questionnaire surveys and VR-based behavioral experiments with 64 participants, pedestrian route choice behaviors were recorded under VR scenarios involving heterogeneous travel purposes, such as transfers arrival, shopping, and ticket purchases. Using pre-training semantic segmentation model and visibility (Isovist software) analysis, visual information, including route visibility and connectivity during the decision-making process, was extracted. This was integrated with spatial physical metrics such as Euclidean distance between areas and route detour rates, forming a comprehensive dataset of heterogeneous pedestrian route choice behaviors. Traveler heterogeneity factors, such as familiarity with spatial layouts, use of two-dimensional navigation assistance, and prior travel modes, were explicitly considered. Subsequently, a dynamic Logit model incorporating a spatial embedding autoregressive term based on historical pedestrian locations (obtained via a graph embedding framework) was constructed. This modeling approach effectively quantifies the temporal evolution of factors influencing route choices, including visual cues, physical spatial attributes, and pedestrian heterogeneity. The overall research framework is illustrated in Figure 2.

Preliminary findings provide valuable insights into how visual information, physical spatial characteristics, and pedestrian heterogeneity influence path-choice decisions dynamically over time, offering an innovative theoretical perspective and technical approach for pedestrian behavior modeling. This study contributes a novel theoretical viewpoint and methodological innovation to pedestrian behavior modeling in complex spatial contexts.

Bibliography

[1] Feng, Y., Duives, D. C., Hoogendoorn, S. P., *Development and evaluation of a VR research tool to study wayfinding behaviour in a multi-story building*, Safety Science , 147, 1-22, 2022.

[2] Dai, Z., Li, D., Feng, Y., Yang, Y., Sun, L., *A study of pedestrian wayfinding behavior based on desktop VR considering both spatial knowledge and visual information*, Transportation Research Part C: Emerging Technologies , 163, 104651104659, 2024.

*Email of the corresponding author: `lidw@bjtu.edu.cn`

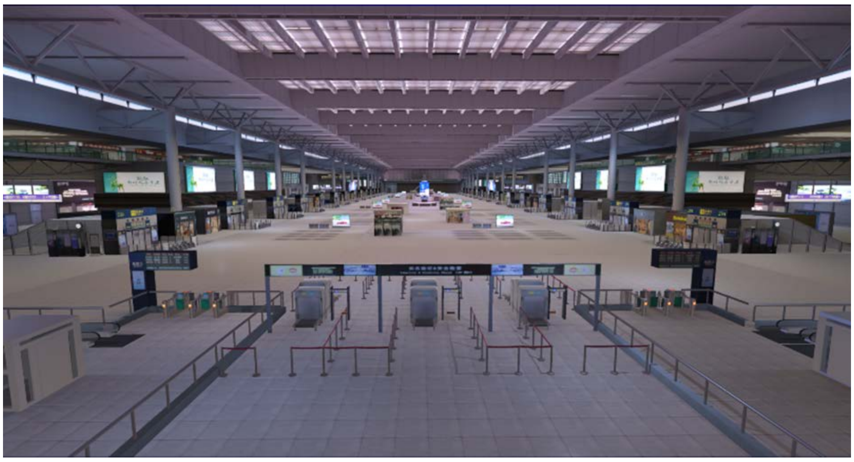

Figure 1: The comprehensive transportation hub VR scenario constructed in this study.

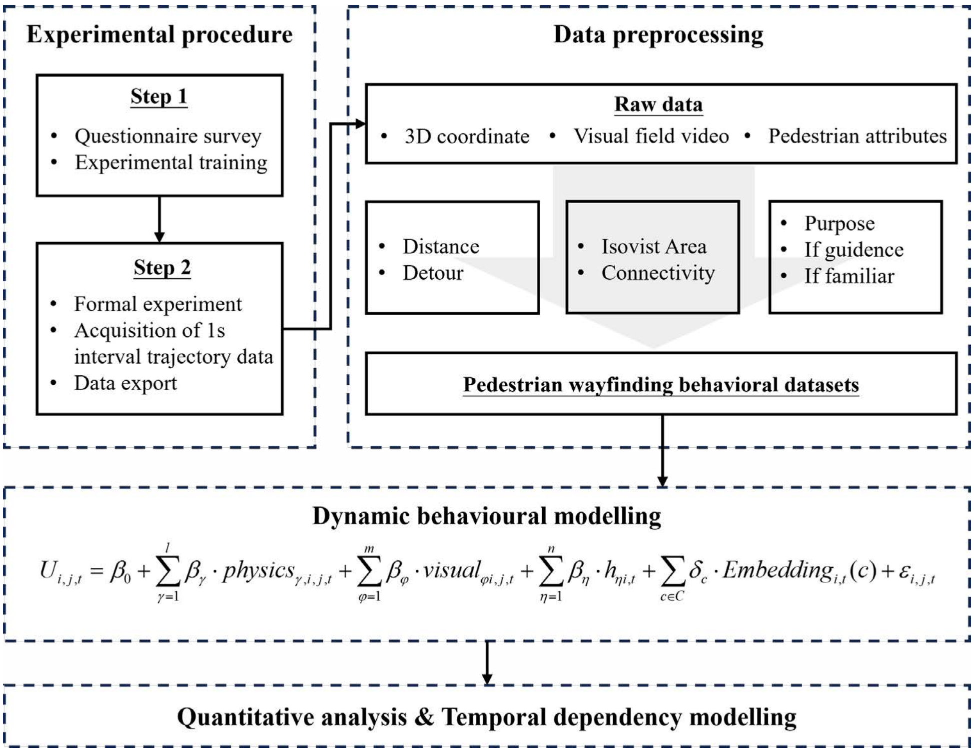

Figure 2: Research framework.

12th International Conference on Pedestrian and Evacuation Dynamics (PED 2025)
Prague, Czech Republic – September 9-12, 2025

Predicting the unseen: Improving robustness in Koopman surrogate models for crowd dynamics at a bottleneck

Sabrina Kern*[1] and Gerta Köster[1]

[1]Hochschule München - University of Applied Sciences

Abstract Crowds moving through bottlenecks form a dynamical system, with its density fluctuating in time and space. The system dynamics can be learned and predicted using the Koopman operator framework. But how reliable are predictions for previously unseen situations? How significant is the impact of stochastic observations? In this work, we show that using Taken's embedding and diffusion maps as part of our learning pipeline facilitates robustness of the surrogate model.

Keywords pedestrian bottleneck, dynamical system, data-driven modeling, Koopman operator, diffusion maps, manifold learning

Koopman surrogate models for crowds in a bottleneck

Modeling and predicting the behavior of pedestrian flows during evacuation, especially in constrained environments such as bottlenecks, is crucial for improving public safety. However, to effectively support practitioners in their decision making, models must provide reliable predictions even for unseen situations.

This work investigates the robustness of the Koopman operator, a promising AI technique suitable for predicting the behavior of various dynamical systems [1]. In the context of pedestrian dynamics at a bottleneck, a Koopman surrogate model may allow us to forecast potentially critical levels of density upfront. Training such a surrogate model can use various learning pipelines, including the Dynamic Mode Decomposition (DMD) [2] or the Extended Dynamic Mode Decomposition (EDMD) [3]. While DMD is designed to predict only linear dynamics, EDMD allows to include non-linear transformations such as Taken's embedding [4] or diffusion maps [5].

Given the great flexibility of the learning pipeline, this work focuses on the following question: How does using techniques such as Taken's embedding and diffusion maps enhance the robustness of Koopman surrogate models? Here, robustness refers to the model's ability to accurately predict unseen data variants, in particular: (1) Unseen crowd sizes in pedestrian inflow, being larger, smaller or between crowd sizes present in the training data, and (2) unseen stochastic observations, containing trajectory-induced noise which is not present in the training data.

Taken's temporal embedding enriches the state space of a dynamical system by adding past snapshots to each observation. We expect that this additional information supports inter- and extrapolation. Diffusion maps on the other hand are a dimensionality reduction technique. They learn a low-dimensional embedding via a diffusion process which aims to preserves essential geometric structures of the data. Overall, reducing the dimensionality increases computational efficiency; in extreme cases, this makes working with large temporal embeddings tractable at all.

Experiments on surrogate model robustness

We simulate the crowd dynamics at a bottleneck using the microscopic simulator Vadere [6]. All virtual pedestrians want to exit through a single bottleneck simultaneously. We generate data for seven crowd sizes, from 10 to 70 people, creating varying density patterns. For each size, we generate two time series: one average of 50 simulations, and one stochastic from a single run. The data is discretized into a spatial grid of 20cm $\times$ 20cm cells, leading to $55 \times 40 = 2200$ cells per snapshot, with snapshots taken every 0.2 seconds.

To analyze surrogate model robustness, we use three learning pipelines. The first employs the classical Dynamic Mode Decomposition (DMD). The second integrates Taken's embedding, adding four frames to each state. In the third and most advanced pipeline, the Taken's embedding is followed by diffusion maps which embed the enriched observations into a lower dimensional state space. This learning approach was previously suggested in [7].

*Email of the corresponding author: sabrina.kern@hm.edu

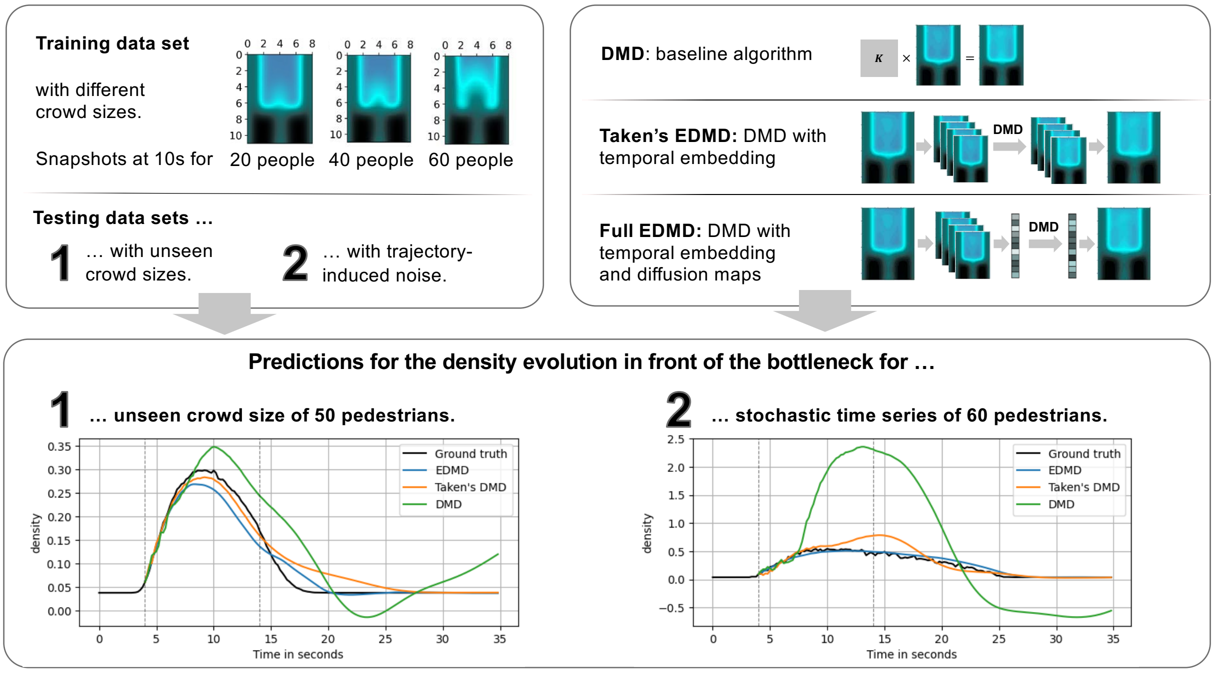

Figure 1: Graphical abstract, showcasing the improvements in prediction accuracy for two exemplary time series from the training data set.

Starting from pure DMD, which leads to infeasible predictions especially for stochastic time series, our experiments show significantly better predictions for the two EDMD learning pipelines. Here, we can largely attribute the main improvements in robustness to using Taken's embedding. At the same time, diffusion maps are able to reduce the dimensionality by a factor of 100, while maintaining the prediction accuracy achieved with Taken's embedding alone. Such a reduction becomes inevitable once we need to increase the amount of training data, increase the spatial resolution, or add more snapshots to the temporal embedding to capture more complex dynamics.

In summary, our comparative analysis shows that using Taken's embedding and diffusion maps significancy improves the accuracy in predictions for unseen crows sizes and stochastic observations while keeping the problem computationally tractable. Further investigations will also incorporate data from laboratory experiments as the stochastic time series.

References

[1] Marko Budišić, Ryan Mohr, and Igor Mezić. Applied koopmanism. *Chaos*, 22:047510, 2016.

[2] Jose Nathan Kutz, Brunton, Steven L. Brunton, Bingni W. Brunton, and Joshua L. Proctor. *Dynamic Mode Decomposition: data-driven modeling of complex systems*. Society for Industrial and Applied Mathematics, Philadelphia, PA, 2016.

[3] Matthew O. Williams, Ioannis G. Kevrekidis, and Clarence W. Rowley. A data-driven approximation of the koopman operator: Extending dynamic mode decomposition. *J. Nonlinear Sci.*, 25(6):1307–1346, 6 2015.

[4] Floris Takens. Detecting strange attractors in turbulence. *Lecture Notes in Mathematics*, pages 366–381, 1981.

[5] Ronald R. Coifman and Stéphane Lafon. Diffusion maps. *Applied and Computational Harmonic Analysis*, 21(1):5–30, 07 2006.

[6] Benedikt Kleinmeier, Benedikt Zönnchen, Marion Gödel, and Gerta Köster. Vadere: An open-source simulation framework to promote interdisciplinary understanding. *Collective Dynamics*, 4, 2019.

[7] Daniel Lehmberg, Felix Dietrich, and Gerta Köster. Modeling Melburnians—Using the Koopman operator to gain insight into crowd dynamics. *Transportation Research Part C: Emerging Technologies*, 133:103437, December 2021.

Multi-Level Crowd Estimation with Limited Data

Yanyan Xu*[1], Neil Yorke-Smith[1], and Serge Hoogendoorn[1]

[1]Delft University of Technology, Netherlands

Abstract Data scarcity is one of the main challenges for real-world crowd estimation tasks, as most of the existing (deep) machine learning approaches rely on having sufficient training data. This study proposes a graph-based multi-task learning model to address data insufficient scenarios for multi-level crowd estimation. In a case study, we first illustrate the utilization of potential open datasets for data augmentation and then implement the proposed model for crowed estimation at neighbourhood and node levels. In comparison with baseline models and single task learning approaches, we illustrate how multi-task learning enables knowledge-sharing that maximum feature learning when data is limited. We also analysis the performance under various percentage of missing data to gain insights into which levels of data absence critically impact the estimation accuracy.

Keywords Crowd estimation, multi-task learning, data scarcity

1 Motivation and Approach

Crowd estimation is one of the crucial tasks for safety management and traffic optimization. Efficiently modelling and forecasting crowd density and flows supports mitigating congestion and optimizing resource allocation [1]. For special events which often bring a sudden surge within a short period, precise crowd estimation will provides authorities sufficient response time and early warnings in emergencies to ensure public safety.

Recent studies on crowd estimation use machine learning and deep learning methods on multiple resources such as sensors, road networks, and GPS data. However, the performance of these methods is highly dependent on the availability of sufficient training data, which is often difficult to obtain in real world scenarios [2]. *Data scarcity* is a common problem in reality as data collection can be time-consuming, expensive, or privacy-limited. Lack of sufficient data will model accuracy and reliability, thus brings difficulties in estimating crowd variations in extreme scenarios, making emergency response systems less effective [3].

To address the data challenge mentioned above, this study proposes a graph-based multi-task learning integration of data augmentation to enhance crowd estimation performance under data scarcity scenario (Fig 1 (a)). The utilization of potential open data not only increase the amount of available datasets but also reduce the cost with data insufficiency. The implementation of multi-task learning enable knowledge-sharing to maximize the available features across related tasks with limited data. We validate the proposed framework for multi-level crowd estimation at Scheveningen area in Netherlands.

2 Case Study

The case study at the Scheveningen area of The Hague, Netherlands is focused on the crowd estimation at both neighbourhood level and node level. Available data has been used in the neighbourhood level which contains hourly and daily visit volumes at 16 neighbourhoods, shown in the grey boundaries in Fig 1 (b). For the node level, we only have three parking lots data that contains hourly parking occupancy and occupancy percentages within the case study area. To enrich node level data, we collect open Points of Interest (POI) data from Google Place API. The POI data contains 265 points with static features (categories, ratings, check-in number, etc) and dynamic features (average and live popularity times). We use popularity time to present crowd density levels from 0 to 100 for which 0 represents the closed hour, 1 and 100 are the percentages of the lowest and highest visits per hour. The standard popularity time represents the average density over the past few weeks and the live popularities is the real-time crowd density that updates hourly. We visualize the case study area and crowd density spatial-temporal variances within a week in Fig 1 (b).

*Email of the corresponding author: `Y.Xu-10@tudelft.nl`

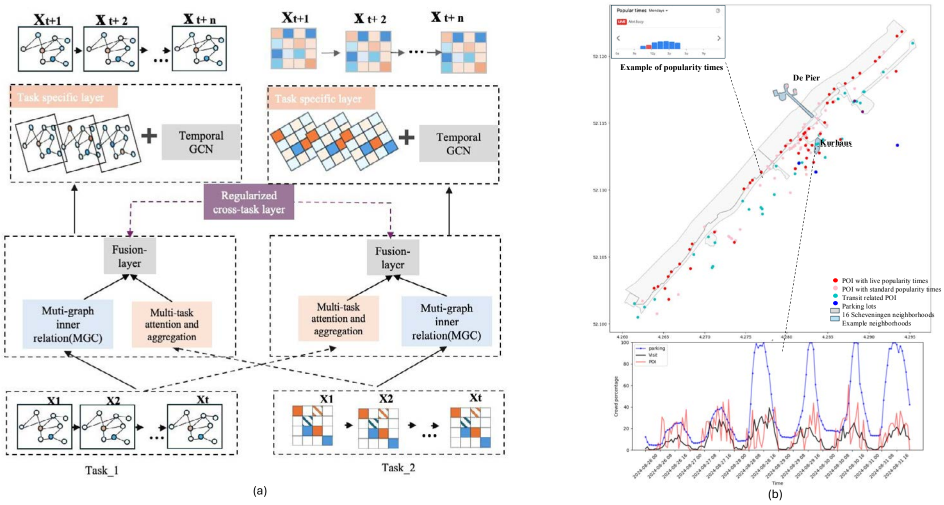

Figure 1: Left: Approach. Right: Data of case study.

Fig 1 (a) illustrates our proposed framework for the multi-level crowd estimation. For the case study, task 1 refers to node-level (POI and parking) crowd estimation and task 2 is neighbourhood-level hourly visits estimation. The experiment conducted from 1 July 2024 to 1 October 2024. As crowd-related data inherently multi-dimensions (spatial, temporal, contextual), we first model them as graph data to represent heterogeneous spatial dependencies (geographic, semantic). After acquiring the inner-task graphs and cross-task graphs, we integrate them using multi-graph convolution with self-attention fusion methods that developed from the Graph Convolution Network (GCN) [4]. After acquiring the multi-relation features in the shared layer, the Temporal GCN is then used for task specific layer. To investigate the performance of our proposed framework on different data insufficient scenarios, we evaluate the model by masking 10% to 40% percentage of training data as missing values for each task. We compare our proposed model with the baseline model: LSTM, GCN, STGCN [5] and MRGCN [6] and implement the ablation analysis to evaluate performance between single task learning and multi-task learning.

Acknowledgements. Partially supported by TULIPS, a project funded by EU Horizon 2020 research and innovation programme under grant number 101036996.

Bibliography

[1] Jiang, H., Gai, Z., Wang, Z., Wang, C., Fan, Z., Chen, Q., Tsubouchi, K., Song, N., and Shibasaki, R., *DeepCrowd: A deep model for large-scale citywide crowd density and flow prediction*, IEEE Transactions on Knowledge and Data Engineering **35**(1), 177–190, 2021.

[2] Mustapha, S., Kassir, A., Hassoun, K., Dawy, Z., and Abi-Rached, H., *Estimation of crowd flow and load on pedestrian bridges using machine learning with sensor fusion*, Automation in Construction **112**, 103092, 2020.

[3] Poon, W. H., Wong, P. K. Y., and Cheng, J. C. P., *Long-time gap crowd prediction using time series deep learning models with two-dimensional single attribute inputs*, Advanced Engineering Informatics **51**, 101482, 2021.

[4] Kipf, T. N. and Welling, M., *Semi-supervised classification with graph convolutional networks*, arXiv preprint arXiv:1609.02907, 2016.

[5] Han, H., Zhang, M., Huo, M., Zhang, F., Wang, Z., Chen, E., Wang, H., He, X., and Liu, Q.,*STGNN: a spatial-temporal aware graph learning method for POI recommendation*, Proceedings of the 2020 IEEE International Conference on Data Mining (ICDM), 1552–1557, 2020.

[6] Huang, Z., Li, X., Ye, Y., and Ng, M. K., *MR-GCN: Multi-Relational Graph Convolutional Networks based on Generalized Tensor Product*, In Proceedings of the 20th International Joint Conference on Artificial Intelligence (IJCAI), 1258–1264, 2020.

12th International Conference on Pedestrian and Evacuation Dynamics (PED 2025)
Prague, Czech Republic – September 9-12, 2025

Probabilistic Time-Series Crowd Forecasting at Scheveningen Beach, The Netherlands

Theivaprakasham Hari*[1], Winnie Daamen[1], Yanan Xin[1], Sascha Hoogendoorn-Lanser[1], Jeroen Steenbakkers[2], and Serge Paul Hoogendoorn[1]

[1]Delft University of Technology, The Netherlands, 2618 CN
[2]Argaleo B.V, 's-Hertogenbosch, The Netherlands, 5223 AL

Abstract
Accurate forecasting of visitor crowd count enables crowd safety managers, municipal authorities, and organizers to anticipate potential risks, deploy personnel strategically, and implement timely interventions. Using the case study at Scheveningen beach, Netherlands, we propose a probabilistic approach, using Conformalized Quantile Regression (CQR) to generate reliable uncertainty prediction intervals for the 14-day hourly forecast. Compared to the quantile regression method, CQR offers better coverage reliability. Our study improves uncertainty quantification of crowd forecasting, supporting crowd management in a dynamic beach environment

Keywords Pedestrian Crowd forecasting, Uncertainty Quantification, Probabilistic forecasting, Conformal prediction, Crowd management

Problem Statement and Objectives

Effective crowd management is critical for ensuring safety, optimizing resources, and enhancing visitor experiences. Accurate and reliable crowd forecasting is integral to the success of crowd management. For example, a 14-day hourly forecast provides valuable information for mid-term planning at tourist destinations such as Scheveningen Beach, Netherlands. Over this time frame, crowd safety managers need reliable staffing, logistics, security arrangements, and resource procurement estimates. In addition to improving forecasting accuracy, quantifying the uncertainty of predictions has garnered increasing attention from researchers and practitioners as it enhances the reliability and explainability of forecasting outcomes.

Traditional forecasting methods (e.g., linear or autoregressive models) often fail to capture these dynamics and struggle with reliable uncertainty estimation. Probabilistic forecasting methods such as Quantile Regression (QR) and bootstrapped residual approaches face limitations in extrapolation and computational efficiency [1]. To overcome these issues, this study applies Conformalized Quantile Regression (CQR), a distribution-free probabilistic approach providing robust uncertainty quantification, to generate reliable 14-day hourly crowd forecasts [2]. Our objectives are to evaluate CQR's performance against standard methods (QR and bootstrapping) regarding prediction interval coverage, interval width, and computational feasibility, specifically to enhance planning and risk mitigation at Scheveningen Beach, Netherlands.

Methodology

A time-stamped dataset, comprising historical visitor counts, weather features (e.g., temperature, rainfall, wind), and calendar variables, was chronologically split (80:15:5) into training, calibration, and testing sets. We trained XGBoost and LightGBM models and their quantile versions (10th and 90th quantiles) using grid-search tuning to minimize errors on the training set. As baselines for uncertainty, we employed (i) Quantile Regression (QR), directly producing upper/lower bounds, and (ii) a bootstrapped residual approach, sampling from past residuals to approximate prediction intervals. CQR further refined the quantile estimates: residuals from the calibration set were used to derive non-conformity scores and adjust interval widths, ensuring empirical coverage at the desired nominal level. Finally, performance on the test set was evaluated using Mean Interval Coverage (MIC), Mean Interval Width (MIW), and the Mean Interval Winkler Score (MIWS).

*Email of the corresponding author: t.hari@tudelft.nl

Table 1: Performance metrics for different uncertainty estimation methods applied to XGBoost and LightGBM forecasting models with prediction interval 0.10-0.90 quantiles

Methods	XGBoost			LightGBM		
80% Prediction Interval (10th - 90th Quantile)	Mean Interval Coverage	Mean Interval Width	Mean Interval Winkler Score	Mean Interval Coverage	Mean Interval Width	Mean Interval Winkler Score
Bootstrapped Residual	0.67	1317.8	2610.4	0.72	1418.41	2435.70
Quantile Regression	0.80	1601.76	2637.27	0.81	1439.26	2415.87
Conformal Prediction	0.81	2052.40	3558.24	0.87	2075.12	3423.75
Conformalized Quantile Regression	0.83	1438.69	2561.92	**0.87**	**1401.38**	**2312.28**

Results and Discussion

Our results (Table 1, Figure 1) demonstrate clear advantages of Conformalized Quantile Regression (CQR) for crowd forecasting at Scheveningen Beach. The MIC evaluates how frequently actual visitor counts fall within predicted intervals (target coverage of 0.80), MIW measures interval precision (narrower is better), and MIWS assesses overall prediction quality (lower scores indicate higher accuracy and precision). Based on these metrics, the bootstrapped residual method underestimated prediction uncertainty, showing coverage below the desired 0.80, potentially causing inadequate preparedness during unexpected visitor increases. Naive Quantile Regression and standard Conformal Prediction methods generated overly broad intervals, indicated by larger interval widths and higher MIWS, making precise resource planning difficult. Figure 1 shows clear visitor peaks, representing periods of significantly increased attendance. CQR effectively captures these peaks with narrower intervals and meets the desired metrics (e.g., the peak on 2023.11.11), enabling managers to anticipate high-attendance periods and to make informed decisions about resource allocation, risk mitigation, and strategic planning.

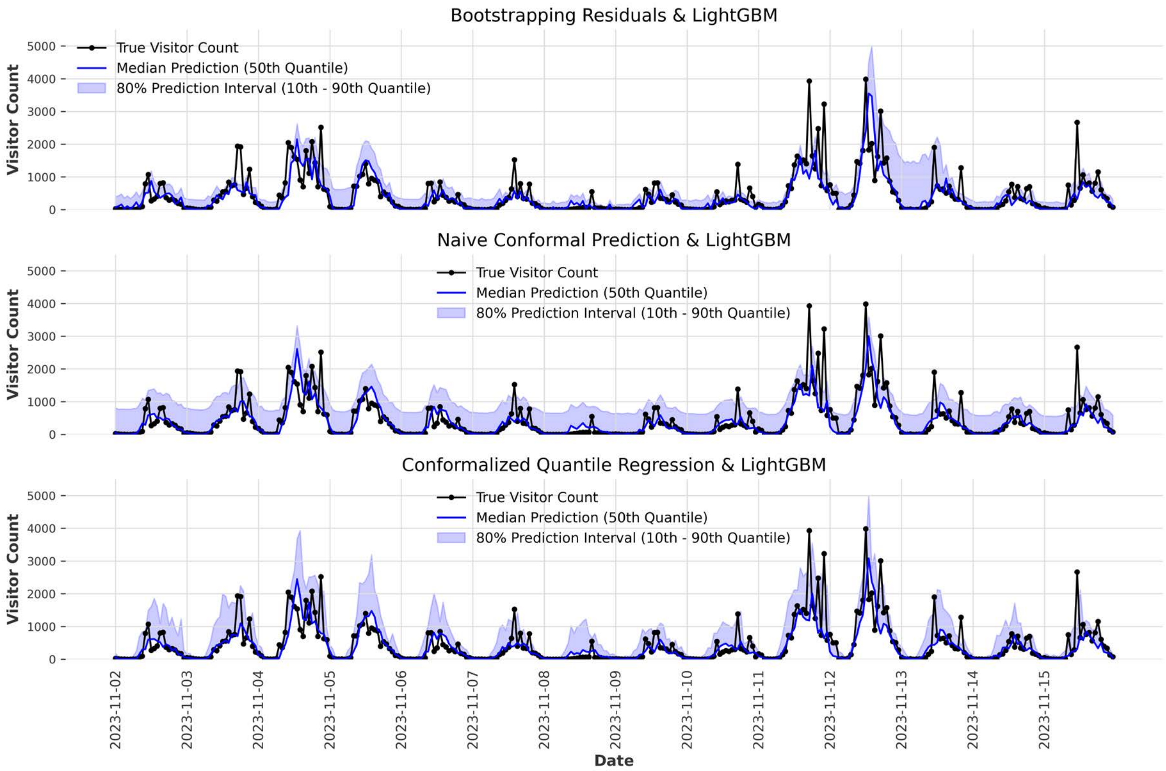

Figure 1: Comparison of 14-Day visitor crowd forecasts with different uncertainty estimation

Bibliography

[1] Anastasios N. Angelopoulos., Stephen Bates., *Conformal Prediction: A Gentle Introduction*, Foundations and Trends® in Machine Learning, 16(4), 494-591, 2023. http://dx.doi.org/10.1561/2200000101

[2] Romano, Yaniv., Evan Patterson., Emmanuel Candes., *Conformalized quantile regression*, Advances in neural information processing systems, 32, 2019. https://doi.org/10.48550/arXiv.1905.03222

12th International Conference on Pedestrian and Evacuation Dynamics (PED 2025)
Prague, Czech Republic – September 9-12, 2025

Micro-Scale Spatial Modification and Pedestrian Behavior

Calvin Breseman*[1], Francesco Zanlungo[1, 2], Igor Moiseev[1], and David M. Woollard[1]

[1]Standard AI, San Francisco, USA
[2]Department of Physics and Chemistry, University of Palermo, Italy

Abstract This study explores how subtle modifications to spatial design can significantly alter pedestrian behavior. Leveraging machine vision-based 3D tracking and existing security cameras to collect uncontrolled ecological data of shoppers in their natural environment (i.e. , retail stores), we created a framework for classifying pedestrian behavior throughout their trip. On this basis, we conducted an experiment which introduced a constriction in a retail aisle and measured the resulting behavioral shifts. Our findings indicate a marked rise in traversing and navigating behaviors at the expense of browsing or deliberating (thought-intensive periods of consideration) events—a demonstration that relatively small changes in spatial design can nudge shoppers in a significant way. These results not only provide a framework for analyzing changes in a retail environment, but also provide a framework for modeling the impact of changeable design elements on pedestrian behavior more broadly, with applications in planning public and private spaces where loitering, dwell time, or free flow of traffic are relevant design considerations.

Keywords Pedestrian Behavior, Spatial Design, Machine Vision, Behavior Classification

Introduction

The ability for the spatial design of an area to instill a sense of hostility or placidity, and doing so, shape pedestrian behavior, has drawn considerable public and scholarly attention over the last decades [1, 2, 3]. In a context with important ethical and practical ramifications, there remains a need for systematic methods to quantify and model how subtle alterations to an environment can shape pedestrian behavior. In the realm of pedestrian and evacuation dynamics, most established models emphasize large-scale crowd flow or emergency contexts. However, there is growing interest in the effects of smaller-scale interventions—such as aisle width or signage placement—on localized behavior [4]. In this analysis, we introduce a framework for measuring the behavioral response of pedestrians to changes in their physical environment at a micro-scale, based on fine-grained body pose detections, and provide an example of such an experiment.

Methodology

We conducted a six-week observational study in a specialty retailer using Standard AI's Vision ML platform. Finetuned 2D pose detection models, each run at 10 FPS on pre-existing overhead security cameras, are synthesized into three-dimensional poses based on triangulation of the 2D poses from the separate cameras, allowing for continual data collection in a manner which minimizes observational bias. Using the 3D pose of the individual shopper at every time step in their shopping trip, we clustered the individual's journey into distinct behavioral events composed of self-similar and externally dissimilar windows. We then performed unsupervised learning on embeddings extracted from segment-level trajectories, leading to the emergence of 25 distinct clusters of shopper behavior. Human labeling of these segments means that we have a precise understanding of the rates at which a variety of different attributes are displayed within these clusters, from the presence of confusion to whether pedestrians were looking at their phones.

Three weeks into the study, following the agreed-upon design, the retailer relocated promotional shelving to make space for additional units on the aisle's south side, which previously had no promotional material. This was done in accordance with their existing store design and promotional principles, and so was intended to introduce a situationally plausible but physically significant constriction. Doing so reduced the effective navigable width by approximately one-third, from 2.5 meters to 1.7 meters. The design goal was to nudge shoppers away from behaviors associated with shopping to those associated with movement by increasing the sense of constriction and decreasing the area available for comfortable

*Email of the corresponding author: `calvin.breseman@standard.ai`

browsing. Over the subsequent four weeks, we captured another large set of trajectories and classified them using the same behavioral segmentation schema. Then, by using a chi-square test, we determined how significant the change in behavioral patterns is after the change to the physical environment. No other layout changes were made in the aisle during this period. Although prices and packaging are continually in flux, the choice of a specialty retailer for the study minimizes the effects of seasonality, as shoppers are highly brand loyal and radical changes to the product paradigm are rare.

Results and Discussion

Chi-square analysis revealed a significant shift in pedestrian behavior ($p < 10^{-16}$). Traversal behaviors increased by 3.7%, while browsing and deliberating declined by 2-3%. The strong statistical significance indicates that subtle aisle modifications can measurably influence pedestrian activity. Although real-world confounding factors—such as daily variations in store traffic—are inevitable in a naturalistic setting, the large sample size and robust clustering approach lend confidence to our conclusion that a physically narrower channel prompted an immediate and quantifiable change in pedestrian activity. With a p value so functionally close to zero, future studies of behavioral changes could take place over shorter windows of time, reducing the chance for confounding factors like seasonality to impact the results.

Table 1: Behavioral shift after aisle modification.

Behavior	Pre-Modification (%)	Post-Modification (%)
Traversal	45.2	48.9
Browsing	25.1	22.3
Deliberation (Consideration)	18.7	16.0

These findings suggest that modest spatial modifications can exert an outsized influence on pedestrian dynamics—even at relatively low densities—and underscore the importance of analyzing micro-scale interactions for both retail and urban planning. Our framework can be extended to other contexts by equipping spaces with camera-based tracking, applying unsupervised behavior classification, and systematically varying layout features. In these contexts, potential applications include determining optimal bench placement in public squares, testing signage efficacy in transportation hubs, or gauging how to balance foot traffic flow with dwell time in museum galleries.

By combining high-resolution trajectory tracking, track segmentation, behavioral clustering, and controlled spatial interventions, this study offers a novel lens on how design choices aimed at nudging pedestrians toward or away from different behaviors can be measured and analyzed. Beyond retail, these insights and methodologies have the potential to enrich the field of pedestrian and evacuation dynamics by enabling fine-grained, data-driven tests of spatial design.

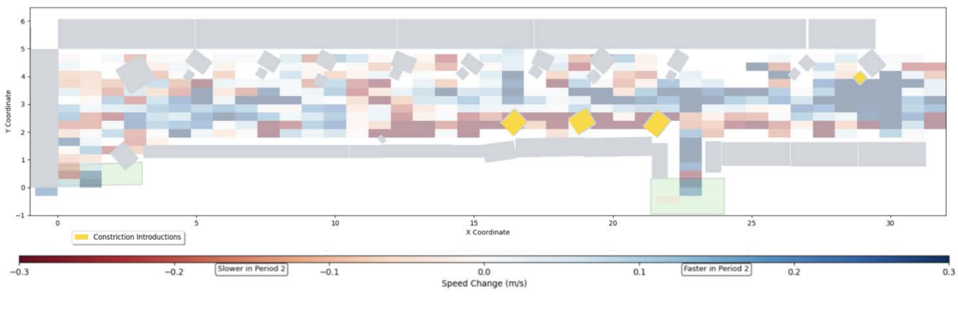

Figure 1: Change in speed throughout the aisle from the control to test phase.

Bibliography

[1] Garcimartín, A., Maza, D., Pastor, J. M., Parisi, D. R., Martín-Gómez, C., & Zuriguel, I., *Redefining the Role of Obstacles in Pedestrian Evacuation*, *New Journal of Physics*, **20**(12), 123025, 2018.

[2] Zhang, J., Seyfried, A., *Quantification of Bottleneck Effects for Different Types of Facilities*, *Transportation Research Procedia*, **2**, 51–59, 2014.

[3] Dubey, R. K., et al., *Cognitively Grounded Floorplan Optimization to Nudge Occupant Route Choices*, Available at SSRN, 2022. `https://papers.ssrn.com/sol3/papers.cfm?abstract_id=4003119`

[4] Feliciani, C., et al., *Nudging Crowds: When It Works, When It Doesn't, and Why*, *Traffic and Granular Flow'22*, **443**, 11, 2024.

Abstracts of Posters

12th International Conference on Pedestrian and Evacuation Dynamics (PED 2025)
Prague, Czech Republic – September 9-12, 2025

Solving Trade-off between Speed and Safety: Decentralized Control of Mobile Agents Based on Modified Social Force Model

Takeshi Kano*[1] and Kentstar Samuel Harsono[2]

[1]School of Systems Information Science, Future University Hakodate, Japan
[2]Department of Biomedical Engineering, University of California, Irvine, USA

Abstract Navigation of multiple mobile agents is an intriguing topic because of various possible applications, such as robots in warehouses and flying drones. A challenge here is that agents avoid collisions without losing their velocities. We previously addressed this issue by adding a prediction term to the social force model, a model of pedestrian dynamics, and succeeded quick, smooth, and safe movement of mobile agents. In this work, we explored another method without the prediction term: we added a force to follow the preceding agent and demonstrated through simulations that agents can avoid collisions without losing their velocities.

Keywords Mobile agents, Decentralized control, Social force model

Introduction

There are growing applications of multiagent systems in which each mobile agent moves towards its destination while avoiding others: e.g. robots in warehouses, self-driving cars, and flying drones. In these systems, it is desirable that each agent moves quickly and safely. However, speed and safety have a trade-off relationship.

Pedestrian dynamics becomes a source of inspiration for solving the problem because pedestrians smoothly avoid collisions with minimal loss of velocity. In our previous work, we tackled this problem by drawing inspiration from the social force model [1], a model of pedestrian dynamics. We added prediction terms to selectvely avoid agents with high collision risk and succeeded in realizing quick, smooth, and safe movement of agents [2, 3].

In this work, we explore another method for solving the trade-off without the prediction. It was previously reported that incorporation of the effect of following preceding pedestrians to the social force model increases traffic efficiency [4]. By simplifying and extrating the essence of this model, we propose a decentralized control scheme for mobile agents and demonstrate through simulations in which agents move in random directions such that they can avoid collisions with little loss of their velocities.

Model

The original social force model in the absence of obstacles or walls is written as [1]:

$$m\ddot{\mathbf{x}}_i = a\left(v_0\mathbf{e}_i - \dot{\mathbf{x}}_i\right) + \sum_{j\neq i}(\mathbf{f}_{ij}^{\mathrm{phys}} + \mathbf{f}_{ij}^{\mathrm{soc}}), \tag{1}$$

where m is the mass of the agent, $\mathbf{x}_i$ is the position of agent i, $\mathbf{e}_i$ is a unit vector representing the direction in which agent i aims to move, v_0 is the target speed, and a is a positive constant. The term $\mathbf{f}_{ij}^{\mathrm{phys}}$ denotes the physical repulsion and friction forces when agents contact with each other. The term $\mathbf{f}_{ij}^{\mathrm{soc}}$ denotes a psychological repulsive force when agents are close to each other.

Here, we redefined $\mathbf{f}_{ij}^{\mathrm{soc}}$ as a control input for an artificial agent and describe it as:

$$\mathbf{f}_{ij}^{\mathrm{soc}} = -A\mathrm{exp}\left(-\frac{d_{ij}-2r}{B}\right)\mathbf{n}_{ij} + C\max((\mathbf{e}_i\cdot\mathbf{n}_{ij}),0)\max((\mathbf{e}_i\cdot\mathbf{e}_j),0)\mathrm{exp}\left(-\frac{d_{ij}-2r}{D}\right)\mathbf{n}_{ij}, \tag{2}$$

where $\mathbf{n}_{ij} = (\mathbf{x}_j - \mathbf{x}_i)/|\mathbf{x}_j - \mathbf{x}_i|$, $d_{ij} = |\mathbf{x}_j - \mathbf{x}_i|$, r denotes the radius of the agent, A, B, C, and D are positive constants, and $D > B$. The first term on the right-hand side is the repulsive force which originates form the social force in the original model [1]. The second term is the newly introduced attraction term. The term $\max((\mathbf{e}_i\cdot\mathbf{n}_{ij}),0)\max((\mathbf{e}_i\cdot\mathbf{e}_j),0)$ mean that attractive force of agent i is generated when agent j precedes agent i and moving directions of agents i and j are similar. Thus, agents follow preceding agents that move in the similar direction.

*Email of the corresponding author: tkano@fun.ac.jp

Simulation

We performed simulations with 50 agents in a circular field of radius 30 (Fig. 1). 50 circular terminals of radius 3 are aligned along the edge of the field. The destination of each agent is chosen from the terminals randomly. The vector $\mathbf{e}_i$ is defined as the unit vector pointing the center of the destination terminal with respect to $\mathbf{x}_i$. When an agent reached the destinaion, next destination is randomly chosn from the distant terminals.

Indices for the speed, smoothness, and safety, E_1, E_2, and E_3, are defined as $E_1 = \langle 1 - \frac{\dot{\mathbf{x}}_i \cdot \mathbf{e}_i}{v_0} \rangle$, $E_2 = \langle |\ddot{\mathbf{x}}_i|^2 \rangle$, $E_3 = \langle |F_{i,phys}| \rangle$, respectively. Lower values of E_1, E_2, and E_3 indicate that agents move quickly, smoothly, and safely, respectievly. Here, $\langle ... \rangle$ denotes the average over $t > 2$ and over agents within the circle of radius 27 with its center at the center of the field. Thus, acceleration at the beginning of the simulation and sharp turns around the destination are removed from the evaluation.

Figure 2 shows the results when A and C are varied with other parameters fixed. We find that E_1 is low for small A and large C, while E_2 and E_3 are low for large A and small C. For the original social force model ($C = 0$), speed and safety are balanced around $A = 0.8$. At $A = 0.8$ and $C = 0.0$, $E_1 = 0.2398, E_2 = 0.0299, E_3 = 0.0110$. In contrast, at $A = 1.6$ and $C = 0.8$, $E_1 = 0.1585, E_2 = 0.0444, E_3 = 0.0003$ (the simulation videos for these two cases are uploaded at https://youtube.com/shorts/FCIPweZu5kA). Thus, introducing the attraction term to follow preceding agents leads to solve the trade-off between speed and safety, although smoothness is slightly lost.

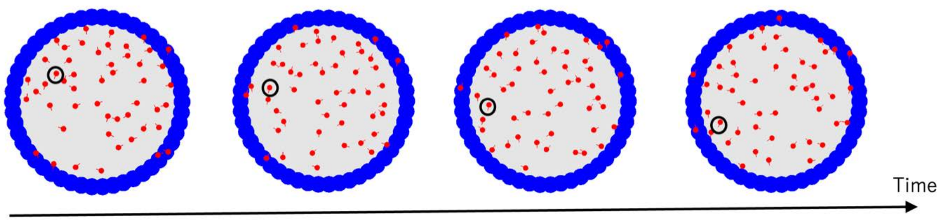

Figure 1: Snapshots for the case of $A = 1.6$ and $C = 0.8$ Agents (red color) move in a gray circular field. Blue circles denote terminals. Black circle follows one of the agents.

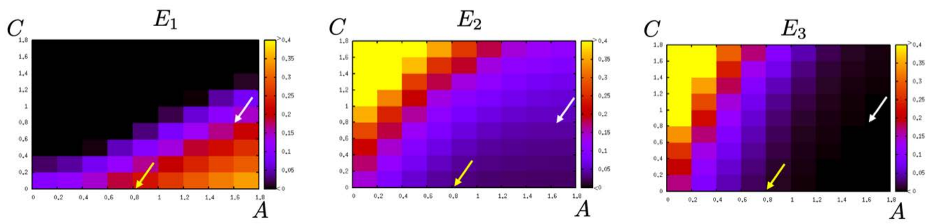

Figure 2: Color maps of E_1, E_2, and E_3. The yellow and white arrows indicate $A = 0.8$ and $C = 0.0$ and $A = 1.6$ and $C = 0.8$, respectively.

Conclusion and future works

We modified the social force model to follow the preceding agent and demonstrated through simulations that agents can avoid collisions with little loss of their velocities. However, smoothness (E_2) was slightly worse than the original social force model. This is probably because movements of nearby agents are not predicted. In the future, we would like to combine the proposed model with our previous models [2, 3].

Acknowledgement

The authors thank Prof. Akio Ishiguro of Tohoku University and Dr. Daiki Wakita of University of Tokyo for their helpful suggestions.

Bibliography

[1] Helbing, D., Molnár, P., *Social force model for pedestrian dynamics*, Phys. Rev. E **51**, 4282-4286, 1995.

[2] Kano, T., Iwamoto, M., Ueyama, D., *Decentralised Control of Multiple Mobile Agents for Quick, Smooth, and Safe Movement*, Physica A **572**, 125898, 2021.

[3] Kano, T., Kanno, T., Mikami, T., Ishiguro, A., *Active-sensing-based Decentralized Control of Autonomous Mobile Agents for Quick and Smooth Collision Avoidance*, Frontiers in Robotics and AI **9**, 992716, 2022.

[4] Yuan, Z. et al., *Simulation model of self-organizing pedestrian movement considering following behavior*, Frontiers of Information Technology & Electronic Engineering **18**, 1142-1150, 2017.

12th International Conference on Pedestrian and Evacuation Dynamics (PED 2025)
Prague, Czech Republic – September 9-12, 2025

Modeling Dynamic Queue Formation and Decision Making in Pedestrian Systems

Ander García *[1,2], Dariel Hernández-Delfin[3], Dae-Jin Lee[4], and Marco Ellero[1,5,6]

[1]Basque Center for Applied Mathematics (BCAM), Alameda Mazarredo 14, 48009 Bilbao, Spain
[2]Department of Mathematics, University of the Basque Country UPV/EHU, P.O. Box 644, 48080 Bilbao, Spain
[3]Department of Civil and Environmental Engineering, Imperial College London, South Kensington, London SW7 2AZ, UK
[4]IE University - School of Science and Technology, Paseo de la Castellana 259, E-28029, Madrid, Spain
[5]Complex Fluids Research Group, Department of Chemical Engineering, Faculty of Science and Engineering, Swansea University, Swansea, SA1 8EN, United Kingdom
[6]IKERBASQUE, Basque Foundation for Science, Calle María Diaz de Haro 3, 48013 Bilbao, Spain

Abstract This study proposes a novel approach to simulating dynamic queue formation and route decision-making in pedestrian systems. Queue formation is modeled by detecting pedestrians within a specific range, adjusting movement forces to create organized behaviors. Two methods are introduced to simulate dense or elongated queues, with a parametric analysis of how model parameters affect queue dimensions. A simple criterion for route selection is presented, prioritizing time efficiency while accounting for queue-induced delays. Finally, the combined approach reveals how queue types influence pedestrians' route choices.

Keywords Pedestrian Dynamics, Social Force Model, Queue Formation, Route Choice

Main Abstract Text

Queuing is a fundamental aspect of pedestrian systems, characterized by organization, low average velocity, and a consistent distance maintained between individuals. It emerges in various scenarios where people share a common objective. Another crucial crowd-related aspect is route choice, as pedestrians continuously make decisions based on multiple environmental stimuli to select the most efficient path. Despite their significance, the modeling of these two features has been limited due to their inherent complexity and the scarcity of empirical data for validation. Most studies on queuing focus on one-dimensional lines, where pedestrians are confined and compelled to queue, or on simplified geometries [1]. Similarly, while several approaches to decision-making modeling have been proposed, they are often validated solely against the specific experiments for which they were developed [2, 3].

In this work, we present a novel numerical method to simulate the dynamic formation of queues in unconfined two-dimensional environments. The model identifies queuing individuals based on a predefined interaction radius and adjusts both the driving and social repulsive forces to achieve equilibrium inter-pedestrian distances consistent with those observed in real queues. To simulate various queue configurations, including elongated and narrow lines as well as compressed and wider formations, we propose two distinct approaches for defining the desired velocity field of pedestrians.

In the **Competitive Queuing Model (CQM)**, pedestrians follow a vector field directed towards the exit, enabling them to join the queue from any direction upon encountering a queuing agent. This results in organization patterns resembling compressed formations. Conversely, in the **Ordered Queuing Model (OQM)**, the desired velocity of non-queuing pedestrians is oriented towards the last agent in the queue when they enter a perception distance d_p, which represents the moment they become aware of the queue. This process is illustrated in Figure 1 (Left).

*Email of the corresponding author: angarcia@bcamath.org

Subsequently, we propose a novel criterion to simulate dynamic decision-making in pedestrians. This approach introduces a mechanism for simulating route choice based on transitions between desired velocity maps. For a geometry with multiple exits, we compute a static navigation field for each exit, allowing agents to choose the gate g that minimizes their estimated egress time, $T_i^{(g)}$. The calculation of the egress time considers the distance to exit g when the gate is free and accounts for both the distance to the last queuing agents and the queuing time if a queue exists at gate g'. Figure 1 (Right) illustrates the components involved in the route choice efficiency calculation.

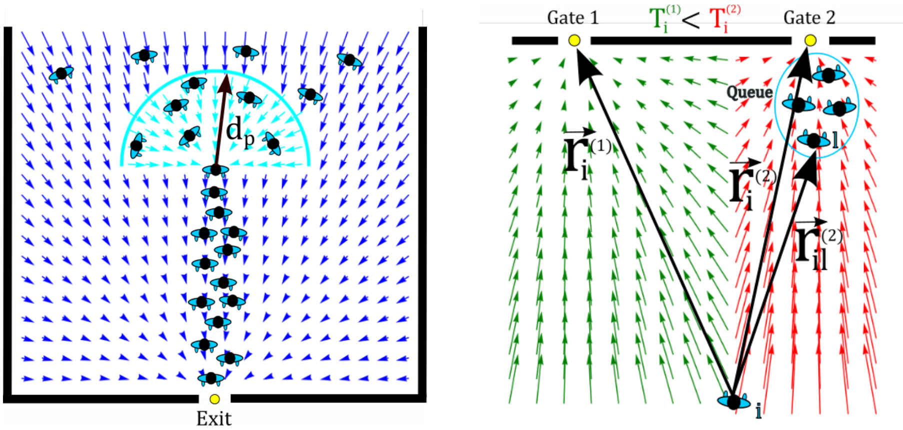

Figure 1: (Left) Sketch illustrating the organized queuing model, aiming to reproduce thin and elongated lines. (Right) Sketch of the route choice algorithm for a reference pedestrian i in a multi-exit scenario.

Our results indicate that multiple types of queues can be effectively captured by appropriately tuning the parameters of the queuing models. In the CQM, the model reproduces compressed formations with variable inter-pedestrian distances, while in the OQM, it captures queue formations ranging from single-file lines (see Figure 2 (Left)) to broader queues two to four people thick. Additionally, the route choice algorithm showed strong agreement with an extensive experimental dataset comprising 12 runs across four distinct geometries and varying participant numbers. The model accurately reproduces the average number of people choosing each gate (see Figure 2 (Right)) and falls very short in instances where the experimental data were particularly sparse.

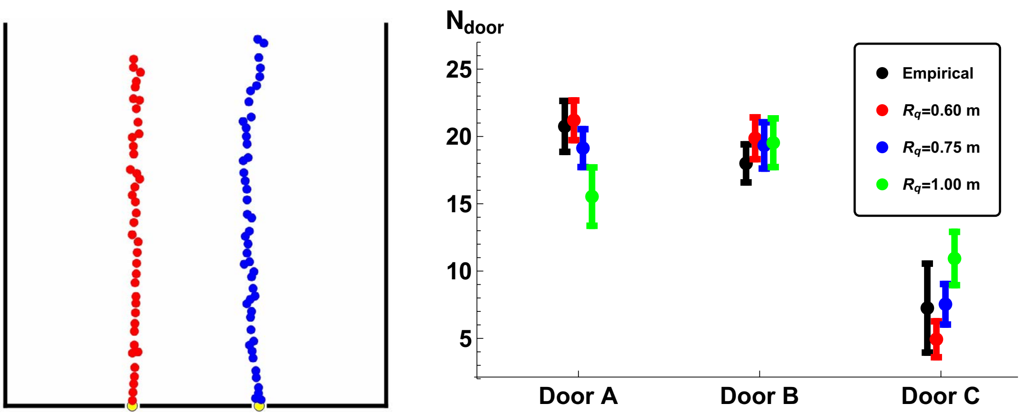

Figure 2: (Left) Snapshot representing queuing agents before the left and right doors in the OQM. (Right) Empirical and numerical route choice of pedestrians in a experiment performed in [2].

Bibliography

[1] Wu, P.-Y. and Guo, R.-Y. *Simulation of pedestrian flows through queues: Effect of interaction and intersecting angle*, Physica A: Statistical Mechanics and its Applications **570**, 125804, 2021.

[2] Crociani, L., Vizzari, G., et al., *Route choice in pedestrian simulation: Design and evaluation of a model based on empirical observations*, Intelligenza Artificiale **10**, 163-182, 2016.

[3] Liao, W., Wagoum, K., Armel, U., and Bode, N., *Route choice in pedestrians: Determinants for initial choices and revising decisions*, Journal of The Royal Society Interface **12**, 20160684, 2017.

12th International Conference on Pedestrian and Evacuation Dynamics (PED 2025)
Prague, Czech Republic – September 9-12, 2025

Behavior of Evacuees on Podium Decks after Building Fire Evacuation

Yoshikazu Minegishi*[1]

[1]Building Research Institute, Japan

Abstract Evacuees' behavior on podium decks after evacuating a building fire was investigated using virtual simulations. The experiment analyzed various aspects of their behavior, including evacuation direction and distance, the percentage of evacuees descending to the ground versus remaining on the podium deck, and the crowd density at which evacuees experience anxiety and have difficulty relocating.

Keywords Podium deck, Evacuation, Building fire, Route choice, Density, Virtual Reality

Introduction

In Japan, the central districts of major cities are centered around railway stations, which are often connected to bus terminals and taxi stands. Therefore, podium decks or pedestrian bridges are often built in the central district to separate pedestrian and car traffic. Many large-scale buildings, such as retail, offices, theaters, hotels, etc., are built connecting to the podium decks. When a fire occurs in ordinary buildings, the occupants evacuate to the outside of the building, i.e., the ground. If the buildings are facing the podium decks, evacuees may evacuate to the podium decks. However, how evacuees behave on the podium decks is not well understood, such as how far they will evacuate, what kind of route they prefer, and where they will wait. When a huge number of evacuees gather on the podium decks, the density becomes large. However, there is no knowledge about the density level at which evacuees voluntarily begin to move, nor the movement is possible. This study examines the characteristics of evacuees' behavior affected by the built environment and evacuation crowd.

Materials and Methods

Two computational urban district models, including podium decks, were prepared. One is a square-type podium deck (Figure 1), and the other one is a walkway-type podium deck (omitted in this abstract). Fifty-six participants were immersed in the virtual environment using the wireless head-mounted display, MetaQuest2. Two kinds of experiments were conducted.

One is the "route choice" experiment. At the beginning of the trials, the participants were located in a shopping mall or retail store (point 1 in Figure 1). They were on the floor, which is the same ground level as the podium decks. They heard the voice alarm that said a fire had occurred within the building and ordered them to evacuate to the outside of the building; subsequently, they exited the building (point 2 in Figure 1). They were instructed to look around, especially at the building where they had been, and informed that no fire or smoke could be seen from their position. Additionally, the participants could navigate themselves in the virtual environment by walking in the physical environment of a 12 m × 10 m size meeting room to check the surroundings. After that, they were asked where or in which direction they wanted to move or stay they were standing. The researcher relocated their position to one of the candidate standpoints in Figure 1, considering their answers. Repeating this procedure, evacuation routes were acquired. When the participants arrived at the edge of the podium decks or choose to wait at the point, the trial ended. There were no other people or evacuees in the virtual environment in this experiment. The other one is the "density" experiment. The settings were common until the participants exited the building and stood at point 2. After that, the scene changed to appear with other evacuees waiting on the podium. Six density patterns, including 0.25, 0.5, 1.0 (Figure 1(d)), 2.0, 3.0, and 4.0 people/m^2 were prepared, and each participant experienced three patterns of them. The combinations and their orders varied among participants. After experiencing each trial, the participants were asked two questions: 1) How did you feel waiting in this density situation (five alternative choices), 2) What did you want to do, and was it possible to do that? (four alternative choices).

*Email of the corresponding author: `minegishi1@kenken.go.jp`

Timetable
Poster index

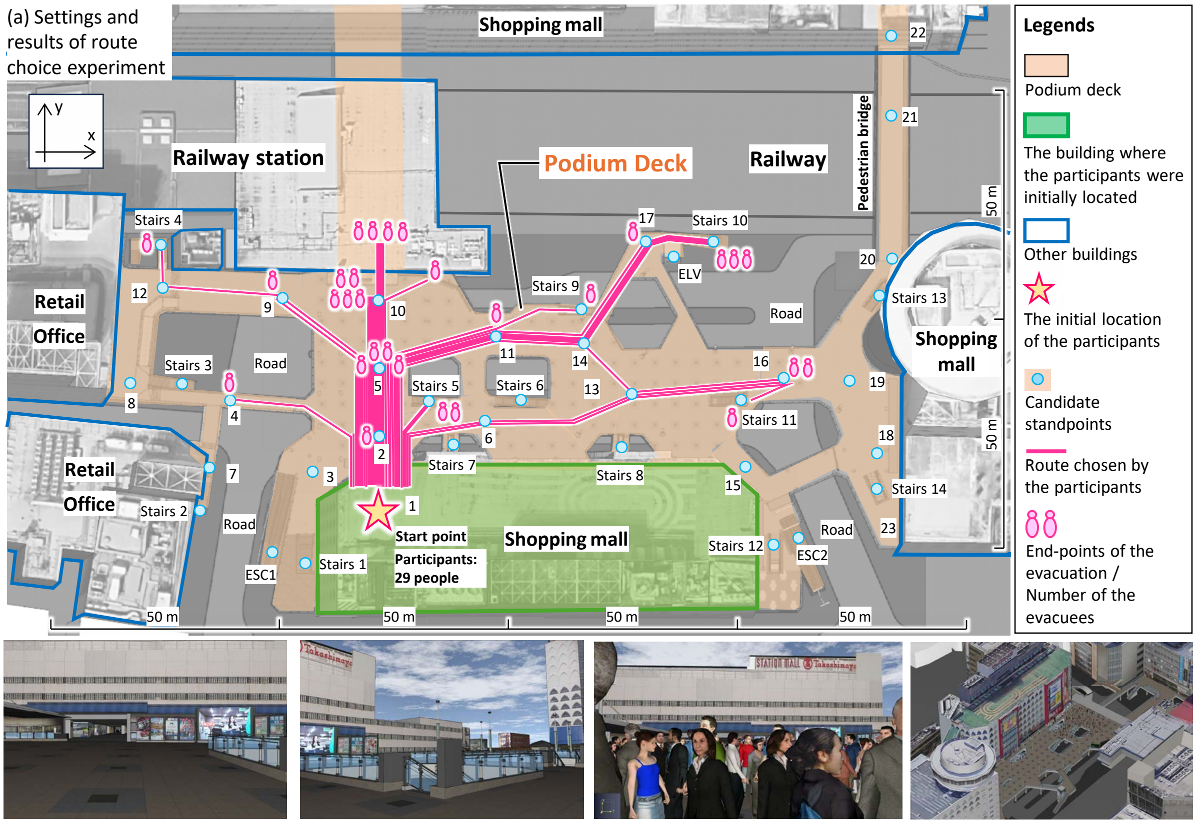

(b) At Point 2, looking to the Points 5 and 10

(c) At Point 2, looking to the Stair 5

(d) Density experiment, at Point 2, 1.0 people/m^2

(e) Bird's-eye view

Figure 1: Paths and end-points of the evacuation by participants on the square-type podium deck

Results

Figure 1 shows the result of the route choice experiment on the square-type podium deck. When the occupants evacuated perpendicular to the building where a fire might occur, 48% of them evacuated in the opposite direction from the building. They tend to get away from it with the directions that allow them to move as far as possible and then wait there. 28% of the participants descended the podium deck, and 72% of them remained on it. In the density experiment, when the evacuees gathered and waited on the podium decks, more than half of them felt anxious about waiting there when the density was more than 0.5 people/m^2, and more than half of them felt strong anxiety when the density was more than 2.0 people/m^2. In addition, when the density becomes large, some evacuees will relocate; however, moving to relocate becomes difficult when the density exceeds 2.0 people/m^2.

Discussions and Conclusion

There is an example of an actual fire case where the fire was not severe; the evacuees on the ground remained near the building [1]. In this study, even though the participants were informed that fire and smoke could not be seen from their position, most of them assumed a severe fire had occurred, and evacuated as far as possible. Characteristics of route choice identified in this study should be considered in the severe fire case. This study does not address the influence of the presence of others on route choice; this topic will be presented in a future study. Meanwhile, approximately 70% of the participants remained on the podium deck, and the result of the density experiment suggests that evacuees may begin to move to distant locations only after the density becomes high. Therefore, personnel guidance will be important on podium decks where the flow of the building exit is relatively large compared to the dispersed flow, which is restricted by the width of the walkway or stairs, i.e., the walkway-type podium decks.

Bibliography

[1] Japan Kagoshima News KTS, *"Something is burning in the bedding section": Fire breaks out at Kagoshima's long-established department store, Yamagataya, in Kagoshima City 2023.11.08 18:30*, https://www.youtube.com/watch?v=svWHLF3rKHI (2024.12.28 accessed, in Japanese)

12th International Conference on Pedestrian and Evacuation Dynamics (PED 2025)
Prague, Czech Republic – September 9-12, 2025

Anchoring and judgment biases of pedestrians in exit choice: A discrete choice model based on Virtual Reality experiments

Can Huang[1], Jun Zhang*[1], and Weiguo Song[1]

[1] State Key Laboratory of Fire Science, University of Science and Technology of China, China

Abstract This study examines the anchoring effect in evacuation exit decisions through WebGL-based online VR experiments (800 participants). Preliminary results confirm its presence, with evacuees over-relying on initial anchors (exit distance, width, crowd density) under time pressure, leading to cognitive biases and suboptimal path deviations. A discrete choice model integrating Expected Utility Theory and emergent value principle is developed and calibrated using experimental data. The findings provide theoretical frameworks and actionable strategies to enhance evacuation efficiency in building design and emergency management protocols.

Keywords Virtual reality, Exit choice, Decision-making behavior, discrete choice model, Building evacuation

Introduction

When an emergency occurs within a building, the exit choice of evacuees plays a crucial role in the evacuation efficiency and the safety of occupants. Understanding the decision-making rules of pedestrians during evacuation can help crowd managers to evaluate evacuation risks and develop appropriate plans in specific scenarios. Due to cognitive resource limitations caused by time pressure and anxiety, evacuees often cannot fully evaluate the available information and tend to choose exits based on heuristics or simplified strategies that are susceptible to cognitive biases.

Anchoring effect is a type of cognitive bias that refers to an individual's excessive reliance on initial information (anchor points) during decision-making, resulting in subsequent judgments deviating from the objective optimal solution. In this study, we selected exit distance, exit width, and number of people around the exit as the anchoring information to study whether they could influence evacuees' decisions. Based on the standard anchoring effect experimental paradigm, we designed a Virtual Reality (VR) based exit-choice task (as shown in Figure 1), where participants firstly receive anchor information and then make decisions under time pressure.

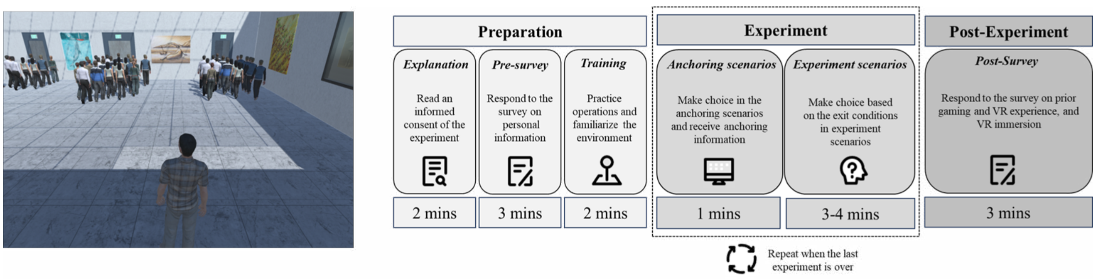

Figure 1: Left: Screenshots of the virtual experience. Right: Experimental procedure.

To overcome the problem of small sample size from offline VR experiments with head-mounted displays (HMD) and cave automatic virtual environments (CAVE), desktop VR based on WebGL technology is adopted in this study to expand sample diversity with a wider range of social group characteristics. A sample of up to 800 participants was obtained and their decision times and decision outcomes in the experiment are recorded. Besides, a survey is used to collect information including socio-demographics, prior gaming and VR experience, and VR immersion.

*Email of the corresponding author: junz@ustc.edu.cn

Through series of online VR experiments, the existence and strength of anchoring effect in exit selection during evacuation are tested and the influence of tested anchoring information on decision making time, the exit selection ratio as well as path deviation rate are investigated. Furthermore, a new discrete choice model is developed based on Expected Utility Theory (EUT) and emergent value principle [1] and calibrated using the experiment data. The results of this study offer new theoretical insights and practical guidance for building design and emergency management.

Methodology

In this section we describe the approaches proposed to assess the susceptibility and subjective valuation of the anchoring effect. The methods use a discrete choice multinomial logit model that accounts for the Anchoring information subjective valuation and susceptibility from the coefficient of an emergent value term differentiated by classes of individuals.

This approach is elaborated as an extension of the emergent value model proposed by Fukushi [2] for the detection of the decoy effect in choice models, which consists in implementing what can be interpreted as a version of the emergent value principle for this context. This is achieved by incorporating a dichotomous variable into the utility function of the alternative influenced by anchoring information in each discrete choice experiment. This approach enables quantification of the anchoring effect's magnitude on individual decision-makers within the sample through the coefficient estimate of this dichotomous variable. Furthermore, systematic taste variations are introduced to the coefficient of this dichotomous variable across deterministic classes. This methodological extension facilitates identification of specific population segments exhibiting differential susceptibility to anchoring effects while simultaneously accounting for heterogeneity in anchoring sensitivity.

To illustrate the method, consider, for example, that the choice under study corresponds to the selection of a exit i by individual based on distance d_i, exit width w_i and the number of evacuees near the exit n_i following a random utility model (RUM) with parameters β, error ϵ and utility U_i, as shown in Eq.(1).

$$U_i = \beta_i + \beta_d d_i + \beta_w w_i + \beta_n n_i + \epsilon_i \tag{1}$$

Under this setting, the emergent value method for the detection of the anchoring effect would correspond to the addition of a variable a_i to the utility, as shown in Eq.(2).

$$U_i = \beta_i + \beta_d d_i + \beta_w w_i + \beta_n n_i + \beta_a a_i + \epsilon_i \tag{2}$$

where a_i is built as a dichotomous variable that equals 1 when alternative i is favored by individual in each choice context and takes value zero otherwise. The subjective valuation of the anchoring information will then be captured by the estimator of the coefficient β_a of variable a_i.

Using the model shown in Eq.(2), the susceptibility of the anchoring effect can be elicited by considering different parameters β_a for deterministic classes of individuals, which are defined by a combination of characteristics s such as age and gender, as shown in Eq.(3).

$$U_i = \beta_i + \beta_d d_i + \beta_w w_i + \beta_n n_i + \sum_{s \in S} \beta_a a_i s_n + \epsilon_i = V_i + \epsilon_i \tag{3}$$

And the probability of choosing exit i is given by Eq.(4).

$$P_i = \frac{e^{V_i}}{\sum_{j=1}^{J} e^{V_j}} \tag{4}$$

Bibliography

[1] C. Angelo Guevaraa, *Modeling the decoy effect with context-RUM Models:Diagrammatic analysis and empirical evidence from route choice SP and mode choice RP case studies* , Transportation Research Part B **93**, 318-337, 2016.

[2] Mitsuyoshi Fukushi, *A discrete choice modeling approach to measure susceptibility and subjective valuation of the decoy effect, with an application to route choice* , Transportation Research Part B **38**, 100256, 2021.

Analysis of Metro Network Passenger Flow Based on Flow Type Classification

Qi Pan[1], Jun Zhang*[1], Weiguo Song[1], and Xiaolian Li[2]

[1] State Key Laboratory of Fire Science, University of Science and Technology of China, China
[2] Fujian Police College, China

Abstract To predict metro passenger flow dynamics, this study proposes a method to classify flows into three types: bidirectional tidal flow (BTF), sustained outbound flow (SOF), and high-volume flow (HVF). By conducting feture analysis on different types of passenger flows, we can obtain valuable insights for understanding and predicting metro passenger flow dynamics. When integrated with analyses of passenger transfer dynamics within the metro network, this approach offers a more comprehensive understanding of overall passenger flow.

Keywords Flow type classification, Metro system, Crowd estimation, Data mining

Introduction

Predicting pedestrian density distribution in metro stations is a challenging yet significant task, as it requires understanding both the overall metro network passenger flow [1] and individual pedestrian behavior in stations [2]. For the former, many existing studies employ deep learning models based on spatio-temporal features to forecast metro network passenger flow. These approaches utilize distinct prediction models tailored to different traffic dynamic [3]. For example, applying separate processing frameworks for the passenger flow controlled by morning peaks and normal passenger flow. While these models generally follow similar analytical frameworks across various scenarios and perform well under typical conditions, they often struggle with atypical situations due to insufficient research on underlying passenger flow patterns, such as large-scale festivals or sudden surged in demand.

To address this limitation, this study processes the automatic fare collection (AFC) data from the metro network in City F, categorizes passenger flows and reveals the characteristics of passenger flow under varying scenarios, to provide actionable reference methodologies for addressing different types of passenger flow patterns.

Method

We first aggregated the AFC data at 30-minute intervals to calculate daily inbound and outbound flow for each station, then systematically categorize the data into workday and rest-day subsets. Ultimately, four combinatorial line charts (inbound/outbound flows on workdays and rest-days) are generated for every station.

This study categorizes metro network passenger flow into three primary types:bidirectional tidal flow (BTF), sustained outbound flow (SOF), and high-volume flow (HVF) (Fig. 1). These categories encompass nearly all possible passenger flow scenarios.

Bidirectional tidal flow (BTF): Characterized by two opposing peaks—manifesting as morning inbound/evening outbound phases, or vice versa—predominantly observed in residential and work areas during commuting hours.

Sustained outbound flow (SOF): Refer to consistently high outbound passenger flow on non-working days, frequently identified in leisure-commercial areas where weekend/holiday travel demand prevails.

High-volume flow (HVF): Exhibit high and fluctuating passenger volumes under various conditions, primarily found in railway stations and airports. These categories encompass nearly all possible passenger flow scenarios.

*Email of the corresponding author: junz@ustc.edu.cn

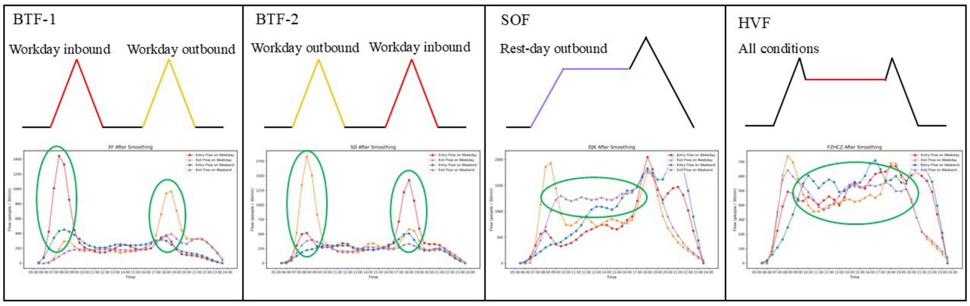

Figure 1: Basic characteristics of different flow types

Analysis and Results

By performing flow pattern recognition across different stations, we can determine the proportion (P) of each flow type within a station's overall traffic.Subsequently, we conduct statistical analysis on each flow type using relative flow data, where relative flow is defined as the passenger volume within a given time interval (30 minutes or 5 minutes in this study) divided by the total daily volume. This approach effectively captures the characteristics of flows of varying magnitudes. Finally, by normalizing relative flow by P, we can better extract the intrinsic characteristics of each specific flow type.

We found that BTF-type flow appears in most metro stations and exhibits highly distinct characteristics. According to the boxplot analysis (Fig. 2 (a)), the boundary flow and peak flow of both the morning and evening peaks are nearly identical. The morning peak starts with an initial relative flow close to zero, while the evening peak begins at approximately 1.5×10^2. The peak values for both periods consistently reach around 4.2×10^2 before declining to approximately 1.3×10^2. For BTF-1, the interval between the morning and evening peaks is typically around 10.5 hours, whereas for BTF-2, the interval is approximately 10 hours. Additionally, the peak start and end times for BTF-2 are more consistent (Fig. 2 (b)). Although being a weekday commuting phenomenon, BTF-type flow's influence extends to weekends, where peak values reach up to 46% of weekday morning peaks and 54% of evening peaks (Fig. 2 (c)). In contrast, SOF-type and HVF-type flows occur in relatively few stations, constrained by the limited number of corresponding building types in the city. For stations with SOF-type flow, after removing the influence of bidirectional tidal flow on weekend passenger flow, the remaining weekend inbound and outbound passenger flows exhibit strong consistency.

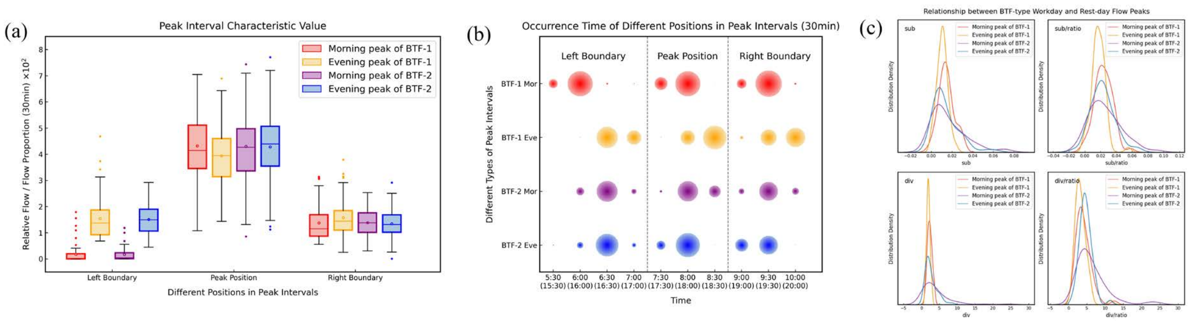

Figure 2: Characteristic BTF-type flow: (a) Peak interval values; (b) Occurrence time of peaks; (c) Relationship between workday and rest-day flow

References

[1] Q.C.Xue, et al. *Passenger flow forecasting approaches for urban rail transit: a survey*, International Journal of General Systems, 2023.

[2] J.Zhang, et al. *State-dependent multi-agent discrete event simulation for urban rail transit passenger flow*, Physica A: Statistical Mechanics and its Applications, 2024.

[3] H.Y.Li, et al. *Short-term passenger flow prediction under passenger flow control using a dynamic radial basis function network*, Applied Soft Computing, 2019.

Cooperation and Competition During Pedestrian Evacuation

Hongpeng Qiu[1], Xuanwen Liang[1], Dongli Gao[1], and Eric Wai Ming Lee*[1]

[1]City University of Hong Kong

Abstract Cooperation and competition are critical evacuation behaviours in pedestrian evacuation and have received extensive attention. However, previous studies were mostly based on their own understanding of cooperation and competition and lacked a solid theoretical foundation. Based on the solid definition of cooperation and competition over the past half century, we propose an evacuation model and verify and compare the model through experiments. We found that cooperative and competitive pedestrians have different evacuation paths, patterns, and efficiencies. Our findings contribute to the understanding of the evacuation process to effectively manage emergencies and reduce chaos during emergencies.

Keywords competition and cooperation, cellular automaton, pedestrian evacuation simulation

Instruction

Every second in an emergency is critical for life and property [1], so an accurate understanding of evacuation behaviour is important to facilitate reliable prediction and implementation of effective control strategies. To improve the accuracy of evacuation prediction of the CA model, many studies have studied various factors of the classic CA model. The psychological states of cooperation and competition of pedestrians during the evacuation process have also been a topic of interest to researchers because it is a comprehensive response of pedestrians to internal and external factors, which seriously affects the evacuation dynamics and efficiency.

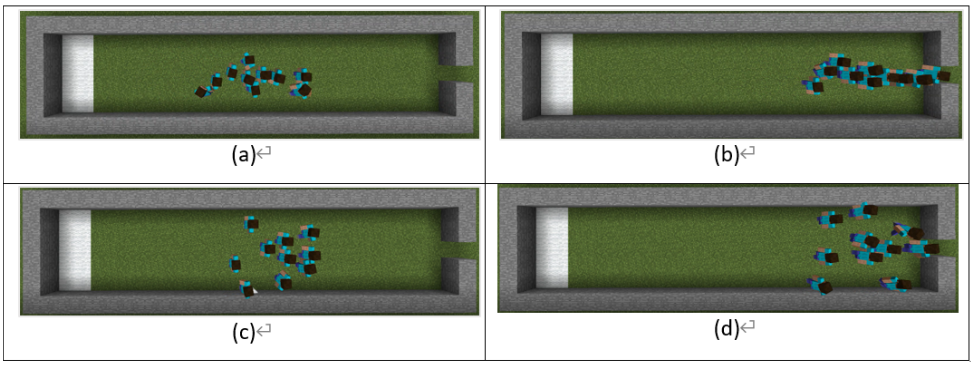

Figure 1: Evacuation patterns of different personality groups

In psychology, cooperation and competition are defined as follows: Cooperation is when one person moves toward goal achievement, and others will also move toward goal achievement. Cooperative people view conflicts as common problems that should be considered and solved together. Competition is when one party succeeds, and the other party fails. Competitive people tend to view conflicts as a win-lose struggle; if the other one wins, they lose. Deutch [2] first proposed this theory in 1948 and then further developed it [3, 4], and it was later recognized and cited by other psychologists, e.g. Tjosvold [5, 6], Alper et al. [7]. It is still recognised more than half a century later [8]. The definition of cooperation and competition is undoubtedly correct. Therefore, we introduce this theory into the cellular automaton model to guide pedestrians with different personalities (cooperation and competition) in making path selection and conflict resolution and better simulate and predict actual pedestrian evacuation. The model deeply explains the cooperative and competitive behaviours of pedestrians during the evacuation process and is compared and verified with actual evacuation experiments, reproducing different evacuation trajectories, evacuation times, evacuation shapes, etc., that occur during the evacuation process.

*Email of the corresponding author: ericlee@cityu.edu.hk

We used the CA model to study cooperation and competition and used Minecraf to conduct evacuation experiments to verify it. We found that cooperative pedestrians and competitive groups showed different evacuation patterns during the evacuation process, as shown in figure 1, where (a) and (b) are the evacuation patterns of competitive pedestrian groups, and (c) and (d) are the evacuation patterns of cooperative pedestrian groups. It can be seen that the competitive pedestrian group gradually moves towards the middle during the evacuation process, and the length gradually stretches, forming a long strip, while the cooperative pedestrian group is relatively dispersed during the evacuation process, with a shorter length and a rectangular shape. We also see this evacuation phenomenon in the CA model.

Bibliography

[1] Hosseini Omid, Maghrebi Mojtaba, Maghrebi Mahmoud Faghfour, *Determining optimum staged-evacuation schedule considering total evacuation time*, **congestion severity and fire threats**, 139: 105211, 2021.

[2] Deutsch, Morton, *The effects of cooperation and competition upon group process*, Journal Name **Massachusetts Institute of Technology**,1948.

[3] Deutsch, Morton, *The resolution of conflict: Constructive and destructive processes*, Journal Name **American Behavioral Scientist**, 248-248, 1973.

[4] Deutsch, Morton, *Sixty years of conflict*, Journal Name **International journal of conflict management**, 237-263, 1990.

[5] Tjosvold, Dean, *Cooperative and competitive goal approach to conflict: Accomplishments and challenges*, Journal Name **Applied Psychology**, 285-313, 1998.

[6] Tjosvold, Dean, *Effects of crisis orientation on managers' approach to controversy in decision making*, Journal Name **Academy of Management Journal**, 130-138, 1984.

[7] Alper Steve, Tjosvold Dean, Law Kenneth S., *Conflict management, efficacy, and performance in organizational teams*, Journal Name **Personnel psychology**, 625-642, 2000.

[8] Tjosvold Dean, Wong Alfred S.H., Feng Chen Nancy Yi, *Constructively managing conflicts in organizations*, Journal Name **Annu Rev Organ Psychol Organ Behav**, 545-568, 2014.

12th International Conference on Pedestrian and Evacuation Dynamics (PED 2025)
Prague, Czech Republic – September 9-12, 2025

Simulation and empirical analysis of pedestrian game-behavior under terrorist attacks

Ran Su[1], Qing-Yi Hao[2], Zhi-gang Shi[1], and Zhi-Ming Fang*[1]

[1]Business School, University of Shanghai for Science and Technology, Shanghai, 200093, China
[2]School of Mathematics and Physics, Anqing Normal University, Anqing, 246133, China

Abstract This study proposes an evolutionary game model to analyze pedestrian evacuation behavior during terrorist attacks. The model focuses on interactions between altruistic and egoistic strategies under panic and varying tactics. Using replicator dynamics, the study examines equilibrium stability and the impact of reward mechanisms on strategy selection, validated by empirical data. The results demonstrate that positive rewards enhance altruistic behavior, improving evacuation efficiency, while negative rewards increase avoidance strategies and risks.

Keywords Altruistic behavior, Replicator dynamics, Terrorist attack, Evacuation process

Model

Terrorist attacks that cause casualties and property losses pose an essential challenge to human society[1]. Developing efficient evacuation strategies is crucial to minimizing losses. This study introduces an innovative evolutionary game model to analyze pedestrian behavior during terrorist attacks. It centers on the interaction between altruistic and egoistic strategies under different levels of panic and terrorist tactics. Due to varying levels of panic among pedestrians[2], the model divides pedestrian strategies into two types: the avoidance strategy, where pedestrians avoid contact with terrorists to minimize casualties, and the defense strategy, where pedestrians overcome panic and altruistically approach the terrorist area to confront terrorists during the attack. Moreover, terrorists commonly hold two strategies according to the relevant experiments[3], namely proximity attacks and movement attacks.

Replicator dynamics is used to analyze the stability of equilibrium points, exploring how various reward values influence pedestrians' strategy choices. And, the payoff of pedestrians adopting different strategies in evacuation is expressed as shown in Table 1. Fitness is used to measure the relative success of a strategy adopted by pedestrians in a crowd. It is typically directly related to the payoff of pedestrians. In the evolutionary game model, pedestrians tend to learn and imitate strategies of higher fitness. According to the replicator dynamics, the change rate of pedestrians who adopt the avoidance strategy $N(x, y)$ is as Eq.(1):

$$N(x, y) = y \cdot (E_y - \overline{E_2}) = y \cdot (1 - y)[A \cdot x + (C_2 - C_1 - A)], \tag{1}$$

where y is the proportion of the pedestrians who adopt the avoidance strategy, E_y is the fitness of pedestrians with the avoidance strategy, and $\overline{E_2}$ is the average fitness of the pedestrians.

Table 1: Payoff matrix of pedestrians.

Strategy	Avoidance strategy	Defense strategy
movement attack strategy	$P_3 - C_1$	$P_3 - C_2$
proximity attack strategy	$P_4 - C_1 - A$	$P_4 - C_2$

Results

The proposed model is validated using experimental data from an evacuation scenario involving attacks[3]. Taking the pedestrian benefit of a movement attack P_3 and the benefit of a proximity attack P_4 as

*Email of the corresponding author: zhmfang2015@163.com

examples, we can acquire temporal data on the number of survivors for different strategies of terrorists as the calculation basis in the model. A is the average distance of motion for pedestrians choosing avoidance strategies. B is difference in casualties compared to a scenario without a terrorist. The simulation

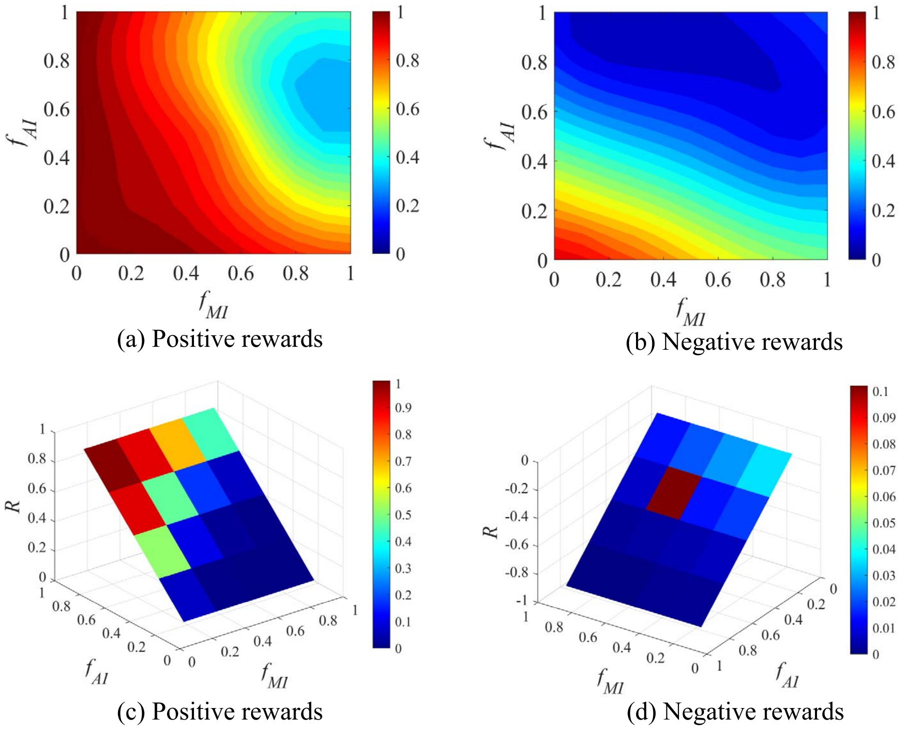

Figure 1: The heat map of the altruistic frequency for positive rewards and negative rewards. Positive rewards mean that pedestrians are rewarded for altruistic behaviors. While negative rewards denote punishments to altruists. The intervals of variation of the parameters are both 0.1.

results reveal that positive rewards significantly promote altruistic behavior, especially under proximity attack strategies. This leads to more efficient evacuations and fewer casualties. Because the number of pedestrians with defense strategy in the system is constantly changing over time, the proportion of altruists could be calculated based on the approximate calculation strategy. Specifically, the number of frames when the altruists appear is recorded as t_0. Moreover, the number of altruists under t_0 is N_{t_0}, and the number of surviving pedestrians under t_0 is S_{t_0}. The initial proportion of the altruists f_{AI} can be obtained as Eq.(2).

$$f_{AI} = \frac{N_{t_0}}{S_{t_0}}. \tag{2}$$

As depicted in Figure 1, the proportion of altruists increases and reduces casualties. The more terrorists initially adopt the proximity attack strategy, the more conducive it is to altruistic behavior in the system under positive rewards. Conversely, negative rewards drive pedestrians towards avoidance strategies, heightening the risk of casualties. This research provides theoretical insights for optimizing evacuation strategies during terrorist attacks.

Bibliography

[1] Zhang, Z. W., Ling, W., Yang, Z. H., Wei, X., Wang, H., A congestion prediction model for optimizing emergency evacuation design of university libraries in China, J. Build. Eng. 99, 111537, 2025.

[2] Helbing, D., Farkas, I., Vicsek, T., Simulating dynamical features of escape panic, Nature 407, 487 - 90, 2000.

[3] Xie, S., Ye, R., Li, X., Huang, Z., Cao, S., Lv, W., He, H., Zhang, P., Fang, Z., Zhang, J., Song, W., Nonreciprocal interactions in crowd dynamics: Investigating the impact of moving threats on pedestrian speed preferences, Transport Res. C-Emer. 162, 104586, 2024.

Optimization of exit-restricted aircraft evacuation with a dual-axis rotation cellular automaton model

Xingwen Xiong[1], Juan Chen[2], Qiao Wang[1], and Jian Ma*[1]

[1]School of Transportation and Logistics, Southwest Jiaotong University, Chengdu 610031, China

[2]Faculty of Geosciences and Engineering, Southwest Jiaotong University, Chengdu 610031, China

Abstract The emergency evacuation efficiency of civil aviation aircraft plays a critical role in determining passenger safety, especially under exit-restricted conditions. Overcrowding can be expected when available exits are limited and unevenly distributed. Such scenarios can be frequently observed in forced landings resulted aircraft fires, demanding safe and efficient evacuation strategies. As a consequence, this study proposes organized evacuation strategies to improve evacuation safety and efficiency considering the variations in the number and locations of exits. Specially, the dual-axis rotation mechanism which mimics the bipedal feature of the human body, as shown in Figure 1, is integrated into a fine discrete floor field cellular automaton (FFCA) to better address evacuation challenges in constrained spaces like aircraft cabins. Using the FFCA with dual-axis rotation, evacuation strategies (e.g., random, back-to-front, front-to-back, zone rotation, outside-in, reverse pyramid, and row-by-row) is analyzed. Effects of passenger numbers, distribution, and available evacuation exits combinations will be investigated. Simulation results show that organized evacuation sequences significantly enhance efficiency and reduce congestion compared to traditional proximity-based methods. Under extreme conditions with limited exits, certain sequences outperform others. The findings provide theoretical support for developing emergency evacuation plans and improving on-site management, offering practical implications for aviation safety.

Keywords Civil aviation aircraft, Emergency evacuation, Evacuation strategies, Floor field cellular automaton, Rotation behavior

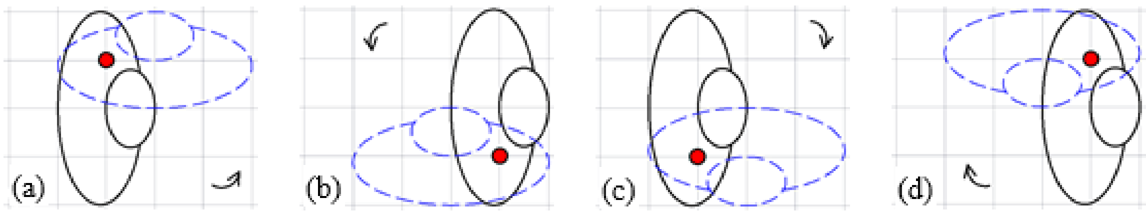

Figure 1: Configurations of rotation with the dual-axis: (a) left around the left axis, (b) left around the right axis, (c) right around the right axis. The solid black and dashed blue lines show the pedestrian before and after rotation respectively. The red dots indicate the rotation axis.

*Email of the corresponding author: majian@mail.ustc.edu.cn

12th International Conference on Pedestrian and Evacuation Dynamics (PED 2025)
Prague, Czech Republic – September 9-12, 2025

Cyclists' Braking Behavior in Response to Crossing Pedestrians

Floor Bontje*[1,2], Leendert van Maanen[1], Bas Spierings[1], Roland J. Geraerts[1], Taoufik Bakri[2], and Christian P. Janssen[1]

[1]Utrecht University, Netherlands
[2]TNO Sustainable Urban Mobility and Safety, Netherlands

Abstract This study examines how pedestrian density, road design, time-to-arrival (TTA), and distance influence cyclists' braking behavior when encountering a crossing pedestrian using four controlled video simulation experiments. While cyclists are known to adapt their decision-making to their environment, controlled studies isolating specific influencing factors remain limited. Our findings indicate that cyclists are more likely to brake in high pedestrian-dense environments, particularly under shorter TTA conditions. In addition, braking decisions take longer than decisions to continue, with this effect being more pronounced in low-density environments, shared spaces, and longer TTA conditions. Our insights highlight the strong influence of pedestrian density on cyclists' braking behavior. The insights of this research could be incorporated into the parametrization of urban traffic and may lead to improved simulations of digital twins of urban areas.

Keywords Decision-making, Cyclist-pedestrian interaction, Digital-Twins, Road design

Motivation

In the field of urban development, traffic models are used to predict and manage traffic scenarios. In recent years, policy makers have increasingly explored the possibilities of using digital twins [1]. A digital twin aims to reflect the physical world as completely as possible, and preferably updates through a bi-directional information flow between the physical and virtual word. Digital twins simulate traffic including potential hazards. To make reliable simulations of human behavior, the underlying models of human decision-making should be accurate and valid; however, there is still significant room for improvement [2]. For this, more knowledge about human traffic behavior is needed. To contribute to this, this study examines the interaction between cyclists and pedestrians.

Previous studies have shown that cyclist-pedestrian interactions are affected by how well they can anticipate each other, which involves negotiation and adaptation to social norms [3]. This ability can be influenced by environmental factors, the number of traffic participants, and the design of the road [4], as well as the kinematics of approaching traffic, such as the time gap (TTA) and the distance gap, as demonstrated in studies on car drivers [5]. However, these factors (and their interaction effects) should be quantified in order to incorporate them in traffic models.

In this research, we investigate how TTA, and distance gap, pedestrian density, and road design (specifically, the presence of a cycling lane) affects cyclists' braking behavior with the use of a video simulation experiment. We focus on both decision outcomes and response times when encountering a crossing pedestrian.

Method

We conducted four experiments (of which two replications) using controlled video simulations. Video stimuli were created using the crowd simulation software SimCrowds [6]. Participants viewed a virtual urban environment from a cyclist's perspective, while moving at a constant speed. On each trial, a pedestrian would cross the road. Participants had to decide as fast as possible, whether they would "continue cycling" (K key) or "brake" (S key).

Across the four different experiments, we manipulated the TTA (4/6 s), distance gap (15/25 m), pedestrian density (high/low), and the impact of road design (shared space/cycling lane) on cyclists' braking decisions (decision outcome, response time) using within-subject designs.

*Email of the corresponding author: f.bontje1@uu.nl

The study was approved by the Ethical Review Board of the Faculty of Social and Behavioral Sciences at Utrecht University (FETC 24-0145). All participants (total N = 114) volunteered and provided written informed consent.

We analyzed the relationships between dependent and independent variables with generalized linear mixed-effects models, incorporating random intercepts per participant to account for individual differences.

Results and Implications

Consistent across all experiments, a high pedestrian density resulted in more "brake" decisions (in all linear models, $p < .05$). Additionally, cyclists in general decided to brake more often when they had a smaller decision time (TTA). Participants also decided to brake more frequently when the distance was small in combination with a larger time gap. Moreover, we found that the time gap (TTA) has a stronger influence on the decision behaviour than the distance gap. We did not find conclusive evidence regarding the effect of road surfaces on braking behavior. Figure 1 shows the decision outcome across the two replication experiments.

Regarding response times, the results suggest that braking decisions take longer, especially in low pedestrian density conditions and shared spaces. We found that cyclists also took longer to decide when more time was available ($p < .05$), especially in the trials where they decided to brake. This effect of TTA was more pronounced in areas with low pedestrian density.

Taken together, the results of this controlled study show that multiple factors influence the decision outcomes and the response times of cyclists in anticipatory decisions. Pedestrian density and TTA especially seem to influence the decision behaviour, whereas road surface seems to not influence that much. Our quantification of the factors of influence could inform the design of digital twins (cf. [2]), for example by specifying how pedestrian density impacts decisions.

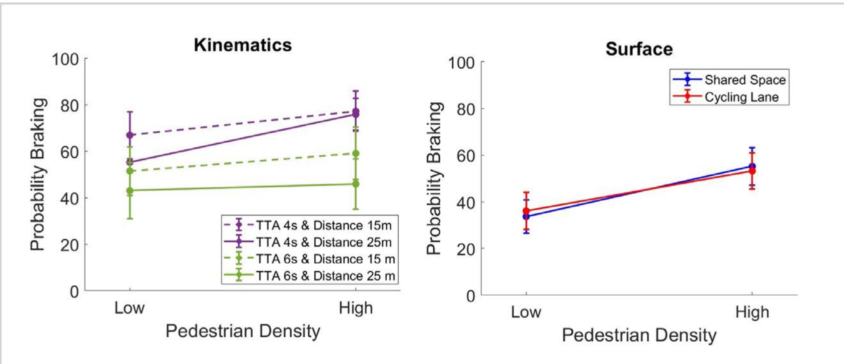

Figure 1: Group average probability of “brake” decisions, the error bars represent the 95% CI. A) Kinematics experiment (N = 30), B) Surface experiment (N = 31)

Bibliography

[1] Marcucci, E., Gatta, V., Le Pira, M., Hansson, L., & Bråthen, S. (2020). *Digital Twins: A Critical Discussion on Their Potential for Supporting Policy-Making and Planning in Urban Logistics*. Sustainability, **12**(24). https://doi.org/10.3390/su122410623

[2] Marçal Russo, L., Dane, G., Helbich, M., Ligtenberg, A., Filomena, G., Janssen, C. P., Koeva, M., Nourian, P., Patuano, A., Raposo, P., Thompson, K., Yang, S., & Verstegen, J. A. (2025). *Do urban digital twins need agents?*, Environment and Planning B: Urban Analytics and City Science. https://doi.org/10.1177/23998083251317666

[3] Edquist, J., & Corben, B. (2012). *Potential application of Shared Space principles in urban road design: effects on safety and amenity*. Report to the NRMA-ACT Road Safety Trust, MONASH University, Accident Research Centre.

[4] Dozza, M., & Werneke, J. (2014). *Introducing naturalistic cycling data: What factors influence bicyclists' safety in the real world?* Transportation Research Part F: Traffic Psychology and Behaviour, **24**, 83–91. https://doi.org/10.1016/j.trf.2014.04.001

[5] Bontje, F., & Zgonnikov, A. (2024). *How Sure is the Driver? Modelling Drivers' Confidence in Left-Turn Gap Acceptance Decisions*, Computational Brain & Behavior, **7**(3), 437-456.

[6] UCrowds (2024). SimCrowds (Version 1.60 - b.1) [Desktop App] https://ucrowds.com/simcrowds/

Timetable
Poster index

Revisiting counter-current pedestrian flow as a non-equilibrium phase transition

Peter Wan[1] and Christopher Ness[1]

[1]School of Engineering, University of Edinburgh, Edinburgh EH9 3JL, United Kingdom

Abstract We explore the fundamental parameter space of Helbing's social force model through agent-based simulations using a counter-current pedestrian flow environment with periodic boundary conditions. The mean agent velocity is used as an order parameter to characterise the phase transition that emerges between fully established lane flow and gridlock. We show that the time evolution of this order parameter can be fit with an exponential decay, allowing us to probe the diverging timescale that arises at the transition. Future work will refine the understanding of these transitions by probing different parameters in the model, and exploring the mechanisms behind lane formation.

Keywords Pedestrian Dynamics, Social Force Model, Non-Equilibrium Phase Transition

Introduction. Pedestrian dynamics modelling [1] has gained significant recent interest due to its ability to address crowd safety concerns in contexts such as emergency evacuations [2] and increasing infrastructure efficiency [3]. Many models have been proposed, with Helbing's Social Force Model [4] being the most popular due to its ability to reproduce self-organised phenomena.

In order to match experimental data, various modifications to SFM have been proposed, including limited vision [5] and modeling group behaviour [6]. These are typically validated by parameter calibration with experimental data [7], and by employing fitting techniques [8]. Although each parameter in the SFM has a well-motivated physical meaning, their collective effect on pedestrian behaviour remains complex: multiple parameters can influence self-organisation, and one parameter can affect multiple observables [9]. Few systematic studies have examined the full parameter space, focusing on aspects such as the relaxation time τ [10], where a drifting effect was measured at different values of τ.

Here, the aim is to gain a physical understanding of the SFM in its most basic form through an agent-based simulation using various values of B, the relaxation distance of long distance force. A periodic bi-directional flow environment is used to eradicate pedestrian-wall interactions, and we quantify flow rate, gridlock and lane formation to characterise the parameter space.

Model. SFM is a self-driven agent-based simulation describing how individuals respond to their environment.This is captured through three interaction forces: the driving force $\vec{F}_i^d$; the repulsive force $\vec{F}_{ij}^r$ between agent pairs; and the contact force $\vec{F}_{ij}^c$. The governing equation is thus

$$m_i \ddot{\vec{x}}_i = \vec{F}_i^d + \sum_{j=1, j\neq i}^{N} \vec{F}_{ij}^r \mu + \vec{F}_{ij}^c, \tag{1}$$

where m_i and $\vec{x}_i = (x_x, x_y)$ are the mass and position of agent i and N is the total number of agents. The driving force is defined as $\vec{F}_i^d = \frac{m_i}{\tau}(\dot{\vec{x}}_i^d - \dot{\vec{x}}_i)$, where $\dot{\vec{x}}_i^d$ and $\dot{\vec{x}}_i$ are the desired velocity and current velocity of the agent. The repulsive force between two agents is $\vec{F}_{ij}^r = A \exp\left(-\frac{\epsilon_{ij}}{B}\right) \vec{e}_{ij}^{\,n}$, where $\epsilon_{ij} = d_{ij} - 2r$ and A and B are parameters defining the force at contact and force relaxation distance. d_{ij} is the distance between two agents, r is their radius, and $\vec{e}_{ij}^{\,n}$ is the unit vector parallel to $\vec{x}_j - \vec{x}_i$.

The contact force F_{ij}^c is defined as $\vec{F}_{ij}^c = [(-k\epsilon_{ij})\vec{e}_{ij}^{\,n} - (\kappa\epsilon_{ij}(\dot{\vec{x}}_j - \dot{\vec{x}}_i)\cdot \vec{e}_{ij}^{\,t})\vec{e}_{ij}^{\,t}]$, evaluated when $\epsilon_{ij} < 0$, and where $\dot{\vec{x}}_{ji}^{\,t}$ is the tangential velocity difference, and $\vec{e}_{ij}^{\,t}$ is the unit vector perpendicular to $\vec{x}_j - \vec{x}_i$. The angle factor μ is unity when $\vec{e}_{ij}^{\,n} \cdot \dot{\vec{x}}_i \geq |\dot{\vec{x}}_i| \cos(\varphi)$, where $\varphi = 100°$, and otherwise 0.5. We use the following non-dimensionalised parameters: $m = 1$, $r = 1$, $A = 25$, $B = 0.16$, $\tau = 1$, $\dot{\vec{x}}_d = (\pm 1.5, 0)$, $k = 15$, $\kappa = 30$. We initialised $N = 1000$ agents, placing them randomly on the nodes of a predefined lattice, with $N \leq$ number of nodes within a rectangular domain of height $H = 50$ and varying lengths L corresponding to different densities ρ. $\frac{N}{2}$ agents are assigned a desired velocity pointing either left or right, and are initialised with $\dot{x}_x$ and $\dot{x}_y$ chosen uniformly between ± 0.5. Simulations were conducted for $\rho = 0.1$ to 0.6 in fixed intervals, using 50 realisations of each case, and run to time $t = 200$ with a time step of $dt = 0.0001$. Figure 1 a) shows snapshots with $\rho = 0.2$.

Analysis. The system exhibits both lane formation and gridlock. The former is defined as a group of more than six agents with same $\dot{\vec{x}}_d$ moving on a similar trajectory. Gridlock is defined when an agent has

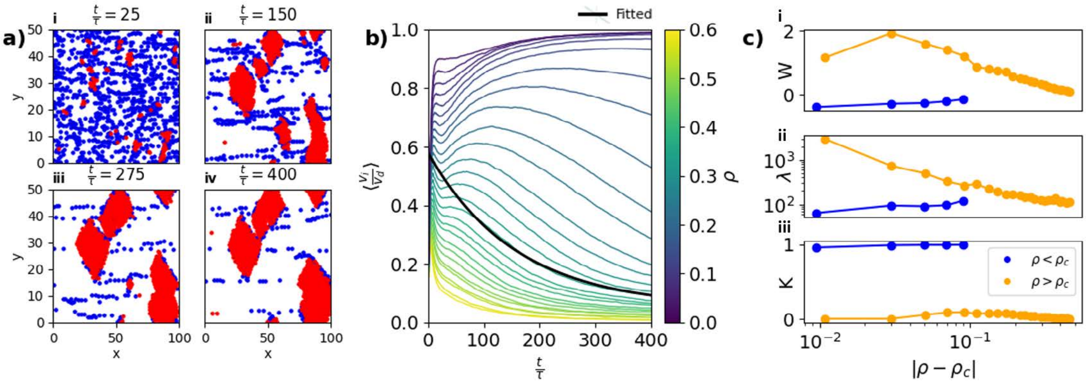

Figure 1: Simulation results. (a) Snapshots for $\rho = 0.2$ at various times. Red agents are gridlocked; (b) $\langle \hat{v}(t) \rangle$ averaged over 50 realisations. An example of curve fitting using $y = W \exp\left(-\frac{t}{\lambda}\right) + K$ is shown in black. (c) fitting parameters shifted through $\rho_c = 0.130$. λ against $|\rho - \rho_c|$ can be fitted with the equation $\lambda = 49.2|\rho - \rho_c|^{-0.80}$

.

$|\vec{\dot{x}}_i| < 0.5$. In order to obtain a quantitative understanding of the system, the mean velocity ratio $\langle \hat{v}(t) \rangle$ is used. It is defined as $\langle \hat{v}(t) \rangle = \frac{1}{N} \sum_{i=1}^{N} \left(\dot{x}_{i0}(t) / \dot{x}_{i0}^{d} \right)$ where $\dot{x}_{i0}$ and $\dot{x}_{i0}^{d}$ are the horizontal components of $\vec{\dot{x}}_i$ and $\vec{\dot{x}}_i^{d}$. $\langle \hat{v}(t) \rangle$ approaches unity when every agent is moving at their desired velocity, whereas it vanishes under full gridlock. An intermediate values suggest coexisting gridlock and lane formation.

Figure 1b) shows $\langle \hat{v}(t) \rangle$ as a function of ρ. A few features are shown; first is the peak at $10 \leq \frac{t}{\tau} \leq 20$ for all densities, and a second peak at around $\frac{t}{\tau} = 150$ for intermediate densities. It is speculated that the first peak is due to initiation method, where agents accelerate towards their $\vec{\dot{x}}_d$, which increases $\langle \hat{v}(t) \rangle$, while collision effect eventually take over, reducing it. The second peak is speculated to be due to competing effects between lane formation and gridlock effects. The system exhibits an exponential decay behaviour, tending towards one or zero. We fit the $\langle \hat{v}(t) \rangle$ using the function $y = W \exp\left(-\frac{t}{\lambda}\right) + K$ in the region after the second peak. The fitting parameters have the following meanings; the sign of W defines the shape of the curve (decaying towards 1 or 0), B is the exponential decay relaxation time, and K is the final steady state velocity. The probed parameters can be found in Figure 1 c), where we measured $\rho_c = 0.130$. For $\rho < \rho_c$, K tends to 1 with W negative, suggesting lane formation dominates, while gridlock dominates for $\rho > \rho_c$. λ is expected to reach infinity at ρ_c, more data points are needed to correctly verify this behaviour.

Project Projection. The goal of the project is to thoroughly understand the transition that emerges in the SFM, in order to gain a fundamental physical understanding of the nature of each of the parameters. This will be done through the following steps. First, an understanding of mean velocity ratio's shape will be established quantitatively, the initialization method will be evaluated, and changes might be made to the curve fitting method and the length of length of the simulation. Second, an understanding of the lane formation will be deeply evaluated. Involving quantitative understanding of lane formation conditions and effects on the system. Third, simulations will be run for different values of B, and the corresponding W, λ and K will be obtained. We anticipate a transition from contact force dominated system to a long range repulsive force system as B decreases.

Bibliography

[1] F. Martinez-Gil, M. Lozano, I. Garc´ıa-Fern´andez, and F. Fern´andez, ACM Computing Surveys **50**, 5 (2017).

[2] M. Li, Y. Zhao, L. He, W. Chen, and X. Xu, Safety Science **79**, 243 (2015).

[3] X. Yang, X. Yang, F. Pan, Y. Kang, and J. Zhang, Physica A: Stat. Mechanics and its Applications **565**:125566 (2021).

[4] D. Helbing, I. Farkas, and T. Vicsek, Nature **407**, 487. (2000).

[5] X. Yang, H. Dong, Q. Wang, Y. Chen, and X. Hu, Physica A: Stat. Mechanics and its Applications **411**, 63 (2014).

[6] Moussa¨ıd, N. Perozo, S. Garnier, D. Helbing, and G. Theraulaz, PLOS ONE **5**, 1 (2010).

[7] I. M. Sticco, G. A. Frank, and C. O. Dorso, Physica A: Statistical Mechanics and its Applications **561**, 125299 (2021).

[8] C. Rudloff, T. Matyus, and S. Seer (2014) pp. 657–672.

[9] T. Kretz, J. Lohmiller, and P. Sukennik, Transportation Research Record **2672**, 228 (2018).

[10] F. Johansson, D. Duives, W. Daamen, and S. Hoogen- doorn, Transportation Research Procedia **2**, 300 (2014).

Rigid body agent-based crowd simulation framework utilizing simplified ray casting social forces and heat map parameters fitting

Tomasz Hachaj*[1] and Jarosław Wąs[1]

[1]Faculty of Electrical Engineering, Automatics, Computer Science and Biomedical Engineering, AGH University of Krakow, Al. Mickiewicza 30, 30-059 Krakow, Poland

Abstract This paper presents a novel rigid body agent-based crowd simulation framework utilizing a simplified Social Forces Model based on ray cast. This approach is specially designed to be integrated with simulation engines (that which enables ray cast-based collision detection) and take advantage of their other functionalities. We also present a parameter fitting method that minimizes the root mean square error between heat maps generated by real-world and simulated crowd motion.

Keywords Crowd modeling, Social forces, Parameters fitting, Heat map, Agent system, Rigid body

Material and methods

The Social Forces Model [1] is one of the most popular models used in the crowd simulation process. This is due to the ease of interpretation of its components and its effectiveness in the simulation process. Thanks to the availability of experimental data on the crowd's behavior, for example, [2], it is possible to calibrate the model's parameters based on actual human motion trajectories. The Social Forces Model can be adapted for use in simulation environments that use rigid body collision systems, A* pathfinding, and ray casting mechanisms by analyzing each agent's closest environment with a beam of rays that have a given radius and different weights of influence on the final resultant force acting on the agent (see Algorithm 1).

An easy-to-interpret way of representing simulation results is all kinds of heat maps (see Algorithm 2), which allow us to visualize the distribution of people in space during the analyzed case. Simulation parameters can be adjusted with the help of minimizing the root mean square error between heat maps of real data and simulation results (see Figure 1).

Algorithm 1 Ray cast-based social forces calculation

Require: $n > 0, d_{agent} \geq 0, d_{wall} \geq 0, w_{A*} \geq 0, w_{agent} \geq 0, d_{wall} \geq 0, a, sa_{\beta}, sw_{\beta}$ ▷ a is an agent
  $\alpha \leftarrow \frac{2 \cdot \pi}{n}; \overrightarrow{f_{agent}} \leftarrow \overrightarrow{0}; \overrightarrow{f_{wall}} \leftarrow \overrightarrow{0}$
  for $\beta \leftarrow 0; \beta < 2 \cdot \pi; \beta += \alpha$ **do**
    $o \leftarrow raycast(rotate(\overrightarrow{dir}, \beta), max(d_{agent}, d_{wall}))$
    if $o \in agents$ **then**
      $w \leftarrow \frac{\|\overrightarrow{a} - \overrightarrow{o}\|}{d_{agent}}$
      if $w \leq 1$ **then** $\overrightarrow{f_{agent}} \leftarrow \overrightarrow{f_{agent}} + sa_{\beta} \cdot lerp(\overrightarrow{a} - \overrightarrow{o}, \overrightarrow{0}, w)$
      end if
    end if
    if $o \in walls$ **then**
      $w \leftarrow \frac{\|\overrightarrow{a} - \overrightarrow{o}\|}{d_{wall}}$
      if $w \leq 1$ **then** $\overrightarrow{f_{wall}} \leftarrow \overrightarrow{f_{wall}} + sw_{\beta} \cdot lerp(\overrightarrow{a} - \overrightarrow{o}, \overrightarrow{0}, w)$
      end if
    end if
  end for
  return $\overrightarrow{f} \leftarrow (w_{A*} \cdot \overrightarrow{f_{A*}} + w_{agent} \cdot \overrightarrow{f_{agent}} + w_{wall} \cdot \overrightarrow{f_{wall}}) \cdot \Delta t$ ▷ impulse force acting on the agent

*Email of the corresponding author: thachaj@agh.edu.pl

Integrating our solution with, for example, game engines allows us to build quickly configurable experiments using both real-world data and theoretical scenarios (see Figure 2). Source codes for our approach can be downloaded from `https://github.com/browarsoftware/crowd_kinetic`.

Algorithm 2 Heat map generation

Require: $n \geq 0$; **return** M
  $M \leftarrow zeros(n, m)$
  for $a \in A$ **do**
    for $a^i \in a$ **do**
      $x \leftarrow round(lerp(0, n, a^i_x))$; $y \leftarrow round(lerp(0, n, a^i_y))$
      $M[x, y] \leftarrow M[x, y] + 1$
    end for
  end for

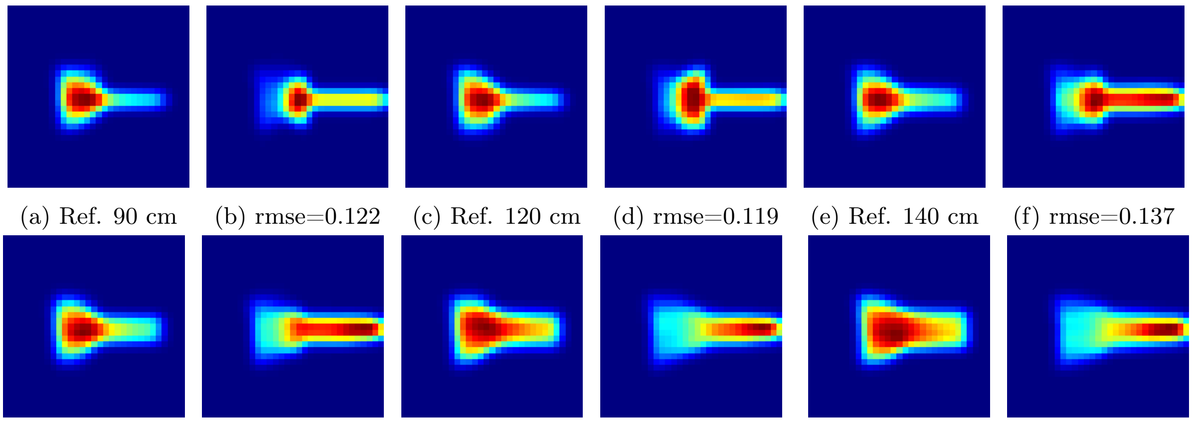

(a) Ref. 90 cm (b) rmse=0.122 (c) Ref. 120 cm (d) rmse=0.119 (e) Ref. 140 cm (f) rmse=0.137

(g) Ref. 160 cm (h) rmse=0.134 (i) Ref. 220 cm (j) rmse=0.138 (k) Ref. 250 cm (l) rmse=0.143

Figure 1: In the first and second rows, we present pairs ((a,b), (c,d), (e,f), (g,h), (i,j), (k,l) of heat maps of reference data (Ref.) for various width of bottleneck and example (without parameters optimization) simulations done with Algorithm 1, rmse is the value of root mean square deviation between reference and simulated heat map. Values in heat maps are in the range [0,1]; blue color represents the lower value, and red is the highest value.

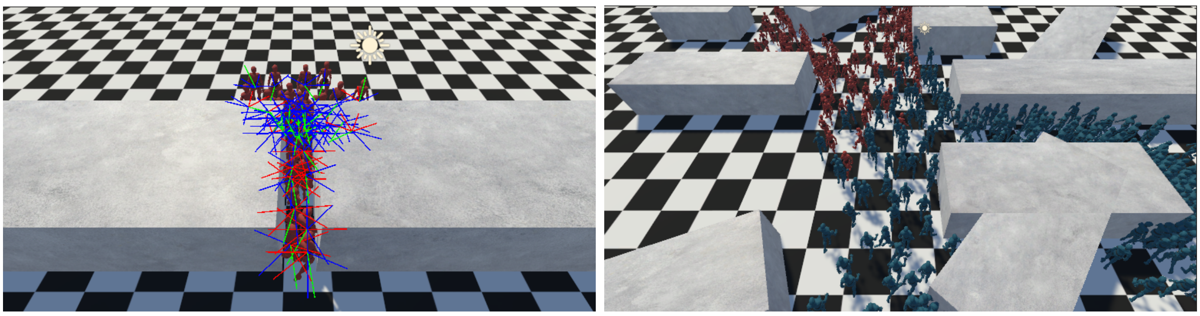

Figure 2: Left - example visualization of bottleneck simulation based on real-world data, right - theoretical scenario. The red line is the repulsion vector from walls, the blue line is the repulsion vector from other agents, and the green line is the direction of motion (the resultant of all forces acting on the agent).

References

[1] Helbing, D., Molnar, P.: Social force model for pedestrian dynamics. Physical Review E **51** (05 1998). https://doi.org/10.1103/PhysRevE.51.4282

[2] Seyfried, A., Passon, O., Steffen, B., Boltes, M., Rupprecht, T., Klingsch, W.: New insights into pedestrian flow through bottlenecks. Transportation Science **43**(3), 395–406 (2009)

Timetable
Poster index

12th International Conference on Pedestrian and Evacuation Dynamics (PED 2025)
Prague, Czech Republic – September 9-12, 2025

The Impact of Distraction on Pedestrian Collision Avoidance Process: An Energy Cost Perspective

Chenrui Xuan and Wei Xie*

Sichuan University-The Hong Kong Polytechnic University Institute for Disaster Management and Reconstruction, Sichuan University, Chengdu 610207, China

Abstract The impact of pedestrian distraction caused by mobile phone use on collision avoidance process has not been well understood. This study investigates this phenomenon through well-controlled head-on walking experiments. We found that distracted behaviour significantly increased the energy expenditure and walking burden of the non-distracted ones. Non-distracted pedestrians walked a longer distance with an average increase of 0.16 m compared to the free walking condition. The metabolic rate difference between two head-on pedestrians in the distracted condition exceeded 0.6 W/kg.

Keywords Collision avoidance, Distracted behaviour, Energy cost, Experiment, Pedestrian dynamics

Studies have shown that mobile phone use significantly distracts pedestrians and reduces their ability to perceive and react to their surroundings, thus increasing the risk of collision [1, 2]. Although studies have explored the effects of distraction on individual walking efficiency [3, 4], the specific mechanisms of its influence on collision avoidance, particularly in terms of energy expenditure, have not been fully investigated.

We conducted controlled experiments in June 2024 at Sichuan University, China. 32 groups (two participants per group) were instructed to walk head-on from opposite ends of the corridor, with one starting at point A and the other at point B (see Figure 1(a)). Two experimental conditions were set up: (i) Free walking condition: Both participants walked freely with no distraction; (ii) Distracted condition: One participant walked freely, while the other was distracted by solving simple arithmetic task on the mobile phone. As shown in (see Figure 1(b)), the trajectory length of each pedestrian was measured. In the distracted condition, the trajectory length of free walking pedestrian was 3.42±0.19 m, while it was only 3.26±0.23 m in the free walking condition. The free walking pedestrians travelled a longer distance with an average increase of 0.16 m to avoid collision with the distracted ones. This agrees well with the finding of Murakami et al. [5] that avoidance maneuvers are a cooperative process and that self-organization in human crowds is facilitated by mutual anticipation.

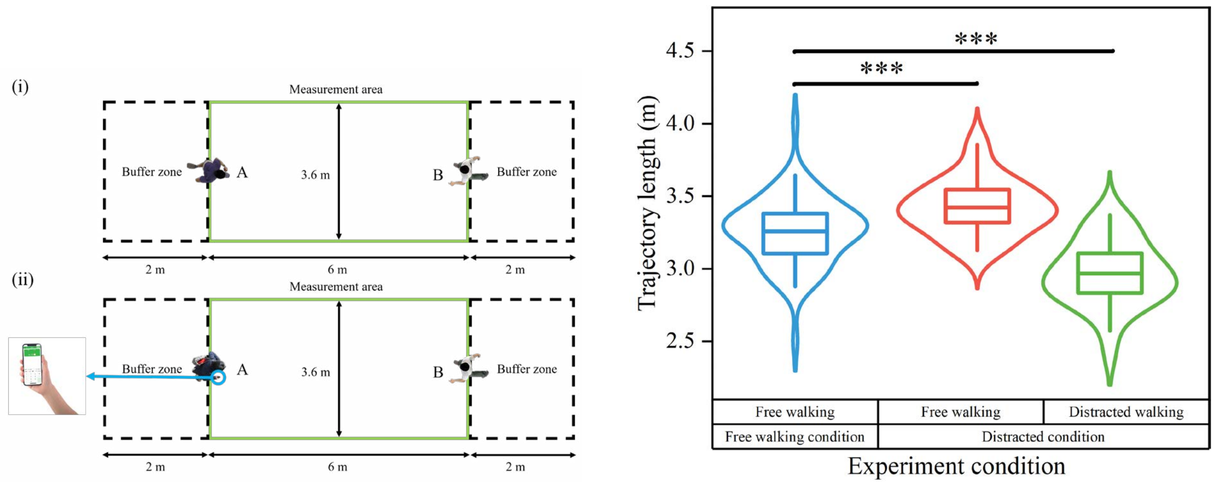

(a) (b)

Figure 1: Experimental setup and results. (a) Illustration of the experimental corridor with (i) Free walking condition and (ii) Distracted condition, (b) The trajectory length of pedestrian.

*Email of the corresponding author: xie_wei@scu.edu.cn

Researchers have extensively shown that the metabolic rate increased nonlinearly with linear and angular velocities, and the metabolic rate could be described by a quadratic function of linear velocity v and angular velocity ω with the following equation [6]:

$$\dot{E} = \alpha_0 + \alpha_1 v^2 + \alpha_2 \frac{v^2}{R^2} = \alpha_0 + \alpha_1 v^2 + \alpha_2 \omega^2$$

Here, $\alpha_0 = 2.204 \pm 0.079\, W/kg$, $\alpha_1 = 1.213 \pm 0.054\, W/kg/(ms^{-1})^2$, $\alpha_2 = 0.966 \pm 0.061\, W/kg/(rad \cdot s^{-1})^2$, giving the metabolic rate $\dot{E}$ in W/kg (normalized by body mass), where v is in ms^{-1}, R is in meters, and ω is in $rad \cdot s^{-1}$. The metabolic rate difference is illustrated in Figure 2. As the forward distance increased, the metabolic rate difference among the pedestrians predominantly ranged between 0.3 and $0.5\, W/kg$ in the free walking condition (see Figure 2(a)). In contrast, in the distracted condition, the metabolic rate difference between the distracted and free walking pedestrian exceeded $0.6\, W/kg$ (see Figure 2(b)). It indicates that under the interference of distracted pedestrians, the free walking pedestrians took on a greater responsibility for collision avoidance, resulting in higher energy expenditure.

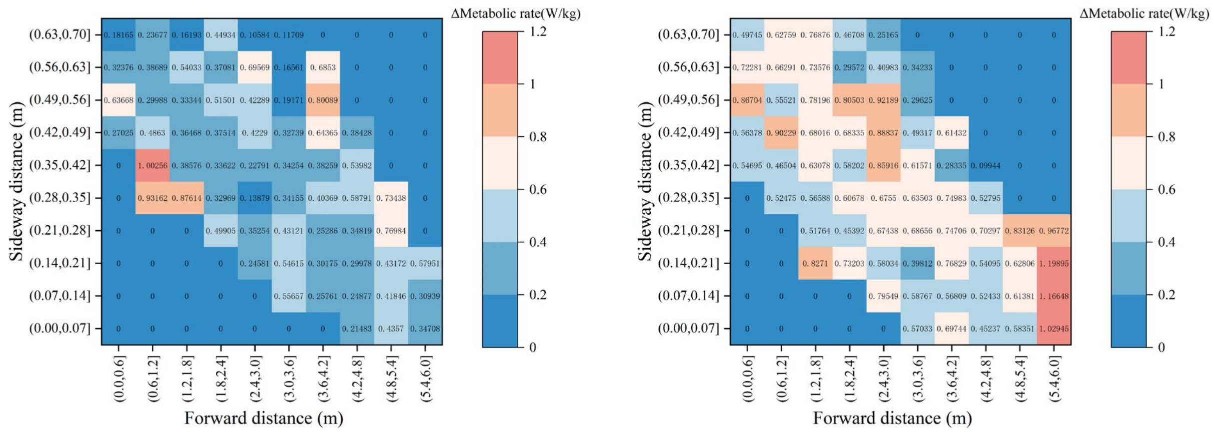

(a) **(b)**

Figure 2: The metabolic rate difference between two participants. (a) Free walking condition, (b) Distracted condition.

Bibliography

[1] Alagbé, J. A., Han, H., & Jin, S. (2023). Effect of Technological Distractions on Pedestrian Safe-Crossing Performance during Mixed Pedestrian–Bicycle Flow Overlapping with Turning Vehicles: A Case Study of Hangzhou, China. *Journal of Transportation Engineering, Part A: Systems*, 149(1), 05022007.

[2] Alsharif, T., Lanzaro, G., & Sayed, T. (2024). Distracted Walking: Does it impact pedestrian-vehicle interaction behavior? *Accident Analysis & Prevention*, 208, 107789.

[3] Alejalil, N., & Davoodi, S. R. (2017). Mobile phone usage and its effects on pedestrians' distraction. *Int. J. High. Risk. Behav. Addict*, 6, e35431.

[4] Jiang, K., Ling, F., Feng, Z., Ma, C., Kumfer, W., Shao, C., & Wang, K. (2018). Effects of mobile phone distraction on pedestrians' crossing behavior and visual attention allocation at a signalized intersection: An outdoor experimental study. *Accident Analysis & Prevention*, 115, 170-177.

[5] Murakami, H., Feliciani, C., Nishiyama, Y., & Nishinari, K. (2021). Mutual anticipation can contribute to self-organization in human crowds. *Science Advances*, 7(12), eabe7758.

[6] Brown, G. L., Seethapathi, N., & Srinivasan, M. (2021). A unified energy-optimality criterion predicts human navigation paths and speeds. *Proceedings of the National Academy of Sciences*, 118(29), e2020327118.

12th International Conference on Pedestrian and Evacuation Dynamics (PED 2025)
Prague, Czech Republic – September 9-12, 2025

Walking in super-aged society: simulating pedestrian stress with real-time adaptive social force model

Jinsoo Kim[1], Changhoon Shin[2], and Hoontae Park*[3]

[1]MIMLAB Co., Ltd.

Abstract Social Force Model(SFM) is modified to dynamically adjust walking behaviors in real-time, responding to environmental factors. A large-scale pedestrian simulation environment is constructed based on a high-definition 3D pedestrian map, in which the modified model is effectively implemented. The system is then employed to evaluate pedestrian stress levels as the proportion of elderly pedestrians increases within the simulation environment.

Keywords Large-scale pedestrian simulation, Super-aged society, Social Force Model, Real-time adaptation, 3D simulation, Pedestrian stress

Extended Abstract

With the global emergence of super-aged societies, pedestrian mobility patterns are undergoing significant transformations. As aging populations continue to rise, the need for understanding and simulating their walking behaviors becomes imperative for urban planning, infrastructure design, and pedestrian-friendly policy development.

Social Force Model (SFM) has been widely utilized in pedestrian simulations, modeling movement dynamics based on interaction forces between individuals and their environment. However, traditional deterministic SFM models rely on fixed parameters, limiting their ability to adapt to real-time pedestrian-environment interactions.

In recent years, pedestrian models based on AI and deep learning have emerged, demonstrating remarkable accuracy in predicting pedestrian trajectories. While these models excel at handling complex pedestrian interactions, their high computational demands and reliance on extensive training datasets make them impractical for real-time, large-scale pedestrian simulations. This study proposes a real-time adaptive SFM-based pedestrian simulation model designed for super-aged societies, effectively bridging the gap between deterministic models and AI-based prediction approaches.

Our approach integrates GIS-based 3D pedestrian mapping to construct a large-scale pedestrian simulation capable of dynamically adjusting pedestrian interaction forces based on environmental constraints. Unlike deep learning-based methods that require intensive computational resources, our model introduces a real-time parameter adaptation mechanism that allows for efficient and scalable pedestrian flow modeling. In this framework, the interaction forces within the SFM model are modified in response to environmental factors, such as road slope, road width, and congestion levels, allowing pedestrians to adapt their movement in real-time.

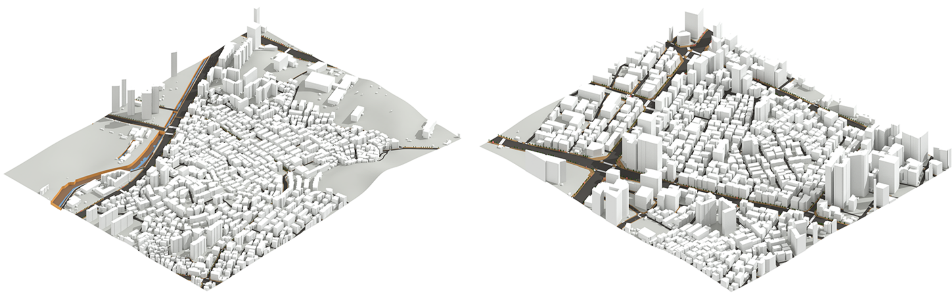

Figure 1: Example of large-scale 3D pedestrian environments

*Email of the corresponding author: htpark@mim-lab.co.kr

The core of our real-time adaptive SFM model is a dynamically modifiable parameter system that controls pedestrian motion. Let V and $V_{desired}$ be the actual and the preferred walking velocity of a pedestrian respectively. Define velocity ratio as $V_p = \frac{|V|}{|V_{desired}|}(0 \leq V_p \leq 1)$. The adaptive parameters P in SFM are updated in the form of $P = f(V_p)$, where relaxation time is inversely proportional to V_p, while other parameters(such as repulsive force) scale directly. This adaptive mechanism enables the real-time modification of pedestrian behavior, allowing for a realistic and responsive pedestrian simulation in large-scale environments.

To evaluate the performance of our modified model, we have conducted a validation process using Fruin's empirical data, which analyzes the average walking speed of pedestrians across different density environments, ranging from low to high density. The results show that while the traditional SFM approach struggled to match the data, particularly in high-density scenarios, our modified model demonstrated enhanced alignment across the entire density spectrum, closely following the empirical trends.

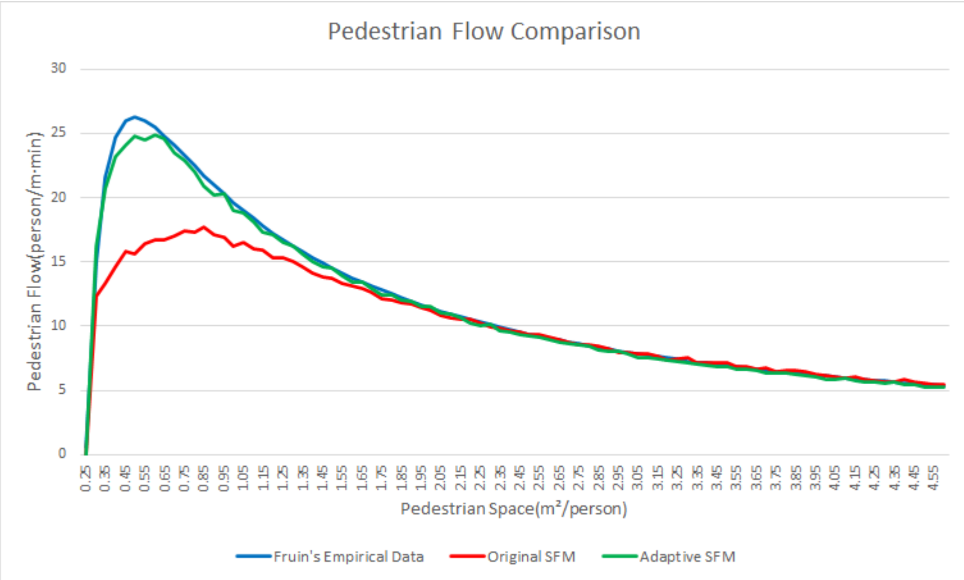

Figure 2: Validation via comparison with pedestrian flow

The validation process with Fruin's empirical data confirmed that our modified model accurately represents pedestrian behavior in general populations. However, as the proportion of elderly pedestrians increased, the validation results deviated from the data distribution. It suggests that existing models may not fully account for the complexities of aging pedestrian behaviors.

Additionally, our model integrates a real-time pedestrian stress evaluation system that analyzes movement deviations, congestion levels, and environmental constraints across various conditions. The stress analysis reveals that as the proportion of elderly pedestrians increased, measured stress levels rise consistently in all environments. These findings underscore the necessity of prioritizing elderly pedestrian considerations in urban planning, particularly in super-aged societies.

In conclusion, this paper presents a real-time adaptive SFM-based pedestrian simulation model tailored for super-aged societies. By integrating real-time parameter adjustments and GIS-based pedestrian mapping, our approach enhances pedestrian mobility analysis and stress quantification in urban environments. Future research will focus on refining elderly pedestrian behavioral models and expanding our simulation framework for real-world urban planning applications.

Bibliography

[1] Helbing, D. *A mathematical model for the behavior of pedestrians*, Behavioral science **36.4**, 298-310, 1991.

[2] Helbing, D., Molnar, P. *Social force model for pedestrian dynamics*, Physical Review E **51**, 1995.

[3] Helbing, D., et al. *Simulating dynamical features of escape panic*, Nature, 487-490, 2000.

[4] Lakoba, T. I., et al. *Modifications of the Helbing-Molnar-Farkas-Vicsek social force model for pedestrian evolution*, Simulation **81.5**, 339-352, 2005.

[5] Farina, F., et al. *Walking ahead: The headed social force model*, PloS one **12.1**, 2017.

[6] Chen, Xu., et al. *Social force models for pedestrian traffic–state of the art*, Transport reviews **38.5**, 625-653, 2018.

[7] Wang, P., Wang, X. *Social force in pedestrian crowd*, arXiv preprint arXiv **2109.12597**, 487-490, 2021.

Timetable
Poster index

12th International Conference on Pedestrian and Evacuation Dynamics (PED 2025)
Prague, Czech Republic – September 9-12, 2025

How Humans in the Loop Adapt Dynamic Lane Allocation Plans at Airport Security: A Decision-Making Analysis

Xiaoting Yuan*[1,2], Tieqiao Tang[1], and Nikolai W.F. Bode[2]

[1]School of Transportation Science and Engineering, Beihang University
[2]School of Engineering Mathematics and Technology, University of Bristol

Abstract This study investigates how humans in the loop adapt dynamic lane allocation plans through a decision-making framework combining optimization and human expertise. We develop a dynamic lane allocation model using constraint-based optimization and discrete-event simulation, then engage human participants to refine the algorithm-generated plans. We hypothesise that, compared to pure algorithmic solutions, which only keep passenger wait times within the threshold, the plans adjusted by human intervention focus more on improving service levels during peak periods.

Keywords Dynamic lane allocation, Security checkpoint management, Queue optimization, Human decision-making

Introduction

The aviation industry has been developing year by year and has become an important mode of passenger transportation. The number of passengers at nearly all airports worldwide is continuously increasing. Airport security screening processes are essential to ensure the safety of passengers and the aviation industry. However, the screening process reduces passenger comfort and satisfaction. To minimize screening time delays, airports often install multiple screening lanes. The operation of security screening lanes is challenging due to various uncertainties. For instance, while passenger flow can be estimated based on flight schedules, the exact time at which passengers arrive at the security checkpoint before departure remains uncertain. In such an uncertain environment, airport managers may have to dynamically open and close security screening lanes. Therefore, determining the optimal configuration of security screening lanes is crucial for managing passenger queues and for ensuring efficient airport operations.

Finding the right balance between maintaining acceptable wait times to ensure a positive passenger experience and controlling operational costs is challenging. Numerous studies have developed models and policies to support the efficient management of airport security checkpoint resources [1]. These studies aim to determine the minimum number of security screening lanes required while ensuring that passenger wait times remain below a predefined threshold. After obtaining a solution that "only meets the minimum requirements" through optimisation, we seek to understand how actual security checkpoint managers may respond, thus introducing humans in the loop. Do they directly adopt these solutions, or do they make adjustments based on their past operational experience?

Methods and Results

We first develop a dynamic lane allocation plan using optimization algorithms and simulation models. Then, we invite human participants in a virtual experiment simulating arrival rates and queues to adopt or adjust this plan. Simulation provides feedback on the impact of participants' choices. Finally, we assess the revised plans to understand the key factors that humans in the loop prioritize in security checkpoint operations.

(I) Optimized Dynamic Lane Allocation: We require that the proportion of passengers with a waiting time of less than 10 minutes must be greater than or equal to 85% as a constraint. Based on an assumed arrival rate, we generate the minimal lane opening configuration, as shown in Figure 1. Additionally, provide the simulation results of the system, including passenger queue waiting times and queue lengths (see Figure 2 and 3).

*Email of the corresponding author: yuanxiaoting@buaa.edu.cn

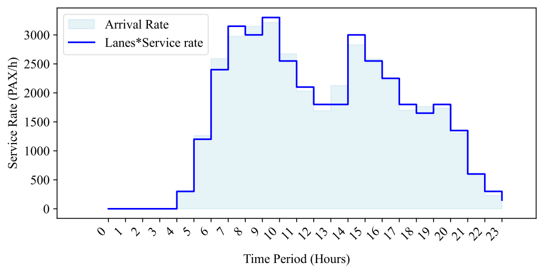

Figure 1: Security checkpoint lane allocation plan.

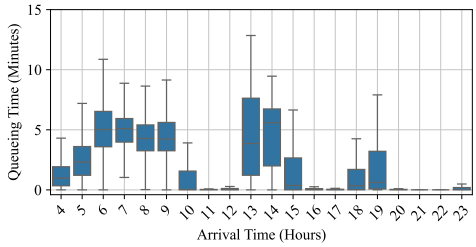

Figure 2: Passenger queue waiting times.

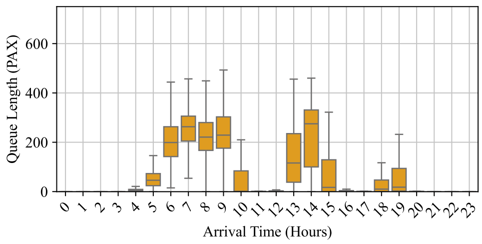

Figure 3: Passenger queue lengths.

(II) Adjustments by human participants: We will invite volunteers to participate in an experimental study. They will be provided with the original lane allocation plan for every hour of the day, as shown in Table 1, and a simulation model to evaluate their adjusted plans. They will then be asked to propose what they consider to be the optimal allocation scheme. Results will be available in time for the conference.

Table 1: Lane Opening Configuration.

Time Period	0	1	2	3	4	5	6	7	8	9	10	11
Num	0	0	0	0	2	8	16	21	20	22	17	14
Time Period	12	13	14	15	16	17	18	19	20	21	22	23
Num	12	12	20	17	15	12	11	12	9	4	2	1

(III) Evaluation of Key Operational Priorities: In the context of airport security management, we focus on the utilization of counters, queue lengths, and queue waiting times to understand how humans in the loop make decisions and manage resources.

The results could show that introducing humans in the loop results in spontaneous responses to stochastic fluctuation during peak hours, even if this results in deviation from optimal plans.

Conclusion

This study is intended to investigate effective lane allocation asking if a collaborative approach between computational optimization and human expertise is useful. While algorithms excel at meeting quantitative constraints, humans in the loop, e.g., security managers' historical experience contributes essential operational insights, such as time buffer management, and anomaly handling. Future work should focus on developing adaptive systems that combine real-time data with expert knowledge bases, particularly for handling irregular operations and evolving demands. These findings are of significant importance for the design of human-centered decision support systems in the management of critical transportation infrastructure.

Bibliography

[1] Brun, A., Feron, E., Alam, S., and Delahaye, D., *Schedule optimization and staff allocation for Airport security checkpoints using Guided Simulated Annealing and Integer Linear Programming*, Journal of Air Transport Management **124**, 102746, 2025.

12th International Conference on Pedestrian and Evacuation Dynamics (PED 2025)
Prague, Czech Republic – September 9-12, 2025

Passenger Data-Integrated Network Analysis of Tokyo Metro

Xi Lin*[1], Daichi Yanagisawa[1], and Katsuhiro Nishinari[1]

[1]School of Engineering, The University of Tokyo

Abstract This study analyzes the Tokyo Metro network by integrating passenger data with traditional topology-based metrics. Compared to conventional approaches, this method provides a more realistic assessment of station importance by incorporating actual usage patterns. Although Shibuya Station is only one of several key stations based on topological perspective, it emerges as the most critical station when passenger data are considered, with simulated disruptions highlighting its vulnerability.

Keywords Passenger data, Metro network, Centrality analysis, Station resilience.

Metro systems play a vital role in urban mobility, with security and stability as key concerns. Network analysis models metro systems as graphs, with stations as nodes and connections as edges, to assess station importance. Complex Network Theory (CNT) facilitates centrality-based identification of critical stations and has been applied to aviation [1], railway [2], and multimodal transport [3]. However, metro research is limited due to data scarcity, often relying solely on topology while overlooking interactions between network structure and empirical traffic data, such as passenger volume. This study addresses this gap by integrating passenger data (boarding and deboarding volumes) of Tokyo Metro into network topology analysis to assess station importance and evaluate network resilience under disruptions. Considering both distance and passenger data as weights, the analysis incorporates three centralities as follows:

a) Strength degree centrality: Defined as the sum of the weights of all edges connected to a node, representing the overall connectivity intensity of a station within the network. Traditional analysis primarily considers edge weights between stations, but this study incorporates station-level passenger data. To ensure a comprehensive measure, both distance and passenger volumes (boarding and deboarding) are integrated.The strength degree centrality of station i is given by:

$$S(i) = \sum_{j\in\Gamma(i)} w_{ij} = \sum_{j\in\Gamma(i)} \frac{\frac{P_i}{d_i} + \frac{P_j}{d_j}}{2 \cdot \text{distance}(i,j)}, \tag{1}$$

where, w_{ij} is the weight between stations i and j. P_i and P_j are the total passenger volumes of stations i and j. d_i and d_j are the numbers of edges connected to stations i and j. distance(i, j) is the Haversine distance between stations i and j. $\Gamma(i)$ is the set of stations directly connected to station i.

b) Betweenness centrality: Defined as the fraction of shortest paths passing through a node, reflecting network connectivity. Unlike strength degree centrality, it preserves geographical distance in shortest-path calculations instead of weighting edges by passenger volume. A node-weighted adjustment incorporates passenger volume while maintaining spatial constraints for a more accurate representation of key transit hubs. The betweenness centrality of station i is given by:

$$B(i) = \sum_{s\neq t\neq i} (P_s \cdot P_t) \cdot \frac{\sigma_{st}(i)}{\sigma_{st}}, \tag{2}$$

where, σ_{st} represents the number of shortest paths between stations s and t (conducted using distance). $\sigma_{st}(i)$ represents the number of these shortest paths that pass through station i.

c) Closeness centrality: Closeness centrality measures a node's importance by the inverse of its total shortest path distances to all other nodes. Similar to betweenness centrality, after computing the shortest paths, the weighting of passenger data is considered. The closeness centrality of station i is given by:

$$C(i) = \frac{\sum_{j\neq i} P_j}{\sum_{j\neq i} P_j \cdot \text{distance}(i,j)}. \tag{3}$$

Considering the three centrality measures, the importance of a station $I(i)$ can be defined as:

$$I(i) = S^*(i) + B^*(i) + C^*(i), \tag{4}$$

*Email of the corresponding author: lin-xi@g.ecc.u-tokyo.ac.jp

where, $S^*(i)$, $B^*(i)$ and $C^*(i)$ are obtained after normalizing three centralities.

Figure 1 presents the strength degree, betweenness, and closeness centrality results for each station, comparing traditional topology-based measures with the proposed passenger data-integrated approach.

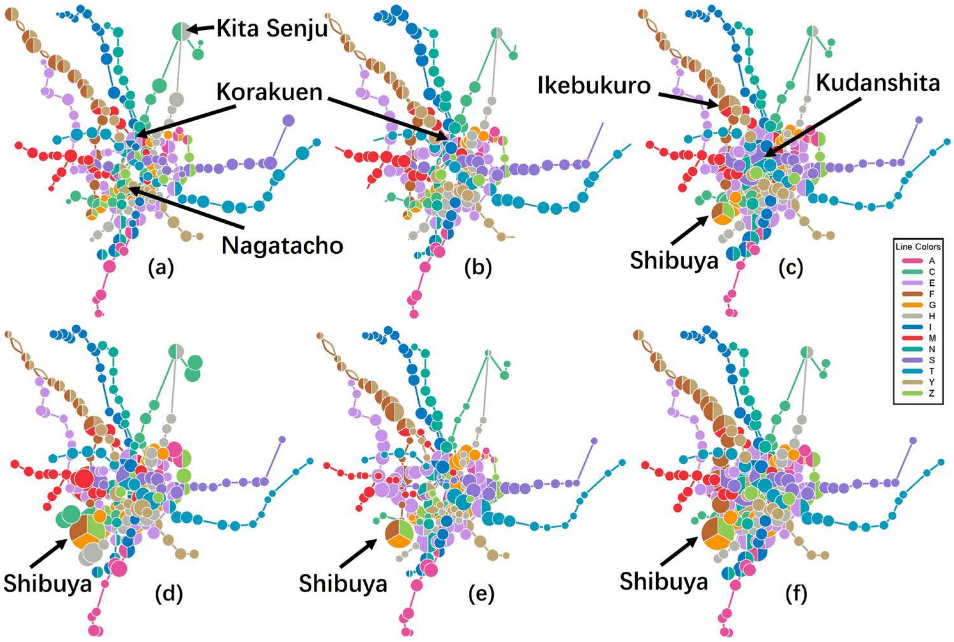

Figure 1: (a-c) Traditional topology-based: Strength, Betweenness, and Closeness centrality. (d-f) Passenger data-integrated: Strength, Betweenness, and Closeness centrality.

Figure 1 shows that traditional topology-based centrality measures highlight stations like Ikebukuro and Korakuen as key nodes due to connectivity and network position. However, integrating passenger data significantly shifts centrality values, emphasizing the impact of passenger volume on network importance. Stations are ranked by $I(i)$, identifying Shibuya Station as the most critical due to its high $I(i)$ and its role as a key hub for the F, Z, and G lines. Resilience is evaluated by simulating line disruptions and analyzing changes in closeness centrality, reflecting accessibility variations. Figure 2 presents the impact of individual disruptions to the F, Z, and G lines.

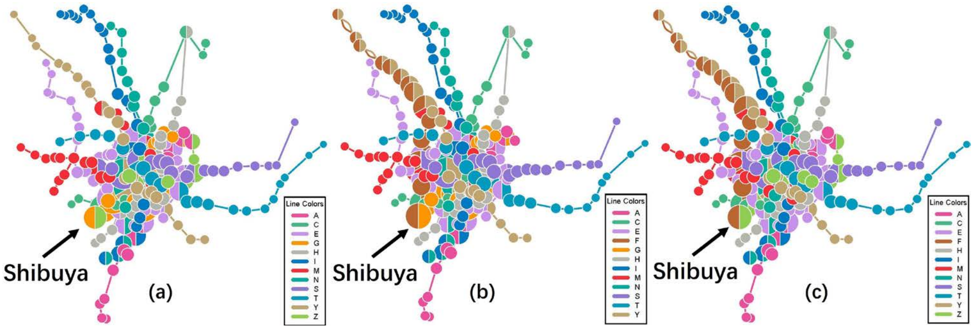

Figure 2: Removal of (a) Line F; (b) Line Z; (c) Line G.

When the F, Z, and G lines are attacked and out of service, the accessibility of Shibuya Station decreases by 37.75%, 27.26%, and 35%, respectively, compared to the fully operational metro network.

Bibliography

[1] Kong, T., *Analysis of China's aviation network and the key node*, Applied and Computational Engineering **5**, 667-677, 2023. DOI: 10.54254/2755-2721/5/20230674.

[2] Liu, S., Wan, Y., Zhang, A., *Does China's high-speed rail development lead to regional disparities? A network perspective*, Transportation Research Part A: Policy and Practice **138**, 299-321, 2020. DOI: 10.1016/j.tra.2020.06.010.

[3] Zhou, Y., Kundu, T., Goh, M., Sheu, J.-B., *Multimodal transportation network centrality analysis for Belt and Road Initiative*, Transportation Research Part E: Logistics and Transportation Review **149**, Article 102292, 2021. DOI: 10.1016/j.tre.2021.102292.

12th International Conference on Pedestrian and Evacuation Dynamics (PED 2025)
Prague, Czech Republic – September 9-12, 2025

Modeling Passenger Selection Behaviour in Vertical Transportation Facilities at Deeply Buried Subway Station

Shanshan He[1], Mohcine Chraibi[2], Juan Chen[3], Qiao Wang[1], and Jian Ma*[1]

[1]School of Transportation and Logistics, Southwest Jiaotong University, Chengdu, 610031, China
[2]Institute for Advanced Simulation, Forschungszentrum Jülich, 52425, Jülich, Germany
[3]Faculty of Geosciences and Engineering, Southwest Jiaotong University, Chengdu 610031, China

Abstract As underground space development intensifies, more subway stations are built at greater depths, making conventional stairs and escalators insufficient for vertical transportation demands. Coordinating the use of stairs, escalators, and elevators can help improve travel efficiency in these deeply buried stations. However, few studies have investigated how passengers choose vertical transportation at such stations' entrances and exits. This paper examines the selection behaviour of outbound passengers, focusing on five key factors: burial depth, passenger flow intensity, number of elevators, elevator egress time (including waiting and travel times), and passenger familiarity with the station. Field investigations were conducted at Hongyancun Station, Liyuchi Station, and Min'an Av. Station in Chongqing, China, collecting data on burial depth, vertical facility configurations, elevator installations, and operation times. Building upon existing field survey data, a specialized questionnaire was developed to investigate passenger selection behaviour for vertical transportation facilities at deeply buried station exits. The questionnaire employed a combined pictorial-textual question format, with strategically distributed decision points across different locations to capture psychological decision-making dynamics of respondent, as shown in Fig.1. Building upon the analysis of selection behaviours, the selection behaviour logistic regression model was established, which is important for optimizing vertical transportation system design and enhancing operational efficiency in deeply buried subway stations.

Keywords Deeply buried subway station, Travel efficiency, Vertical transportation facilities, Selection behaviour modeling, Questionnaire analysis

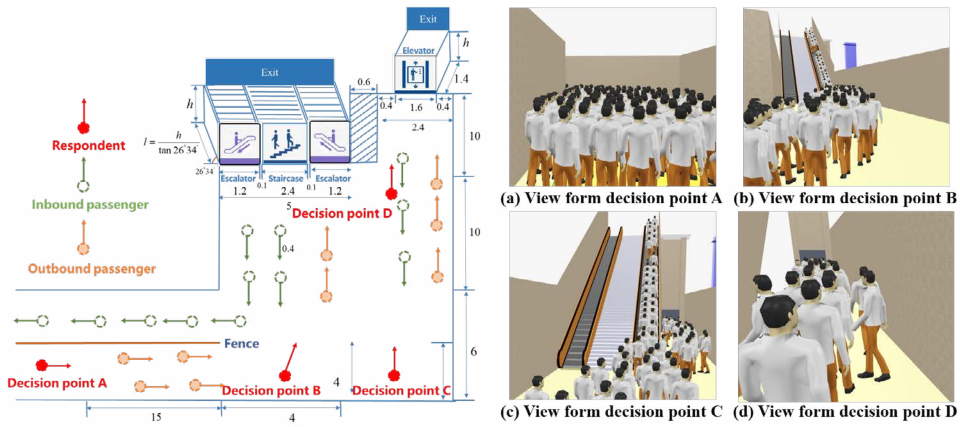

Figure 1: Different decision points in the questionnaire.

*Email of the corresponding author: `majian@swjtu.edu.cn`

12th International Conference on Pedestrian and Evacuation Dynamics (PED 2025)
Prague, Czech Republic – September 9-12, 2025

The Effect of Desired Speed Variability on Pedestrian Dynamics in Social Force-based Simulations of a closed bi-directional Flow Setting

Peter Sukennik*[1] and Tobias Kretz †[1]

[1]PTV Group, Haid-und-Neu-Str. 15, D-76131 Karlsruhe

Abstract When a corridor is used by pedestrians for walking in both directions they form lanes. It has been found in a lab experiment that the stability of the lanes is finite over time and that it depends on the degree of heterogeneity of (free or desired) walking speeds. Here we investigate the topic by means of simulation with closed boundary conditions, i.e. a ring.

Keywords pedestrians, bi-directional, simulation, heterogeneity

Introduction

When two streams of pedestrians of a certain density meet in bi-directional traffic, they spontaneously form lanes. This is probably the most prominent example for the spontaneous emergence of structure and order in pedestrian dynamics. It was observed in a lab experiment [1] that the stability of the lanes depends on the heterogeneity of free walking speeds of the pedestrians. This is plausible: when everyone wants to walk the same speed, then there is no incentive to jump out of an existing lane, once it has been formed, to overtake the slower walking pedestrian ahead. On the contrary, when there are very slow and very fast walkers in the scene, then the fast walkers are tempted to jump out of their current lane. Eventually, they will meet oncoming pedestrians head on and be forced – and forcing the other pedestrian – to slow down. Pedestrians following behind in either direction will close up, evade, and eventually the lanes get destroyed.

1 Methods: Simulation Model

We have replicated the geometry from the lab experiment (a ring with inner radius 2.5 and outer radius 4.5 meters) as well as the number of pedestrians in a simulation model implemented in PTV Viswalk 2025. Additionally, we go far beyond the number of pedestrians who participated in the experiment (a maximum of 210 instead of 60 pedestrians) as well as number of repetitions (100 for each setting) and duration (one hour per run). Desired speeds are distributed stochastically equal around 1.25 m/s, variability ranges from zero to ± 0.9 m/s, i.e. [0.35..2.15]. Here, we present results for zero variability of desired speeds, ± 0.3, ± 0.6, and ± 0.9 m/s. The simulation runs are evaluated by counting the number of pedestrians which conclude a full circle, i.e. flow over a cross section. Time interval for evaluation is always 60 seconds.

2 Results

Since in [1] it is reported that pedestrian traffic dynamics oscillates between ordered (high flow in lanes) and unordered (low flow with collapsed lanes), i.e. that the system can recover from a collapsed state, naturally, the time evolution is of high interest. Figure 1 shows averages of 100 simulation runs. It can be seen that for zero variability and few pedestrians (30 to 50) flow relaxes over time to a high value. For a medium sized number of pedestrians (60 and to a lesser degree 70) flow first grows to decline afterward. For higher densities, the highest flow is measured in the first minute and then it decays to a stable small value. For higher values of desired speed variability it can be seen that the maximum flow is smaller and that the maximum flow is achieved with a higher density. This is summarized in Figure 2 (left) which

*Peter.Sukennik@ptvgroup.com
†Email of the corresponding author: Tobias.Kretz@ptvgroup.com

shows the flow averages of 100 simulation runs for minute 30 – when in Figure 1 flows have stabilized – plotted vs the number of pedestrians, thus the fundamental diagram.

The fact that in Figure 1 flows do stabilize is not self-evident. Alternatively, flow could collapse progressively in various simulation runs over time and then remain collapsed, such that for all settings flow would continue to decline over time. Therefore and with respect to the above mentioned main result from [1] we are interested in the distribution of flows for those times of the simulation where the average values appear to be stable in Figure 1 which is after about 600 seconds. This is shown with a box plot in Figure 2 (right) which summarizes flow measurement from single time intervals and single simulation runs. For zero speed variability and 30 pedestrians the flow is practically identical in all simulation runs, with 50 pedestrians, during some minutes reduced flows compared to the average were found and with 60 pedestrians flow values span from zero to capacity. With a further increasing number of pedestrians the flow value stabilizes progressively to small values. Increasing speed variability the picture changes insofar that the flow varies also for very small as well as for very large numbers of pedestrians.

This result is interesting, because when there is a variation in the flow from various time intervals and simulation runs, while at the same time the simulation averages appear to be near constant then some simulation runs stabilize at high and some at low flow values, or flow oscillates between high and low values. To decide this, one has to look at individual simulation runs. We found (plot will left out due to limited space) that for each variability of desired speeds there is at least one number of pedestrians, where flow oscillates between low and high: for zero variability it is 60 pedestrians, for ±0.3 m/s it is 60 and 70 pedestrians, for ±0.6 m/s it is 90 pedestrians, and for ±0.9 m/s it is 150 pedestrians.

We conclude that on one hand we found a confirmation for the conclusion from [1] that in such situations flow oscillates between high and low. On the other hand, we find that this is only the case for specific combinations of density and variability of desired speeds. A general conclusion is that the setting appears to be promising to produce further insights and deserves further empirical investigation. At the same time one could imagine that it could serve to asses or compare simulation models.

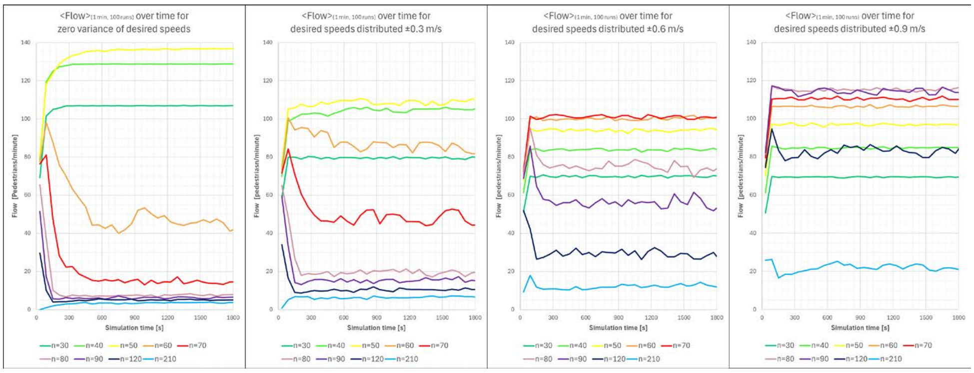

Figure 1: Flow – measured in intervals of one minute – for zero variability of desired speeds (left), and variabilities ±0.3, ±0.6, and ±0.9 m/s (right), averaged over 100 simulation runs each. n gives the number of pedestrians.

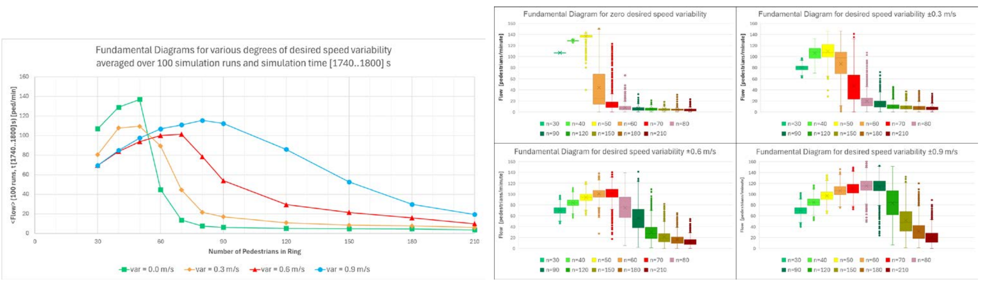

Figure 2: Left: Flow vs. number of pedestrians for speed variabilities 0.0, ±0.3, ±0.6, and ±0.9 m/s as average of 100 simulation runs for time 29:00 .. 30:00 minutes of the simulation. Right: Box plot of all flow values from all simulation runs and all minute intervals later than 600 seconds into the simulation, i.e. each value as an individual count is an integer number, not an average over something.

Bibliography

[1] Moussaïd, M., *Traffic Instabilities in Self-Organized Pedestrian Crowds*, PLoS comp. biol., 8(3), e1002442, 2012.

12th International Conference on Pedestrian and Evacuation Dynamics (PED 2025)
Prague, Czech Republic – September 9-12, 2025

Integrated Analysis of Environmental Qualities and Pedestrian Movement Using Simulations

Stefan Seer*[1], Thomas Matyus[1], and Viktoria Sandor[1]

[1]AIT Austrian Institute of Technology

Abstract Pedestrian simulation models typically focus on interactions with physical objects while neglecting environmental factors like solar radiation, which can significantly influence outdoor movement behavior. This paper introduces a novel framework that integrates environmental qualities, particularly sunlight exposure, into pedestrian movement simulations to support urban design. Using tools such as Rhino/Grasshopper and the Ladybug plugin, solar radiation is evaluated and incorporated into routing algorithms that model pedestrian preferences based on environmental comfort. The results demonstrate enhanced flexibility in modeling movement choices and the ability to assess urban design options in terms of spatial and environmental qualities. This approach facilitates data-driven, collaborative urban planning processes by linking environmental analysis with pedestrian simulation.

Keywords Pedestrian Simulation, Environmental Comfort, Solar Radiation, Urban Design, Movement Behavior Modeling

Extended Abstract

Microscopic simulation models of pedestrian movement have been predominantly focusing on representing interactions of individuals with physical objects such as walls, barriers, and other pedestrians [1]. However, they often neglect critical environmental factors like exposure to sunlight, which can significantly influence human behavior in outdoor spaces. Evidence that these aspects influence outdoor movement behavior has been found in [2] [3]. The importance of incorporating non-physical factors has been highlighted in related work, such as emergency evacuation scenarios that model movement in the presence of smoke or fire. For instance, [4] model behavioral process of individuals perceiving or receiving external cues from their environment such as flames and other hazards. The lack of integration of environmental aspects limits the applicability of these models in urban design processes, where factors like sunlight exposure play a vital role in shaping public space usage.

This paper introduces a novel approach to pedestrian simulation that integrates environmental qualities, particularly solar radiation, into movement behavior modeling. This method aims to facilitate urban design by enabling a more comprehensive assessment of spatial and movement qualities. As such the aim was to develop a simulation framework that enables urban designers to evaluate how pedestrians interact with both physical design choices (e.g., urban furniture, vegetation) and environmental conditions (e.g., sunlight or shading). This integrated approach allows for the assessment and quantification of design choices in terms of spatial and movement qualities, fostering better decision-making in urban planning.

The proposed framework has been demonstrated on a case study focusing on revitalizing the public urban realm and it consists of the following components:

1. **Environmental Analysis:** Using *Rhinoceros 3D* [5] a widely-used 3D modeling software in architecture design, and its native plugin *Grasshopper* [6], geometries of urban environments are generated. Figure 1a shows the base scenario of the case study and Figure 1d the redesign with trees and different urban furniture. In addition, location and time specific solar radiation are calculated with the *Ladybug* [7] plugin (see Figure 1b, c, e and f). The heatmap visually represents areas from low (blue) through medium (yellow) to high (red) levels of solar radiation, indicating the amount of sunlight energy reaching a surface, measured in watts per square meter (W/m²).

2. **Simulation Model Extension:** The grid-based routing algorithm from [8] using the simulation framework from [9], is extended with a heuristic that minimizes the disutility function by considering the effects of the sunlight exposure derived from the environmental analysis. Thus the simulation is

*Email of the corresponding author: stefan.seer@ait.ac.at

enabled to reflect seasonal differences, such as seeking shade in summer or sun exposure in winter as shown in Figure 1b and 1c. The operational model is calibrated according to [9], though empirical validation of the extended routing algorithm remains an area for future research.

3. **Integrated Quantitative Analysis:** Simulated pedestrian trajectories, densities, and other movement characteristics are combined with environmental comfort data, enabling a holistic evaluation of urban designs (see Figure 1e and 1f). The workflow also connects to visualization platforms, e.g. Unreal Engine, to render realistic environments, highlighting atmospheric qualities like sunlight, which in this study had an effect on the simulated pedestrian trajectories and movement patterns.

The integration of environmental factors into pedestrian simulations provides greater flexibility in modeling movement choices and preferences. By manipulating routing weights based on solar radiation, the approach is also able to represent adapted behaviors induced through 'soft' interventions where changes in behavior are influenced subtly rather than rigidly. In future, this extended modeling approach could improve pedestrian decision making where movement is overly restricted. For instance, a common approach to modeling pedestrian dynamics on sidewalks is the use of virtual walls along sidewalk edges, ensuring that pedestrians do not step off the designated path, even in collision-avoidance situations.

This method enables the assessment and quantification of urban design choices with respect to both spatial and movement qualities, supporting iterative, data-driven design processes. Furthermore, the approach was tested in co-creation workshops, demonstrating its applicability in collaborative urban design settings. The approach offers a valuable tool for urban designers, enabling them to evaluate and optimize design choices with respect to both environmental comfort and pedestrian behavior. Future research will focus on the empirical validation of the model and exploring additional environmental factors beyond solar radiation.

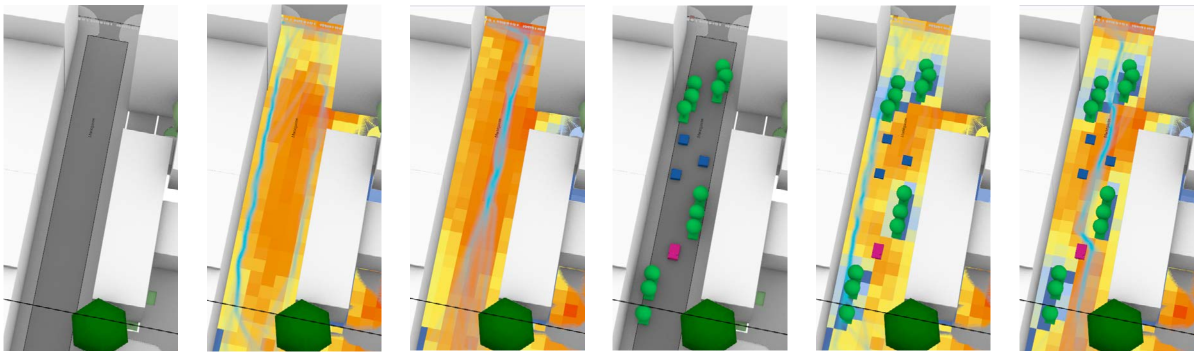

(a) (b) (c) (d) (e) (f)

Figure 1: Integrated analysis of pedestrian movement based on (a) geometries of the base scenario, (b) solar radiation in summer, (c) solar radiation in winter, (d) geometries of the design scenario including trees (green) and other urban furniture (magenta and blue), (e) solar radiation in summer, and (f) solar radiation in winter.

Bibliography

[1] Duives, D., Daamen, W., Hoogendoorn, S.P., *State-of-the-art crowd motion simulation models*, Transportation Research Part C: Emerging Technologies, **37**, 193-209, 2013.

[2] Huang, Kuo-Tsang and Lin, Tzu-Ping and Lien, Hsiao-Chi, *Investigating Thermal Comfort and User Behaviors in Outdoor Spaces: A Seasonal and Spatial Perspective*, Advances in Meteorology, **1**, 2015.

[3] Kim, S.W., Brown, R.D., *Pedestrians' behavior based on outdoor thermal comfort and micro-scale thermal environments, Austin, TX*, Science of The Total Environment, *808*, 2022.

[4] Kuligowski, E. *Modeling Human Behavior during Building Fires*, Technical Note (NIST TN), National Institute of Standards and Technology, Gaithersburg, MD, 2008.

[5] Rhinoceros 3D from https://www.rhino3d.com accessed January 24, 2025.

[6] Grasshopper from https://www.grasshopper3d.com/ accessed January 24, 2025.

[7] Ladybug from https://www.ladybug.tools/ accessed January 24, 2025.

[8] Stubenschrott, M., Matyus, T., Schrom-Feiertag, H., Kogler, C., Seer, S., *Route-choice modeling for pedestrian evacuation based on infrastructure knowledge and personal preferences*, Transportation Research Record, **2623**, (1), 82-89, 2017.

[9] Seer, S., *A unified framework for evaluating microscopic pedestrian simulation models*, Dissertation, 2015.

12th International Conference on Pedestrian and Evacuation Dynamics (PED 2025)
Prague, Czech Republic – September 9-12, 2025

Wheelchair pedestrians' road-crossing behavior - A Virtual Reality Study

Yan Feng*[1] and Zhenlin Xu[1]

[1]Department of Transport Planning, Delft University of Technology

Abstract This study utilizes Virtual Reality to investigate wheelchair pedestrian road crossing behavior in urban traffic. Using a developed VR wheelchair simulator, a VR experiment was conducted with 32 participants where we collected both subjective data and objective data. Specifically, we aim to understand the impact of (1) traffic user behavior and (2) traffic flow (i.e., cyclist and vehicle) on wheelchair pedestrian road crossing behavior regarding crossing decision, crossing performance, and road attention. This extended abstract details the VR experiment.

Keywords Wheelchair pedestrian, Road crossing, Virtual Reality, Road safety

Introduction

Pedestrians with reduced mobility (PRM) are particularly vulnerable when it comes to road safety. Research on PRM's interactions with other road users is still lacking [1, 2]. Understanding PRM's road crossing behavior is crucial for designing accessible, inclusive, and safe mobility systems. However, little attention has been paid to PRM and existing studies often focus on qualitative insights through interviews and focus groups. Virtual Reality (VR) provides opportunities to study PRM road crossing behavior by immersing PRM in virtual road scenarios with high experimental control and without exposing them to real risk [3]. In our previous study, we developed a high-fidelity and low-cost VR wheelchair simulator to investigate wheelchair pedestrians' interaction with other road users in diverse traffic scenarios. Utilizing this VR wheelchair simulator, we conducted a VR experiment to investigate wheelchair pedestrians' interaction with other road users in diverse traffic scenarios. During the experiment, we collected subjective data (e.g., wheelchair pedestrians' movement trajectories and gaze points) and objective data (e.g., perceived safety and risk). This allows us to closely examine how wheelchair pedestrians navigate in traffic scenarios for their movement dynamics, decision-making process, stress level, and physical exertion.

Methodology

The VR experiment aims to examine how wheelchair pedestrians cross urban traffic and the impact of traffic flow and road user behavior on their road crossing behavior. This section details the experiment design, experiment procedure, apparatus and data collection.

Experiment scenario design. The VR scenario was designed based on the same urban road setup used for the field observation in [4]. It features a two-lane roadway that is 16 meters wide with a separate cyclist path along the side. Additionally, curbs are present to separate the motorized lane from the cyclist's path. Figure 1 shows the virtual and real-life road scenarios. In our previous study [4], we conducted semi-structured interviews and field observations with wheelchair users to identify the key factors influencing their road crossing safety. From the six factors we identified, we selected two for further investigation in the current study: (1) traffic flow and (2) rule-breaking behavior of other road users. Regarding traffic flow, we examined both bike and vehicle flow, each with two levels: high and low traffic flow. Similarly, for rule-breaking behavior, we considered the actions of cyclists and drivers, specifically whether they yield or fail to yield at traffic lights. Additionally, we incorporated a baseline scenario that mirrors real-life traffic conditions. The VR experiment consisted of a total of eight scenarios. To control for individual differences, a within-subject design was employed in this study. Participants were requested to cross the road from one side to another side. Each participant experiences all experimental scenarios in a random order.

*Email of the corresponding author: y.feng@tudelft.nl

Figure 1: Illustration of VR (left) and real-life road crossing scenario(right).

Experiment apparatus. The VR experiment used the previously developed VR wheelchair simulator, which includes an HTC VIVE Pro Eye headset (resolution: 1440 × 1600 pixels per eye, 110° field of view, 90Hz refresh rate) and HTC VIVE 2.0 Trackers. Participants experienced a first-person view of the virtual environment through the headset and controlled their movement using the wheelchair's wheel. Custom 3D-printed mounting parts were designed to attach the trackers to the wheelchair. Participants had 360-degree freedom of movement in the real world with the VR wheelchair, and their movements were synchronized in the virtual environment.Figure 2 shows a participant wearing the VR headset and sitting in a wheelchair.

Figure 2: A participant using the VR wheelchair simulator

Experiment procedure. The experimental procedure consisted of four main stages: (1) Introduction, where participants were informed about the purpose of the study and provided their consent; (2) Familiarization with the VR Wheelchair System, during which participants were instructed on how to use the VR headset and wheelchair simulator, ensuring they could operate the system comfortably before the official experiment; (3) Official experiment, where participants performed the experimental task described above; and (4) Completion of the post-questionnaire, in which participants provided answers on simulator sickness, feelings of presence, perceived risk and safety, as well as feedback of their experience during the experiment.

Data collection. Two types of data were collected during the experiment: objective data (e.g., movement trajectory, gaze point) and subjective data (e.g., Simulator Sickness Questionnaire, Perceived behavioral control and risk questionnaire, Presence Questionnaire). These data allow us to have a detailed analysis of wheelchair users' movement dynamics, decision-making process, and stress level regarding their road crossing behavior and interaction with other road users. At PED, we will present the results of the analysis and findings.

Bibliography

[1] Schwartz, N., Buliung, R., Daniel, A., & Rothman, L. *Disability and pedestrian road traffic injury: A scoping review*, Health & Place, **77**, 102896, 2022.

[2] Pecchini, D., Giuliani, F., *Street-crossing behavior of people with disabilities*, Journal of Transportation Engineering **141(10)**, 04015022, 2015.

[3] Feng, Y., Duives, D., Daamen, W., Hoogendoorn, S., *Data collection methods for studying pedestrian behaviour: A systematic review*, Building and Environment **187**, 107329, 2021.

[4] Kwakernaak, N., Boess, S., Hiemstra-van Mastrigt, S., Feng, Y., *Understanding wheelchair pedestrians' road crossing behaviour and traffic safety needs in the Netherlands*, **International Co-operation on Theories and Concepts in Traffic Safety**, 2024.

12th International Conference on Pedestrian and Evacuation Dynamics (PED 2025)
Prague, Czech Republic – September 9-12, 2025

Beyond Landmarks: Investigating Cognitive Maps in Crowds

Ezel Üsten*[1]

[1]Institute for Advanced Simulation (IAS-7), Forschungszentrum Jülich

Abstract Cognitive maps have traditionally been studied in static environments with fixed landmarks, yet little is known about how humans spatially represent dynamic elements such as crowds. Individuals appear to maintain a sense of position and movement within crowds, either by mapping their immediate surroundings or forming broader representations of group structures. This research examines cognitive mapping in dynamic social contexts, integrating perspectives from spatial cognition, social psychology, and visual perception to explore how people perceive and navigate crowds.

Keywords Cognitive maps, Entitativity, Eye-tracking, Spatial perception

Introduction

Cognitive maps—our mental representations of the physical environments around us [1]—have been extensively researched. However, nearly all studies on cognitive maps, whether focused on navigation, memory, recall, or problem-solving, have examined only static environments, such as city-wide layouts , predetermined locations, and buildings [2, 3]. These environments typically feature landmarks (e.g., Big Ben, a school, a kiosk, a specific room), to which individuals could attribute social meaning [4]. These landmarks help individuals form mental representations, serving as fixed anchors or reference markers that enable them to estimate distances and plan routes with relative accuracy. When dynamic elements, such as other people, were included in research, they were usually treated as interference that disrupted the cognitive mapping process [5].

The aim of this contribution is to report preliminary results and discuss future studies on the extent to which humans can spatially represent dynamic elements—namely, crowds and groups gathering at a specific location—in their minds as a 'mental map.' To ground this idea, two perspectives must be discussed, and several research methods need to be considered. The first perspective, an *inside* perspective, examines whether individuals can mentally project the crowd they are part of. This corresponds to experiencing a crowd from within, such as attending a concert. The second perspective takes an *outside* view, focusing on how people perceive crowds and groups from an external standpoint. This relates to navigating through or observing a crowded environment from a distance, where different groups or crowds are within visual perception but without directly participating in them. Both perspectives involve a dynamic setting where individuals in groups and crowds behave naturally within their given context, rather than remaining static.

Regarding the *inside* perspective, a key question is how individuals perceive their position within a crowd despite the challenges of a dynamic environment. Unlike static settings, crowds lack stable landmarks, are constantly shifting, and present limited visibility—both due to the forward-facing nature of human vision (unlike birds, which have lateral vision) and obstructions caused by nearby individuals. Despite these limitations, people appear to have a sense of their relative position and movement within a crowd, either by loosely mapping their immediate surroundings or forming a broader representation of the entire crowd, using various sensory inputs such as vision and auditory cues. Preliminary results suggest that individuals can recall the position and shape of a crowd from a bird's-eye perspective after being part of a crowd formation (of up to 15 people) when asked about a specific moment in time. Figure 1 shows a drawing by one of the participants, illustrating a specific moment from their formation. Notably, participants received no explicit instructions regarding the perspective they should adopt, how to incorporate environmental cues, or the shape in which they should represent people.

The *outside* perspective—observing a crowded environment from a distance—incorporates the long-standing social psychology concept of entitativity, which addresses whether a group or crowd is perceived as a cohesive unit. From this viewpoint, people seem able to recognize and interpret the social context of a group accurately [6] from an outside point of view, potentially projecting and representing it within a

*Email of the corresponding author: e.uesten@fz-juelich.de

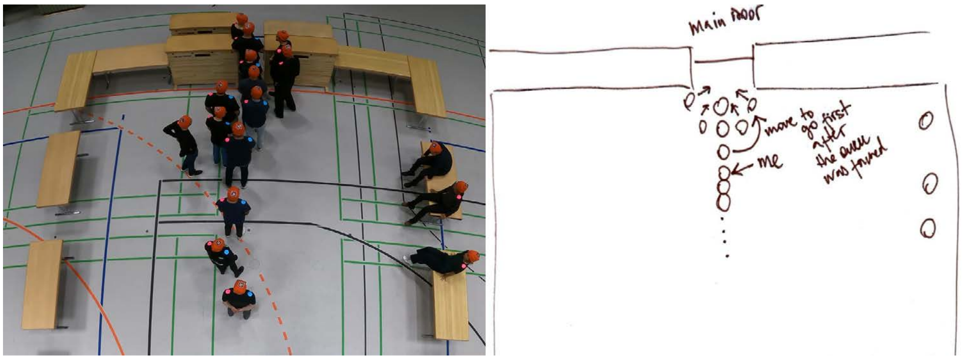

Figure 1: An exemplary representation of a crowd formation.

spatial framework in their minds, as the group's occupation of space is one of its defining characteristics. However, whether this mental representation is driven primarily by the group's social meaning, its physical presence in space, or a combination of multiple factors remains unexplored. While existing literature suggests that group characteristics significantly influence entitativity perceptions [6], the specific role of spatial occupation itself has not yet been investigated.

To study both perspectives, visual perception—particularly gaze patterns—can provide insight into how people perceive groups. Investigating fixation points may help determine whether individuals focus on socially significant elements (e.g., a tour guide in a tour group) or whether their gaze moves across the entire crowd, scanning its borders, peripheries, or other focal points—not only for spatial awareness and group cohesiveness but also potentially for navigation. Integrating this knowledge with research on spatial mapping could offer a more detailed understanding of how cognitive maps of groups and crowds function. Additionally, sound perception (the sound of the crowd or the broader soundscape) also plays a role, particularly from the *inside* perspective, where individuals must rely on occasional visual checks and auditory cues to stay aware of people behind them.

To investigate and explore the assumptions outlined above, a comprehensive study of the phenomenon is required. For this purpose, a field study is being planned at Kirchentag, one of Germany's largest events—a Protestant church gathering held in Hannover, which attracts approximately 100,000 people from around the world. In this study, a predetermined route will be used to navigate streets with crowds to examine the 'outside' perspective. Additionally, an event venue and the crowd in front of the participants will serve as the setting for investigating the 'inside' perspective, as participants will be instructed to remain within this crowd. Eye-tracking data, first-person videos, and audio recordings will be collected using NEON eye-trackers [7]. Participants will also complete questionnaires and self-drawn representations to assess their cognitive representations of the environment and their perception of group cohesiveness when encountering crowds or being part of one.

Investigating these aspects and examining how they perform in real-world contexts would broaden our understanding and hold significant relevance for various topics within pedestrian dynamics. In particular, spatial representation plays a crucial role in how individuals choose routes and make decisions within a social environment, making it a key factor in navigation. Fields such as robotics are already trying to integrate insights from cognitive mapping into their research [8]. Additionally, this research could contribute to a better understanding of the limits of mental representations, as it uniquely focuses on dynamic elements rather than static ones.

Bibliography

[1] Whittington, J. C. R., McCaffary, D., Bakermans, J. J. W., et al., *How to build a cognitive map*, Nature Neuroscience **25**, 1257–1272, 2022.

[2] Maguire, E. A., Frackowiak, R. S., Frith, C. D., *Recalling routes around London: activation of the right hippocampus in taxi drivers*, Journal of Neuroscience **17**(18), 7103-7110, 1997.

[3] Andresen, E., Chraibi, M., Seyfried, A., *A representation of partial spatial knowledge: a cognitive map approach for evacuation simulations*, Transportmetrica A: Transport Science **14**(5-6), 433-467, 2018.

[4] Couclelis, H., Golledge, R. G., Gale, N., Tobler, W., *Exploring the anchor-point hypothesis of spatial cognition*, Journal of Environmental Psychology **7**(2), 99-122, 1987.

[5] Merriman, N. A., Ondřej, J., Rybicki, A., Roudaia, E., O'Sullivan, C., Newell, F. N., *Crowded environments reduce spatial memory in older but not younger adults*, Psychological Research **82**(2), 407-428, 2018.

[6] Lickel, B., Hamilton, D. L., Wieczorkowska, G., Lewis, A., Sherman, S. J., Uhles, A. N., *Varieties of groups and the perception of group entitativity*, Journal of Personality and Social Psychology **78**(2), 223, 2000.

[7] Baumann, C., Dierkes, K., *Neon Accuracy Test Report*, Pupil Labs, 2023.

[8] Fan, T., Wang, D., Liu, W., Pan, J., *Crowd-driven mapping, localization and planning*, in *Experimental Robotics: The 17th International Symposium*, Springer International Publishing, pp. 354-368, 2021.

12th International Conference on Pedestrian and Evacuation Dynamics (PED 2025)
Prague, Czech Republic – September 9-12, 2025

User Preference-Based Parallel Coordinate Plots: Its Application in Guidance Planning

Chisa Mori*[1,3], Shuhei Watanabe[2,3], Masaki Onishi[3], and Takayuki Itoh[1]

[1]Ochanomizu University
[2]Preferred Networks, Inc.
[3]National Institute of Advanced Industrial Science and Technology

Abstract Parallel coordinate plots (PCPs) are a prevalent method to interpret the relationship between control parameters and a metric of simulations. PCPs deliver such interpretation by the color gradation based on a single metric, but it is challenging to provide such gradation given multiple metrics in each simulation. To this end, this paper proposes a novel mathematical approach to compute the color gradation for bi-metric problems and demonstrates its effectiveness through a real-world application of pedestrian flow guidance planning.

Keywords Visualization, High-Dimensional Data Visualization, Parallel Coordinate Plots, Real-World Application, Pedestrian Flow Simulation

1 Introduction

Simulation plays a crucial role in pedestrian flow guidance planning assessments as large-scale real-world experiments are often infeasible. As pedestrian flow simulations involve several control parameters that determine performance metrics of a simulation, a comprehensive understanding of their relationship is essential for effective pedestrian flow guidance planning. Parallel coordinate plots (PCPs) [1] are widely employed to interpret such relationships. Although PCPs can highlight key control parameters and patterns by color gradation based on a metric, it is not obvious to determine appropriate color gradation for simulations with multiple metrics. To address this problem, we propose a principled approach to theoretically calculate color gradation in PCPs based on a user preference chosen from the Pareto front yielded via the control parameter optimization. In this paper, we provide the coloring algorithm and demonstrate that it elucidates some patterns of control parameters that lead to desirable results in simulations.

2 Parallel Coordinate Plots for Bi-Metric Problems

In this paper, we consider a pedestrian flow simulation controlled by D-dimensional parameters $\lambda \in \mathbb{R}^D$ with two metrics $f := [f_1, f_2]$ to be minimized. Due to the space limit, we defer the definitions of Pareto solutions and Pareto front to [2]. An experiment performs simulations multiple times each with a different control parameter set λ_n that yields the corresponding two metrics f_n, leading to the scatter plot in Figure 1 (**Left**). Since there are two metrics, we need to consider the trade-off between them and think of how to encode such trade-off into a single metric to color PCPs. To this end, we first approximate the Pareto front by fitting the coefficients a, b of the function $g(f_1) := f_2 = \frac{a}{f_1+b}$ using the least squares method. The fitting is performed using the Pareto solutions $\mathscr{P} \subseteq \{f_n\}_{n=1}^N$ obtained during an experiment where $N \in \mathbb{Z}_+$ is the number of performed simulations in an experiment. Since there are infinitely many trade-off choices on the Pareto front, the selection highly depends on the user's preference. Therefore, we let users choose a point $f^c := [f_1^c, g(f_1^c)] = [f_1^c, f_2^c]$ on the approximated curve, e.g., see the red dot in Figure 1 (**Left**), and consider encoding this preference into a weighted metric $E := w_1 f_1 + w_2 f_2$ where $w_1 + w_2 = 1$.

Now, we present how to compute the optimal weight pair. Assume that the true Pareto front is convex, there actually exists an optimal weight pair $[w_1^\star, w_2^\star]$ such that the weighted metric E attains its minima (optima) at the selected point f^c. More specifically, suppose metrics are normalized to $[0,1]$ and $E_{w_1} := \{w_1 f_1 + (1 - w_1) f_2 | f_1 \in [0,1], f_2 \in [g(f_1), 1]\}$ is a set of possible weighted metric values, we would like to calculate $w_1^\star$ such that $f_1^c = \mathrm{argmin}_{f_1 \in [0,1]} E_{w_1^\star}$. As $E = w_1 f_1 + w_2 f_2$ can be transformed as $f_2 = -\frac{w_1}{w_2} f_1 + \frac{E}{w_2}$ with $w_2 \neq 0$, we can regard $\frac{E}{w_2}$ as the intercept in the scatter plot, e.g., see Figure 1 (**Left**), and this can be rephrased as a problem that involves considering the intercepts of a line. Since $g(f_1)$ is a convex function and there exist lines of the form

*Email of the corresponding author: g2020539@is.ocha.ac.jp

Timetable
Poster index

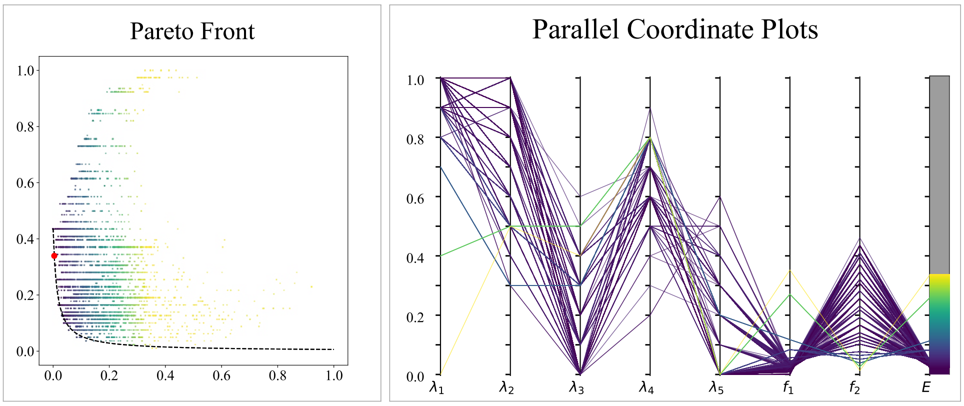

Figure 1: Visualization results using the proposed method. Scatter plot of metric values obtained in our experiment (**Left**): The black dashed line represents the approximate Pareto solution curve. The color gradation of each dot indicates the weighted metric value E ranging from yellow (worse) to purple (better) and it is calculated by assuming that the user selects the red dot as its preference. PCP with the color gradation calculated by the selected user preference (**Right**): The plots highlight patterns in control parameters that lead to desirable simulation results.

$f_2 = h(f_1) := cf_1 + d$ such that $g(f_1) \geq h(f_1)$ for $f_1 \in [0,1]$. In particular, when the weight pair is fixed, i.e. to fix the slope c to $-w_1/w_2$, the minimum possible intercept is attained when the line is tangent to $f_2 \geq g(f_1)$. To achieve $f_1^c = \mathrm{argmin}_{f_1 \in [0,1]} E_{w_1^\star}$, f^c must be on the tangential line, ensuring $f_2^c = cf_1^c + d = g'(f_1^c)f_1^c + d = -\frac{w_1^\star}{w_2^\star} f_1^c + d$. Note that the tangential line has only one tangent point, which is at f^c, with $f_2 \geq g(f_1)$ ($f_1 \in [0,1]$). Therefore, the optimal weight pair $[w_1^\star, w_2^\star]$ can be obtained by solving $g'(f_1^c) = -\frac{w_1^\star}{w_2^\star}$ and $w_1^\star + w_2^\star = 1$. Then, the weighted metric E for each observation is computed using the calculated weight pair, resulting in the colored PCP shown in Figure 1 (**Right**).

3 Application to Pedestrian Flow Guidance Simulation Data

In this section, we present an application example of our proposed method to simulation data collected by Crowd-Walk [3] that simulates an evacuation from a station to a designated evacuation site. Each simulation has the following five parameters normalized in $[0,1]$: the time interval λ_1 of the start of evacuation between two pedestrian groups, the guidance ratios to the less congested route at two different branches λ_2, λ_3, and the guidance ratios to the underground λ_4, λ_5. Each simulation was evaluated with two metrics: The first metric f_1 represents the degree of congestion and the second metric f_2 represents the total evacuation time. Both f_1 and f_2 were normalized to the range $[0,1]$ for visualization purposes, so E falls within $[0,1]$.

Figure 1 (**Left**) visualizes a scatter plot of the metric values obtained in our experiment and the black dotted line is the approximated Pareto front. Based on the figure, users select a point f^c, such as the red dot in Figure 1 (**Left**), to calculate the optimal weight pair $[w_1^\star, w_2^\star]$. Once the point is selected, the scatter plot is colorized accordingly and PCPs in Figure 1 (**Right**) is rendered. In our PCP example, we only used the Pareto solutions and simulation results with $E \in [0, 0.05]$. Each PCP line was colored such that yellow represents the worse weighted metric E and purple represents the better weighted metric. Figure 1 (**Right**) shows the PCPs when less congestion f_1 was observed, which can be obtained by selecting the red dot in Figure 1 (**Left**). When taking a closer look at λ_1 of our PCPs, purple lines are concentrated at high values (around 0.9 and 1.0). This indicates that delaying the evacuation start time and ensuring sufficient capacity in the flow networks are effective strategies for reducing congestion. Due to the space limit, we omit any further analysis, but similar analyses are possible for various different trade-offs. A key advantage of our method is that it enables direct comparisons between different trade-offs side-by-side by generating PCPs based on varying user preferences.

References

[1] J. Heinrich and D. Weiskopf. State of the art of parallel coordinates. *Eurographics*, 2013.

[2] S. Watanabe. Python tool for visualizing variability of pareto fronts over multiple runs. *arXiv:2305.08852*, 2023.

[3] T. Yamashita, T. Okada, and I. Noda. Implementation of simulation environment for exhaustive analysis of huge-scale pedestrian flow. *Journal of Control, Measurement, and System Integration*, 6, 2013.

12th International Conference on Pedestrian and Evacuation Dynamics (PED 2025)
Prague, Czech Republic September 9-12, 2025

Cross-cultural comparison of wayfinding behavior in a multi-level building between The Netherlands and China - A Virtual Reality Study

Chenyi Yang[1], Yan Feng*[2], and Dewei Li[1]

[1]Department of Traffic and Transportation, Beijing Jiaotong University, Beijing, China
[2]Department of Transport & Planning, Delft University of Technology, y.feng@tudelft.nl

Abstract VR technology is widely used in pedestrian wayfinding behavior studies, yet most focus on a single cultural background. Culture impacts wayfinding behavior, but cross-cultural influence remains insufficiently explored.Based on an previous pedestrian wayfinding experiment conducted in the Netherlands, this paper compares cross-cultural pedestrian wayfinding behaviors between Netherlands and China. By analyzing the wayfinding behaviors, observation behaviors, wayfinding performance, and user experiences, it was found that there are significant differences in some aspects such as wayfinding and observation behaviors.

Keywords Virtual reality, Pedestrian wayfinding, Cross-cultural, Evacuation, Route and exit choice

Instruction

Virtual Reality (VR) technology is being widely used in the study of pedestrian wayfinding behavior. Currently, existing studies that applied VR for pedestrian wayfinding behavior often focus on a single cultural background. Research has shown that culture plays a important role in pedestrian wayfinding behavior. For example, cultural backgrounds significantly affect the firefighters' wayfinding performance [1]. Cultural context significantly impacts pedestrian behavior during various crossing phases [2]. However, the influence of cultural background on pedestrian wayfinding behavior remains insufficiently explored, particularly in pedestrian wayfinding behavior across different cultural backgrounds.

Previously, a pedestrian wayfinding behavior study was conducted in the Netherlands [3], in which the authors developed a VR tool called WayR, designed a VR experiment, and evaluated the validity and usability of WayR using objective and subjective indicators. Based on this study, this paper uses HMD VR technology and the WayR software adopted in the previous study to investigate the wayfinding and evacuation behaviors of pedestrians in China, as shown in Figure 1. Participants are required to complete the exact wayfinding tasks, including three wayfinding tasks and one evacuation task, and then fill out a user experience questionnaire upon completion. By analyzing the differences in wayfinding behaviors and user experiences between the studies conducted in The Netherlands and in China, this paper aim to compare pedestrians wayfinding behaviors across different cultural backgrounds.

A total of 40 participants took part in this study in China. We collected data on pedestrians movement trajectories and gaze points through the VR system and recorded user experience data via questionnaires. This enabled a detailed analysis and comparison of route and exit choice behavior, observation behavior, wayfinding task performance, and user experiences between the two cultural backgrounds. The research results found significant differences between the participants in the Netherlands and China, such as path choice ($p < 0.001$), use of decision points ($p = 0.011$), and stair selection ($p = 0.003$), while the differences were not significant in the evacuation tasks. Moreover, Chinese pedestrians had a larger head rotation angle and higher variances during the experiment. The average head rotation of China group is 18.33°/s, while Netherlands is 14.79°/s.

During PED conference, we will present a more comprehensive and in-depth comparison, covering pedestrians wayfinding behaviors, observation behaviors, wayfinding performance, and user experience.

*Email of the corresponding author: Y.Feng@tudelft.nl

Bibliography

[1] Jieyu Chen, Nan Li, Yangming Shi, Jing Du, *Cross-cultural assessment of the effect of spatial information on firefighters wayfinding performance: A virtual reality-based study*, International Journal of Disaster Risk Reduction **84**, 103486, 2023.

[2] Leidy Marcela Barón Acela, Emanuel Sousa, Susana Faria, Raul Almeida, Elisabete Fraga Freitas, *Pedestrian crossing behavior in social groups: Exploring cultural contexts through a comparative study*, Case Studies on Transport Policy **19**, 101333, 2025.

[3] Feng, Y., Duives, D. C., Hoogendoorn, S. P., *Development and evaluation of a VR research tool to study wayfinding behaviour in a multi-story building*, Safety Science **147**, 105573, 2022.

Figure 1: One participant was using the HMD display and hand controller during the VR experiment.

12th International Conference on Pedestrian and Evacuation Dynamics (PED 2025)
Prague, Czech Republic – September 9-12, 2025

Insights from Pedestrian Tracking Data for Railway Safety

Ernst Bosina*[1] and Stephanie Baumann[1]

[1]SBB AG

Abstract This study investigates the use of the danger zone adjacent to the platform edge, which is a critical part of pedestrian safety in railway stations. Through the analysis of tracking data from multiple stations across Switzerland, we examine the influence of platform design, pedestrian demand, and train presence. Our findings indicate correlations between the use of the danger zone and different influences, which help to identify and mitigate safety critical situations in the future.

Keywords railway platform, danger zone, safety, pedestrian tracking, real-life observation

Introduction

In light of the increasing passenger demand and the limitations of existing railway stations, of which many were designed and constructed several decades ago, safety considerations on platforms have become increasingly important. A key safety concern from a passenger flow perspective is the utilization of the danger zone, defined as the area between the safety line and the edge of the platform. In this area, whose width depends on the speed of passing trains [1], dangerous situations due to train movements are possible. Previous studies have indicated that the likelihood of pedestrians stepping into the danger zone is influenced by pedestrian density and platform width [2, 3]. Notably, Thurau and Keusen [3] demonstrated that the use of the danger zone is greater in areas where the safety zone width is less than two meters. In addition to a linear correlation between density and the number of people stepping into the danger zone, Thurau et al. [2] also found an exponential correlation between them, particularly in areas characterized by narrow safety zones or high circulation. It was also concluded that other factors are likely to influence the use of the danger zone.

However, the datasets utilized in these studies were restricted to one respectively two measurement areas with data for about one month. Meanwhile, data from new measurement areas is available that can be used to compare different platform layouts and similar situations at different stations and for longer time intervals. The goal of this study is to get more detailed insights into the previously observed influences and to include further parameters, such as the presence of trains.

Method

The study employs anonymous tracking data from five distinct railway platforms across Switzerland, yielding positional accuracy within a few centimeters. This precision allows for accurate identification of pedestrian movement within the danger zone. As the data reflects the head position and entering the danger zone is defined by the foot position, an offset of 10 cm was added to take this difference into account. Additionally, the presence of trains is detected for each adjacent track, categorizing periods into scenarios with no trains, one train, or two trains present. Times with two trains present were removed from the data, as entering the danger zone is safe when a train is stationary. For times with one train, only the opposite danger zone was analyzed.

For each measurement area we created a geometry, which displays each danger and safety zone for the whole measurement area as well as for 21 subareas with a narrow safety zone. For each of these areas, the average length, speed and duration and the number of overstepping events is calculated, utilizing data spanning 6 to 18 months. As this data is intended to observe trends in the overstepping behaviour, a temporal resolution of one hour is used. This limits the direct correlation between the current pedestrian density and the overstepping behaviour, but this time resolution allows to compare longer time periods.

*Email of the corresponding author: `ernst.bosina@sbb.ch`

Results and Discussion

On average, individuals within the danger zone traverse 5.26 m in 6.2 seconds, yielding an average walking speed of 0.85 m/s. This indicates that walking in the danger zone primarily occurs as pedestrians attempt to pass one or more individuals. The availability of data from different situations enables the examination of various parameters influencing danger zone utilization. Initial comparisons between periods with no trains and those with one train present reveal that the proportion of time spent in the danger zone is higher during train-free intervals, accompanied by lower walking speeds. In most areas, the distance traveled is marginally shorter, resulting in similar durations spent in the danger zone. These findings can be partially explained as in situations with one train present, only the opposing danger zone is considered and the share of boarding and alighting people differs between these two situations.

Analysis of pedestrian demand reveals varying behaviors across locations. Similar to previous studies, some sites exhibit an increase in the proportion of pedestrians entering the danger zone with rising pedestrian volumes, while others do not display this trend. The relationship between demand and danger zone utilization also varies based on train presence, suggesting distinct pedestrian behaviors or differing platform load capacities.

In the 21 subareas characterized by narrow safety zones, the data does not reveal a clear distinction across varying train scenarios. Additionally, the impact of pedestrian volume is inconsistent. With the exception of Zürich Hardbrücke, where a slight increase in danger zone utilization is observed, most narrow areas show no correlation or a negative relationship. This may be attributed to high volumes of waiting pedestrians, resulting in a lower fraction actively walking compared to wider areas. In Zürich Hardbrücke, the short train headways may contribute to the observed deviation from the other locations.

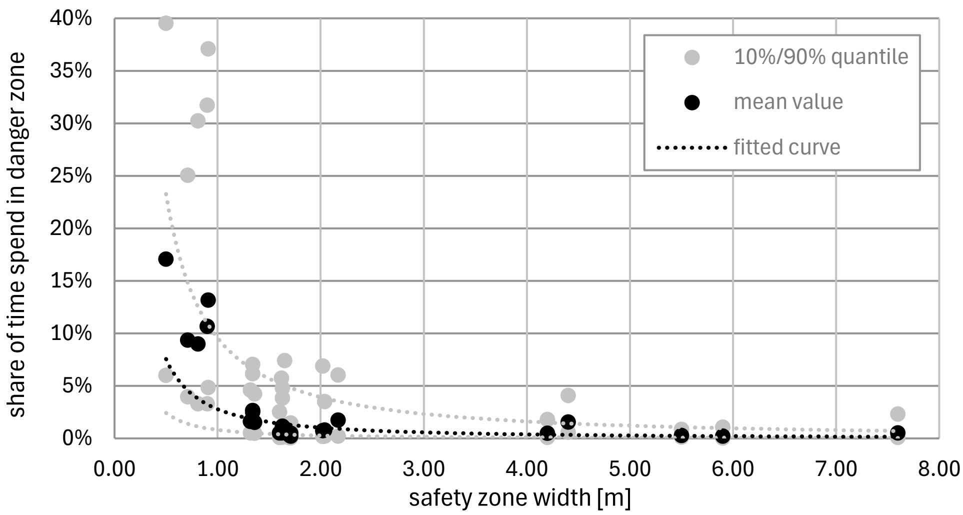

Figure 1: Range of share of time spent in danger zone for different widths of the safety zone

A pronounced influence of the width of the safety zone is evident in the data (see Figure 1). Areas with safety zones narrower than 1.0 m exhibit a significantly higher proportion of time spent in the danger zone, while a correlation persists even within wider zones. This also corresponds to the existing regulations, where 0.90 m is the minimum design width for short bottlenecks [1].

In conclusion, the comprehensive dataset provides valuable insights into the factors influencing danger zone utilization. Future research will focus on further investigating these factors and the observed discrepancies, with particular attention to variations among stations. This understanding is crucial to enhance the safety and operational efficacy of railway stations.

Bibliography

[1] BAV, *Forschungsbericht – Abstände auf Perrons*, Bundesamt für Verkehr BAV, 2011.

[2] Thurau, J., van den Heuvel, J., Keusen, N., van Ofwegen, M., Hoogendoorn, S.P., *Influence of Pedestrian Density on the Use of the Danger Zone at Platforms of Train Stations*, In: Hamdar, S. (eds) Traffic and Granular Flow '17, 287-296, Springer, Cham, 2019.

[3] Thurau, J., Keusen, N., *Influence of Obstacles on the Use of the Danger Zone on Railway Platforms*, Collective Dynamics **5**, A84, 2020.

[4] BAV, *Ausführungsbestimmungen zur Eisenbahnverordnung AB-EBV*, Bundesamt für Verkehr BAV, 2024.

12th International Conference on Pedestrian and Evacuation Dynamics (PED 2025)
Prague, Czech Republic - September 9-12, 2025

Investigating Contributing Factors to Older Pedestrian Traffic Crashes

Elisabeta Mitran *[1], Xiaoduan Sun[1], Farooq Azam Khanzada[1]
[1]Department of Civil Engineering
University of Louisiana at Lafayette

Abstract

Pedestrian safety has persistently remained one of the most pressing issues of the last decade. The purpose of this study is to identify critical factors contributing to older pedestrian crashes in Louisiana to be able to implement effective countermeasures to improve safety and mobility for all road users. A descriptive crash analysis as well as modelling is performed to determine the contributing factors. A comparison of the crash profiles of pedestrians (65 and older) with middle-aged (25 to 64 years) and younger (15 to 24 years) is also included to identify older pedestrians overrepresentation. The geospatial analysis identified parishes with high crash risk for older pedestrians across Louisiana.

Keywords: older pedestrians, crash contributing factors, safety risk factors, elderly pedestrian crashes

Extended Abstract

Introduction

Over the last decade, the United States experienced a significant increase in older population (65 and older) accounting for 57.8 million people (17 percent of total population) in 2022 [1]. This increase in the older population has also led to a rise in pedestrian fatalities at a faster rate than the U.S. population growth. Crashes involving pedestrians have become more frequent and with more severe outcomes. According to the National Highway Traffic Safety Administration, in 2022 there were 7,522 pedestrians killed in traffic crashes, being the highest number since 1981 [2]. Older people made up 20% of all pedestrian fatalities in 2022, a 64% increase from 2013 [1]. The same increasing trends were observed in the state of Louisiana. In 2022, Louisiana had a fatality rate of 19.10 per 100,000 population for individuals aged 65 and older, a 38 percent higher than the national fatality rate of 13.79 [1]. At the state level, the State Highway Safety Plan (SHSP) has continued to recognize an urgent need to curb older pedestrian crashes by incorporating strategies and tactics in all emphasis areas.

Previous studies have shown that multi-vehicle crashes, daylight condition, weekdays, non-intersection locations, age-related deteriorations in perceptual and cognitive abilities are among the crash-contributing factors for older pedestrians. Few studies examined pedestrian crashes in Louisiana. Therefore, the aim of this study was to investigate older pedestrian crashes in Louisiana to identify critical crash contributing factors to be able to implement effective countermeasures to improve safety for all road users. The research focused on Louisiana roadways and drivers at-fault. Twelve years of police-reported crash data (2010-2021), obtained from the Louisiana Department of Transportation and Development was used for the analysis. A comparison of the crash profiles of older pedestrians (65 and older) with middle-aged (25 to 64 years) and younger (15 to 24 years) was also performed to identify overrepresentation. In addition to crash data, demographic information was obtained to understand the distribution of older population across Louisiana. Population data was obtained from the U.S. Census Bureau for the years 2010 and 2020.

*Email of the corresponding author: elisabeta.mitran@louisiana.edu

Results and Discussions

Selected results from the comprehensive analysis of all older pedestrian crashes are presented here. An in-depth descriptive analysis of the factors that contributed to the injury severity of older pedestrians crashes by considering human, vehicle, roadway, and environmental characteristics was performed. Figure 1 displays the percentage distribution by severity level in the final dataset showing that crashes with fatal, severe, and moderate injury represented more than 60% of older pedestrian crashes. Older pedestrians fatal crashes were most frequent between 6 pm and 12 am, under dark conditions without streetlights, on weekdays, involving vehicles that proceed straight ahead, at locations without proper traffic control. Crossing at non-intersection locations emerged as a major risk factor, accounting for the highest proportion of fatal crashes (28%). Older males were overrepresented in pedestrian crashes, accounting for 78% of fatal crashes and 61% of severe crashes.

The results from the comparison of pedestrian crash characteristics by age groups showed that older pedestrians are involved in a higher proportion of intersection-related crashes (46%) compared to middle-aged (39%) and younger pedestrians (38%). This trend highlights the increased crash risk older pedestrians face in complex traffic environments, particularly at intersections where multiple conflict points exist. Furthermore, 64% of older pedestrian crashes occurred during daytime (between 8 am and 5 pm), which was significantly higher than middle-aged (44.94%) and younger pedestrians (47.02%).

The geospatial analysis of older pedestrian crashes identified high-risk parishes across Louisiana by examining spatial crash distribution patterns. Figure 2 shows the distribution of older pedestrian crash rate, measured per 1,000 older population. The spatial distribution highlights the urban-rural divide, where urbanized regions tend to have elevated crash rates most likely due to higher interaction between pedestrians and vehicles.

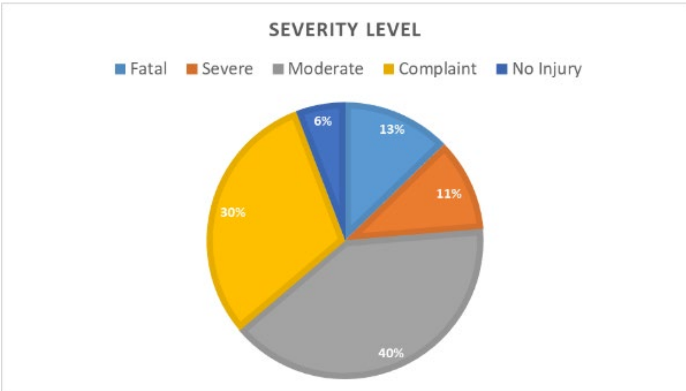

Figure 1: Older Pedestrian Crashes by Severity Level

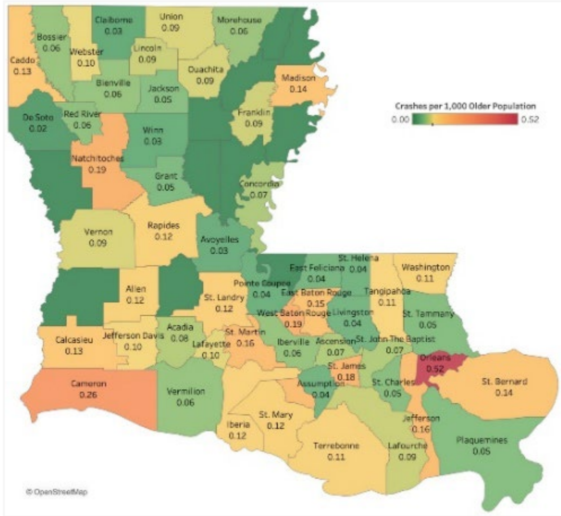

Figure 2: Spatial Distribution of Older Pedestrian Crash Rates across Louisiana Parishes

Findings of this study are expected to guide traffic safety engineers and other highway safety stakeholders in implementation of effective countermeasures to address current increasing crash trends to improve safety and mobility of older pedestrians and to justify safety improvement investments.

Bibliography

[1] National Highway Traffic Safety Administration, "Traffic Safety Facts 2022 Data: Older Population," U.S. Department of Transportation, DOT HS 813 616, Aug. 2024.

[2] National Highway Traffic Safety Administration, "Traffic Safety Facts 2022 Data: Pedestrians," U.S. Department of Transportation, DOT HS 813 590, July 2024.

Consideration of the data range of Biosignal sensors in response to the rating scale ~Laboratory Experiments Focusing on the Personal Space Region~

Risa Kagaya[1], Fumie Iwata [2], and Hideaki Takayanagi [3]

[1]Ph.D. Student, Research Assistants/Tokyo City University
[2]Master's course Student/Tokyo City University
[3]Professer, Department of Urban Life/ Tokyo City University, Dr.Eng.

This study explores pedestrian conditions in human flow using Biosignal sensors and questionnaires. An experiment simulated human flow with subjects at five distance intervals (500–900 mm). Results showed changes in perceived distance, comfort, and congestion, aligning with Biosignal data trends. Findings suggest Biosignal sensor data could serve as a mathematical scale for subjective evaluations in future human flow research.

Keywords Biological response, rating scale, human flow analysis, personal space, sensitivity evaluation

Instruction

In areas such as Shibuya and Shinjuku, where large amounts of human flow occur, there have been many simulation analyses [1] and proposals for reducing congestion [2]. These studies have mainly focused on human flow itself, with little research focusing on the conditions of the pedestrians who make up the human flow. In the future, it will be important to analyze the state of pedestrians in the human flow to create a sustainable and walkable city.

Biosignal sensors used for analyzing pedestrian conditions are generally difficult to carry, making it difficult to measure pedestrians during human flow. On the other hand, although questionnaires on human flow are widely used, there are limitations in deriving specific sensory evaluations of subjects from the numerical values of the evaluation scale.

In this study, we focused on the personal space of individual pedestrians who constitute human flow and conducted measurements using Biosignal sensors and a questionnaire. Specifically, we calculated the mean, standard deviation, and standard error of the Biosignal sensor data for each response number on the questionnaire and aimed to clarify the range of Biosignal sensor data for each response number.

In the experiment, an experimental space was created to simulate a situation in which human flow was occurring. In this environment, since the presence of others inside the personal space occurs, the distance range to be measured was divided into five steps (at 100 mm intervals), from 500 mm, the closest distance at which shoulders make contact, to 900 [mm][3], which is considered the personal space area. At each distance, one subject was surrounded by eight neighbors, and measurements were taken for one minute.

Two types of Biosignal sensors were used: a skin potential sensor and an electrocardiogram sensor. The questionnaire contained three response items: "distance," "comfort," and "crowdedness," and a six-point rating scale was used.

The results of the experiment showed that for "distance," most respondents felt that the closest distance was the closest, and the number of responses tended to increase as the distance between neighbors increased (Table 1).

As for "comfort," respondents tended to feel more comfortable as the distance between neighbors increased, but there was some variation in the evaluation of comfort within the personal space area. As for "congestion," the sense of congestion tended to decrease as the distance from the neighbor increased, but it did not completely disappear.

Based on the results of the above responses, the mean, standard deviation, and standard error for each

Table1: Questionnaire Response Tables by Distance

feeling of distance	500[mm]	600[mm]	700[mm]	800[mm]	900[mm]
1 : close	**14**	5	0	0	0
2	4	**10**	3	0	0
3	0	3	**13**	3	2
4	0	0	1	**13**	6
5	0	0	1	2	**8**
6 : distant	0	0	0	0	2

comfort	500[mm]	600[mm]	700[mm]	800[mm]	900[mm]
1 : unconfortable	**10**	3	0	0	0
2	6	6	2	2	1
3	1	**8**	**9**	3	2
4	0	0	5	**7**	**5**
5	1	0	0	3	**5**
6 : confortable	0	1	2	3	**5**

crowding	500[mm]	600[mm]	700[mm]	800[mm]	900[mm]
1 : feel crowd	**13**	2	0	0	0
2	3	**9**	2	0	0
3	2	6	**10**	6	2
4	0	1	4	**8**	**8**
5	0	0	0	2	5
6 : not crowd	0	0	2	2	3

Figure1: the results of the detection range of the Biosignal sensor in distance

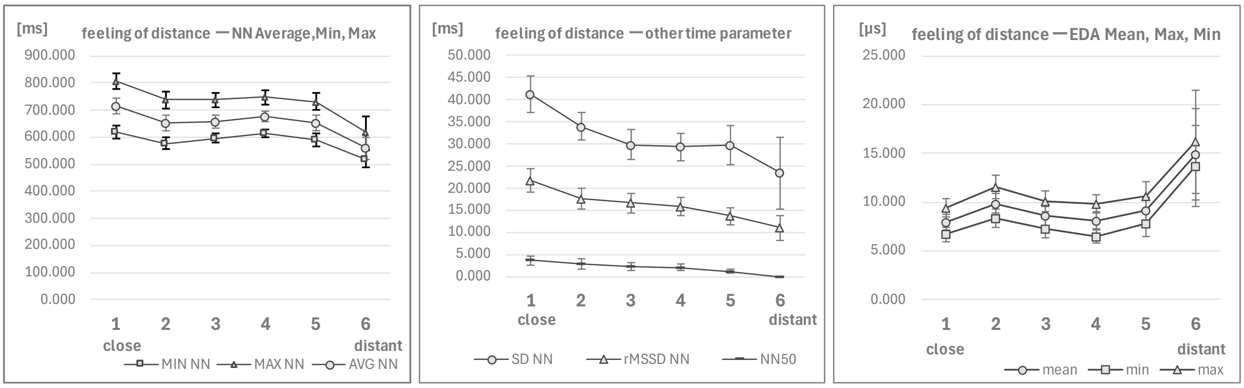

response number were calculated, and the results are shown in Figure 1.

The Biosignal sensor data were analyzed using OpenSignals provided by Plux. The results show that the meaning of the maximum and minimum NN intervals tends to appear as small numbers, and the difference in standard deviation is not large, indicating that there is a certain trend in the NN maximum and minimum values.

The above results reveal the mean and standard error of the Biosignal sensor data corresponding to the rating scale, suggesting the possibility of using the rating scale of the questionnaire survey as a mathematical scale for the Biosignal sensor in future human flow measurements.

[1] Hiroto Sunouchi, Tatsuto Kihara, Yuichi Sueshige, Kei Saito, Hideaki Takayanagi, A STUDY ON THE LVEL OF SERVICE OF WALKING SPACE FOR COEXISTENCE OF PERSONAL VEHICLES, AIJ Journal of Technology and Design, Vol.31, No.77, pp449-pp.454,2025.

[2] Yui Horishita, Yoko Tsushima, Hideaki Takayanagi, Risa Kagaya, Kimihiro Sato, A STUDY ON THE CONTROL AND GUIDANCE OF PEOPLER FLOW IN THE TERMINAL STATION WITH MOVABLE SIGNAGE ELEMENTS, AIJ Journal of Technology and Design, Vol.30, No.75, pp.885-890, 2024.

[3] John J. Fruin: Pedestrian Space: Theory and Design, Kajima Publishing, Tokyo, pp. 45-pp.58, 1974.

Enhancing Evacuation Efficiency in Low-Visibility Scenarios through AR-based Smoke Simulation and BIM-guided Navigation

Saizhe Ding[1], Kristian Börger[2], Mohcine Chraibi[2], Yuxin Zhang*[1], and Xinyan Huang†[1]

[1]Research Center for Smart Urban Resilience and Firefighting, Department of Building Environment and Energy Engineering, The Hong Kong Polytechnic University, Hong Kong

[2]Institute of Advanced Simulation, Forschungszentrum Jülich GmbH, Wilhelm-Johnen-Straße, Jülich, 52428, Germany

Abstract This study explores a novel approach to improving evacuation efficiency under low visibility conditions by integrating immersive technologies and BIM models. Fire Dynamics Simulator results are employed for volume rendering to create realistic smoke simulation. These simulations are then deployed to AR devices, overlaying the real environment for a near-authentic experience. In addition, a BIM-based guidance system overlays outlines and indicators on the simulated smoke, helping evacuees navigate buildings more efficiently.

Keywords visibility, smart evacuation; augmented reality; fire dynamics simulator.

Introduction

Large complex buildings, such as underground transportation systems and skyscrapers, often have more complicated layouts than regular buildings. Meanwhile, most people are unfamiliar with the layout of such buildings, especially under low visibility conditions, which leads to a passive effect on the psychological and physiological state of evacuees. This, in turn, influences their behavior and reduces evacuation efficiency [1]. Numerous studies have been conducted on participants' performance under limited vision conditions [2]. However, despite their findings, there are still some issues that remain to be addressed:

Firstly, for ethical and safety considerations, low visibility simulations are often achieved by requesting participants to wear eye patches or semi-transparent glasses [3] or by producing artificial smoke [4]. For the former, such wearable devices often fail to reflect the dynamic characteristics of smoke movement in real indoor environments, while the latter requires a significant investment of manpower and material resources, as each experiment typically occupies a specific floor or even an entire building, and repeated experiments require a long wait for the smoke to clear. In addition, it cannot replicate the black smoke generated by incomplete combustion, which is commonly encountered in real-life fire scenarios. Consequently, it is necessary to find an approach that not only simulates the dynamic movement of smoke but also allows for repeated and multiple experiments at minimal cost while being able to modify the characteristics of the smoke according to specific needs.

Secondly, there are currently few studies that offer more feasible suggestions on how to optimize evacuation efficiency under such low visibility conditions. The reason for this is that the indication of safety exits is usually obscured and loses efficacy in such adverse environments, leading to failure of remote visual guidance. At the same time, real person guidance has also become impossible in this situation. Therefore, a more suitable and effective alternative is needed to provide guidance to evacuees and help facilitate the evacuation process.

Methodology

To address the above issues, this study provides a novel solution by integrating emerging immersive technologies and BIM models.

*Email of the corresponding author: yx.zhang@polyu.edu.hk
†Email of the corresponding author: xy.huang@polyu.edu.hk

Regarding the reliability simulation of low-visibility scenarios, we utilize the volume rendering method based on AR devices, which enables us to achieve realistic smoke (as shown in Figure 1). First, we obtain simulation results from the Fire Dynamics Simulator (FDS) such as Pyrosim and export the data of the soot density for each voxel at each timestamp. This data is then imported into the game engine such as Unreal Engine 5 that provides volume rendering functionality, which can update the volume texture with each time step to simulate the flow pattern. Subsequently, we deploy the entire smoke animation as an executable file into the AR headset to verify the feasibility. After the validation step, we will further deploy it to the mobile application and consider proceeding with the next phase of evacuation assistance development.

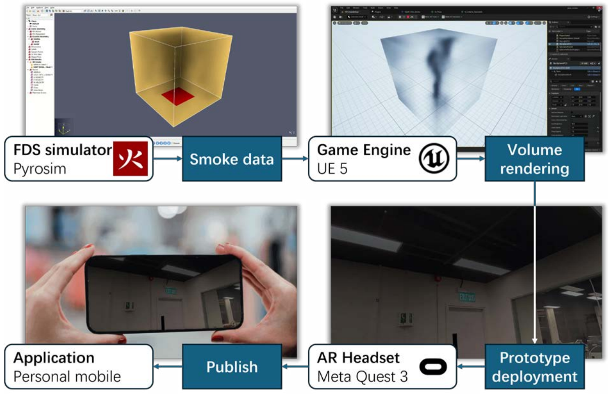

Figure 1: Schematic demonstration of volume rendering.

In terms of how to promote evacuation efficiency under low visibility, we further overlay some basic evacuation assistance elements on top of the smoke layer (as shown in Figure 2), based on available BIM information. In detail, when participants stands in the simulated smoke that is generated based on the BIM layout of the building, users can find and scan the nearest QR code displayed on the wall. By doing so, the algorithm can identify the specific location of users and provide current buildings' outline (*e.g.* doors, walls and stairs) and guidance indicators (*e.g.* evacuation routine, exit signage) in front of the smoke, ensuring that evacuees can still find the correct direction in low visibility by using their personal devices rather than searching distant cues.

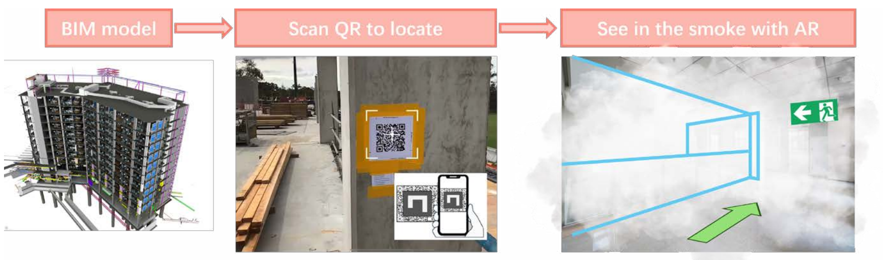

Figure 2: Demonstration of BIM-based Instruction.

In this setup, we believe our proposed system not only meets the needs of routine evacuation drills in smoke environments and the observation of human behavior under low visibility, but also helps users quickly find the fastest escape routes using personal devices under low visibility, whether in training scenarios or emergencies.

Bibliography

[1] Zhang, Y., Xie, W., Chen, S., & Li, T., *Experimental study on descent speed on stairs of individuals and small groups under different visibility conditions*, Fire technology, 54, 781-796, 2018.

[2] Cao, S., Fu, L., Wang, P., Zeng, G., & Song, W., *Experimental and modeling study on evacuation under good and limited visibility in a supermarket*, Fire safety journal, 102, 27-36, 2018.

[3] Xue, S., Shi, X., Jiang, R., Feliciani, C., Liu, Y., Shiwakoti, N., & Li, D., *Incentive-based experiments to characterize pedestrians' evacuation behaviors under limited visibility*, Safety Science, 133, 105013, 2021.

[4] Zhang, J., Zhao, J., Song, Z., & Gao, J., *Evacuation performance of participants in an offshore platform under smoke situations*, Ocean Engineering, 216, 107739, 2020.

12th International Conference on Pedestrian and Evacuation Dynamics (PED 2025)
Prague, Czech Republic – September 9-12, 2025

Finding relations between pedestrian count time series at different locations for footfall forecasting

Wentao Chen*[1] and Nikolai W.F. Bode[1]

[1]School of Engineering Mathematics and Technology, University of Bristol, Bristol BS8 1TW, UK

Abstract We investigate the relationships between pedestrian count time series measured at locations across Melbourne city. By evaluating the accuracy of different models in predicting future pedestrian counts, we examine which spatiotemporal feature best captures the properties of this system. Initial results show that for this data, overall prediction accuracy does not increase when information from other locations is being introduced. However, these relations change with specific time and location.

Keywords Macroscopic pedestrian movement, demand forecast, structure learning, time series

Introduction

Understanding macroscopic pedestrian movement is important, as it is a significant component in modern traffic systems. Information on pedestrian movement can be obtained in different ways. Capturing pedestrian counts at locations by privacy-reserving sensors is one popular method. Recording pedestrian counts simultaneously using many sensors in different locations can be regarded as a partial observation of pedestrian movement on a city scale. Data from such systems can be treated as a new dynamical system where the locally observed counts arise from the movement of pedestrians in a city.

Studying the governing equation of this dynamical system promises fundamental insights into the functioning of cities and is directly useful for predicting future traffic demand for transportation management. However, this dynamical system is neither time-invariant nor closed. For example, people may show different travel behavior in the morning and afternoon peaks. The sparsity of sensors means that key information may not be observed.

To address these problems, data-driven methods are applied to approximate the governing equation and perform prediction tasks. For example, Koopman operator methods have been used to linearly approximate the process [1]. Alternatively, machine learning methods such as Long Short-Term Memory (LSTM) can be used. However, few studies have focused on explaining characteristics of the fitted dynamics. Here, we focus on the question of whether for predicting the counts at one location, it is useful to consider information from other locations, and if so, which locations should be used. We compare prediction accuracies under different assumptions to find explainable relations between locations [2].

Formal Description

Assuming the dynamics of pedestrian counts $\vec{N}^t$ captured by sensors can be described by a governing equation $F_{\Delta t}$, where Δt is a time step:

$$\vec{N}^{t+\Delta t} = F_{\Delta t}(\vec{N}^t, t). \tag{1}$$

This process is usually time-variant and not closed. Here, we employ LSTM models to learn the dynamics and compare the prediction accuracy under different assumed relations between sensor locations.

Introducing data from other locations, N_i^t, will benefit model performance if there are non-redundant stable relations between the given N_i^t and the predicted target $N_j^{t+\Delta t}$ (i can be any place with observations in the system). To explore this, we train different LSTM models to approximate the map between $\{N_i^t\}$ and $\{N_i^{t+\Delta t}\}$ and compare the prediction accuracy according to different hypothesis.

Assumptions can be made for different relations between count time series. For example, nearby sensors may provide more information due to the continuity of pedestrian movement or similarity of locations. Here, we consider a range of different assumptions for relations between locations (Table 1).

*Email of the corresponding author: wentao.chen@bristol.ac.uk

Table 1: Different assumptions for relations between count time series compared in this work.

Component	Assumptions
Spatial scale	1. Using historical data of the target sensor. 2. (Spatial) Using historical data from the target sensor and nearby sensors. 3. (Correlation) Using historical data from the target sensor and sensors that are highly correlated to the target sensor. 4. (Opposite) Using historical data from the target sensor and sensors that are not highly correlated to the target sensor nor are close to the target sensor.
Temporal scale	A. The same spatial relation appears at any time point. B. Distinct spatial relations appear at different time.

Results

We train LSTM models to approximate $F_{\Delta t}$ (Eq.1) according to the different assumptions on spatial relations and check the prediction accuracy at different hours to gain insights about the dynamics on temporal scales. For the overall prediction accuracy, we do not see significant increases in model performance when information from additional sensors is introduced into the models (Figure 1c). However, considering prediction accuracy at different hours of the day, the results indicate that assumption B from Table 1 holds on the temporal scale and assumptions 1-4 on the spatial scale hold on a case-by-case basis (Figure 1d,e).

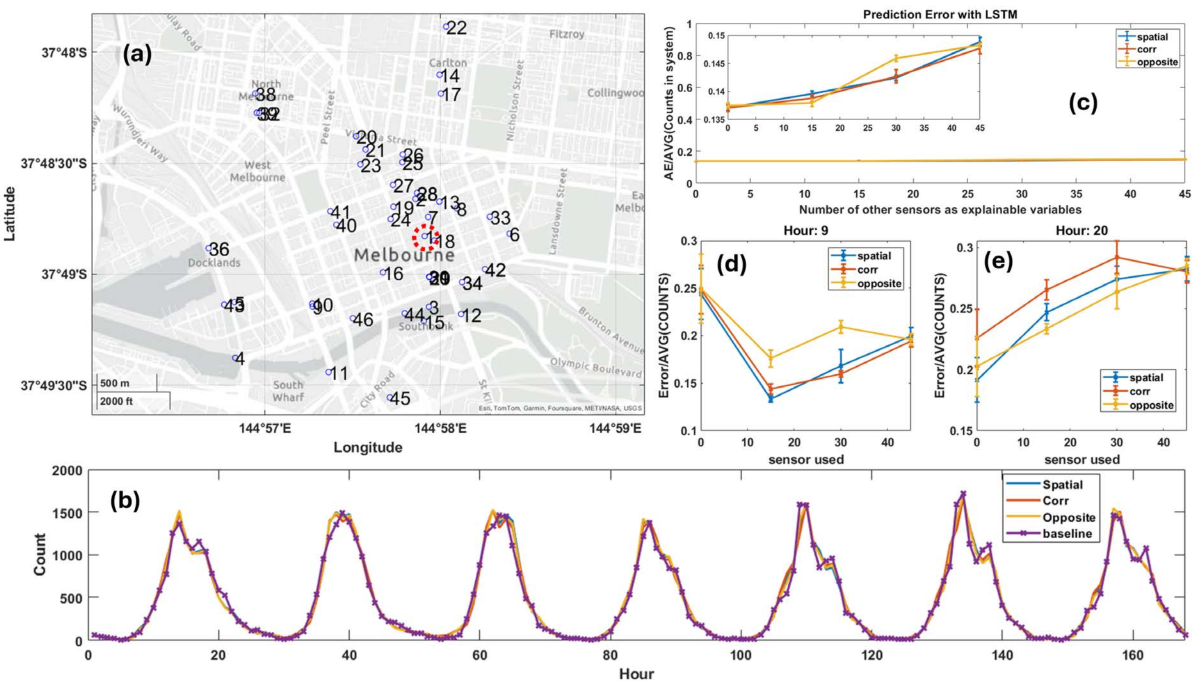

Figure 1: Using LSTM models to compare support for relations between locations when predicting future counts. (a) The spatial layout of all sensors in the system. For example, we consider predicting the counts at sensor 1 in the next hour using historical data from sensor 1 and other sensors in the system. (b) One example of predicted counts at sensor 1 from Friday, Sept.13th, 2024, to Thursday, Sept.19th, 2024. (c) The overall prediction error does not change much when data from an increasing number of additional locations (x-axis) is used for prediction. We show results based on assumptions 2-4 in Table 1, indicated by different colors. Every experiments are repeated for five times. The standard deviations are presented by error bars. (d) and (e) show how the same information as panel (c) but only for selected hours of the day. (d) and (e) show distinct patterns, which suggests B is the correct assumption on the time scale.

Bibliography

[1] Daniel Lehmberg, Felix Dietrich, and Gerta Köster. "Modeling Melburnians—Using the Koopman operator to gain insight into crowd dynamics." Transportation Research Part C: Emerging Technologies **133**, 103437, 2021.

[2] Gustau Camps-Valls, et al. "Discovering causal relations and equations from data." Physics Reports **1044**, 1-68, 2023.

A Body Size Measurement Method Using Aligned Depth Cameras: A Preliminary Experiment

Hana Najmanová*[1], Pavel Hrabák†[2], Dominik Košík[1], and Vít Pospíšil[2]

[1]Faculty of Civil Engineering, Czech Technical University in Prague, Czechia
[2]Faculty of Information Technology, Czech Technical University in Prague, Czechia

Abstract This paper presents a 3D point-cloud measurement method for acquisition of static physical dimensions of people relevant for pedestrian dynamics and fire safety applications. The method was validated beyond laboratory settings through an initial field experiment and proved sufficient reliability and applicability for estimating the body size of pedestrians.

Keywords Data Extraction, Body Dimensions, Experiment, 3D Point Cloud, Pedestrian

Introduction and Measurement Method

The size of the individuals' bodies affects the use of the surrounding space and, in turn, has a direct impact on variables such as pedestrian flow and density during crowd evacuation. Although the idea of considering the occupied area in evacuation and building planning emerged in the 1970s [1], the changing anthropometric traits of the population call for recent updates [4]. The vertical projection of a single pedestrian is typically approximated as an ellipse, with the axes representing shoulder width and chest-level depth [2]. Therefore, the use of anthropometric measurements can provide valuable insights [3].

This study introduces a static measurement method of person's body size dimensions by means of two aligned Intel RealSense Depth Cameras D435. This method aims at providing a fast and reliable way to accurately capture a wide range of data sets outside of laboratory conditions. As illustrated in Fig. 1, a 3D point cloud in XYZ coordinates can represent the entire human body by merging front and rear depth maps. Due to proper alignment and extrinsic calibration of the cameras, the desired body dimensions (e.g., height H, shoulder width S, maximal width W, depth D) can be extracted algorithmically. In addition, body projection area A is determined using a concave polygon of the XY projection of all points in the cloud.

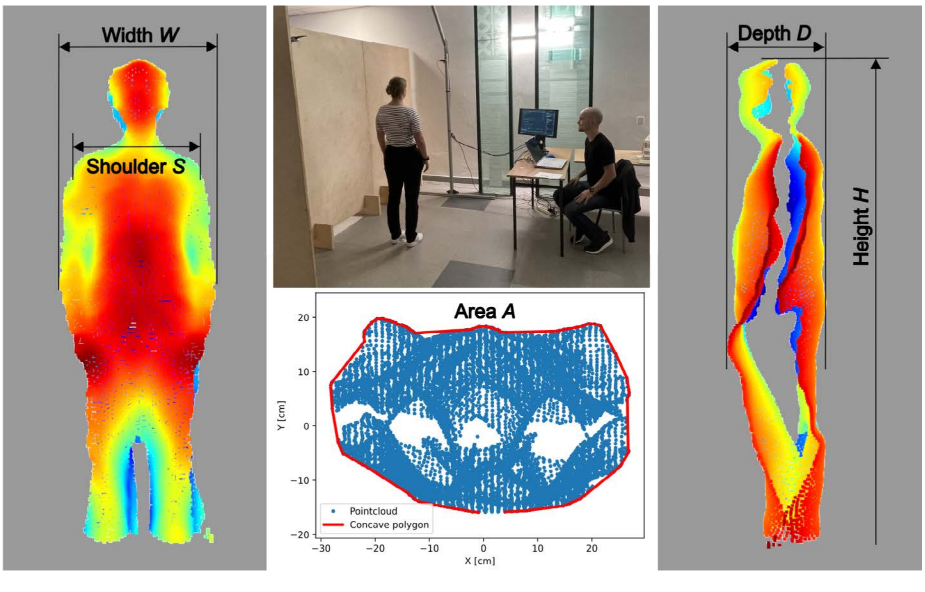

Figure 1: Illustration of the measurement method and the target body dimensions for collection

*Email of the corresponding author: `hana.najmanova@cvut.cz`
†Email of the corresponding author: `pavel.hrabak@fit.cvut.cz`

Experiment and Results

After an optimization process under controlled laboratory conditions, the proposed method was preliminary tested and validated in a field experiment carried out in October, 2024 at the Faculty of Civil Engineering of the Czech Technical University (CTU) in Prague. The experiment involved 111 students and faculty employees recruited on a voluntary basis. Participants were captured with and/or without wearable accessories. With 23 participants recorded both with and without accessories, the sample size consisted of 134 body measurement records in total. In addition to anonymous automatic measurements, information on the age group and gender of the participants was gathered, and their height and shoulder width were manually measured for validation purposes. The experiment was approved by CTU in Prague's Committee for Ethics in Research of the CTU Scientific Council.

Table 1: Descriptive statistics of the body dimensions without any accessories based on 104 samples. Δ is the difference between automatic and manual measurement; Mean and Std stand for average and standard deviation of the sample, corr X denotes the Pearson's correlation coefficient of the row variable and X.

Variable		Δ mean$\pm$std	Mean	Std	corr S	corr W	corr D	corr A
Height	[cm]	0.92 ± 1.13	179.48	10.32	0.52	0.52	0.12	0.36
Shoulder	[cm]	1.08 ± 2.41	48.66	3.86	-	0.82	0.50	0.75
Width	[cm]	-	56.39	5.09	0.82	-	0.55	0.84
Depth	[cm]	-	36.10	4.08	0.50	0.55	-	0.84
Area	[cm^2]	-	1552.72	249.19	0.75	0.84	0.84	-

Table 1 presents several statistics of the measurements without accessories. The mean difference between automatic and manual measurement indicates that the method was sufficiently reliable. The average body projection area of 0.15 m^2 corresponds to maximal density 6.44 ped/m^2. For comparison, in [1], it is estimated that the horizontal projection area of an adult is 0.1 m^2 when wearing a summer dress and 0.125 m^2 when dressed for winter. The relatively low correlation coefficient between width and depth signalizes that considering depth to be proportional to width is not a dependable model. In contrast, comparing the measured area A with the ellipse area $E = \frac{\pi}{4} \cdot W \cdot D$, where the width and depth serve as axes, we obtain the difference $A - E = -55.07 \pm 98.2$ cm^2 and $\mathrm{corr}(A, E) = 0.95$. The average measurements showed that men's dimensions were marginally greater than those of women. The main influence of gender was observed in the correlation between width W and depth D, which was slightly higher for men (0.61) compared to women (0.52). The measurements involving participants with accessories differed in depth and projection area, reading $D = 53.79 \pm 5.48$ and $A = 2189.77 \pm 288.06$. The results lean over [5], which can be considered as supplementary material to the contribution.

Conclusions

Initial results indicate that the suggested measurement method provides a fast, non-contact, and accurate way of gathering data on the body sizes of people. The 3D scans collected were considered sufficiently detailed to enable automatic extraction of the desired variables, including body ground projection. Our findings offer a starting point for discussing the application of anthropometric measurements in estimating pedestrian body size and further use in pedestrian and evacuation design, especially relevant to significantly heterogeneous crowds.

Acknowledgments: The project was carried out with significant support from the FIT CTU in Prague Image Processing Laboratory, namely Alexander Bazko, Robin Gaignoux, and Justýna Frommová.

Bibliography

[1] Predtechenskii, V. & Milinskii, A. Planning for Foot Traffic Flow in Buildings. (Amerind,1978)

[2] Korhonen, T. & Hostikka, S. Fire Dynamics Simulator with Evacuation: FDS+Evac: Technical Reference and User's Guide. (VTT Technical Research Centre of Finland,2009)

[3] Erkan, I. A system proposal for rapid detecting of anthropometric data and affecting design strategies. *Journal Of Engineering, Design And Technology.* **18**, 1793-1822 (2020,3), Publisher: Emerald Publishing Limited

[4] Thompson, P., Nilsson, D., Boyce, K. & McGrath, D. Evacuation models are running out of time. *Fire Safety Journal.* **78** pp. 251-261 (2015,11)

[5] Dominik Košík, *Experimental data acquisition for modelling pedestrian and evacuation dynamics*, Master thesis, Czech Tecnical Univesity in Prague, 2025. `http://hdl.handle.net/10467/121209`

12th International Conference on Pedestrian and Evacuation Dynamics (PED 2025)
Prague, Czech Republic – September 9-12, 2025

The Sound of Crowds: Perceiving and Understanding Pedestrian Dynamics through Visual and Auditory Data

Dilge Dakman*[1] and Anna Sieben[1,2]

[1]Faculty of Human and Social Sciences, University of Wuppertal, Wuppertal, Germany
[2] Institute for Advanced Simulation (IAS-7), Forschungszentrum Jülich, Jülich, Germany

Abstract Studies in pedestrian dynamics primarily focus on visual aspects, neglecting the auditory elements of crowds. This study seeks to highlight the significance of sound in crowd experiments by conducting a think-aloud study, incorporating both visual and audio data. It is expected that the inclusion of audio will deepen the understanding of the experimental atmosphere.

Keywords Sound, Think-aloud, Atmosphere, Bottleneck, Social Psychology

Introduction

While pedestrian dynamics have been extensively studied across various disciplines, most research predominantly focuses on visual and spatial aspects, largely neglecting the role of sound in examining crowd behavior. The aim of this study is to bridge this gap by analyzing the auditory dimension of pedestrian movement and bringing in new insights into the field.

Environmental sounds such as traffic noise, sounds of nature and human activity often carry valuable information [1]. This study, however, focuses specifically on human-generated sounds—those produced by people, such as voices, footsteps, and other forms of human activity. These sounds can be essential for understanding the context and structure of crowds: For example, chanting or booing in a stadium, which may be visually or spatially indistinguishable. Research has shown that auditory material serves as a complementary source of information, with its importance increasing as visual input becomes more limited [2].

A study comparing video and audio material in emotion recognition found that while auditory information is less accurate than visual data, their combination achieves an accuracy rate of 63.6 percent, compared to 58.2 percent for video alone [3]. Therefore, sound, such as laughter—recognized as a universal indicator of positive emotions —becomes highly detectable in crowd behavior audios, making it a valuable auditory cue for emotional analysis.

The primary aim of this study is to introduce a new perspective in the analysis of crowd behavior by focusing on the auditory experience of the crowd rather than observing them in silence. The importance of sound has often been overlooked, yet it is crucial for a complete understanding of crowd dynamics.

To explore this idea, a think-aloud study involving 5-10 participants is created, where participants are asked to observe and comment on videos from previously conducted experiments. The videos are from experiments where participants were asked to navigate through a bottleneck [5]. Participants first watch the short video clips without sound and then with sound to observe whether and how their own impression of the atmosphere changes. In some videos, pushing behavior is observable (Figure 1a). Without sound, the situation may appear dangerous, however, when the sound is added, laughing and chatting is evident. The other videos do not consist of pushing behavior, but the overall context remains the same (Figure 1b). Video data from camera glasses are shown to complement top-view videos with a within-perspective experience (Figure 1c). It is expected that this additional perspective will allow participants to engage more deeply with the material, advancing their understanding of the situation as if they are part of the crowd. In addition to the sound from the top-view perspective, this perspective allows participants to identify where the sound is specifically coming from, enhancing their interaction with the material. In total, the think-aloud study includes 21 videos but each participant is presented with half of them.

The think-aloud method is chosen as it provides insights into the inner speech of participants allowing other people to follow their thoughts [4]. While watching the videos from previously conducted experiments, participants are instructed to think aloud and share all their impressions and thoughts.

*Email of the corresponding author: dakman@uni-wuppertal.de

By systematically reflecting on both the visual and auditory data, the impact of sound on participants perception of the video is becoming clear. This includes identifying whether certain auditory cues direct attention to specific visual elements, evoke particular emotional responses or shape interpretations of the crowd dynamics depicted in the video materials. Therefore, the think-aloud method is particularly effective in this context, as it provides direct insights into how naive participants process and engage with the audio material, allowing for a deeper understanding of how sound modulates their experience of the videos.

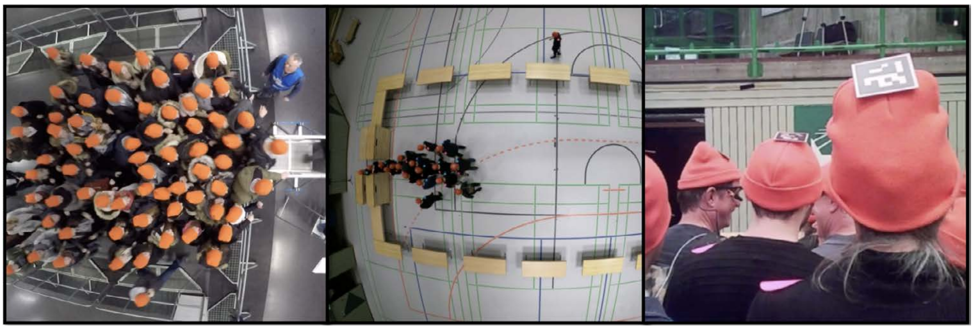

Figure 1: a: Pushing behavior; b: Top-view perspective of bottleneck situation; c: Within-perspective of bottleneck situation

It is expected that the audio material will provide significant information regarding the atmosphere of the observed crowd, offering a richer understanding of crowd behavior. While video footage provides a general overview of the situation and people's actions, combining both elements allows participants to gain a more comprehensive understanding of the crowd's behavior and emotional state. Based on this, new methods for analyzing crowd dynamics can be developed in the future.

Bibliography

[1] Aletta, F., Kang, J., Axelsson, Ö., *Soundscape descriptors and a conceptual framework for developing predictive soundscape models*, Landscape and Urban Planning **149**, 65–74, 2016. doi:10.1016/j.landurbplan.2016.02.001.

[2] Burr, D., Alais, D., *Combining visual and auditory information*, Progress in Brain Research **155**, 243–258, 2006. https://doi.org/10.1016/S0079-6123(06)55014-9.

[3] Cao, H., Cooper, D. G., Keutmann, M. K., Gur, R. C., Nenkova, A., Verma, R., *CREMA-D: Crowd-sourced Emotional Multimodal Actors Dataset*, IEEE Transactions on Affective Computing **5**(4), 377–390, 2014. https://doi.org/10.1109/TAFFC.2014.2336244.

[4] Charters, E., *The Use of Think-aloud Methods in Qualitative Research: An Introduction to Think-aloud Methods*, Brock Education Journal **12**(2), 2003. https://doi.org/10.26522/brocked.v12i2.38.

[5] Adrian, J., Seyfried, A., Sieben, A., *Crowds in front of bottlenecks at entrances from the perspective of physics and social psychology*, Interface **17**(165), 20190871, 2020. https://doi.org/10.1098/rsif.2019.0871.

Pedestrian Trajectory Prediction Focusing on Environmental Object and Social Interaction Modeling through Graph Attention Networks

Wen-Xin Qiu*[1] and Eiji Hato[2]

[1]Institute of Engineering Innovation, The University of Tokyo, Japan
[2]Department of Civil Engineering, The University of Tokyo, Japan

Abstract This paper proposes a pedestrian trajectory modeling approach that integrates pedestrian-object interactions through extending the spatial-temporal (ST) graph representations by introducing heterogeneous nodes to consider objects in environments. A deep learning (DL) model is designed to learn the features that capture interactions at the object level. The experimental results show that the proposed approach performed better than the baseline, especially in scenes with small objects.

Keywords Deep Learning, Graph Neural Network, Walking behavior, Interaction

Introduction

Understanding pedestrian behavior is essential for designing safe and comfortable environments. Conventional operational-level pedestrian behavior models, including social force and discrete choice models, have indicated that interactions are crucial factors in pedestrians' trajectories. Those models primarily consider avoidance of obstacles and other pedestrians and following others, but they cannot capture the diversity of human reactions to the same object.

DL-based models have recently been widely applied for pedestrian trajectory modeling [1]. With a ST graph that can represent the pedestrian relationships [2, 3], graph neural networks can learn detailed interactions with invariant weights of the graph. Also, the approaches considering environmental features typically process entire images or maps using convolutional neural networks [4]. Still, their end-to-end structure makes it difficult to assess the impact of individual objects, which is essential in spatial design.

This study proposes a pedestrian trajectory modeling approach that integrates pedestrian-pedestrian and pedestrian-object interactions. By extending the ST graph representations of previous studies on trajectory prediction to consider objects in environments, the model captures complex avoidance and attraction relationships at the object level, improving its applicability to spatial planning.

Approach

This study aims to predict humans' future trajectories given their trajectories in a time period and the coordinates of the objects in the scene. The framework of the proposed approach is shown in Figure 1.

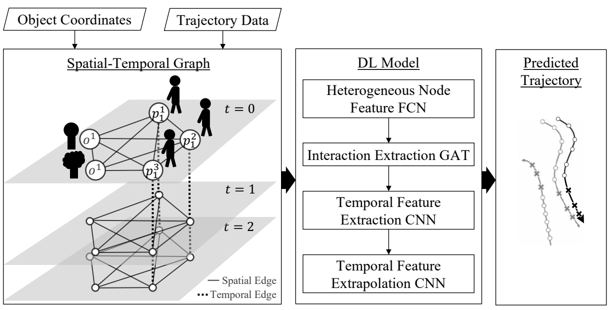

Figure 1: Framework

*Email of the corresponding author: `qiu@bin.t.u-tokyo.ac.jp`

The ST graph consists of two kinds of nodes: pedestrians (p) and objects (o). The features of both kinds of nodes are their coordinates and a dummy variable indicating if it is an object or a pedestrian. The spatial edges connect the nodes of the same time step, representing their interactions. The temporal edges connect the pedestrian nodes in each time step, representing the trajectories. The object nodes remain with the same features, which are assumed static, but the edges in different time steps could represent different interactions due to the human movements through learning features from the connected nodes.

A DL model is designed to learn the features from the ST graphs and predict the future trajectories. The first part is a fully connected network (FCN) that encodes features of heterogeneous nodes. The following interactions extraction part adopts the graph attention network (GAT) [5] to learn the weights representing each pedestrian perceiving the others and the objects. The following steps are CNN layers to extract temporal features and to extrapolate future trajectories, adopting the same model structure as [6]. The distributions of future trajectories are then predicted, and the trajectories are sampled. The loss function is the negative log likelihood of the predicted distribution and the ground truth.

Experiment Results and Discussion

The proposed approach is experimented with the ETH/UCY dataset. The evaluation metrics are minimum average and final displacement error (minADE_{20}, minFDE_{20}), defined by [1],

The results are shown in Table 1. The first and second rows are two proposed models of this paper. Model (i) considers the loss of only the pedestrian nodes, and (ii) predicts object coordinates the same as pedestrians and considers the loss of both pedestrian and object nodes. The third row is the model in [6], which can be recognized as only considering homogeneous pedestrian nodes of this study. The last row is a baseline [3]. Both proposed models performed better than the baseline in the UNIV. This density of the UNIV is higher, indicating more interaction, and the directions have larger varieties. Besides, the objects in the UNIV set are a garbage can, a road lamp, and some small obstacles, while there are buildings and cars in the ZARA1 and ZARA2. It indicates that representing large objects only by a pair of coordinates may be improper. Besides, the better performance of model (i) suggests that the object nodes should be treated differently than pedestrian nodes.

Table 1: minADE_{20} and minFDE_{20} results

Model	minADE_{20}						minFDE_{20}					
	ETH	HOTEL	UNIV	ZARA1	ZARA2	AVG	ETH	HOTEL	UNIV	ZARA1	ZARA2	AVG
Proposed (i)	0.272	0.405	0.033	0.183	0.146	0.208	1.288	0.776	0.115	0.561	0.321	0.612
Proposed (ii)	0.595	0.236	0.046	0.818	0.214	0.382	1.546	0.569	0.140	1.790	0.497	0.909
Ped only [6]	0.729	0.248	0.400	0.297	0.252	0.385	1.504	0.343	0.785	0.297	0.481	0.682
Baseline [3]	0.716	0.433	0.495	0.390	0.331	0.473	1.289	0.712	0.893	0.647	0.535	0.815

Conclusions

In this paper, a new approach for pedestrian trajectory prediction that considers environment objects is proposed. It is expected to provide a mathematical understanding of interactions between pedestrians and objects. Nonetheless, the method of describing larger objects should be further investigated.

Bibliography

[1] Alahi, A., Goel, K., Ramanathan, V., Robicquet, A., Fei-Fei, L., & Savarese, S., *Social LSTM: Human Trajectory Prediction in Crowded Spaces.*, 2016 CVPR, 961–971, 2016.

[2] Vemula, A., Muelling, K., & Oh, J., *Social Attention: Modeling attention in human crowds*, ICRA, 4601–4607, 2018.

[3] Mohamed A., Qian K., Elhoseiny M., & Claudel C., *Social-STGCNN: A social spatio-temporal graph convolutional neural network for human trajectory prediction.*, 2020 CVPR, 14412–14420, 2020.

[4] Shafiee, N., Padir, T., & Elhamifar, E., *Introvert: Human trajectory prediction via conditional 3D attention*, CVPR 2021, 16815-16825, 2021.

[5] Veličković, P., Cucurull, G., Casanova, A., Romero, A., Lio, P., & Bengio, Y., *Graph attention networks*, arXiv:1710.10903, 2017.

[6] Qiu, W.-X., & Fuse, T., *Visualization of Pedestrian Interaction through Attention-based Pedestrian Trajectory Prediction*, Asain Journal of Geoinformatics, AJG–2311002, 2024.

A Comparative Study on the Reliability and Validity of Virtual Reality-Based Pedestrian Dynamic Experiments

Jianyu Wang*[1] and Tao Chen†[1]

[1]School of Safety Science, Tsinghua University, Beijing 100084, China

Abstract Virtual reality (VR) technology has been widely applied in the field of pedestrian evacuation dynamics. Variations in hardware and software configurations result in differences in control methods, immersion levels, and distinctions in validity and reliability across systems. To address this, we proposed a novel control scheme utilizing controllers and trackers, conducting comparative analyses through two representative experiments. The results demonstrated that our proposed control solution exhibits significantly reduced motion dizziness and improved authentic experience during actual experimental implementations than the hand controller method.

Keywords Virtual reality, Pedestrian dynamic, Pedestrian experiment, Reliability, Validity

Instruction

Virtual reality (VR) experimental environments have emerged as a novel methodology for pedestrian dynamic and evacuation research where physical experiments are infeasible, owing to their cost-effectiveness, interactivity, operational flexibility, and independence from physical space/equipment constraints. VR technology has been extensively applied in pedestrian dynamic studies investigating complex behavioral patterns, including wayfinding strategies Ref. [1], route selection dynamics Ref. [2], and emotional responses Ref. [3]. However, ensuring naturalistic locomotion comparable to real-world movement remains a persistent challenge in VR implementations. Current mainstream VR systems, including Head-Mounted Displays (HMDs), Desktop VR, and CAVE environments, exhibit significant divergences in locomotion mechanics and control paradigms. To address this, we propose a hybrid locomotion scheme integrating hand controller with body orientation tracker, systematically contrasting it with conventional controller-only approaches. Controlled experiments were conducted involving circular walking trajectories and obstacle negotiation tasks across both systems, supplemented by post-experiment questionnaires. The results show that both experimental control configurations are reliable. The motion control configuration using hand controller with body orientation tracker has better validity by it could effectively reduce dizziness and provide a more authentic experience.

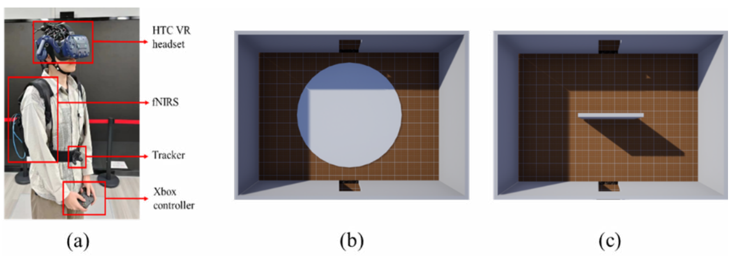

Figure 1: Experimental settings, (a) Still image of test-subject with device, (b) circular walking scenario, (c) obstacle negotiation scenario.

*Email of the corresponding author: jianyuwang0602@163.com
†Email of the corresponding author: chentao.a@tsinghua.edu.cn

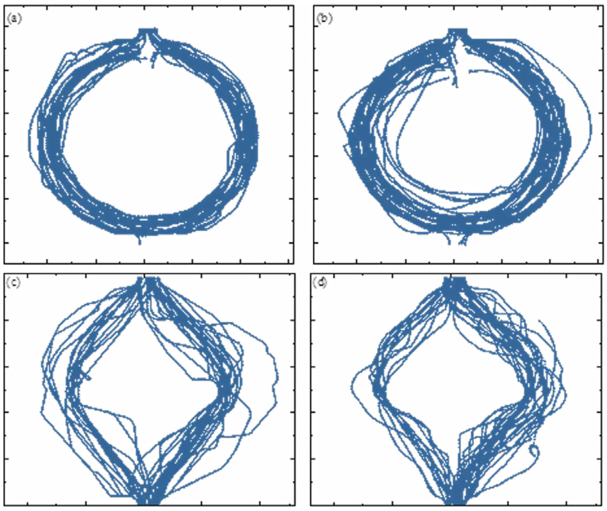

Figure 2: Comparison of trjectory with with two control configurations, (a)(c) with hand controller & tracker, (b)(d) with hand controller.

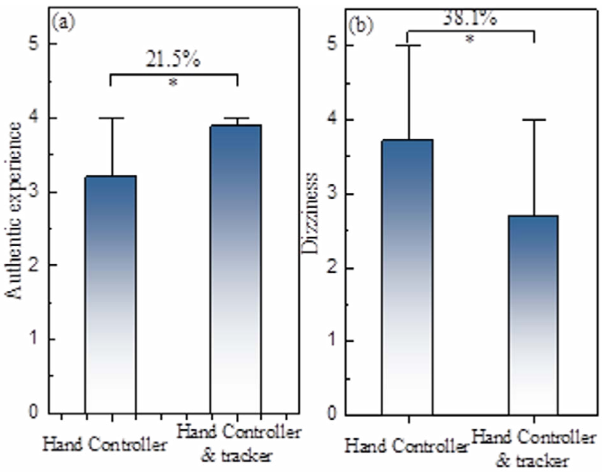

Figure 3: Comparison of dizziness and authentic experience with two control configurations.

Bibliography

[1] Yu L., Wang Z.J., Chen F., Li Y.F., Wang W.T.*Subway passengers' wayfinding behaviors when exposed to signage: An experimental study in virtual reality with eye-tracker*, Safety Science **162**, 106096, 2023.

[2] Lovreglio R., Dillies E., Kuligowski,E., Rahouti A., Haghani, M.*Subway passengers' wayfinding behaviors when exposed to signage: An experimental study in virtual reality with eye-tracker*, Automation in Construction **141**, 104452, 2022.

[3] Deng K.F., Li M., Wang G.N., Hu X.M., Zheng H.J., Tian K.K., Chen T.*Experimental Study on Panic during Simulated Fire Evacuation Using Psycho- and Physiological Metrics* , International journal of environmental research and public health. **19**, 6905, 2022.

12th International Conference on Pedestrian and Evacuation Dynamics (PED 2025)
Prague, Czech Republic – September 9-12, 2025

Interactions of Pedestrian Flow and Stagnation in Front of a Floor Plan in a Commercial Building

Mineko Imanishi*[1], Takuro Okada[1], and Tomonori Sano[2]

[1]Takenaka Research & Development Institute
[2]Waseda University

Abstract The interrelationship between the stagnation areas autonomously formed in front of a floor plan and the compression of pedestrian flows due to the stagnation was analysed by observing an actual corridor in a commercial building. Additionally, a subject experiment with 30 participants was conducted to clarify the psychological discomfort pedestrians felt in this situation. The results show that that people who stop to view floor plan feel uncomfortable about interrupting the flow and, therefore, considerately decide where to stand.

Keywords Pedestrian Flow, Field Observation, Detouring, Signage

Instruction

Walking is the primary activity in corridors of building spaces. However, in the actual corridors in commercial buildings, various other activities besides moving occur, such as waiting for someone, looking at show windows, and organising belongings. Pedestrians moving through the corridor are at the mercy of these temporary 'obstacles' and make detours to avoid people lingering. Consequently, the walkable area is narrowed, pedestrian flow density increases, and congestion intensifies. On the other hand, the people who become obstacles are also pedestrians. Staying people put feel psychologically burdened by the flow of people in the vicinity and try to accomplish their actions with reserve.

To provide a better walking environment for building users, it is necessary to model what is happening in such mixed flow and stagnation situations from the perspective of pedestrian dynamics. However, such situations are difficult to observe in an experimental environment and require investigation in real space. In addition, it is necessary to take into account the psychological situation, rather than just perceiving the phenomenon as a quantitative phenomenon.

This research focuses on the relationship between people who walk and people who stay in such spaces, and aims to unravel their interrelationships. By observing an actual case, a variety of situations can be grasped, and furthermore, by directly questioning people who have experienced the situation, the reasons for their behavioural decisions and their psychological situation could be clarified.

Methodologies

The authors investigated pedestrians' movements in a main concourse in a large complex building in Osaka, Japan and also performed a subject experiment in the same location.

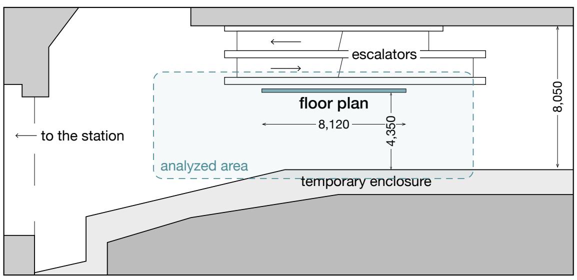

Figure 1: Floor plan of the subject area.

*Email of the corresponding author: imanishi.mineko@takenaka.co.jp

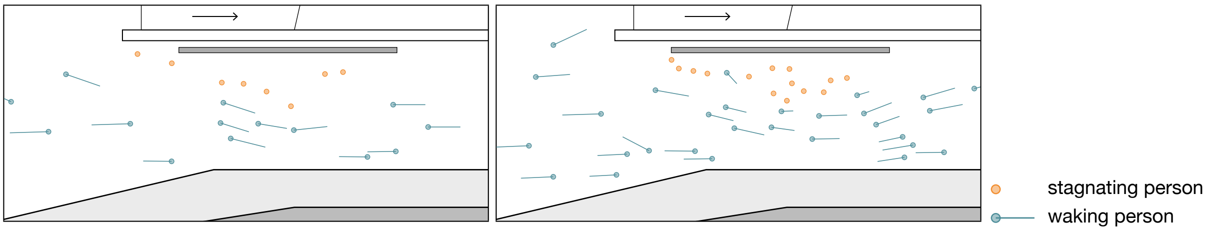

(a) Lunch time (12:26) (b) highly congested moment (16:20)

Figure 2: Pedestrian movements at different aspects. The bars in the diagram indicate walking vector for one second at the moment.

Table 1: Frequency of responses to feeling when looking for the information in front of the floor plan.

statement	frequency
Refrained from the pedestrian stream.	7
Refrained from the stagnating people.	1
Stagnating people were obstructing me.	6
Pedestrian stream was obstructing me.	0
Pedestrians avoided me.	4
Didn't mind.	5
Others	5

The building houses offices on the upper floors and restaurants and shops on the lower floors. A pedestrian deck from the station directly enters the first floor of the building, passing through the main concourse, which is the focus of this survey, and leads to another wing further back. Consequently, the main concourse is filled with commuters during the morning rush and shoppers throughout the day. Figure 1 illustrates the floor plan of the observed area in the main concourse. After the entrance from the station direction, there is a large floor plan that draws many visitors to find their destination.

A video camera mounted on the fence of the bridge on the upper level recorded the subject area from 8 am to 6 pm on a weekday. Pedestrian movements are then extracted from the recorded video. The trajectories and behaviours of pedestrians were analysed in terms of pedestrian density, autonomously developed stagnant space and pedestrian flow compression.

On the same day, 30 participants were given the task of walking down the main concourse one by one, assuming that they were visitors to the building, and finding a restaurant that met certain criteria from the floor plan on the way. They responded with a psychological evaluation during the task, such as the difficulty of walking, the feeling of crowding, and how they felt when they stopped.

Results

Figure 2 indicates the pedestrian movements at lunchtime(0.36 pers./m^2) and at a peak time (0.70 pers./m^2). As the main corridor runs straight, pedestrians in the stream basically walked ahead along the corridor, but had to detour around the stagnant area to get through. In both moments, arc-shaped stagnant areas were developed. When the area in front of the floor panel became congested, people were multi-tiered. At peak times, the stagnant area grew up approximately half the width of the corridor. For legibility, the frontmost layer kept a distance of about 0.4–1.0 metres from the panel, although pedestrians scarcely passed through the gap between this panel and the stagnant area.

Table 1 summarises the frequency by topic from the free-text descriptions of what participants of the experiment felt about people in the vicinity while looking for information in front of the floor plan. From the answers, it was found that the participants took care not to impede the main pedestrian stream, by intentionally choosing their standing position and trying to minimise the stagnation time as much as possible. On the other hand, some also stated that people walking avoided them.

Conclusions

The results indicate that the congestion of the pedestrian flow affected the stagnation area formed, and that people who stagnate choose their standing position with respect to the stream, but once they have stopped, priority shifts to them and the stagnant people influence the people walking.

Differentiating XR Modes to Study Pedestrian Behaviour during Fire Evacuations

Abhinav Azad*[1], Yan Feng[1], and Serge P. Hoogendoorn[1]

[1]Department of Transport & Planning, Delft University of Technology, the Netherlands

Abstract This study systematically evaluates Extended Reality (XR), encompassing Virtual Reality (VR), Augmented Reality (AR), and Mixed Reality (MR), to assess their effectiveness in simulating fire evacuations. Sixty-one participants completed evacuation tasks across four reality modes, including Physical Reality (PR), while their movement patterns, biometric signals, and subjective responses were recorded. This study examines differences in psychophysiological, tactical, and operational behaviours across XR modes in fire evacuations, with emphasis on their ecological validity.

Keywords XR, VR, AR, MR, Fire, Evacuation, Tactical, Operational, Pedestrian behaviour

Introduction

Understanding how individuals navigate fire evacuations is essential for improving emergency protocols and the safety of the built environment. Replicating such dangerous conditions in real-world settings poses significant ethical and safety concerns, making traditional pedestrian study methods impractical for analysing these behaviours [1]. However, fire hazards impose time-sensitive, high-risk decision-making demands, making it crucial to investigate tactical, operational, psychological, and physiological responses. Although VR has been extensively used to replicate hazards, concerns remain regarding ecological validity [2], navigation fidelity, and simulation sickness [4]. AR and MR introduce virtual fire hazards within real-world spaces, potentially enhancing behavioral realism [3]. This study evaluates VR, AR, MR, and PR to determine their ecological validity and effectiveness in simulating fire evacuations.

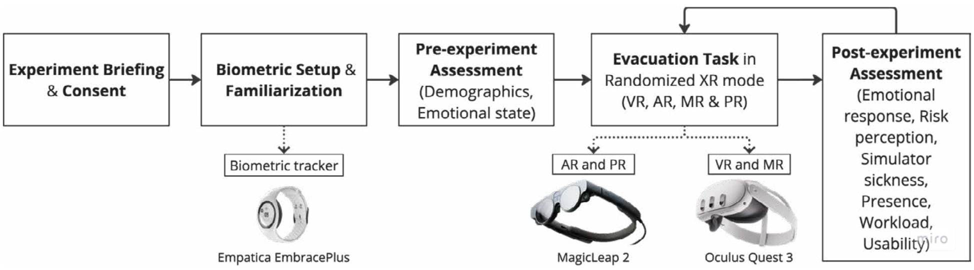

Figure 1: Schematic representation of the experimental procedure

Experimental Design and Setup

A G*Power analysis ($|\rho| = 0.25$, $\alpha = 0.05$, power $= 0.95$) determined a minimum required sample size of 44. To enhance statistical robustness, 61 participants (aged 18–50) were recruited, balanced between those familiar and unfamiliar with the environment.

The experiment followed a structured five-stage process: (1) briefing and consent, (2) biometric setup and familiarisation, (3) pre-experiment assessment, (4) four randomised evacuation tasks across XR modes (VR, AR, MR) and PR, ensuring equal distribution of XR modes as the initial task, and (5) post-experiment assessment. Biometric data were recorded using the Empatica EmbracePlus wristband, while XR evacuations were conducted using the Magic Leap 2 (AR, PR) and the Quest 3 (VR, MR). Tactical, operational, physiological, and subjective responses were recorded. To maintain consistency, all XR environments were developed in Unity 3D using identical 3D assets, visual settings, and audio cues.

*Email of the corresponding author: a.azad@tudelft.nl

The evacuations took place in the sixth-floor common area of TU Delft's Civil Engineering building. AR and MR conditions projected a simulated fire hazard into real-world space via Magic Leap 2 and Oculus Quest 3. The VR condition fully reconstructed the environment within Oculus Quest 3. The PR evacuation task (baseline) involved a real-life evacuation under a fire alarm without any simulated visuals using Magic Leap 2 headset to standardise data collection, ensuring consistency in sensory input across conditions.

Experiment Procedure and Data Collection

Ethical approval for the study was granted by the Human Research Ethics Committee (HREC) of the Delft University of Technology. Figure 1 outlines the experiment procedure, which lasted between 30 and 50 minutes per participant. During the experiment, positional tracking and physiological data were recorded, including evacuation time, route choice, exit selection, and obstacle collisions.

Physiological data, such as blood volume pulse (BVP), electrodermal activity (EDA), and wrist temperature, were recorded using the Empatica EmbracePlus wristband. Subjective measures were assessed through validated questionnaires evaluating risk perception, affective state, presence, simulation sickness, workload, and usability. To enhance validity, all experimental conditions were conducted under similar ambient lighting, temperature, and noise levels to mitigate confounding variables. Each session concluded with an open-ended debriefing to gather qualitative insights into the user experience.

Figure 2 presents biometric data from the Empatica EmbracePlus across all four tasks, illustrating trends in EDA, temperature, and BVP. Figure 3 visualises XZ evacuation trajectories, highlighting navigational differences among XR conditions for a pilot participant. Initial pilots reveal clear circumvention behaviour in XR-induced fire settings and significant trajectory deviations in PR, suggesting differences in hazard perception and route choices.

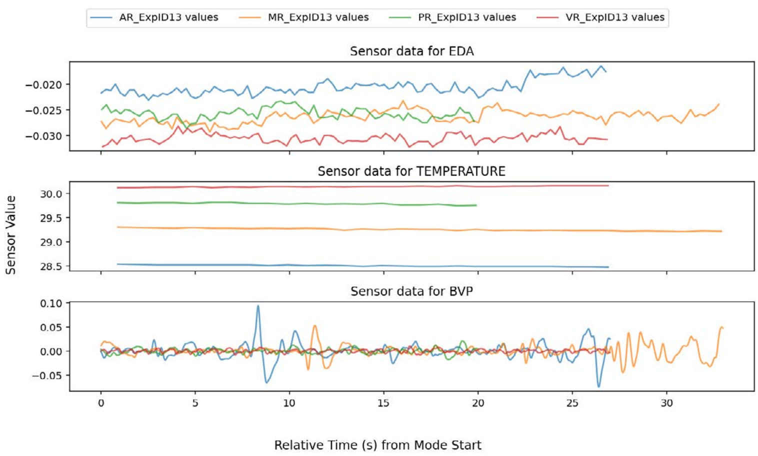

Figure 2: Empatica's biometrics data recorded across four tasks

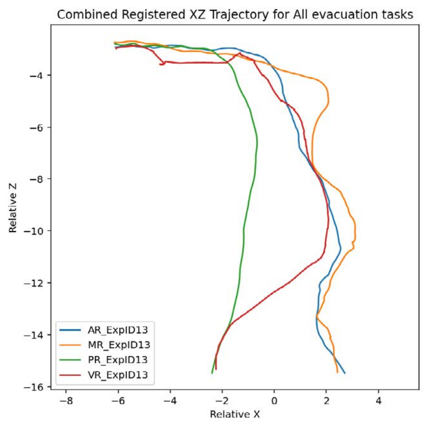

Figure 3: Pilot participant's evacuation trajectories across four tasks

The full paper will further examine how different XR modes replicate real-world evacuation behaviour by analysing spatial decision-making alongside psychological and physiological stress responses. Special emphasis is placed on the ecological validity of XR environments, and their implications for advancing fire evacuation research and safety training.

Bibliography

[1] Feng, Y., Duives, D., Daamen, W., Hoogendoorn, S., 2021. Data collection methods for studying pedestrian behaviour: A systematic review. *Build. Environ.* 187, 107329.

[2] Kinateder, M., Ronchi, E., Nilsson, D., Kobes, M., Müller, M., Pauli, P., Mühlberger, A., 2014. Virtual Reality for Fire Evacuation Research. *Federated Conference on Computer Science and Information Systems*, pp. 313–321.

[3] Ruggiero, L., 2018. A Review of Augmented Reality Applications for Building Evacuation. `https://doi.org/10.48550/arXiv.1804.04186`.

[4] Zhao, H., Thrash, T., Kapadia, M., Wolff, K., Hölscher, C., Helbing, D., Schinazi, V.R., 2020. Assessing crowd management strategies for the 2010 Love Parade disaster using computer simulations and virtual reality. *J. R. Soc. Interface* 17, 20200116.

Impact of individual preferences on route choice model parameters. A case study of Trondheim

Irene Hofmann*[1] and Trude Tørset[1]

[1]Department of Civil and Environmental Engineering/Norwegian University of Science and Technology

Abstract In this study, we developed a route choice model based on individual preferences to evaluate differences from the traditional revealed preferences approach. Employing a mixed-method approach, we conducted intercept surveys to identify key factors influencing route choice, which were converted into objective metrics to estimate a route choice model utilizing a GPS dataset. The model identified significant parameters, including route length, sidewalk width, traffic levels, presence of shops, and historic buildings. Our findings reveal that these parameters are consistent with those in traditional approaches.

Keywords pedestrian route choice, pedestrian behavior, GPS data, subjective measures, objective measures

Introduction

Recent research on pedestrian route choice mainly relies on revealed preference analysis. Researchers use different types of variables associated with route choice from the literature to predict pedestrians' route choices [1].

However, focusing only on revealed preferences might overlook the context of what pedestrians really prioritize. This well-established approach tends to explain behavior at a macro level rather than provide a deeper understanding [2]. Therefore, this research aims to integrate individual preferences into a route choice model to examine how the parameters of the route choice model change compared to traditional approaches. In this research, we answer the following research questions: What factors are important for pedestrians' route choice?(1), how do these factors differ from objective variables?(2), how do these parameters of the route choice model differ from the traditional approach?(3)

To address these research questions, we employed a mixed-method approach in a Trondheim's city center case study.

Method

In this research, we used a mixed-method approach. Initially, we conducted intercept surveys where pedestrians mapped their routes and identified segments as attractive or unattractive, explaining their choices. In total, the surveys included 25 participants. The attractive aspects of their routes were grouped into major categories with the following subjective variables: "community and atmosphere" such as being less crowded, very crowded, a lot ongoing and having shopping possibilities; "aesthetics and design" noted for nice architecture; "green spaces and nature integration" such as green and river views; "traffic and accessibility" focusing on ease of walking and route directness; and "noise and activity levels" characterized by quiet surroundings, no car traffic, or less car traffic. These subjective variables were translated into objective measures.

Subsequently, we calculated the level of agreement between the subjective and objective variables and estimated a route choice model for the city center using map-matched GPS data from 800 walking trips. Prior to estimation, two-sided t-tests were conducted to assess significant attribute changes between alternatives, and a correlation matrix among predictors was calculated.

The model was estimated using a conditional logit model including a path size factor. It considers the shortest path route and the reported route as alternative options. Routes with more than 70 % overlap were excluded from the analysis. One limitation is that individual preferences were applied to the GPS dataset rather than being directly derived from GPS-participants, which may lead to slight differences.

*Email of the corresponding author: irene.hofmann@ntnu.no

Results

1. Important factors for pedestrians' route choice in the city center

   70 % of the participants reported that they chose their route based on attractive features. The most important factors influencing their route choice were the presence of shops, nice architecture, absence of car traffic, and views of greenery and the river.

2. Differences between subjective and objective variables

   On average, the subjective and objective variables exhibited a moderate agreement of 65%. Excellent agreement, indicating no mismatch between perceived and objective variables, was observed for factors such as very crowded, recreational land use associated with "nice architecture", shopping possibilities, wider sidewalks associated with "easy to walk", and both no or reduced car traffic and river views. In contrast, poor agreement was noted for green views and crossing facilities (associated with "easy to walk"), indicating that there are more green spaces and crossing facilities than participants actually perceived.

3. Differences in route choice model parameters compared to traditional approaches

   Using a stepwise estimation approach, four different route choice models were developed. The results of the model with the best fit are presented in table 1.

Table 1: Final route choice model

Variable name	Beta	Z-Value	Sig
Route length	0,001	2,5	0,014*
Presence of shops	0,002	3,5	0,000***
Less car traffic	0,002	2,8	0,006**
Sidewalk width >3m	0,002	2,2	0,026*
Presence of historic buildings	-0,002	-3,2	0,002**
Pathsize factor	3,820	6,0	0,000***

This model includes route length, the presence of shops, reduced car traffic, wider sidewalks, the presence of historic buildings, and a path size factor. Except for the presence of historic buildings, all parameters have a positive sign, indicating a preference for routes with wider sidewalks, less car traffic, and more shops, aligning with literature findings [3]. Conversely, the presence of historic buildings has a negative sign, suggesting that people tend to choose routes with fewer historic buildings compared to the shortest path route. This may be because historic buildings often coincide with narrower sidewalks. The model's Akaike Information Criterion (AIC) of 1044, along with a pseudo R^2 of approximately 0.20, indicates that it accounts for about 20 % of the variance in the observed data.

Conclusion

In this study, we employed a mixed-methods approach to develop a route choice model for Trondheim's city center. Key predictors, including route length, sidewalk width, reduced car traffic, shopping opportunities, and the presence of historic buildings, were analyzed. While these predictors are commonly noted in existing literature, the inclusion of historic buildings is less frequent. A significant challenge was converting subjective factors into objective metrics, often encountering multicollinearity that necessitated their exclusion from the model estimation. Our findings confirm that this approach is consistent with traditional approaches.

Bibliography

[1] Basu, N., Haque, Md.M., King, M., Kamruzzaman, Md., Oviedo-Trespalacios, O., *A systematic review of the factors associated with pedestrian route choice*, Transport Reviews **42**, 672–694, 2022.

[2] Wozniak, M., Filomena, G., Wronkowski, A., *What's your type? A taxonomy of pedestrian route choice behaviour in cities*, Transportation Research Part F: Traffic Psychology and Behaviour **109**, 1257–1274, 2025.

[3] Basu, R., Sevtsuk, A., *How do street attributes affect willingness-to-walk? City-wide pedestrian route choice analysis using big data from Boston and San Francisco.*, Transportation Research Part A: Policy and Practice **163**, 1–19, 2022.

12th International Conference on Pedestrian and Evacuation Dynamics (PED 2025)
Prague, Czech Republic – September 9-12, 2025

Some benefits of high pedestrian density during flood evacuation

Xintong Li*[1,2], Nicolas Duthou[2], Weiguo Song[1], Jun Zhang[1], Alberto Gambaruto[2], and Nikolai W.F. Bode†[2]

[1]State Key Laboratory of Fire Science/University of Science and Technology of China
[2]School of Engineering Mathematics and Technology/University of Bristol

Abstract Flood evacuations often require walking through water, yet the impact of crowd density on pedestrian-water interactions remains understudied. This study uses 3D CFD simulations with the Volume of Fluid (VOF) method in *Simcenter Star-CCM+ v2302* software to analyze hydrodynamic forces on pedestrians. Results show that higher crowd densities reduce individual drag and water resistance due to wake shielding effects, similar to hydrodynamic clustering. These findings can improve flood evacuation models and strategies to minimize individual energy expenditure in water.

Keywords Pedestrian-water interaction, Flood evacuation, Wading simulation, CFD, Drag reduction

Introduction

In the context of emergency evacuations during flooding events, the interaction between pedestrians and water flow introduces significant hazards, often leading to catastrophic consequences. Investigating the dynamics of pedestrian movement in water, particularly the interaction mechanisms between pedestrians and water flow, holds significant research value.

Interestingly, natural phenomena provide potential insights. Yuan et al. [1] revealed through hydrodynamic modeling that ducklings swimming in single-file formation experience up to 158% drag reduction by positioning themselves in the wave troughs created by leading individuals, with this benefit propagating through the formation. For human movement, Li et al. [2] conducted a series of experiments in an 8-meter-long corridor within a swimming pool with a water depth of 0.60 m. Their fundamental diagram of speed versus density revealed that when the pedestrian density exceeds 1.10 ped/m^2, the inhibitory effect of density on speed in water is weaker than that observed on land. This phenomenon is likely influenced by the water flow generated behind moving pedestrians. However, whether pedestrians can benefit from the water flow induced by surrounding individuals remains an open question.

To address this question, we employed computational fluid dynamics (CFD) methods to conduct three-dimensional simulations of pedestrian movement in water. The primary objective was to explore the interaction mechanisms between pedestrians and water flow, specifically the relationship between pedestrian force and density under water flow conditions, rather than providing a detailed description of local fluid characteristics. We aim to determine from an energy consumption perspective whether individuals can derive benefits from the water flow generated by surrounding pedestrians.

Methods and Results

Simulations using the finite volume method were performed with software *Simcenter STAR-CCM+ (v2302)*, solving the incompressible and Newtonian Navier-Stokes equations. Specifically, three-dimensional CFD simulation was carried out using a Eulerian multiphase flow model and the volume-of-fluid (VOF) method to capture the interface of the two-phase water-air system. The computed solution provided a high-resolution description of the flow field and enabled the evaluation of the forces that act on pedestrians.

The Reynolds number was identified to be $Re_{air} = 2.1\times10^4$ in air (laminar flow) and $Re_{water} = 3.2\times10^5$ in water (transitional regime as $Re_{crit} = 4 \times 10^5$ for cylinders [3]), as such both a laminar solver and an Unsteady Reynolds-averaged Navier-Stokes (URANS) solver with $k - \omega$ SST turbulence modeling were employed. Standard no-slip boundary conditions were imposed to the modeled predestrians and the ground surface. To ensure solution accuracy, an adaptive timestepping scheme was used, in addition to surface reconstruction techniques and trimmed cell meshing which were employed to generate high-quality

*Email of the corresponding author: xintongli@mail.ustc.edu.cn
†Email of the corresponding author: nikolai.bode@bristol.ac.uk

computational grids. Adaptive mesh refinement was used to enable higher accuracy at the free surface interface and the pedestrian boundary layer. Several assumptions were made to simplify the simulation:

1. Pedestrians were modeled as smooth rigid bodies. Based on the average shoulder width of the individuals, each pedestrian was approximated as a cylinder of radius 0.2 m and height 1.7 m.
2. Pedestrians were stationary while the water flowed around them. This facilitates specifying a constant water momentum source term, while ensuring the relative velocity between pedestrian and the flow is appropriate

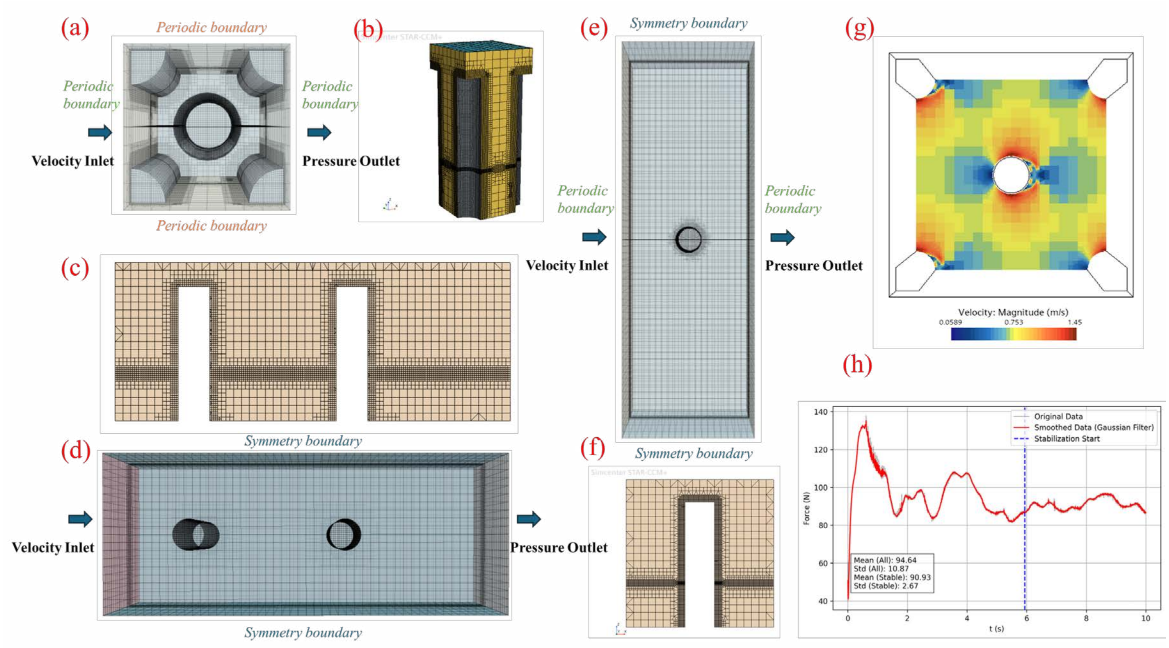

Figure 1: a). Boundary condition of crowd wading simulation; b). Mesh of crowd wading simulation; c). Mesh of dual-pedestrian wading simulation; d). Boundary condition of dual-pedestrian wading simulation; e). Boundary condition of single-file wading simulation; f). Mesh of single-file wading simulation; g). The velocity magnitude field result of crowd wading simulation; h). Time series of pedestrian surface drag.

Based on these assumptions, three simulation scenarios were designed: staggered crowd wading simulation (Figure 1a), dual-pedestrian wading simulation (Figure 1d), and single-file wading simulation (Figure 1e). For crowd wading simulations, periodic boundary conditions were imposed to replicate a large, regularly spaced, crowd, where Figure 1a represents a simplified pedestrian unit within the collective movement. The pedestrian density was varied by adjusting the size of the computational domain. In the dual-pedestrian wading simulation, symmetric boundary conditions with momentum loss compensation were set to establish a quantitative relationship between pedestrian spacing and hydrodynamic forces. Furthermore, a single-file wading simulation was conducted with periodic boundaries, where density variations were again achieved by modifying the domain size. The pedestrian surface forces over time at different densities (Figure 1h) and the corresponding water flow characteristics (Figure 1g) were obtained throughout these simulations. Our preliminary findings suggest that, at a constant velocity, the drag force experienced by pedestrians decreases as pedestrian density increases. These insights could help refine flood evacuation models and inform new strategies to reduce individual energy expenditure in critical water-related scenarios.

Bibliography

[1] Z.-M. Yuan, M. Chen, L. Jia, C. Ji, A. Incecik, *Wave-riding and wave-passing by ducklings in formation swimming*, Journal of Fluid Mechanics **928**, 1-11, 2021.

[2] X. Li, H. Yu, W. Song, J. Zhang, Z. Zhan, X. Ren, H. Xu, *Fundamental diagrams for straight movement of pedestrians in water*, Safety Science **159**, 106018, 2023.

[3] Schlichting, Hermann, and Klaus Gersten. Boundary-Layer Theory. Berlin, Heidelberg: Springer Berlin Heidelberg, 2017. https://doi.org/10.1007/978-3-662-52919-5.

Timetable
Poster index

12th International Conference on Pedestrian and Evacuation Dynamics (PED 2025)
Prague, Czech Republic September 9-12, 2025

Impact of Distribution Shape on Simulated Evacuation Times: Sensitivity Analysis of Agent Parameters

Juraj Kmec*[1], Pavel Hrabák[1], and Daniel Vašata[1]

[1]Faculty of Information Technology, Czech Technical University in Prague

Abstract This study examines how sampling agent velocity and diameter from uniform and truncated normal distributions affects evacuation simulations under different bottleneck conditions. In unconstrained geometries, distribution shape significantly affects evacuation time, while bottlenecks increase the contribution of inherent randomness. Sensitivity analysis reveals mean velocity as the most influential parameter, while parameters related to agent diameter have a comparatively smaller impact on total evacuation time.

Keywords Pedestrian dynamics, Sensitivity analysis, Uncertainty analysis, Agent heterogeneity

Introduction and Problem Setup

Simulating microscopic pedestrian movement requires defining probability distributions for the physical properties of agents. Real-world crowds are often heterogeneous in both their physical parameters and their behavior. One can disregard this variability and simply set every relevant parameter to a constant average value; however, such a homogeneous group may exhibit excessively uniform and robotic behavior, leading to an overly optimistic bias in total evacuation time (TET) or other selected metrics. This contribution examines the effect of sampling selected physical agent properties (free-flow velocity and diameter) from distinct probability distributions (uniform and truncated normal) in a common geometrical setting with multiple bottleneck configurations. A sensitivity analysis is conducted on the location parameters of the distributions (minimum/maximum and mean), as well as an uncertainty analysis of the randomness introduced by the sampling process and the inherent uncertainty in human behavior.

In the Pathfinder simulator, we modeled a common geometrical setting consisting of an initial room of size $5\,\mathrm{m} \times 4\,\mathrm{m}$ connected to a 10 m long and 2 m wide corridor. The exit is located at the far end of the corridor. A bottleneck is placed either at the beginning of the corridor (*early bottleneck* scenario), just before the exit (*late bottleneck* scenario), or not at all (*no bottleneck* scenario). The initial room contains 40 occupants whose goal is to reach the exit. For comparison purposes, the uniform and truncated normal distributions are always normalized to the same range, since the density near the edges of the distribution was observed to significantly influence the total evacuation time [1]. The uniform distribution is fully parametrized by two numbers – in this case we chose the mean, as it is often the only quantity with available empirical measurements; and one of the minimum/maximum pair as we want to determine the sensitivity of TET to a change in the bounds of the distributions (slowest and/or largest occupant). For consistency, we also parametrized the truncated normal distributions with the same two numbers – the second truncation point of the distribution is computed symmetrically around the mean, and the variance is set such that the variance of the unbounded distribution would be equal to that of the uniform one. The values for the mean were chosen based on the simulator defaults and available literature. The bounds of the distribution were designed so as to avoid unrealistically low or high values. Each simulation is repeated 3 to 5 and the results averaged to account for some of the inherent stochasticity of the model.

Simulation Results

We initially assess the effects of distribution shape by comparing the TET values obtained from various parameter samples. The bounds of the distributions in this case were fixed at 0.7 m/s–1.7 m/s for velocity and 0.35 m–0.55 m for diameter. The analysis reveals distinct patterns across geometric configurations. The lack of a bottleneck in the first scenario allows for easy overtaking, limiting the ability of the slower agents to impede others. This results in faster evacuation times when sampling parameter values

*Email of the corresponding author: `juraj.kmec@fit.cvut.cz`

from a truncated normal distribution, as there are, on average, fewer agents significantly slower than the mean. The introduction of a bottleneck disrupts this relationship, leading to a considerably larger overlap between the TET values for different distribution types, suggesting that geometric constraints diminish the impact of the distribution shape on evacuation outcomes. Further analysis reveals that the average of the sampled velocity values is a robust predictor of TET regardless of bottleneck placement or distribution type, with only the intercept term of the regression line varying significantly between configurations (Fig. 1). This consistent linear association suggests that macroscopic flow characteristics remain fundamentally similar despite geometric variations, although the absolute evacuation time is affected by the presence and location of bottlenecks. The diameter distribution has a largely negligible effect on TET, which is consistent with previous research.

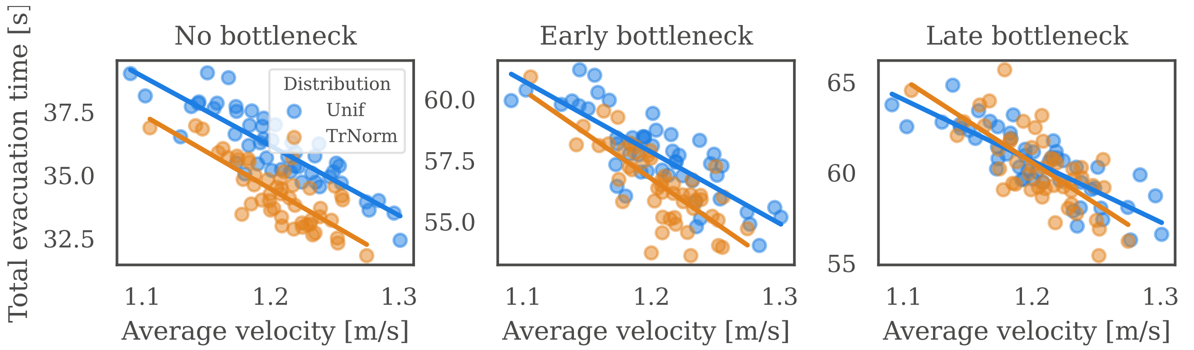

Figure 1: Mean sampled velocity as a predictor of TET.

To better understand TET variability, we applied the Law of Total Variance: $\mathrm{Var}(Y) = \mathrm{Var}(\mathbb{E}[Y|X]) + \mathbb{E}[\mathrm{Var}(Y|X)]$, allowing us to attribute the variance components to different sources. This analysis reveals that without bottlenecks, distribution parameters account for approximately 54% of TET variance, with sampling variability contributing 39% and inherent randomness only 6%–8%. In bottleneck scenarios, the inherent randomness becomes substantially more significant (34%–41%), while the effect of the distribution parameters decreases to 30%, suggesting that in constrained geometries, stochastic pedestrian interactions play a significant role in the overall evacuation dynamics. The standard deviation of TET also increases with geometric complexity, from 2 s without bottlenecks to almost 5 s with a late bottleneck.

To quantify the impact of individual distribution parameters on TET, we computed Sobol' total effect indices (S_T), which measure the percentage of variance that would be lost if a parameter were fixed to an arbitrary (reasonable) value. Table 1 illustrates how parameter importance varies across different geometries. In the no-bottleneck scenario with a uniform distribution, the minimum velocity dominates ($S_T = 0.75$) as the slowest agents determine the evacuation time when overtaking is possible. With a truncated normal distribution, the mean velocity becomes more influential ($S_T = 0.57$). In bottleneck scenarios, the mean velocity consistently shows the highest sensitivity regardless of the distribution type, reaching $S_T = 0.90$ with truncated normal distributions in the early bottleneck configuration. The diameter parameters consistently show lower sensitivity indices in all scenarios (maximum $S_T \approx 0.30$), confirming velocity as the primary determinant of evacuation times.

Table 1: Total-effect indices for different parameters and geometry–distribution pairs.

Geometry	Distribution	$\mathrm{Min}_{\mathrm{vel}}$	$\mathrm{Mean}_{\mathrm{vel}}$	$\mathrm{Max}_{\mathrm{diam}}$	$\mathrm{Mean}_{\mathrm{diam}}$
No bottleneck	Unif	**0.75**	0.32	0.07	0.10
	TrNorm	0.45	**0.57**	0.09	0.10
Early bottleneck	Unif	0.32	**0.68**	0.08	0.23
	TrNorm	0.35	**0.90**	0.11	0.19
Late bottleneck	Unif	0.14	**0.67**	0.15	0.30
	TrNorm	0.10	**0.73**	0.12	0.28

Bibliography

[1] Kmec, J., Hrabák, P., Vašata, D., Bode, N. W. F., *Modelling Physical Heterogeneity of Agents by Means of Correlated Distributions*, Submitted to Web of Conferences Journal (EDP Science), Proceedings of Traffic and Granular Flow 2024, Lyon, November 2024.

12th International Conference on Pedestrian and Evacuation Dynamics (PED 2025)
Prague, Czech Republic – September 9-12, 2025

Two frameworks to identify crowd risks, monitoring metrics and assessment thresholds

Dorine Duives*[1] and Lucia van Schaik[1]

[1]Active Mode Lab/Delft University of Technology

Abstract Within this contribution, we extend [1] analysis into two connected frameworks, the Crowd Risk Identification (CRI) framework, which identifies the main crowd incident risks of a pedestrian space, and the Crowd Risk Assessment Metric (CRAM) framework, which determines which metrics are best suited to quantify those crowding risks by means of a crowd monitoring scheme. In combination, the CRI and CRAM frameworks allow crowd managers to systematically use crowd monitoring systems to monitor crowding risks.

Keywords Crowd management systems, Risk assessment, Crowd dynamics, Guidelines

Introduction

In a crowd, danger or harm to individuals is caused by events including falling, fainting, or being trapped between people, objects, or infrastructure. These are instances indicative of loss of physical control and/or loss of consciousness and could lead to personal injuries, such as blunt trauma, musculoskeletal trauma, and compressive/traumatic asphyxia.

In essence, crowd management revolves around ensuring that all individuals in the crowd are not exposed to conditions where they could lose physical control and/or consciousness. Yet, it is often difficult to establish precisely when a situation moves from being safe to being unsafe. Therefore, in engineering and planning, usually a slightly different formulation is adopted, namely 'crowd incident risk'. Yet, how to identify crowd incident risks systematcially? And if we know which risks to look out for, how can we monitor those risks?

This contribution presents two connected frameworks that systematically identify crowd incident risks and required metrics and thresholds to monitor those risks.

Crowd Risk Identification model

The CRI framework aims to help understand how crowd incidents evolve by structuring relevant information. It helps identify critical conditions that may lead to a crowd incident. Knowledge regarding the events leading up to a crowd incident can be used to anticipate crowd incidents during the planning phase and/or the crowd management operation.

The CRI framework's structure is quite simple and comprises four parts (see figure 1):

- **Adverse environmental conditions:** The conditions leading up to the adverse crowd condition.
- **Adverse crowd conditions:** The conditions inside the crowd leading up to the crowd incident.
- **Crowd incident:** One or more individuals lose control and cannot recover.
- **Consequences of incident:** The physical consequences for any individual in the crowd directly resulting from the incident.

One can use the framework to identify crowd incident risks in two ways. Firstly, one can start by listing the most probable adverse environmental conditions and, accordingly, working forward to identify the adverse crowd dynamics, crowd incidents, and consequences resulting from these environmental conditions, given that one is not proactively intervening in the scenario. Secondly, one can also start by listing the most probable crowd incidents and reason backward to identify the adverse crowd conditions and adverse environmental conditions that might potentially cause these crowd incidents.

*Email of the corresponding author: d.c.duives@tudelft.nl

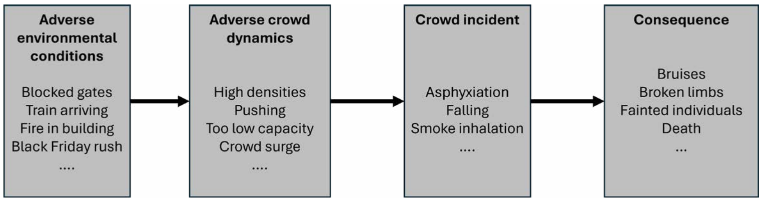

Figure 1: Visualization of Crowd Risk Identification framework.

Table 1: Excerpt of the CRI and CRAM framework implementation.

No.	Crowd incident risks	Metrics	Thresholds
1	Overcrowding of the square	Density	$2P/m^2$
2	Evacuation of the square	Number of people	$50.9\text{m} * 2.25P/m/s * 15\text{min} = 103,073\text{P}$
3	Turbulence on the square	Max. density	$7P/m^2$
4	Entry soccer spectators	Number of people	$(4300 - 500) * 2 - 10\% * 15700 = 6,030P$
5	Fire truck on the square	Number of people	$(4300 - 500 - 10 * 4) * 2 = 7,520P$
		Density	$2P/m^2$
	Final thresholds	Max density	$7P/m^2$
		Number of people	$6,030\text{P}$

Crowd Risk Assessment Metric (CRAM) framework

The CRAM framework aims to identify which metrics and thresholds are relevant to monitor crowd incident risks. It uses the CRI framework as a backdrop. In essence, the CRI framework identifies failure routes. The Swiss cheese model of [2] suggests that effective crowd management mitigates crowding risks by breaking the potential failure routes. This means that the risk metrics and thresholds need to be established so that adverse environmental conditions do not lead to adverse crowd dynamics.

Consequently, we can use the list of adverse crowd dynamics established in the CRI framework to identify the crowding risk assessment metrics. To do so, we translate each adverse crowd dynamics condition into a physical property of the crowd.

Example case study - Carnaval 2025

To test the two frameworks, we have applied both to a national public event in the Netherlands. During this event, large crowds gather on one of the main squares of Breda to meet and party for three days. The square features a large music stage and a number of bars. Crowd monitoring systems are in place on the square and the routes leading up to the square. Yet, which metrics should be used to quantify the crowd incident risks, and which thresholds should be applied per metric?

The CRI and CRAM frameworks were applied to determine the relevant metrics and thresholds for this case. Multiple failure routes have been identified, five of which are mentioned in table . A metric and threshold were defined for each failure route using state-of-the-art literature featuring crowd dynamics. The last three rows of table display the results of the CRAM analysis. Among other works, the Handboek Evenementenveiligheid [3], the Dutch building decree [4], and the works of [5] and [6] have been used to derive relevant numbers. In the full paper, we extend this analysis to account for all relevant crowd incident risks and present a complete flowchart connecting failure routes to metrics and relevant thresholds.

Bibliography

[1] van Schaik, L., Duives, D.C., Hoogendoorn, S.P. *Three indicators to assess crowd safety*, Proceedings of Traffic & Granular Flow.

[2] Reason, James *The contribution of latent human failures to the breakdown of complex systems.* Philosophical Transactions of the Royal Society of London. B, Biological Sciences, **327(1241)**, 475-484, 1990.

[3] Stichting Evenementen Handboek, *Een gemeenschappelijk denkkader omtrent veiligheid*, **1**, 2019

[4] Informatiepunt Leefomgeving, *Inhoud Besluit bouwwerken leefomgeving*, url: https://iplo.nl/ regelgeving/ omgevingswet/ inhoud/besluit-bouwwerken-leefomgeving/

[5] Daamen, W., Hoogendoorn, S. *Capacity of doors during evacuation conditions.* Procedia Engineering, **3**, 53-66, 2010.

[6] Helbing, D., Johansson, A., Al-Abideen, H. Z. *Dynamics of crowd disasters: An empirical study.* Physical Review E—Statistical, Nonlinear, and Soft Matter Physics, **75(4)**, 046109, 2007.

12th International Conference on Pedestrian and Evacuation Dynamics (PED 2025)
Prague, Czech Republic – September 9-12, 2025

Data fusion, state estimation and short term demand prediction for crowd management at SAIL2025

Winnie Daamen*[1], Theivaprakasham Hari[1], Yanyan Xu[1], Yanan Xin[1], Sascha Hoogendoorn-Lanser[1], and Serge Hoogendoorn[1]

[1]Delft University of Technology, the Netherlands

Abstract Every five years, the SAIL event in Amsterdam attracts millions of visitors, making it the largest free event in the Netherlands. We will apply AI models for data fusion, state estimation, and short-term demand prediction using a wide variety of data sources. These data do not only relate to visitor flows and densities, but also to other modes (bicycle, car, and public transport), to identify arrivals and departures of the SAIL visitors. We aim to make the AI models transferable and scalable such that they can also be used at other large scale events.

Keywords crowd management, data fusion, state estimation, short-term demand prediction

Introduction

Every 5 years tall ships from all over the world have been coming to Amsterdam. Over the years, the SAIL event has become the largest free event in the Netherlands. In 2025, SAIL will be extra special, as it combines the 750th anniversary of Amsterdam, the 50th anniversary of SAIL, and the 10th edition of the world's biggest nautical event. This implies that the 5 day event might attract even more than 2-3 million visitors, which was the case in previous editions. To manage such large visitor flows, an extensive crowd monitoring and management organization is set up. For effective performance of crowd management, input is needed on the visitor flows, both real-time using sensor data and for the (near) future using predictions through models. Our research focuses on accurate crowding assessments using data fusion and traffic state estimation and short-term predictions for real-time interventions, all based on AI models.

This research is part of a broader initiative called Aim-TT, which is short for AI Learning Initiative for Multi-modal Traffic and Transportation. This initiative creates a Learning Community, which are long-term strategic collaborations that offer a practical approach for enterprises and civil society organizations to enhance AI knowledge and skills while partnering with AI experts on an educational level. SAIL is a first use case to explore the opportunities of AI for crowd monitoring and management. The use case aims to ensure that the data types, methods, and insights gained during SAIL are preserved and applied not only throughout the SAIL organization but also at other events and by other organizations.

Method

Key in AI models is the presence of data. The first step in this use case is, therefore, to create an overview of all available data sources. The data contain event-specific information (including schedules and historical crowd movement patterns), social media activity, mobile app interactions, weather conditions, and traffic patterns (not only for pedestrians, but also for other modes). More specifically, we intend to use the following data sources:

- Pedestrian density, flow, and sentiment (aggregated as the result of on-device analysis by an image sensor; no video is processed).
- 3D drawings with event layout.
- Bicycle counts (aggregated, number, direction).
- Numbers of passengers boarding and alighting bus, metro, and ferry (aggregated).

*Email of the corresponding author: `w.daamen@tudelft.nl`

- Numbers of passengers boarding and alighting trains (aggregated).
- Traffic flow on highways (aggregated).
- Planned road closures (geo-data) (Melvin data for roads, as well as proprietary event data in geometric form).
- Unplanned blockages (geometry).

Using exploratory data analysis, the characteristics of these data can be understood, patterns can be identified, and anomalies detected. The results of the analysis are input for feature engineering and selection of AI models.

There are a wide variety of AI models to estimate and predict visitor flows and comprehensive insights into crowd dynamics. For this use case, we will look at multitask AI and transfer learning models, given the wide range of model outcomes and the fact that SAIL is a 'one-of-a-kind' event, for which only limited historical data exist. We intend to adapt models for unique events, ensuring applicability to various scenarios and future editions of the SAIL event.

For the actual application within this use case, we combine planning, real-time data, and predictive analytics to provide short-term forecasts. The information will run as a 'shadow' application during the event, to show crowd managers its possibility, without interfering the day-to-day operations.

After the SAIL event, we will continue to improve the models using historical and real-time data. Not only from the SAIL event, but also from other events and situations. In this way, we ensure the accuracy and reliability of the models.

Results

The results will depend on the models being applied to the SAIL data. As the event is still to come, no results are available yet. Figure 1 gives an example of a forecasting result, using historical data of counts at a cross-section as a starting point to forecast the counts over the coming time period. The interaction with the crowd managers during SAIL will help to improve the visualisation of the results, in order to make them intuitive and easy to use in practice.

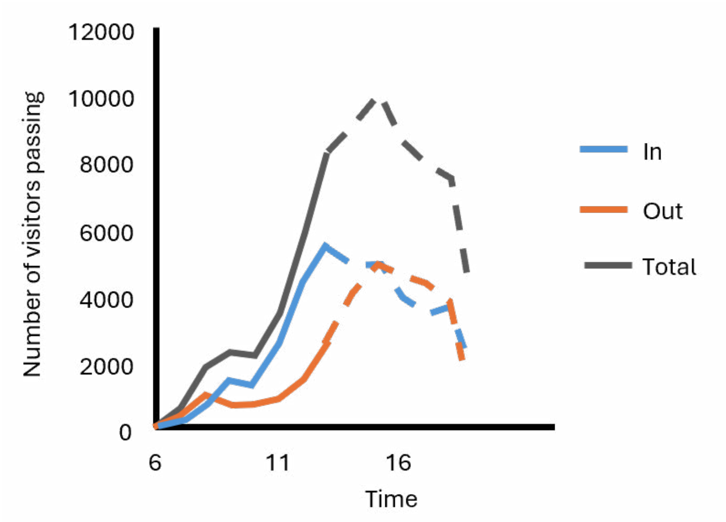

Figure 1: An example of short-term forecasting results, where the dotted lines indicate the forecasts.

Conclusions

After the SAIL event, we will assess not only the quality of the models, but also their applicability during SAIL and other large scale events. Moreover, we will see how, and to what extent, it will be possible to use AI in crowd monitoring and management, not only for researchers, but also for practitioners.

12th International Conference on Pedestrian and Evacuation Dynamics (PED 2025)
Prague, Czech Republic – September 9-12, 2025

Pedestrian movements on stairs in metro stations – an empirical study

Lakshmi Devi Vanumu[1], K. Ramachandra Rao[*,2,3], and G. Tiwari[3]

[1]Transportation Researcher, Vadodara, India
[2]Department of Civil Engineering, IIT Delhi, New Delhi, India
[3]Transportation Research and Injury Prevention Centre, IIT Delhi, New Delhi, India

Abstract Empirical data on pedestrian movements on stairs in the underground metro stations with Uni and bidirectional movements can help assess the evacuation strategies. This study attempts to understand the movements on stairs in various groups, through large sample data (more than 10,000). Congested regimes being rare, are generated through simulations. The design specific flows obtained are comparable, will facilitate in establishing the safe operating zones.

Keywords Stairs, ascending, descending, uni-directional and bi-directional flows, simulations 5

Introduction

Stairways are considered as one of the most important parts of egress routes in the metro stations. Understanding the evacuation dynamics of pedestrians on stairs is crucial particularly to analyse the emergency situations. Since the beginning of research on pedestrian movements on stairways [1], there has been a considerable interest over the past five decades on this topic. This owes partly to the fact that stairways have become one of the means to access to public transport terminals, particularly rail-based modes, which have been an integral part. The rapid proliferation of metro rail systems in many parts of the world (particularly in India and China), primarily has made the stairways as one of the important access points. Further, in evacuation situations stairways are the safe means of egress from the underground metro system.

Data collection in pedestrian movements in a metro station is a bit involved. Usually, it would be difficult to get permissions. A typical pedestrian movement study entails, i) field or empirical data collection, ii) experiments with pedestrian subjects and iii) simulations. In these approaches experiments are generally not permitted on the premises of underground metro stations, thus leaving the option of data collection at the site or simulations. To get a good estimate of the flows, gathering field/empirical data at site will be useful, there are some recent studies on the pedestrian flow measurements on the stairs of the metro stations [2]. Further, few other studies focus on the modelling of the pedestrian movements besides performing simulations [3,4]. There is a gap on how one interprets the data collected on stairs in the underground metro stations. This paper attempts to investigate the data collected extensively on the stairs of the Delhi metro stations. Statistical analysis of the empirical data was conducted to analyse the specific flows, speeds (ascent and descent) and compare with the existing standards/guidelines. For emergency evacuations or collecting data in the congested conditions, simulations were carried out. A detailed cross-sectional data was studied to understand the effect of age group, gender and the luggage carried.

Uni-directional and bi-directional movements

Specific flow – Density relationship for unidirectional pedestrian movements on ascending and descending stairs were obtained. The results of the present study were compared with fundamental diagrams (FD's) under various planning guidelines, empirical and experimental studies from the existing literature (Fig 1 (a) and (b)). A significant difference exists between ascending and descending speeds for stairs; ascending speeds are 15% lower

* Email of tne corresponding author: rrkalaga@civil.iitd.ac.in

than descending speeds. Further, the maximum specific flows for the bi-directional flows are lower compared to uni-directional flows. Simulation studies were performed to study the outcomes where the empirical data is unavailable in the congestion regimes.

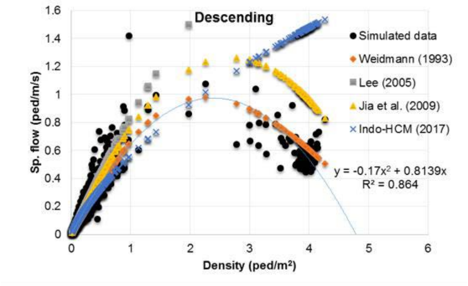

a)

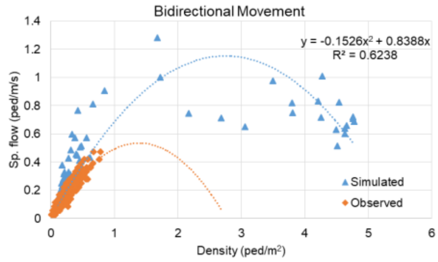

b)

Figure 1: a) Uni-directional, a) Bi-directional movements.

Cross-sectional studies

Extensive studies were carried on the various attributes of pedestrians such as gender, age group and luggage carried and their effect on the speeds. Males show higher average speeds compared to their female counterparts. When conducting pairwise analysis, it was found that there was no significant difference between children and elder pedestrian speeds both in uni and bidirectional movements. While conducting the pairwise analysis, it was found that there was no significant difference between the speeds of pedestrians with no luggage and medium luggage. The speeds in the bidirectional movements are higher compared to unidirectional movement for all the luggage categories except when the pedestrians carry a child.

All the results presented here are specific to the metro stations. Efforts can be made to conduct these types of studies in other transport facilities such as bus terminals, railway stations and airports to get an overall view and enabling robust design of the terminals.

Bibliography

[1] Fruin JJ. Pedestrian planning and design, 1971

[2] Goyal T, Kahali D, Rastogi R. Analysis of pedestrian movements on stairs at metro stations. Transportation research procedia. Jan 1;48:3786-801, 2020

[3] Liu MW, Wang SM, Oeda Y, Sumi TN. Simulating uni-and bi-directional pedestrian movement on stairs by considering specifications of personal space. Accident Analysis & Prevention. Jan 1;122:350-64, 2019.

[4] Qu Y, Gao Z, Xiao Y, Li X. Modeling the pedestrian's movement and simulating evacuation dynamics on stairs. Safety science. Dec 1;70:189-201, 2014..

12th International Conference on Pedestrian and Evacuation Dynamics (PED 2025)
Prague, Czech Republic – September 9-12, 2025

SHAPES: An open-source code base to generate realistic pedestrian shapes and simulate mechanical contacts in two dimensions

Maxime Stapelle*[1], Oscar Dufour[1], and Alexandre Nicolas[1]

[1]Université Claude Bernard Lyon 1, CNRS, Institut Lumière Matière (ILM), 69100 Villeurbanne, France.

Abstract We present the outcome of the SHAPES project, an open-source codebase designed to facilitate agent-based modelling of pedestrian dynamics. It serves two purposes. First, a graphical interface generates 2D and 3D realistic shapes for pedestrians, based on anthropometric data, and can spawn them randomly in space to create a synthetic crowd. Secondly, a shared library, implemented in C++ but callable from Python, is provided to handle mechanical contacts and collisions between agents (and/or static obstacles) in 2D.

Keywords Agent-based modelling, Pedestrian Dynamics, Shapes, C++, `Python`

Extended abstract

The SHAPES project is part of the broad subject of the modelling of pedestrian crowds. Its purpose is to make publicly available, in a convenient way, two features of recent work initiated in [1] and extended in [2]:

- *The ability to model humans by shapes more complicated than a disk or an ellipse.* Basing ourselves on [4], we model a top view (2D) of a pedestrian by the contour of 5 disks (Figure 1). The use of such shapes allows to reach higher densities of pedestrians – typical of mass events, as well as to reproduce the “sneaking” behaviour commonly observed in pedestrians.

  We also offer the possibility to obtain a 3D view of a human in the form of layers of polygons (Figure 2), based on the actual slices of two cadavers done in [4]. In order to generate crowds of such 3D models, the tool can compute realistic variants through a suitable homothety of the polygons.

- *The handling of mechanical evolution of the agents, including collisions, whose treatment is inspired by the physics of granular media.* Given a 2D setting of an assembly of agents, including driving forces and torque for each of them and a duration, this second part will take care of the mechanical evolution of the agents in time.

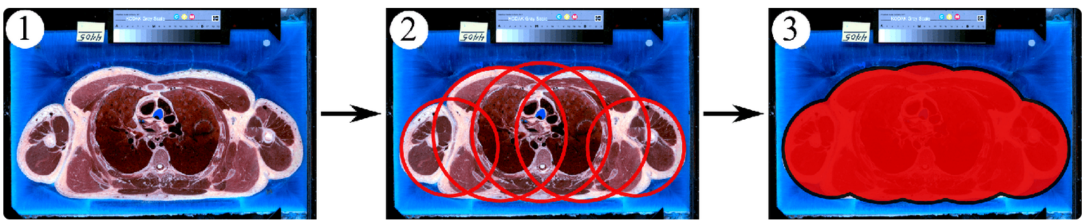

Figure 1: A slice taken at the height corresponding to the bideltoid breadth (coming from [4]), the approximation by 5 disks, and the resulting shape.

The first feature presents itself in the form of a graphical user interface running a `Python` backend, allowing to generate 2D and 3D (Figure 2) realistic shapes of humans, as well as to generate a random distribution of a number of pedestrian in a certain area (Figure 3). The user has direct access to the original data in [4] and [3].

*Email of the corresponding author: `maxime.stapelle@univ-lyon1.fr`

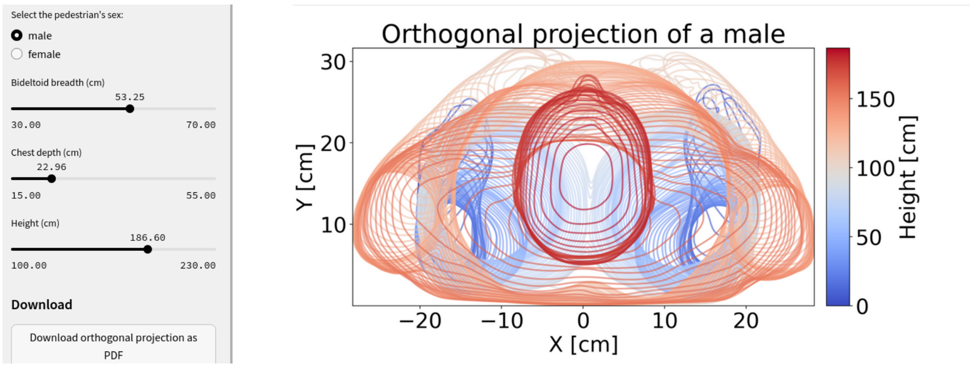

Figure 2: A top view of the layers of polygons derived from the slices in [4], reproducing a realistic shape of the human body. We show here the image embedded in our graphical user interface.

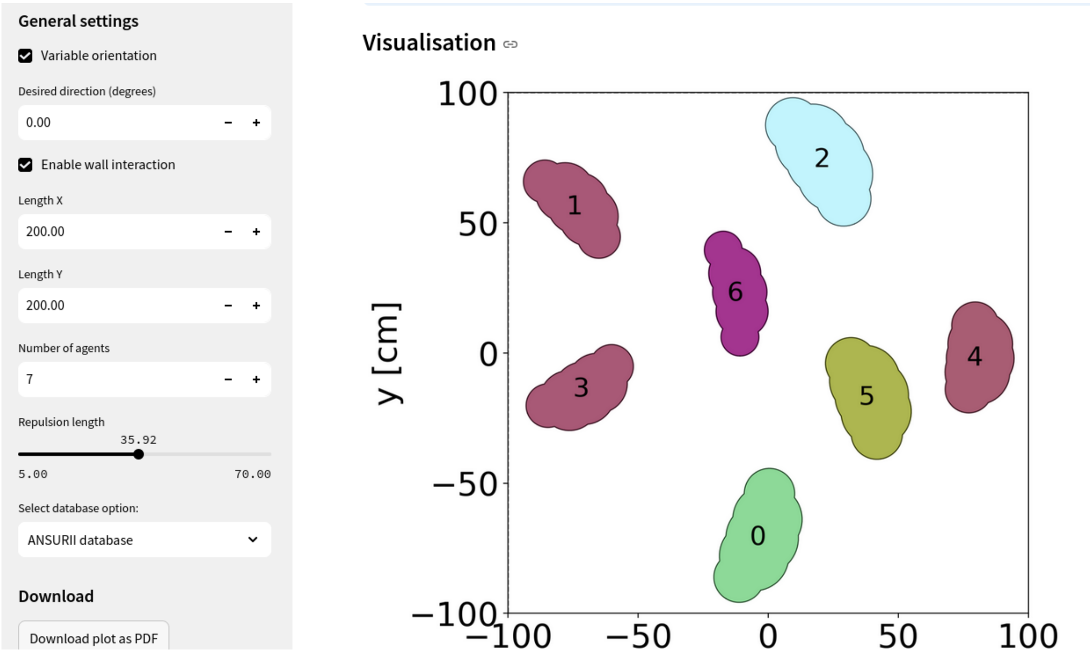

Figure 3: An example of randomly generated crowd.

The second feature is a C++ shared library, easily callable from `Python`. It supports XML files as input and output, for convenience and human-readibility, and takes a setting of pedestrians (positions, size of shapes, orientation...) as well as driving forces and torques given for each of them, and evolves the positions of the agents according to the mechanical laws of granular dynamics, duly handling possible collisions. Users can define their own materials. The output of the library, on top of the new state of each agent, will include the forces on each shape, allowing computation of the pressure exerted on each agent.

Bibliography

[1] Echeverría-Huarte, I., Nicolas, A., *Body and mind: Decoding the dynamics of pedestrians and the effect of smartphone distraction by coupling mechanical and decisional processes*, Transportation Research Part C: Emerging Technologies **157**, 2023.

[2] Dufour, O., *Enhanced agent-based models for pedestrian crowds: insights from empirical data at the Festival of Lights and refinements of mechanical interactions, pedestrian shapes, and decisional aspects*, PhD Thesis, Université Claude Bernard Lyon1, 2024, `https://theses.hal.science/tel-04953804v1` .

[3] Gordon, C.C., Blackwell, C.L., Bradtmiller, B., Parham, J.L., Barrientos, P., Paquette, S.P., Corner, B.D., Carson, J.M., Venezia, J.C., Rockwell, B.M., Mucher, M., Kristensen S., *2012 anthropometric survey of u.s. army personnel: Methods and summary statistics. Technical report*, Defense Technical Information Center, 2012a, `https://apps.dtic.mil/sti/citations/ADA611869` .

[4] U.S. National Library of Medicine, *Visible human project*, 1994, 1995, `https://datadiscovery.nlm.nih.gov/Images/Visible-Human-Project/ux2j-9i9a/about_data` .

12th International Conference on Pedestrian and Evacuation Dynamics (PED 2025)
Prague, Czech Republic – September 9-12, 2025

Top-View Multi-Camera Pedestrian Tracking for Enhanced Evacuation Dynamics Analysis

Hongliu LI[1] and Jacqueline Tsz Yin LO*[1]

[1]Department of Civil and Environmental Engineering, The Hong Kong Polytechnic University, China

Abstract Real-time tracking is crucial for understanding pedestrian dynamics, particularly in evacuation scenarios where timely information can enhance safety and efficiency. This study presents a real-time top-view multi-camera pedestrian tracking method using YOLOv8 and DeepSORT for detection and tracking. We propose a novel cross-camera ID matching technique based on cosine similarity of features and bounding box distance differences in real-world coordinates. Our approach effectively tracks pedestrians across multiple top-view cameras, improving the understanding of evacuation dynamics in complex environments.

Keywords Multi-camera tracking, Top-view perspective, Pedestrian dynamics, Real-time detection, ID matching

Introduction

Understanding pedestrian dynamics is important for enhancing safety and efficiency of pedestrian flow, particularly during emergency evacuations. Real-time tracking can provide critical insights into movement patterns, crowd behavior, and potential bottlenecks, aiding decision-making. While many studies have focused on flat-view tracking, top-view perspectives remain underexplored despite their advantages in monitoring crowd behavior and ensuring privacy.

The top-view perspective provides a comprehensive overview of pedestrian movements, facilitating the identification of interactions and flow patterns that may be obscured in flat-views. This characteristic is particularly beneficial in complex environments, where occlusions and varying angles can hinder tracking accuracy. However, the applications of top-view multi-camera tracking are still limited, hindering our understanding of pedestrian dynamics in critical scenarios.

Recent advances in computer vision, such as YOLOv8 [1] for object detection and DeepSORT [2] for pedestrian tracking, have improved real-time monitoring capabilities.

This study proposes a top-view multi-camera pedestrian tracking method, combining YOLOv8 and DeepSORT with a novel cross-camera ID matching technique based on cosine similarity of features and bounding boxes spatial relationships. By addressing the challenges of top-view cross-camera tracking, our approach aims to provide a robust solution for monitoring pedestrian dynamics during evacuations, ultimately contributing to improved safety and efficiency in emergency management.

Method

This study proposes a top-view multi-camera pedestrian tracking method, integrating advanced object detection and tracking algorithms to enhance the accuracy and robustness of pedestrian monitoring in evacuation scenarios. The methodology consists of the following key components:

Camera setup and calibration: Multiple cameras are strategically positioned to cover the area of interest from a top-view. Each camera's intrinsic and extrinsic parameters are calibrated to ensure accurate mapping of pixel coordinates to real-world coordinates. This calibration is essential for effective cross-camera tracking.

Object detection: We utilize YOLOv8 for real-time pedestrian detection. YOLOv8 is known for its high accuracy and speed, making it suitable for dynamic environments.

Pedestrian tracking: We implement DeepSORT to maintain the identity of detected pedestrians across frames. DeepSORT enhances traditional SORT by incorporating appearance features, allowing for more reliable tracking in crowded environments.

*Email of the corresponding author: `jacqueline.lo@polyu.edu.hk`

Cross-camera ID matching: We propose a novel ID matching method involving: Cosine similarity - Compute similarity between pedestrian features in overlapping views to identify appearance-based matches. Bounding box distance - Analyze spatial relationships by calculating Euclidean distance between bounding boxes in real-world coordinates. Matching threshold - Combine cosine similarity and bounding box distance to determine if detections correspond to the same individual. Data fusion and tracking update - Fuse multi-camera data to update pedestrian positions and identities across the tracking system.

Our approach combines these methodologies to offer a comprehensive solution for real-time top-view pedestrian tracking, enhancing the understanding of pedestrian dynamics in evacuation scenarios.

Results

We tested our multi-camera pedestrian tracking method on a public dataset[3], which consists of 5 hours of video captured from 5 cameras (24 fps, 1280 × 960 resolution) in the UCU dining room. The dataset includes 4000 YOLO-format labeled images, each with a .txt file specifying "person" as the detection class and bounding box positions.

We fine-tuned YOLOv8 on the object detection dataset to optimize its performance for our application and applied the trained model to track pedestrians in videos captured by cameras 1, 2, and 3. Overlapping fields of view between cameras 1-2 and 2-3 enabled accurate cross-camera ID matching. The tracking results are shown in Figure 1, displaying the consistent pedestrian identification across overlapping regions, highlighting the robustness of our method.

Figure 1: Real-time tracking of pedestrians across three cameras with consistent ID assignment

Our approach demonstrates the effectiveness of top-view tracking combined with advanced algorithms for real-time pedestrian monitoring, offering valuable insights for evacuation and crowd management.

Conclusion

In this study, we introduced a novel top-view multi-camera pedestrian tracking method for real-time monitoring of pedestrian dynamics in evacuation scenarios. Leveraging YOLOv8 for object detection and DeepSORT for tracking, we developed a robust framework capable of accurately identifying and tracking individuals across multiple camera views. The cross-camera ID matching method, combining cosine similarity and spatial relationships of bounding boxes, significantly improves tracking consistency.

Future work will refine the algorithms, integrate additional data sources, and validate the system in more real-world environments. Our research aims to enhance emergency management by providing actionable insights into pedestrian dynamics during critical events.

Bibliography

[1] Glenn Jocher, Ayush Chaurasia, Jing Qiu. *Ultralytics YOLOv8*. Version 8.0.0, 2023. `https://github.com/ultralytics/ultralytics`. ORCID: 0000-0001-5950-6979, 0000-0002-7603-6750, 0000-0003-3783-7069. License: AGPL-3.0.

[2] Nicolai Wojke, Alex Bewley, Dietrich Paulus. *Simple Online and Realtime Tracking with a Deep Association Metric*. arXiv preprint arXiv:1703.07402, 2017. `https://arxiv.org/abs/1703.07402`.

[3] Ivan Prodaiko. *Person re-identification in a top-view multi-camera environment*. 2020.